

**Synthesis and isolation of biosynthetic derivatives of
Amphotericin B**

Thesis submitted for the degree of

Doctor of Philosophy

at The University of Leicester

by

Simon X. Walmsley BSc MSc (Leics)

Supervisor: Dr B.J. Rawlings

Department of Chemistry

University of Leicester

Submitted: September 2016

Revised: August 2017



Abstract

Amphotericin B has been used in the clinic for over fifty years in the treatment of serious fungal infections without any evidence of resistance developing, and recently has also become a frontline treatment for the parasite borne disease leishmaniasis, endemic in many poorer regions of the world. Alternative antibiotics are prone to the pathogens developing resistance, however amphotericin B is highly toxic leading to unpleasant side effects. A less toxic liposomal formulation is expensive limiting its use in the UK NHS and, even with a large WHO subsidy, restricting application to treating leishmaniasis. Semisynthetic modification has led to improved analogues, but at prohibitive cost.

This thesis presents work as part of a programme with Dr Caffrey (UCD, Dublin) to use synthetic biology in order to generate *in vivo* improved analogues of amphotericin B at clinically affordable cost. A promising 16-descarboxyl-16-methyl analogue has been identified by a previous student, but only isolated in very small quantities. An efficient protocol for the isolation of decigram quantities of 16-descarboxyl-16-methyl analogue is developed, along with inexpensive semisynthetic modifications to decrease the haemolytic activity in animal cells.

A noted synthetic analogue is the fructosylated disaccharide MFAME (*N*-methyl-*N*-D-fructosyl amphotericin B methyl ester), which has improved antifungal and decreased haemolytic properties, but due to the complex synthesis is not economically viable. Caffrey has produced a plasmid which when transfected into *S. nodosus* bacteria generates a mannosylated disaccharide analogue, the isolation and purification of which is documented in this thesis, along with biological testing where it was discovered to have reduced haemolytic activity compared to the parent molecule.

Acknowledgements

“The impossible often has a kind of integrity which the merely improbable lacks”
-Douglas Adams

Thanks are due to many people, particularly my supervisor, Bernard Rawlings, for allowing me the opportunity to work on this project and providing insights not only into the world of antifungal drugs but also the faults in our political system, benefits of nuclear power generation, what not to do in the event of a building fire, how to format a presentation so as to be readable from an adjacent county and the best routes for a walk in the hills around Gregynog.

Patrick Caffrey generously supplied the genetically modified bacteria samples, along with support and guidance about getting them to grow properly.

I would also like to thank Mick Lee, for running countless mass spectroscopy samples; Gerry Griffith, for helping me to make sense of amphotericin’s horrible NMR spectrum; and Kuldip Singh, for his patience when I kept showing up with sample vials that it turned out didn’t actually contain crystals.

I owe gratitude to Andy Fallows for reminding me of the omnipresent stench in my lab emanating from the incubators; Stu Philips for scarring my retinas; Bunmi Ibrahim for help and advice whilst following in her footsteps with this project; and Naomi, Georgie, Yana, Adam, Luka, Kat, Charlotte, Simran, Vicki, Greg, Lina, and all other colleagues for the morning chats over coffee which were sometimes the highlight of the day.

Contents

6	Abbreviations
8	1. Introduction and literature review
	1.1 Amphotericin B
10	1.2 Leishmaniasis
13	1.3 Antifungal and antiprotozoan action of amphotericin B
16	1.4 Toxicity of amphotericin B
17	1.5 Orientation of mycosaminyl sugar
20	1.6 The polyene antimycotic family
23	1.7 Reducing the toxicity of amphotericin B
25	1.8 Biosynthesis of amphotericin B
34	1.9 Previous biosynthetic derivatives from this group
43	1.10 Important techniques used
48	Results and discussion
	2. Biosynthesis of decarboxylated derivative
50	2.1 Attempted purification of AmNM (33) by existing method.
57	2.2 Second growth and improvements to method
62	2.3 Investigating necessity of XAD16 resin and variations on B2 method.
67	2.4 Contamination of flasks
68	2.5 Further reduction in quantity used of XAD16
70	2.6 Investigating use of Cottonseed flour
73	2.7 Further production of AmNM.
75	2.8 Functionalisation of the amine group
	2.8.1 Oxidation of 3-(Fmoc-amino)-1-propanol
77	2.8.2 Alkylation of mycosyl amine
82	2.8.3 Fmoc deprotection of alkylated AmNM
84	2.8.4 Alkylation with 2-(Fmoc-amino)-1-ethanol
91	2.8.5 Derivatisation with iodoacetic anhydride
94	2.8.6 Derivatisation with acetic anhydride
97	2.9 Biological testing of AmNM derivatives
98	2.9.1 Antifungal activity
99	2.9.2 Haemolytic activity
100	2.10 Summary
101	3. Amphotericin disaccharides
	3.1 Introduction
104	3.2 Mannosyl-amphotericin B
119	3.3 Mannosyl-7-oxo-amphotericin B
134	3.4 Mannosyl-8-deoxy-amphotericin B
157	3.5 Biological testing of mannosyl-8-deoxyAmB

158	4. Crystallisation
159	4.1 Previous work
161	4.2 Crystal growing methods
163	4.3 Pure AmNM
164	4.4 Iodoacetyl derivatisation
166	4.5 7-oxo-AmB <i>N</i> -iodoacetyl
167	4.6 8-deoxy-AmB <i>N</i> -iodoacetyl
	4.7 Amphotericin DI-DII-NM
169	4.8 Co-crystallisation
170	5. Summary and future work
171	6. Experimental
185	7. Appendix – NMR spectra
201	8. References

Abbreviations used

AA	amino acid
AmB	Amphotericin B
AmL	8-dehydroxyl-amphotericin B
AmNM	16-descarboxyl-16-methyl-amphotericin B
BuOH	Butan-1-ol
DCM	Dichloromethane
DMF	Dimethylformamide
DMPC	1,2-dimyristoyl- <i>sn</i> -glycero-3-phosphocholine
DMPU	1,3-Dimethyl-3,4,5,6-tetrahydro-2(1H)-pyrimidinone
DMSO	Dimethyl sulphoxide
EtOAc	Ethyl acetate
EtOH	Ethanol
FAE	2-(Fmoc-amino)-1-ethanal
FAP	3-(Fmoc-amino)-1-propanal
FDA	Food & Drug Administration
GSK	GlaxoSmithKline
Hep	Heptaene (analogue of amphotericin)
HPLC	High-pressure liquid chromatography
IBX	2-iodoxybenzoic acid
IPA	Isopropyl alcohol
KR16	7-oxo-amphotericin B
MeOH	Methanol

MFAME	<i>N</i> -methyl- <i>N</i> -D-fructosyl amphotericin B methyl ester
MHC	Minimum haemolytic concentration
MIC	Minimum inhibitory concentration
NMR	Nuclear Magnetic Resonance (spectroscopy)
ORF	Open reading frame
PKS	Polyketide synthase (enzyme)
Ppt	precipitate
ppm	Parts per million
RT	room temperature
s/n	supernatant
SIBX	Stabilised 2-Iodoxybenzoic Acid
Tet	Tetraene (analogue of amphotericin)
VdW	Van der Waals forces
WHO	World Health Organisation
WT	Wild-type
XRD	X-ray diffraction

1. Introduction and literature review

1.1 Amphotericin B

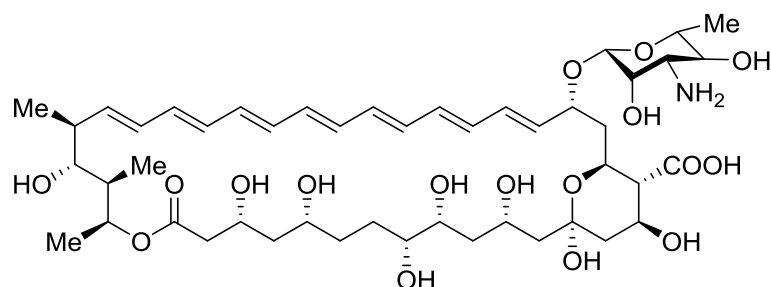


Figure 1: Amphotericin B

Amphotericin B (**1**, AmB) was first¹ isolated² in 1953 from *Streptomyces nodosus*, a filamentous bacterium collected from soil samples taken from the Orinoco River in Venezuela. When first discovered, *Streptomyces* were thought to be fungi, due to their tendency to form spores (at the time unknown in bacteria) hence their original classification as Actinomycetes, although they are now classed as Actinobacteria. A crucial difference is that the spores of fungi are gametes necessary for sexual reproduction, while the spores formed by bacteria are used as a survival mechanism against unfavourable external conditions and to aid dispersal. *Streptomyces* are Gram-positive bacteria, meaning they have a thick murein layer as a protective cell wall and are known for their characteristic odour due to metabolic production of the volatile metabolite geosmin (**2**).

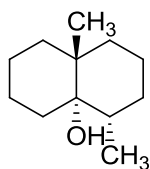


Figure 2: Geosmin

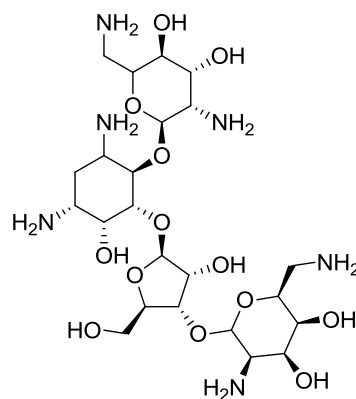


Figure 3: Neomycin

They are widely used to produce many antibiotic and antifungal drugs such as neomycin (3), used as an oral preparation to treat bacterial infection in the gut, and nystatin (4), used to treat *Candida* infections such as thrush. *Streptomyces* have also been used as an alternative to *E. coli* for heterologous protein expression, showing many advantages in terms of correct protein folding and emission.³

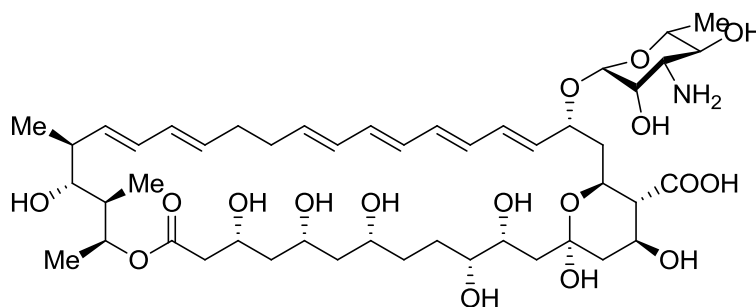


Figure 4: Nystatin

Amphotericin is named for its being amphoteric, meaning it will react both as an acid and as a base. *S. nodosus* produces two amphotericins, A and B⁴. The difference is that A has a single bond between the 28th and 29th carbon, whilst B has a double.

Amphotericin A (5) may be referred to as the tetraene, with B as the heptaene.

Amphotericin A is known to have much lower antifungal activity (MIC₅₀ *C. albicans*: 10.1 µg/ml)⁵ than AmB (MIC₅₀ *C. albicans*: 0.5 µg/ml).⁶

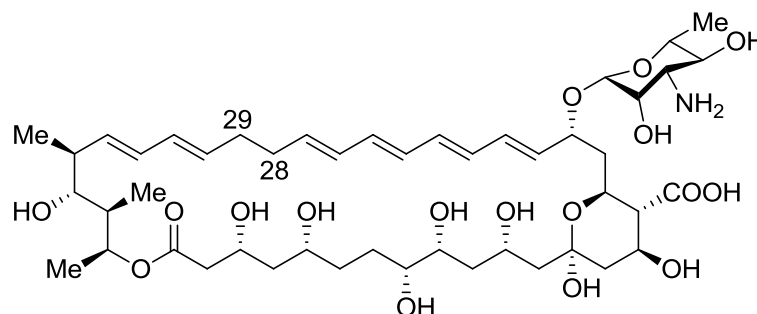


Figure 5: Amphotericin A (aka tetraene)

1.2 Leishmaniasis

Malaria is the world's most prevalent parasitical killer. In 2010 estimates from the WHO placed the number of malaria cases at 219 million, resulting in 660,000 deaths in that year.⁷

However, since not all deaths are recorded it is estimated by the WHO that the true number could be as high as 1.24 million. Malaria is very well known about in the western world, however, the second largest parasitic killer, leishmaniasis, remains far less well known, despite affecting as many as 12 million people worldwide, with up to 2 million new cases each year. Deaths from the most serious form, visceral leishmaniasis were 87,000 in 1990, with a drop to 52,000 in 2010.⁸

Leishmaniasis is present on all continents; though it is most prevalent in Brazil, Nepal, India, Bangladesh and the Sudan. However, the most concentrated centre for leishmaniasis according to the WHO is Kabul, Afghanistan, which experienced 67,500 cases in 2004.⁹ Anecdotal reports¹⁰ suggest that this is due to destruction of the housing and healthcare infrastructure during the regimes of the Mojahedin and Taliban, and ongoing political instability in the war-torn country.



Figure 6: swelling caused by visceral leishmaniasis. Image from WHO.



Figure 7: Ulcer caused by cutaneous leishmaniasis. Image from Australian Society for Parasitology

There are two main types of leishmaniasis, visceral (figure 6)¹¹ and cutaneous (figure 7).¹² Visceral (from latin *viscera*, meaning the internal organs) leishmaniasis is also known as kala-azar or black fever and is the most serious form. The leishmania parasite attacks the internal organs, particularly the liver and spleen causing swelling, and without treatment will nearly always kill the host. Cutaneous (from Latin *cutis*, meaning skin) leishmaniasis affects the skin and is less serious but more common than visceral. However it is possible for cutaneous to progress to visceral. Large red lesions form at the location of the bite from a sand fly, which can progress into ulcers and may suffer secondary infection from bacteria. The lesions often heal but leave significant scarring. A specific form of cutaneous leishmaniasis is mucocutaneous leishmaniasis which forms large disfiguring lesions on the face.

Leishmaniasis is spread by two species of female sand fly (figures 8a¹³ and 8b¹⁴), phlebotominae in the old world and lutzomyia in the new world. Both insects are about 1.5 to 3 mm in length.

Like mosquitoes, female sand flies require a blood meal to produce eggs. They use their mouthparts to produce a wound, then inject agents to prevent blood-clotting

and to stimulate blood flow. It is at this point that the leishmania parasite, if carried by the sand fly, may be transferred to the victim.



Figure 8a: *Phlebotominae*



Figure 8b: *Lutzomyia*

The leishmania parasite is named for William Boog Leishman (1865-1926), a medical officer in the British army. In 1903 he published an account of oval structures he had observed in the spleen of a patient who had died of kala azar. This was later recognised as the protozoan which causes leishmaniasis.¹⁵

Previous treatment of leishmaniasis used two pentavalent antimonials, sodium stibogluconate (Pentostam, GSK) and meglumione antimoniate (Glucantime, Aventis). Both of these contain antimony and require intramuscular injection, however their use is declining due to widespread resistance.¹⁶

Amphotericin B is now the preferred choice of treatment.

1.3 Antifungal and antiprotozoan action of Amphotericin B

Amphotericin B was approved by the FDA in 1958 as an antimycotic drug despite its structure and mechanism being unknown at the time. It remains an effective broad-spectrum antifungal as no effective resistance to it has yet been observed.

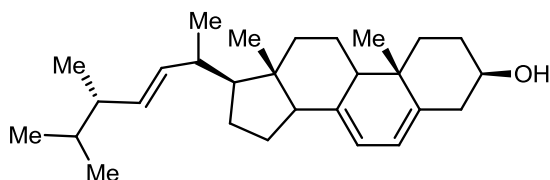
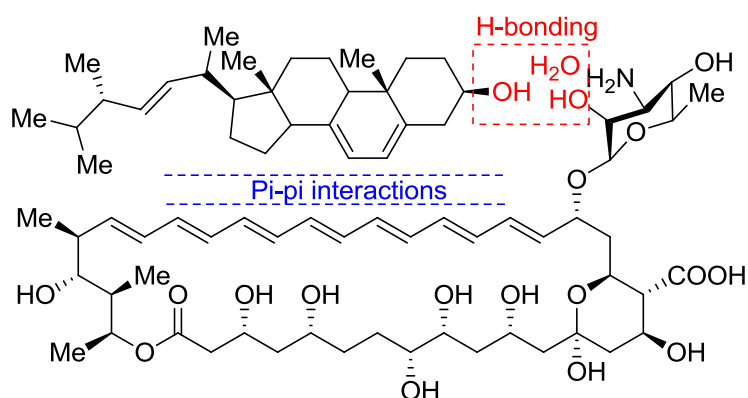


Figure 9: Ergosterol

Early studies of amphotericin showed that the mode of action involved a loss of cellular electrolytes.¹⁷ Finkelstein then showed that this loss could be caused by the formation of barrel stave channels with ergosterol (**9**), an abundant steroid in both fungal and flagellated protozoan cell membranes.¹⁸ Eight amphotericins and eight ergosterols form a cylindrical structure spanning half the cell membrane. Two of these cylinders then join (figure **10**)¹⁹ to span the whole width of the membrane leading to uncontrolled ion loss.



Scheme 1: Formation of amphotericin B-ergosterol unit.

The exact mechanism for this is not fully understood, but is thought²⁰ to proceed thus:

1. Pi-pi interactions between the pi system of ergosterol and the heptaene section of amphotericin B bring the molecules into alignment allowing hydrogen bonding between the axial hydroxyl group on the mycosaminyl sugar of amphotericin and the hydroxyl group on ergosterol.
2. Eight of these units form a barrel stave channel half the width of the membrane.
3. Two of these barrels then coordinate to form a channel spanning the full width of the membrane, with the hydrophilic hydroxyl groups from amphotericin on the inside and the hydrophobic carbon chains on the outside. This causes a significant change in membrane potential, leading to uncontrolled loss of cell electrolytes, leading eventually to cell death through apoptosis.



Figure 10: The completed barrel stave channel

The hydroxyl group on carbon-35 appears to be responsible for the joining of two barrels. Evidence for this theory lies in work by Szpilman *et al* who in 2008 synthesised 35-deoxy amphotericin B methyl ester (**11**), and found that its ability to transport potassium ions out of large unilamellar vesicles was greatly diminished compared to normal AmB.²¹

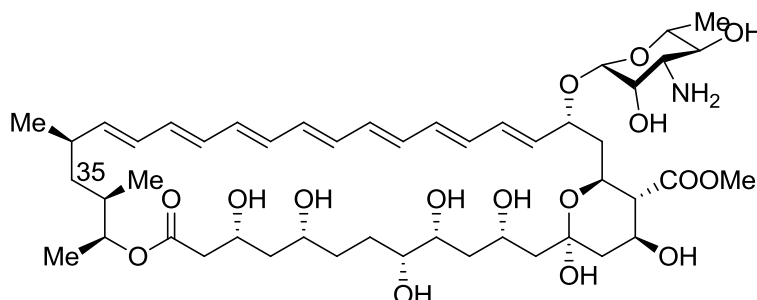


Figure 11: 35-deoxy amphotericin B methyl ester

Burke proposes an alternative theory that the antifungal action of AmB is primarily due to simply binding ergosterol,²² in contrast to the leading model. Previous research by Chen appeared to show that aqueous membrane channels were not central to the lethal action of polyene antibiotics,²³ and by te Welscher found that natamycin bound directly to ergosterol and thus inhibited the membrane fusion of vacuoles in yeast cells without causing membrane permeabilisation.²⁴ Burke proposes that since ergosterol is critical for many aspects of fungal cell physiology, such as the proper functioning of membrane proteins,²⁵ the compartmentalisation of membranes,²⁶ signalling via pheromones,²⁷ endocytosis,²⁸ and the aforementioned vacuole fusion,²⁹ the binding alone of this multifunctional lipid should be sufficient to kill yeast cells.

To test this hypothesis, Burke synthesised 35-deoxy-amphotericin B (figure 12) via iterative cross-coupling. This compound retained the ability to bind to ergosterol but

was unable to form membrane channels and in testing showed no membrane permeabilising activity.

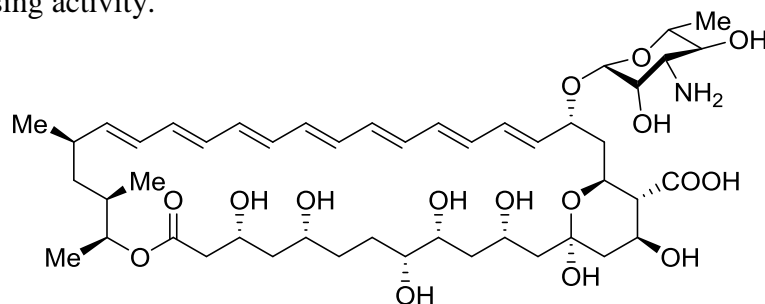


Figure 12: 35-deoxy-amphotericin B

In antifungal testing using a broth microdilution assay against *S. cerevisiae*, 35-deoxy-AmB showed a six-fold fall in potency (MIC: 3 μ M) compared to AmB (MIC: 0.5 μ M), and a comparable level to natamycin (MIC: 2 μ M). Despite this decrease in activity, Burke's research shows that the mechanism of action of amphotericin B and the other polyenes may be more complicated than previously thought.

1.4 Toxicity of Amphotericin B

Amphotericin B is toxic to mammalian cells as well as to fungal and protozoan cells. This arises from the similarity of ergosterol (**9**) to cholesterol (**13**), an abundant steroid in mammalian cell walls.

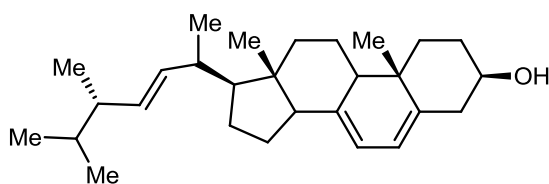


Figure 9: Ergosterol

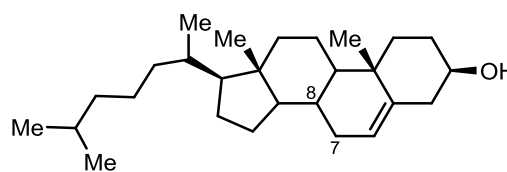


Figure 13: Cholesterol

AmB's binding affinity for cholesterol is lower due to the slight structural differences, particularly the single bond between carbons 7 and 8, giving cholesterol a less planar structure.³⁰ This causes AmB to form weaker VdW and pi-pi interactions with cholesterol, thus reducing the likelihood of hydrogen bonding occurring between

the mycosyl sugar and the steroid hydroxyl.³¹ This reduces the formation of barrel stave channels in mammalian cell walls though they remain prevalent, particularly in the kidneys where AmB forms transmembrane pores using cholesterol causing tubular disfunction.³² This results in complications such as decreased rate of filtration and renal blood flow, azotemia (increased levels of nitrogen containing compounds, such as urea, in the blood) and renal tubular acidosis (accumulation of acids in the body). These complications often lead to acute kidney failure.

AmB is also poorly soluble in most solvents, in the blood it exists as both monomers and as soluble & insoluble oligomers. It also forms complexes with other blood components such as sugars and fats. This can lead to it aggregating in smaller vessels, such as those found in the kidneys. For this reason, AmB requires administration in small doses (~1 mg/kg/day)³³, as an intravenous infusion up to three times a day, for up to six weeks. This can lead to difficulties as leishmaniasis is prevalent in Third World countries, where hospital resources may be scarce and a long journey from the patient's home. The patient may also have animals and children to nurture or crops to tend, making lengthy hospital visits a great inconvenience.

1.5 Orientation of mycosaminyl sugar

The relative geometry of the rigid macrolactone and mycosamine moieties on the AmB molecule is thought to be very important for both the drug's activity and selectivity. Murata examined this hypothesis by forming conformation-restricted derivatives where the amino and carboxyl groups were linked together by varying lengths of alkyl chain²⁰.

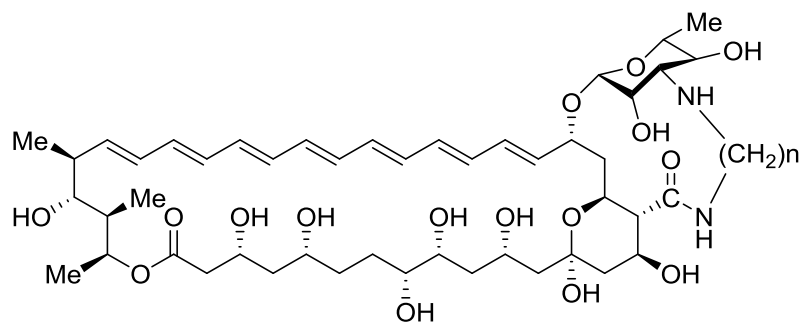


Figure 14: Intramolecular bridged AmB

Three derivatives of **14** were produced; $n=4$ (**14a**), $n=6$ (**14b**) and $n=8$ (**14c**). Their ergosterol selectivity was tested by measuring the concentration at which they permeabilised 50% of ergosterol containing liposomes (EC_{50}). Unmodified AmB has an EC_{50} of 11 $\mu\text{g/ml}$.

For **14a** where the sugar adopts a parallel orientation to the macrolide ring, ergosterol selectivity was reduced (EC_{50} : 50 $\mu\text{g/ml}$) as was also the case for **14c** (EC_{50} : 27 $\mu\text{g/ml}$).

For **14b**, where the plane of the sugar was twisted by $\sim 30^\circ$ with respect to the macrolide, ergosterol selectivity was increased (EC_{50} : 5.8 $\mu\text{g/ml}$)

This runs counter to propositions by Baginski, who suggested that AmB exists as two conformers³⁴, the ‘open’ conformer, where the sugar swings up from the molecule, allowing intermolecular hydrogen bonds between amino and carboxyl groups of neighbouring AmB molecules, and the ‘closed’ conformer, allowing formation of a hydrogen bond between the amino and carboxyl groups of the same molecule (figure 15).

The study by Murata *et al* suggests that such drastic conformational change is not necessary, rather that minute conformational alteration can be attributed to the sterol preference of AmB.

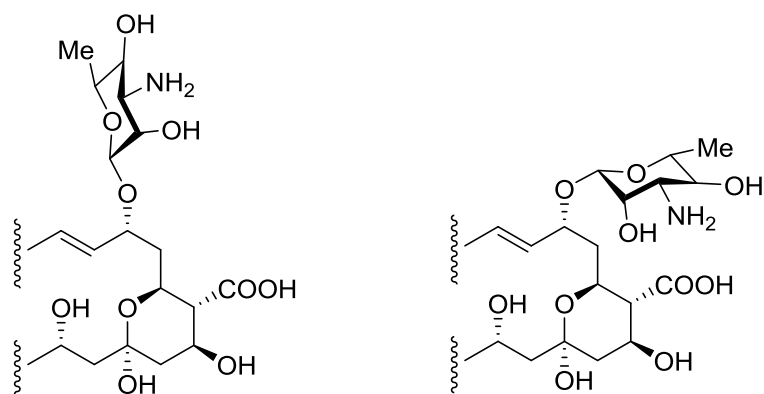


Figure 15: 'Open' (left) and 'closed' (right) conformers of AmB.

Murata's group also synthesised an intramolecularly linked AmB where the chain contained a hydrophilic glycine moiety³⁵ (figure 16), this molecule had almost the same configuration as **14b**, however the antifungal activity was improved significantly, possibly because the increased hydrophilicity enhances fungal cell wall penetration. (MIC: **14b** 20 µg/ml, **16** 10 µg/ml, AmB 5 µg/ml)

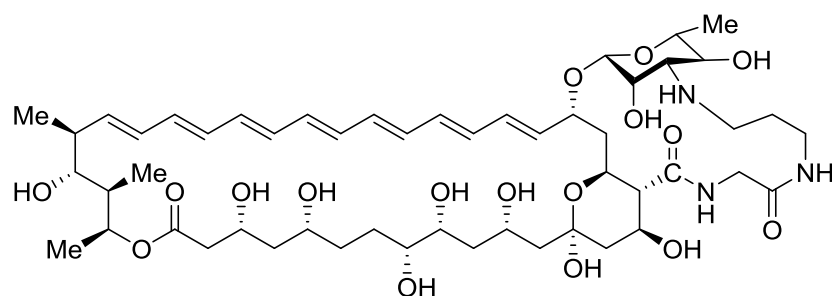


Figure 16: Intramolecularly glycine linked AmB

1.6 The polyene antimycotic family

The class of drugs that includes amphotericin B is sometimes referred to as the polyene antimycotics.³⁶ Characteristic of these molecules, all produced by *Streptomyces* bacteria, is the series of alternating double bonds that form part of the macrolide ring structure, they also usually have an amino-glycoside group attached to the molecule.

Nystatin

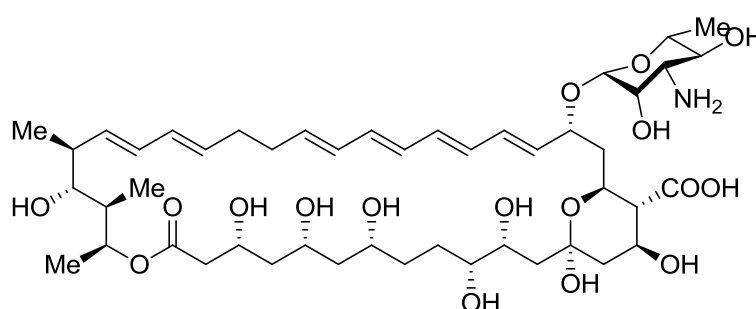


Figure 4: Nystatin

Nystatin was the first of the polyene antimycotics to be discovered, in 1950 by Rachel Brown and Elizabeth Hazen,³⁷ who isolated it from a soil bacterium *Streptomyces noursei* which was discovered near a barn on a dairy farm in Fauquier county, Virginia, and named after the farm's owner William Nourse. The molecule was named nystatin after the New York State Public Health department.³⁸ It is in common use as a topical antifungal to treat *Candida* infections such as vaginal thrush and nappy rash. It is also in use as an oral suspension to treat oesophageal infections and in tablet form for infections in the gut. Since nystatin has negligible absorption in the intestines, toxic side effects similar to those of AmB (chapter 1.4) are not a problem, however diarrhoea and abdominal pain are known side effects.³⁹ *In vitro* experiments with nystatin show an antifungal activity against *C. albicans* of MIC: 4 µg/ml.⁴⁰

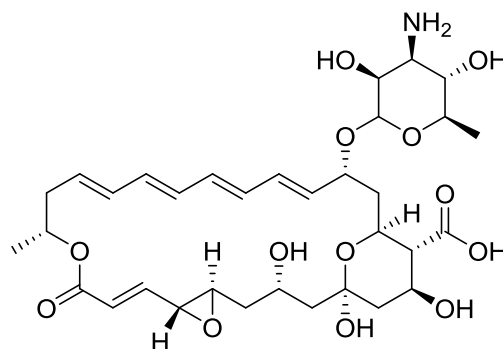
Natamycin

Figure 17: Natamycin

Natamycin was first isolated from *Streptomyces natalensis* in 1955.⁴¹ It is commonly administered as an eye drop for infections such as conjunctivitis and keratitis, as well as a cream for topical administration or a lozenge for gastrointestinal infections. Like nystatin, very little is absorbed from the gut thus avoiding toxic complications in the body. It has also been used extensively in the food industry as a surface preservative for cheese and some meats and carries the E number E235.⁴²

It has an LD₅₀ of 2.5-4.5 mg/kg.⁴³

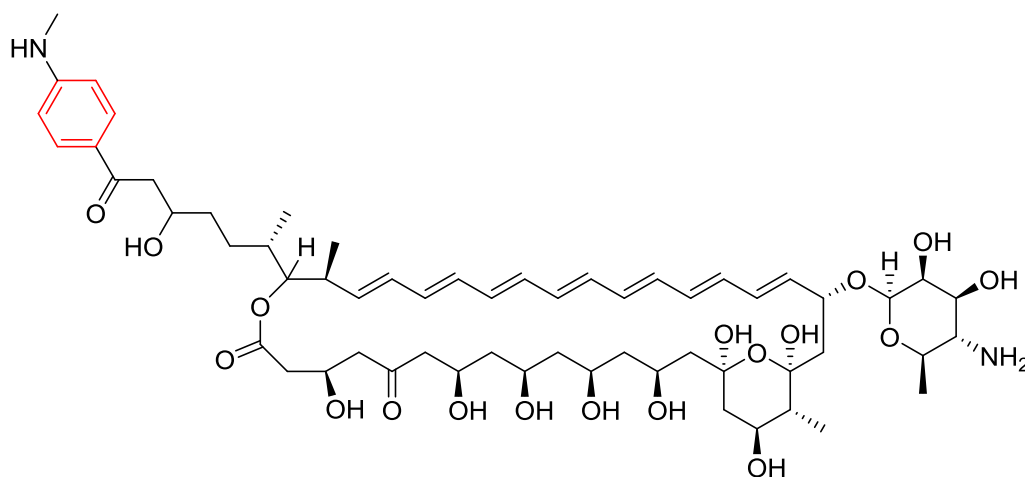
Perimycin

Figure 18: Perimycin A

Perimycin is produced by *Streptomyces coelicolor* and was first described in 1960.⁴⁴ It exhibits good antifungal activity against *C. albicans* and *S. cerevisiae* (MIC: 0.06 $\mu\text{g/ml}$)⁴⁵ but is not currently used clinically.⁴⁶ Perimycin is produced as a mixture of three types; A, B and C, with the largest component being A (figure 18) which has an aromatic group (in red on figure 18). The structures of B and C have not been fully determined.

Hamycin

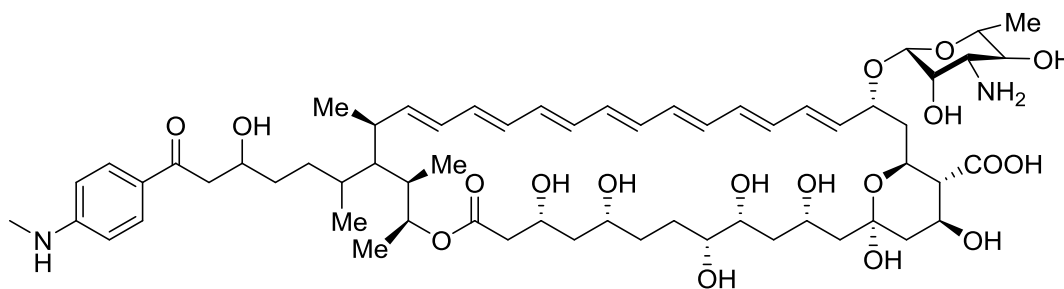


Figure 19: Hamycin B

Hamycin is structurally very similar to amphotericin except for the additional aromatic chain bound to the molecule at carbon-35. Hamycin is also produced in A and B forms analogous to amphotericin A and B. It exhibits very potent antifungal activity (MIC₅₀: 0.006 $\mu\text{g/ml}$ for A, 0.005 $\mu\text{g/ml}$ for B) but also very high haemolytic activity (MHC₅₀: 0.2 $\mu\text{g/ml}$ for A, 0.03 $\mu\text{g/ml}$ for B. AmB was 6.0 $\mu\text{g/ml}$ in the same test).⁴⁷

Since Hamycin can be absorbed after oral administration, this has been the preferred method in most clinical studies.⁴⁸ Encapsulation in a cholesterol-containing liposome managed to reduce the haemolytic activity to a MHC₅₀ of ~ 50 $\mu\text{g/ml}$ whilst maintaining comparable antifungal activity.⁴⁹

1.7 Reducing the toxicity of Amphotericin B

For intramuscular injection, AmB was originally administered as a solution in DMSO, but more recently was used as a complex with sodium desoxycholate (Fungizone) which provides a colloidal dispersion. Injection in such a manner contributes to many of the side effects discussed above (section 1.4). Recently, a unilamellar liposomal formulation of AmB has been developed. This formulation, known as AmBisome, was first registered by the FDA in 1997. In trials AmBisome was shown to be more effective and less toxic than AmB, due to a higher concentration of the drug present in the liver and spleen where it is needed, and a lower concentration in the kidneys and lungs where it causes side effects.⁵⁰ A liposome is a microvesicle composed of a bilayer of lipid amphipathic molecules which enclose an aqueous compartment that traps drug molecules. This could be thought of as a synthetic cell and protects the drug from metabolism in plasma. The liposome's design can be targeted to a specific therapeutic area. A study by Abeer reported that a single-dose treatment of 5 mg/kg/day of AmBisome has a cure rate for visceral leishmaniasis of 97.5% in patients in India.⁵¹ However, the complex synthesis of AmBisome makes it an expensive treatment, the WHO price of 50 USD per vial is unaffordable in many regions where leishmaniasis is prevalent.

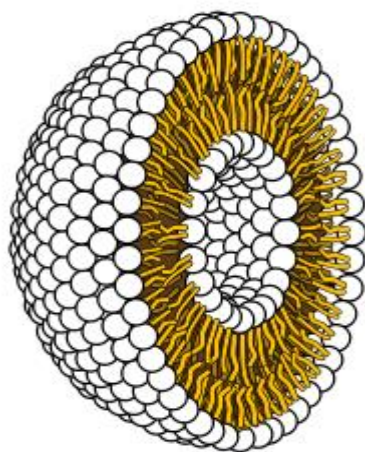


Figure 20: Cartoon representation of a liposome, Wikimedia Commons.

Semi-synthetic analogues of AmB have been produced. The wide array of functional groups in AmB affords many opportunities for chemical modification. For example: the macrolactone heptaene and hydroxyl groups may be oxidised, the lactone ester is liable to saponification (reaction with NaOH to form a sodium salt) and the hemiketal and the mycosamine are acid sensitive.⁵² The most successful synthetic derivative of AmB is *N*-methyl-*N*-D-fructosyl amphotericin B methyl ester (MFAME, **21**).⁵³ This compound retained⁵⁴ similar antifungal activity to AmB (MIC: 5 µg/ml) but showed much reduced toxicity (LD₅₀ 400 mg/kg to AmB's 6 mg/kg).

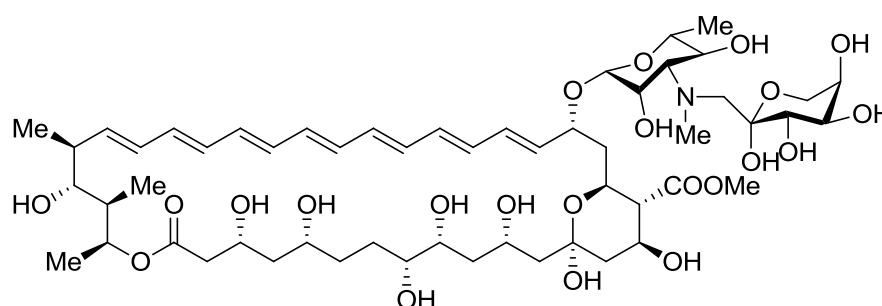


Figure 21: MFAME

However, due to the multi-step synthesis involving a sixteen hour reaction with D-glucose⁵⁵ (yield ~65%) followed by methylation with diazomethane⁵⁶ (yield ~13%), the production cost to use MFAME as a drug would be prohibitively expensive. Despite this, MFAME demonstrates that less toxic analogues of AmB exist in chemical space; the challenge is to produce them cheaply enough to be used medicinally.

1.8 Biosynthesis of Amphotericin B

A less expensive, and therefore more pharmacologically viable (affordable), alternative to chemical modification of AmB could be through alterations to the biosynthesis mechanisms of the *S. nodosus* bacterium by which it is produced.

The biosynthesis of AmB first proceeds by assembly of the lactone bicyclic ring molecule referred to as 'aglycone' (see scheme 2). Formed from sixteen acetate units and three propionate units the ring is assembled by a series of Claisen-like condensations, catalysed by polyketide synthase (PKS). The reactions necessary for the extending chain are summarised in scheme 2 and the modules involved in the formation of algycone are summarised in schemes 3a-3d.⁵³

The PKS module contains 6 domains, acyl transferase (AT) binds the extender unit, ketoreductase (KR) reduces ketone groups to hydroxyl groups, acyl carrier protein (ACP) holds the chain as a thiol ester, ketosynthase (KS) catalyses condensation reactions between the growing chain and the extender units, dehydratase (DH) reduces hydroxyl groups to unsaturated enoyl groups, and enoylreductase (ER) reduces enoyl groups to saturated alkyl groups. The gene cluster for the PKS has been sequenced by Caffrey *et al* and found to contain six genes, *amph ABCIJK*. Each of these genes codes for one of the multifunctional proteins necessary for the different steps of the synthesis.⁵⁷

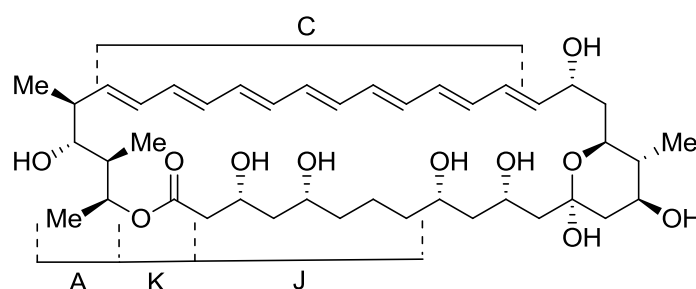


Figure 22: Location of modifications made by PKS genes.

Amph A loads the first acetate unit, Amph B contains the first two extension modules. Amph C assembles the polyene unit, modules 3-8.

In Amph C modules 3, 4, 6, 7 and 8 all contain a DH-KR reduction loop whereas module 5 contains DH-ER-KR, the region preceding ER5 is 45 AAs shorter than ER loops in other PKS proteins, this restricts movement of the ER5 domain allowing some chains to transfer from ACP5 to KS6 before the enoyl reduction occurs, it is this discrepancy that allows both amphotericin A and amphotericin B to be formed. Caffrey theorised⁵³ that inactivation of ER5 by gene replacement could give a *S. nodosus* strain that exclusively synthesised AmB, the more active and therefore more valuable antifungal agent. To date this has not been tried, though work by Zotchev⁵⁸ on the equivalent gene in *S. noursei* resulted in a mutant producing a heptaene analogue of nystatin (S44HP, **23**) tested to have higher antifungal activity against *C. albicans* than the parent compound (MIC₅₀: nystatin 0.45 µg/ml, S44HP 0.07 µg/ml) confirming that there is much more to be done in this area.

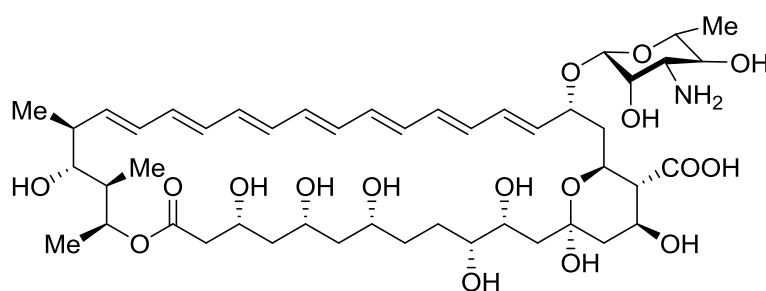
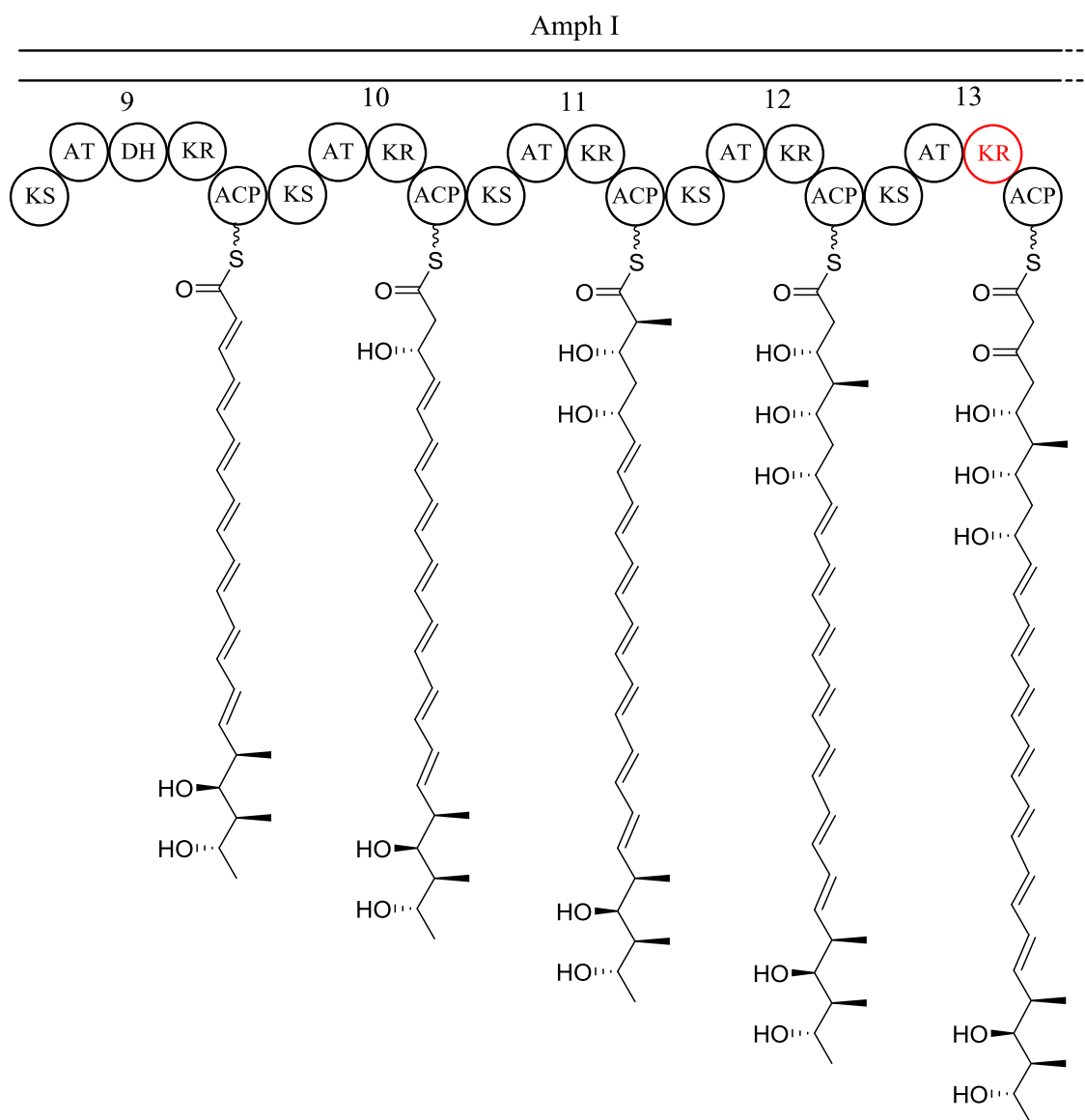


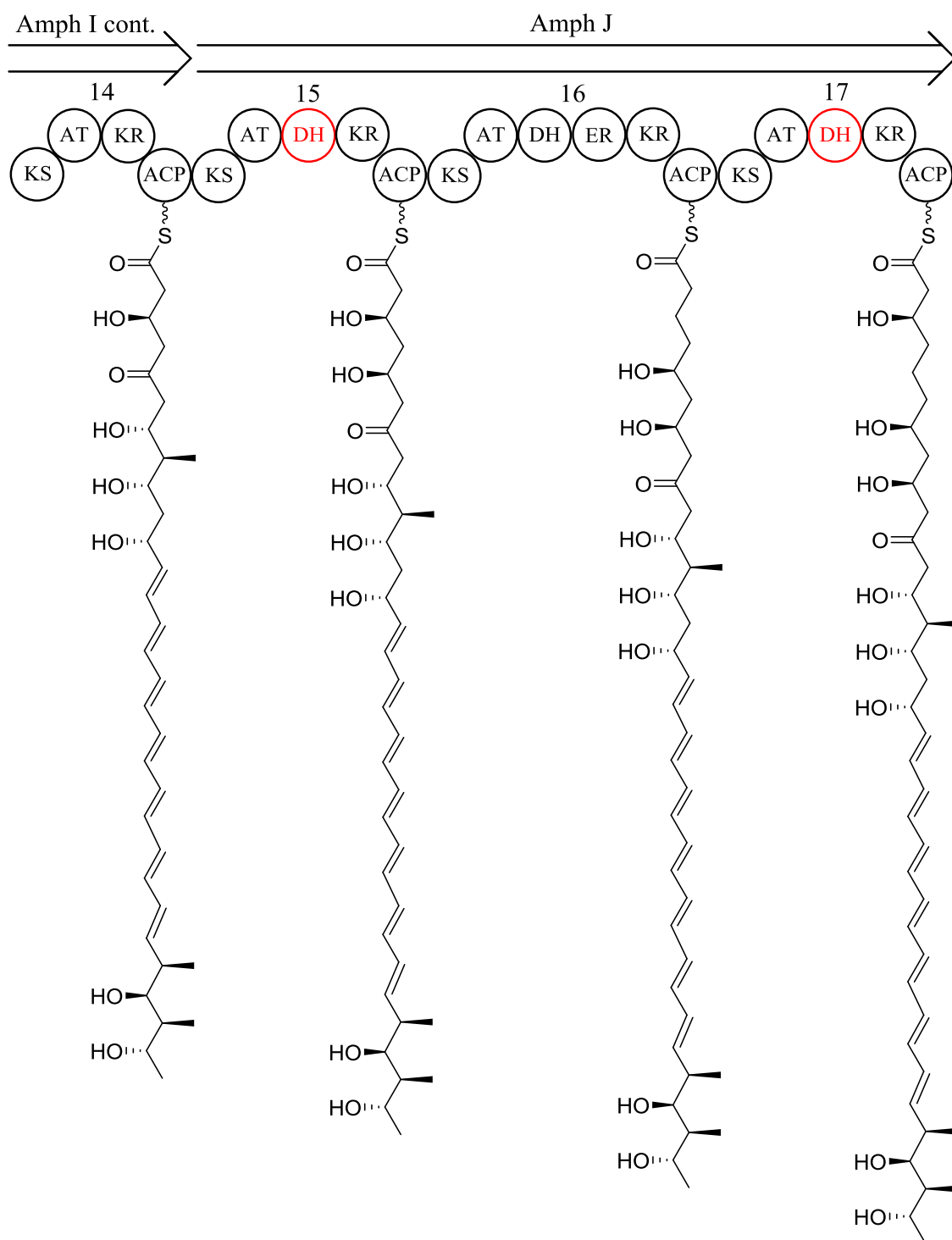
Figure 23: S44HP

Amph I incorporates modules 9-14, 11 contains a methylmalonate specific AT domain resulting in the methyl branch at C41. Amph J incorporates modules 15-17, modules 15 and 17 both contain inactive DH-KR reductive loops while 16 contains a complete DH-ER-KR reductive loop, it is this protein that accounts for the differences between amphotericin and nystatin, the Nys J protein contains a complete reductive loop at 15 with inactive loops at 16 and 17.⁵⁹

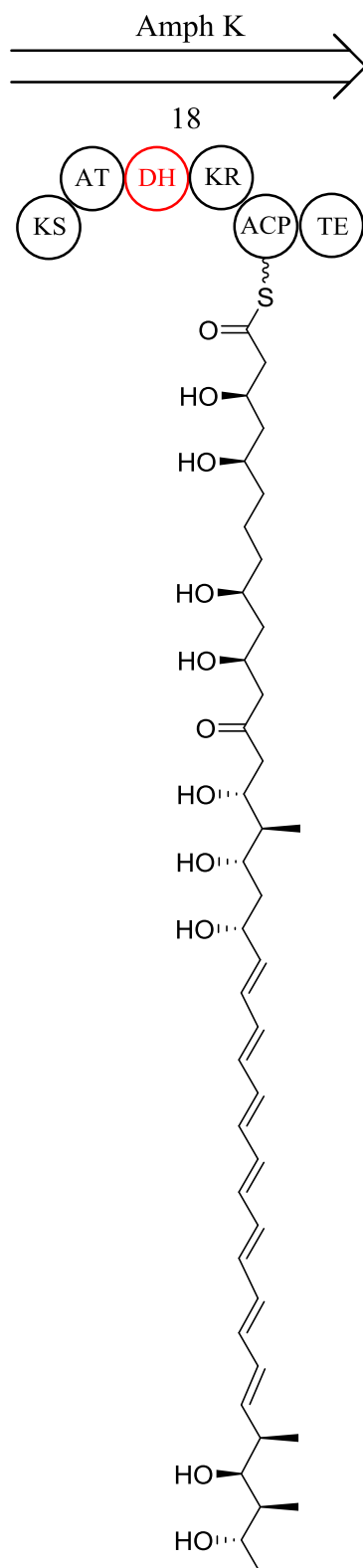


Scheme 3b: Modular structure of the aglycone PKS part 2.

After cyclisation, the macrolactone ring is hydroxylated at C8 by cytochrome-P450 protein Amph L, the hydroxyl group at C19 is mycosaminylated by Amph DI and the propionate-derived C41 methyl group is oxidised by cytochrome-P450 protein Amph N to form the carboxyl group. The order in which these modifications occur is unknown⁵³ though importantly, the Amph N and Amph DI modifications do not appear to be sequence specific.⁶⁰



Scheme 3c: Modular structure of the aglycone PKS part 3.



Scheme 3d: Modular structure of the aglycone PKS part 4.

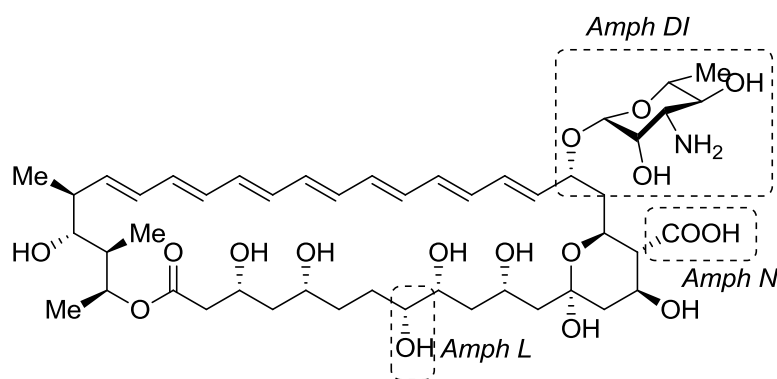
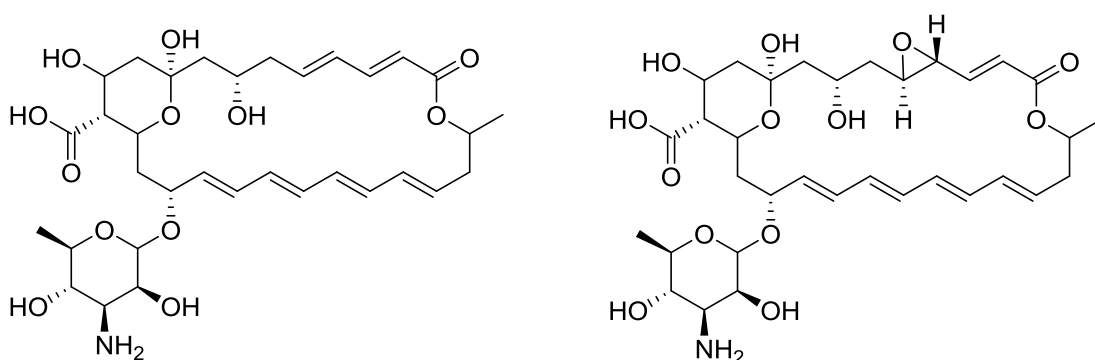


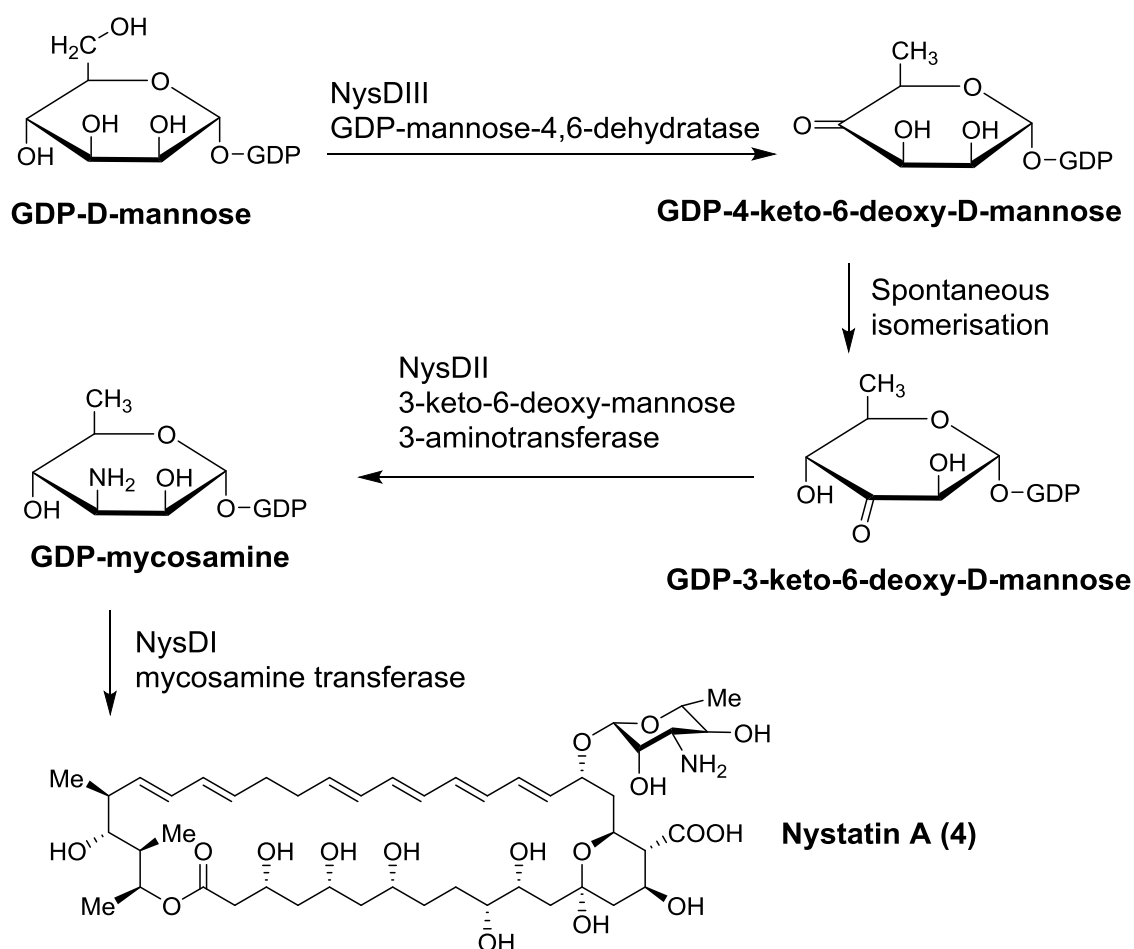
Figure 24: Modifications to aglycone made by post PKS proteins

The sugar group is synthesised separately⁶¹ by Amph DII and DIII, the 4,6-dehydratase DIII dehydrates GDP-mannose to yield 4,6-dideoxy-4-oxo-mannose, which spontaneously isomerises to form GDP-3,6-dideoxy-3-oxomannose (this is assumed to be spontaneous isomerisation because no enzyme has yet been discovered to account for the change,⁶² however in 1998, Sullivan and colleagues used *E. coli* and human GDP-mannose 4,6-dehydratases to generate GDP-4-keto-6-deoxymannose *in vitro*, they observed via NMR that this substrate spontaneously converted to GDP-3-keto-6-deoxymannose⁶³). DII catalyses an amino transfer at C-3 to give GDP-mycosamine. The mycosamination of nystatin has been fully characterised and is shown in scheme 4.⁶⁴ Since AmphDI and NysDI are known to have equal substrate specificity,⁶⁵ this process is assumed to be analogous to that on amphotericin B.



Figures 25a: de-epoxypimaricin (left) and 25b: pimaricin (right)

Gene disruption to the sequence described above leads to development of novel analogues of AmB. Caffrey found gene replacement through transduction to be the preferred method.⁵⁷ In transduction, foreign DNA is introduced to a bacterial cell by a viral vector. The first example of this on a *Streptomyces* bacterium was a pimaricin (**25b**) derivative produced by gene disruption in *S. natalensis* by Mendes *et al.*,⁶⁶ in which a recombinant mutant produced de-epoxypimaricin (**25a**) as a major product. This resulted from the phage-mediated targeted disruption of the gene *pimD*, which codes for the cytochrome-P450 epoxidase enzyme which converts de-epoxypimaricin into pimaricin.



Scheme 4: Synthesis of mycosamine on nystatin.
The process is analogous to that on amphotericin.

1.9 Previous biosynthetic derivatives from this group.

Several other biosynthetic derivatives have previously been produced by this group, mostly via phage transduction.⁶⁷ The actinophage KC515 was found to form plaques on *S. nodosus*,⁵³ allowing it to be used for the introduction of DNA for gene disruption and replacement. Fragments of DNA from genes are cloned into the plasmid pUC118 which is then subcloned into KC515. The recombinant phage is used to infect *S. nodosus* and lysogens (infected bacteria where the phage DNA has been integrated in the host's chromosome) obtained by growing the bacteria in the presence of thiostrepton, genes for the resistance of which are located on the plasmid.

Disruption of the amphDIII gene

A 2091 base pair region which contains the amphDIII gene was amplified by PCR and cloned into plasmid pUC118, which was then digested with BgIII which cuts at a site approximately in the centre of the amphDIII gene. The ends were repaired with T4 DNA polymerase and ligated thus creating a frameshift mutation. This fragment was cloned into KC515 and propagated on *S. nodosus*, lysogens being identified by thiostrepton resistance. The mutant was grown on fructose-dextrin-soya medium and methanol extracts of the mycelia showed tetraenes and heptaenes by UV/Vis assay. ESMS analysis showed that the products present were 8-deoxyamphoterinolides A (**26a**) and B (**26b**) and amphoterinolides A (**26c**) and B (**26d**). The partially purified 8-deoxyamphoterinolides were converted to their methyl esters (**26e** & **26f**). The polyenes were tested for antifungal activity in agar diffusion assays with *Saccharomyces cerevisiae* as the indicator organism. No antifungal activity could be measured, consistent with previous research showing that the positively-charged amino group on the mycosamine is necessary for antifungal activity.⁶⁸

Disruption of the amphL gene

The amphL gene contains a SacI site either side of a 1053 base pair region, this intra-SacI fragment was cloned between the SacI sites of KC515. The recombinant phage was plated with *S. nodosus* and lysogens selected by thiostrepton resistance.

The mutants were grown on fructose-dextrin-soya medium, both heptaenes and tetraenes were found in methanol extractions of the mycelia. Yields were very low (2-5 mg per litre of broth, AmB is usually ~4 g/l). Analysis by ESMS revealed the presence of masses corresponding to 8-deoxyamphotericin A and B (figure 27) as well as homologs with an additional methyl group. Due to their very low abundance and resistance to extraction with alcoholic solvents, pure enough material for NMR spectroscopy was not obtained. Designation of these compounds as 8-deoxyamphotericins rather than e.g. 16-descarboxyl-16-formyl-amphotericins is based on the homology between amphL and pimD. The presence of the methyl homologs may be due to the use of propionate as a starter unit, or an O-methylation on the sugar unit, possibly as a detoxifying process. Antifungal activity of partially purified 8-deoxyamphotericin B was measured against *S. cerevisiae* as MIC: 1.25 µg/ml, suggesting a slightly lower activity than AmB (1 µg/ml).

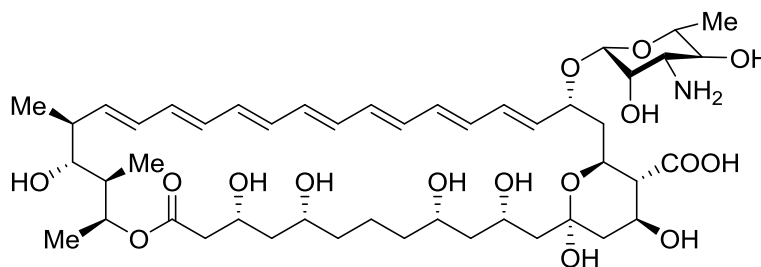


Figure 27: 8-deoxy-amphotericin B

Deletion of two modules from the AmphC polyketide synthase protein

The bifunctional vector was also used to redesign the amphotericin PKS to delete two modules from the AmphC pathway (see chapter 1.8) resulting in production of a pentaene⁶⁷, the hypothesis being that whilst the antifungal activity might be reduced, the water solubility would be improved giving an overall improvement to the therapeutic index. All AmphC modules contain the PKS domains KS-AT-DH-KR-ACP. Codons for the modules KS5 and AT7 were used to target the plasmid resulting in fusion of the coding sequences between these modules, thus producing a truncated yet functional AmphC protein. The resultant polyene showed strong UV/Vis absorbance at 310, 318, 333 and 352 nm, a spectrum characteristic of a pentaene.

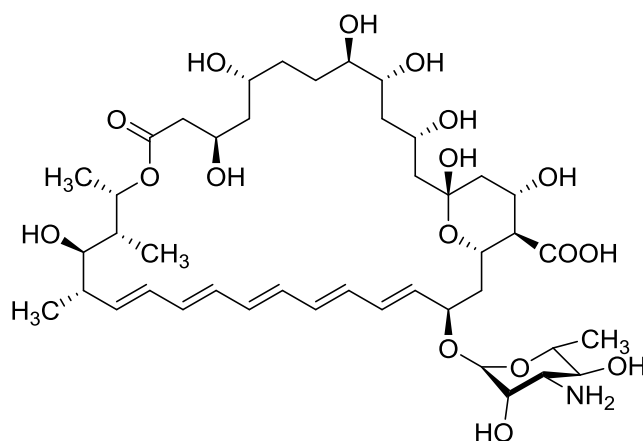


Figure 28: Proposed structure of truncated pentaene.

Inactivation of KR domain in module 16

The KR16 domain is located within the trimodular AmphJ protein. The strategy used⁶⁹ aimed to change the DNA sequence around the active site tyrosine (tyrosine 720 of AmphJ) codon from GCC-AAC-TAC to GCA-AGC-TTC, which would change the sequence from Alanine-Asparagine-Tyrosine to Alanine-Serine-Phenylalanine, thus impairing the active site of the protein at that point. PCR mutagenesis was used to construct plasmids containing the engineered KR16 coding sequence, which was cloned into phage KC-UCD1 to give

recombinant phage KC-KR16, which was used to introduce the engineered DNA into *S. nodosus*.

The mutant *S. nodosus* bacteria were grown and extracted with methanol, the methanolic extracts were slightly purified by gel filtration on Sephadex LH20. ESMS analysis found the major heptaene product to be 7-oxo-amphotericin B (**29**, $M+H^+$ 938.7) and the major tetraene product to be 7-oxo-amphotericin A (**30**, $M+H^+$ 940.5).

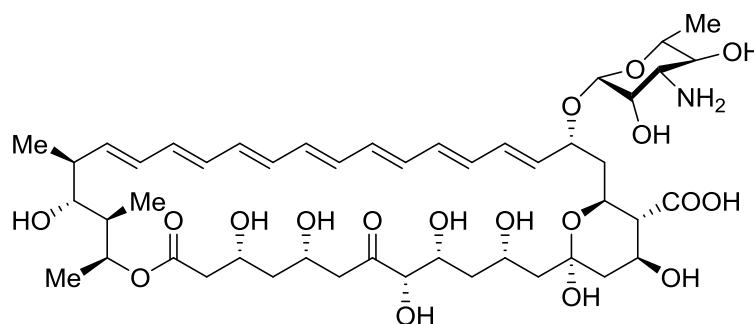


Figure 29: 7-oxo-amphotericin B

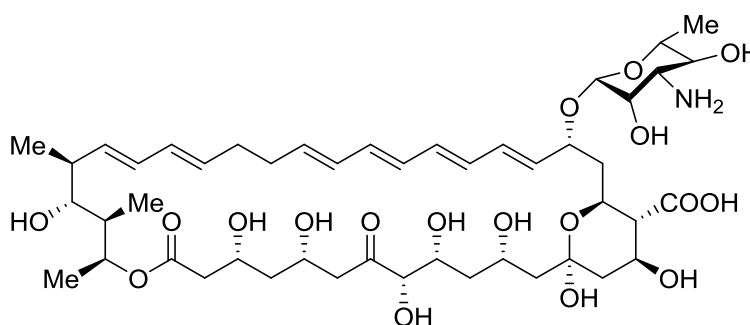


Figure 30: 7-oxo-amphotericin A

The crude 7-oxo-amphotericin B was converted to the *N*-acetyl methyl ester and purified for analysis by NMR spectroscopy. The carbon NMR showed a resonance at 212.67 ppm confirming presence of a ketone. NMR spectra were obtained that strongly consisted with the expected structure, however the large number of near-isochronous resonances in both the carbon and proton NMRs prevented rigorous exclusion of regioisomers. In antifungal and haemolytic assays, the control AmB showed a MIC of 1.25 $\mu\text{g/ml}$ and a MHC of 6 $\mu\text{g/ml}$, whereas 7-oxo-AmB had a lower antifungal activity (MIC: 4.5 $\mu\text{g/ml}$) but a greater relative decrease in haemolytic activity (MHC: 65 $\mu\text{g/ml}$).

Inactivation of AmphN protein

Disruption of the cytochrome P450 gene *amphN* was expected to block oxidation of the C16 methyl group on the macrolactone.⁶⁰ Subsequent glycosylation and C8 hydroxylation would yield 16-descarboxyl-16-methyl-amphotericin B.

Within the amphotericin gene cluster, the *amphN* P450 and *amphM* ferredoxin are located downstream from the *amphDII* and *amphDI* genes.⁵³ Targeted disruption of *amphN* was found to be problematic with phage constructs either not integrating with the genome or else giving unwanted deletions that prevented polyene production altogether, the reason for these failures was unknown. To counter this, a recombinant phage was designed to integrate into the upstream *amphDI* gene, the hypothesis being that this might stop *amphN* expression through polar effects. A fragment containing the 3'-end of *amphDI* and the 5'-end of *amphDII* was cloned into the KC-UCD1 vector to give KC-DI. Correct integration of this phage should leave intact copies of *amphDI* and *amphDII* in the chromosome.

Propagation of this phage gave two lysogens, DI-1 and DI-2. DI-1 was found to contain the *amphDII* region but had lost the *amphDI* region; by contrast, DI-2 contained the *amphDI* region but had lost the *amphDII* region. DI-1 produced no polyenes. DI-2 extracts had the UV spectrum characteristic of a tetraene/heptaene mixture with heptaene as the major product. The antifungal activity was measured as ~10 times lower than AmB. Analysis by ESMS revealed a mass appropriate for an amphotericin analogue with a methyl group instead of the carboxyl and a neutral deoxyhexose sugar (figure 31).

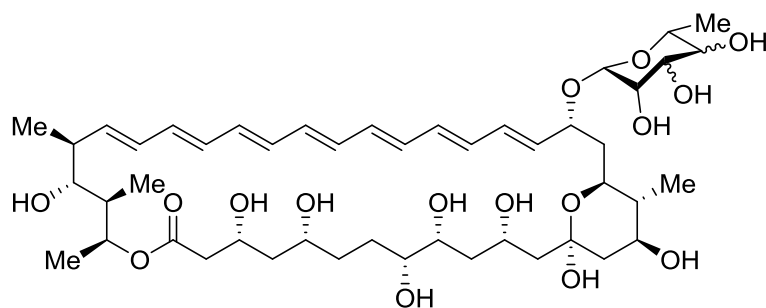


Figure 31: DI-2 lysogen product

The polyenes produced by DI-2 suggested that amphotericins lacking C16 carboxyl groups were not toxic to the producing cell. Renewed efforts were made to achieve targeted disruption of the *amphN* gene that would leave the glycosylation genes intact. A 1200-bp *Stu*I fragment was deleted from a pUC118 plasmid clone of the 6-kb *Pst*I fragment containing the *amphN* region of the amphotericin biosynthetic gene cluster, thus removing the 3'-end of the *amphN* gene, the adjacent *amphM* ferredoxin gene, and part of open reading frame 3. ORF3 has no role in amphotericin biosynthesis. Propagation of this plasmid on *S. nodosus* and extraction of the polyenes produced revealed a tetraene/heptaene mixture. Analysis of the tetraene fraction by ESMS found a mass appropriate for 8-deoxy-16-descarboxy-16-methyl-amphotericin A (**32**, $M+H^+$ 880.5). Analysis of the heptaene fraction by ESMS found a mass appropriate for 16-descarboxy-16-methyl-amphotericin B (**33**, $M+H^+$ 894.6). It is not known why the heptaene was hydroxylated at C8 when the tetraene was not.

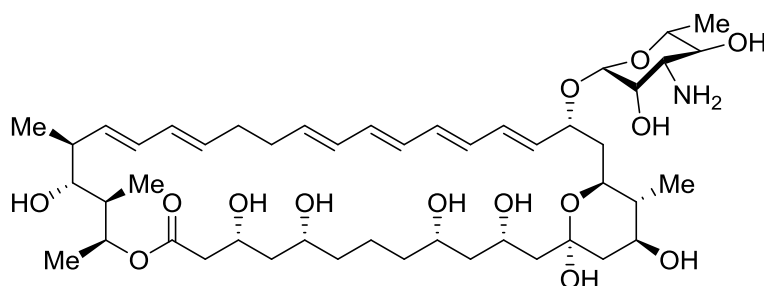


Figure 32: 8-deoxy-16-descarboxy-16-methyl-amphotericin A

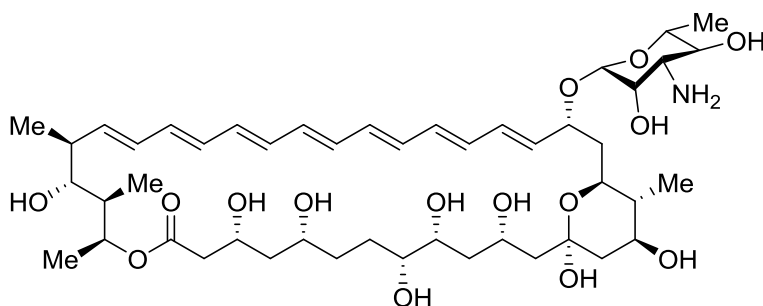


Figure 33: 16-descarboxy-16-methyl-amphotericin B (AmNM)

Antifungal and haemolytic assays of these two compounds showed that **32** was four times less antifungal than AmB (MIC: 5 $\mu\text{g/ml}$ to AmB's 1.25 $\mu\text{g/ml}$) but had a dramatic drop in haemolytic activity (MHC: 166 $\mu\text{g/ml}$ to AmB's 5 $\mu\text{g/ml}$), a 33-fold reduction. **33** had a MIC of 1 $\mu\text{g/ml}$ and a MHC of 50 $\mu\text{g/ml}$ showing comparable antifungal activity with a 10-fold reduction in haemolytic activity.

Perimycin (see chapter 1.6) is an aromatic heptaene that differs from the other polyene macrolides in that it lacks an exocyclic carboxyl group and contains perosamine instead of mycosamine. D-Perosamine is the 4-amino-3-hydroxyl regioisomer of D-mycosamine.⁷⁰ The *perDII* perosamine synthase and *perDI* perosamine specific glycosyltransferase were isolated from *S. aminophilus* and inserted into the *amphNM* mutant in early attempts to engineer the biosynthesis of 16-descarboxyl-16-methyl-19-(O)-perosaminyl amphoterinolides. This strain is theoretically capable of synthesising both GDP-D-mycosamine and GDP-D-perosamine, although no perosaminylated analogues were identified in production cultures. Production cultures of *amphNM+perDIDII* were unpredictable and could yield AmNM or the algycone or both, use of high levels of thiostrepton increased production of AmNM.⁶¹

Studies by previous student Odobunmi Ibrahim found that purifying AmNM from the high levels of cellular debris present in the mixture obtained from methanolic extraction of the *amphNM+perDIDII* mycelia to be very difficult, only about 40% purity by

weight of unmodified AmNM could be achieved.¹⁹ A strain of *S. nodosus* in which the *amphNM* genes were disrupted without the insertion of the *perDIDII* was provided by Caffrey (University College Dublin) which produced increased yields of AmNM (~37 mg/l compared to ~16 mg/l) without the addition of thiostrepton. Despite this increased yield, purity greater than 40% was still not achieved. Because of this, Ibrahim experimented with derivatising the amine group on the mycosamine with an aim to increasing the purity that could be obtained.

Fluorenylmethoxycarbonyl (Fmoc) is a widely used protecting group for free amines, such as in amino acid coupling during solid phase synthesis.⁷¹ It is a popular choice due to its stability in acidic and neutral conditions and its ease of removal in mildly alkaline solvents. The hydrophobicity of the Fmoc group and the masking of the free amine would it was hoped effect enough of a change in the amphotericin molecule's solubility as to facilitate greater purification than had previously been achieved. Ibrahim found that by protecting the AmNM molecule with Fmoc-OSu then running multiple flash chromatography columns on silica, followed by semi-preparative HPLC and finally deprotection with piperidine, AmNM could be obtained in almost pure form. However, this process took much time and resulted only in single-digit milligram yields. It is from this point that the work described in Chapter 2 below continues.

1.10 Important techniques used

UV/Vis assay

A UV/Vis assay is taken by diluting the sample in MeOH, and testing that sample against a blank containing pure solvent. The weight of polyene in the sample is determined using the Beer-Lambert law:

$$A = \epsilon cl$$

Where A is the absorbance, ϵ is the extinction coefficient, c is the concentration in mg/ml and l is the path length in cm. The assays are performed in disposable plastic cuvettes with a path length of 1 cm so l is removed from the equation. Concentration (c) equals mass (m) divided by volume (v), substituting this into the law gives:

$$A = \frac{\epsilon m}{v}$$

Rearranging for mass gives:

$$m = \frac{Av}{\epsilon}$$

An extra term must be added to account for the dilution (d):

$$m = \frac{Avd}{\epsilon}$$

The extinction coefficients are 170,000 for heptaene and 85,000 for tetraene⁷².

Example: if a sample 8.5 ml in volume, is diluted 500 times, which produces an absorbance of 0.500, the equation for heptaene becomes:

$$m = \frac{0.500 * 8.5 * 500}{170,000}$$

Solving for m gives a heptaene mass of 0.0125 g or 12.5 mg.

A UV/Vis assay trace is shown in figure 34. The peaks marked 1,2&3 are from heptaene, the peaks marked 5,6&7 are from tetraene. The absorbance for heptaene calculations is taken from peak 1 (405 nm), the absorbance for tetraene calculations is the difference between peak 5 (319 nm) and the background signal of trough 12 (~325 nm).

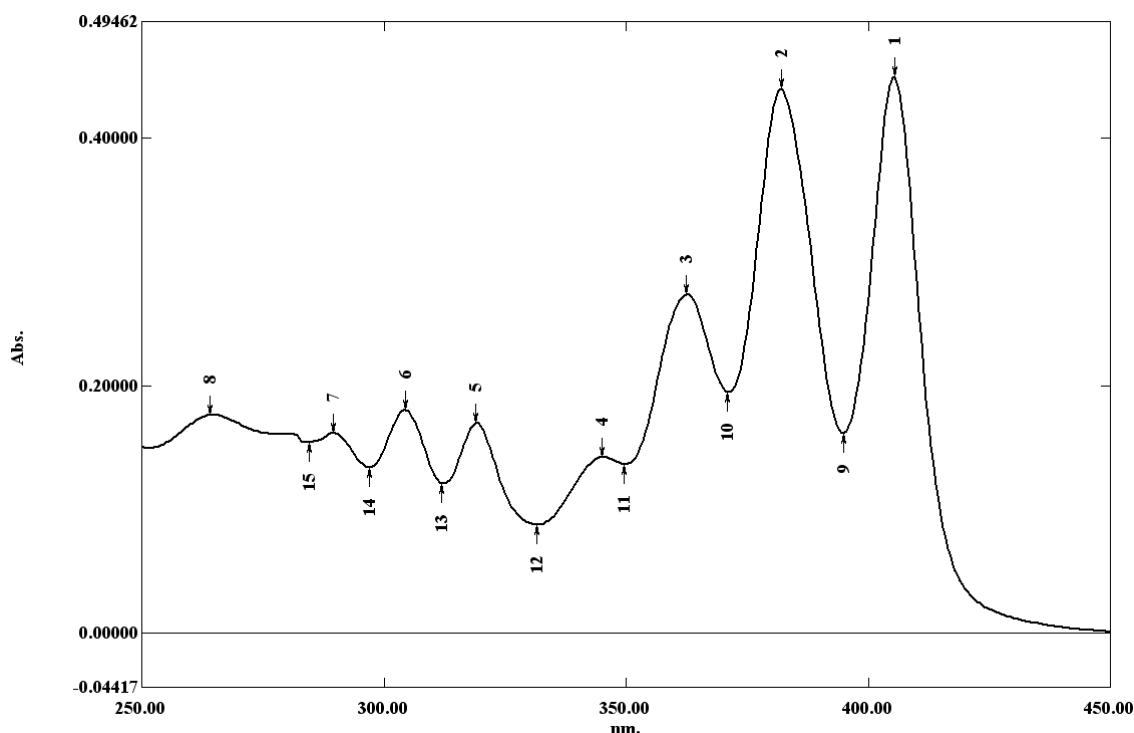


Figure 34: Example of a UV/Vis assay trace of a sample containing hep and tet.

It is important to note that the UV/Vis assay should be treated with caution as the spectrum produced depends upon the state of oligomerisation⁷³. The monomeric form contributes to the peak seen at 405 nm, while the aggregate form contributes to the broad peak observed at 340 nm (labelled 4 in figure 34).

Analytical and semi-preparative HPLC

HPLC stands for either High-Performance Liquid Chromatography or High-Pressure Liquid Chromatography. It uses a column of tightly packed silica resin as the solid adsorbent, the sample being passed over in a mixture of solvents as the liquid eluent. Compounds in the sample interact differently with the adsorbent, some interacting strongly, which increases their elution time, some interacting weakly, which are eluted more quickly. The adsorbent is much finer (5 μm) than would be found in bench chromatography (60 μm), and the pressure is much higher (typically 3000-4000 psi) so the resolution is much increased. 'Normal-phase' HPLC works in a similar manner to bench chromatography, the solid phase is polar (e.g. silica) and the liquid phase begins non-polar and increases polarity (e.g. hexane \rightarrow ethyl acetate), so that the least polar analytes are eluted first. 'Reversed-phase' HPLC has a non-polar stationary phase and a polar mobile phase, so that the most polar analytes are eluted first.

The solvents used on this HPLC system were water and methanol. The columns used were C8 and C18. In these columns, the silica has been modified with RMe_2SiCl , where R is a saturated alkyl group, C8 is C_8H_{17} and C18 is $\text{C}_{18}\text{H}_{37}$. This makes the chains hydrophobic, so that hydrophobic analytes interact more strongly with them in hydrophilic conditions, when the mobile phase contains water. The solvent composition for an analytical HPLC run is shown in figure 35 below. Formic acid (0.01%) is added to the methanol to keep the amphotericin in its protonated configuration giving a single elution signal. Without the formic acid, the retention time of amphotericin becomes a wider range, making purification difficult.

Sugars in the sample are very hydrophilic, so they elute first (typically 3-4 minutes on C18), amphotericin B with the heptaene moiety is less hydrophilic so it elutes later (~20 minutes on C18) and aglycone without the mycosyl sugar is more hydrophobic so elutes last (~33 minutes on C18). AmNM without the carboxylic acid is slightly less polar than AmphB so elutes slightly later (~22 minutes on C18). Retention times on the C8 column are slightly shorter though the order remains the same.

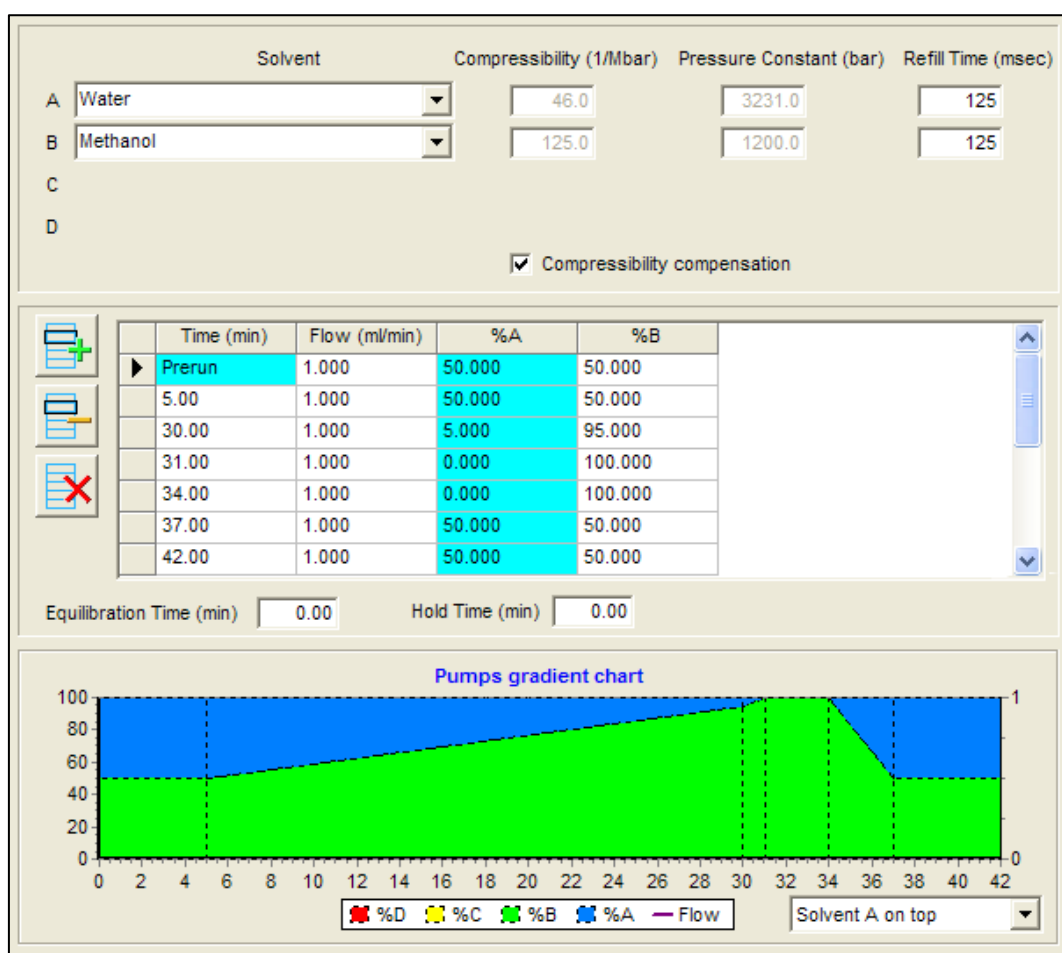


Figure 35: Solvent settings for analytical HPLC run

The detector contains a diode-array and plots a graph of absorbance by wavelength against time. Lowest absorbance is coloured blue, highest absorbance is coloured red, the scale is self-adjusting. Heptaene and tetraene varieties are easily visually identified.

Semi-preparative HPLC runs typically use the same solvent gradient as analytical but with the flow rate increased to 15 ml/min due to the larger column. A small aliquot (100 μ l) of the sample to be purified is run first to test retention time on the column, then the collector programmed to collect a few minutes either side of the desired signal, in fractions of 20 seconds. The sample is purified in injections containing 4-5 mg heptaene per run. A sample might typically be collected in 4 or 5 tubes.

Results and discussion

Chapter 2 discusses work done on a decarboxylated biosynthetic derivative of amphotericin B. Previous student Odobunmi Ibrahim managed, via Fmoc-protecting the amine group, to isolate and characterise a very small (~5 mg) quantity of this derivative. Described below is the work done to improve the yield and efficiency of the isolation of this product, and once improved yields had been obtained, to make simple chemical modifications to the molecule to either improve the antifungal activity, decrease the toxicity, or both. A small decrease in haemolytic activity was achieved.

2. Biosynthesis of decarboxylated derivative.

Amph N oxidises the methyl group at carbon-16 to a carboxylic acid. Disruption of the *amphN* along with the neighbouring *amphM* gene (which encodes for a ferredoxin that acts as an acceptor to mediate electron transfer) prevents oxidation of C16 on the macrolactone. Glycosylation at C19 and hydroxylation at C8 results in the formation of an amphotericin molecule which retains the methyl group on C16. This carboxylic acid had been thought to be essential for antifungal activity, however, in testing this molecule retained comparable antifungal activity (MIC: 1 µg/ml to AmB's 1.25 µg/ml) with reduced haemolytic activity (MHC: 50 µg/ml to AmB's 5 µg/ml).⁶⁰

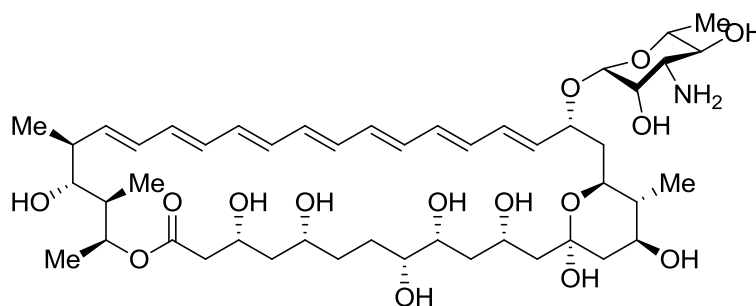
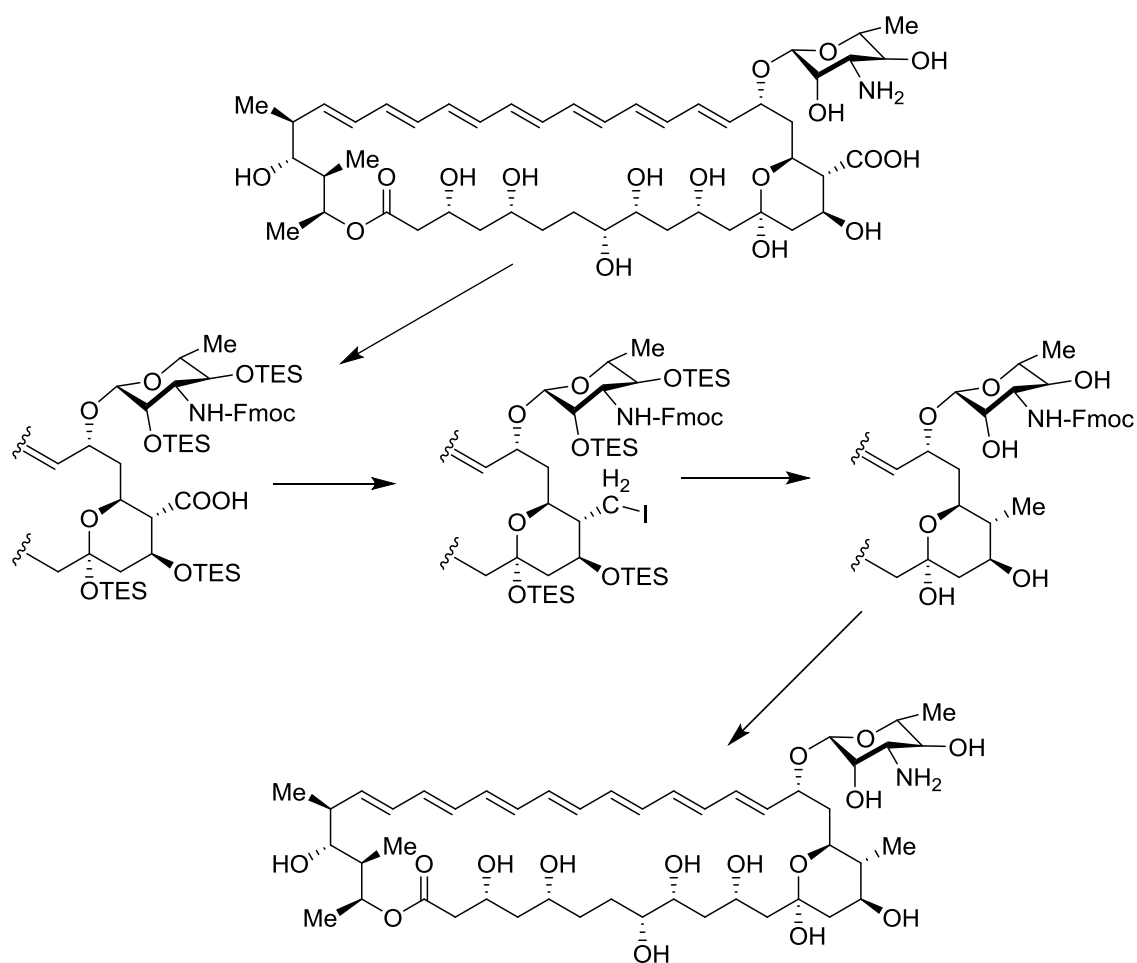


Figure 33: 16-decarboxyl-16-methyl-amphotericin B (AmNM)

This molecule has also subsequently been synthesised from AmB by Burke⁷⁴ who confirmed its therapeutic potential. Burke's group began by protecting the amine group with Fmoc-OSu and the hydroxyls with Triethylsilyl (TES) groups. The carboxylic acid was then reduced to a primary alcohol via a 2-pyridinethiol ester as an intermediate, iodination of this alcohol with PPh_3/I_2 gave an iodomethyl derivative. Reductive cleavage of the iodide with NaBH_4 in DMPU and removal of the protecting groups yielded 16-descarboxyl-16-methyl-AmB. Antifungal activity against *Saccharomyces cerevisiae* was tested qualitatively using a disc-diffusion assay⁷⁵, in which they found it to be roughly equipotent to AmB, this was confirmed quantitatively using a broth dilution assay⁷⁶ (MIC: AmB 2 μM , AmNM 1 μM).



Scheme 5: Synthesis of AmNM from AmB by Burke

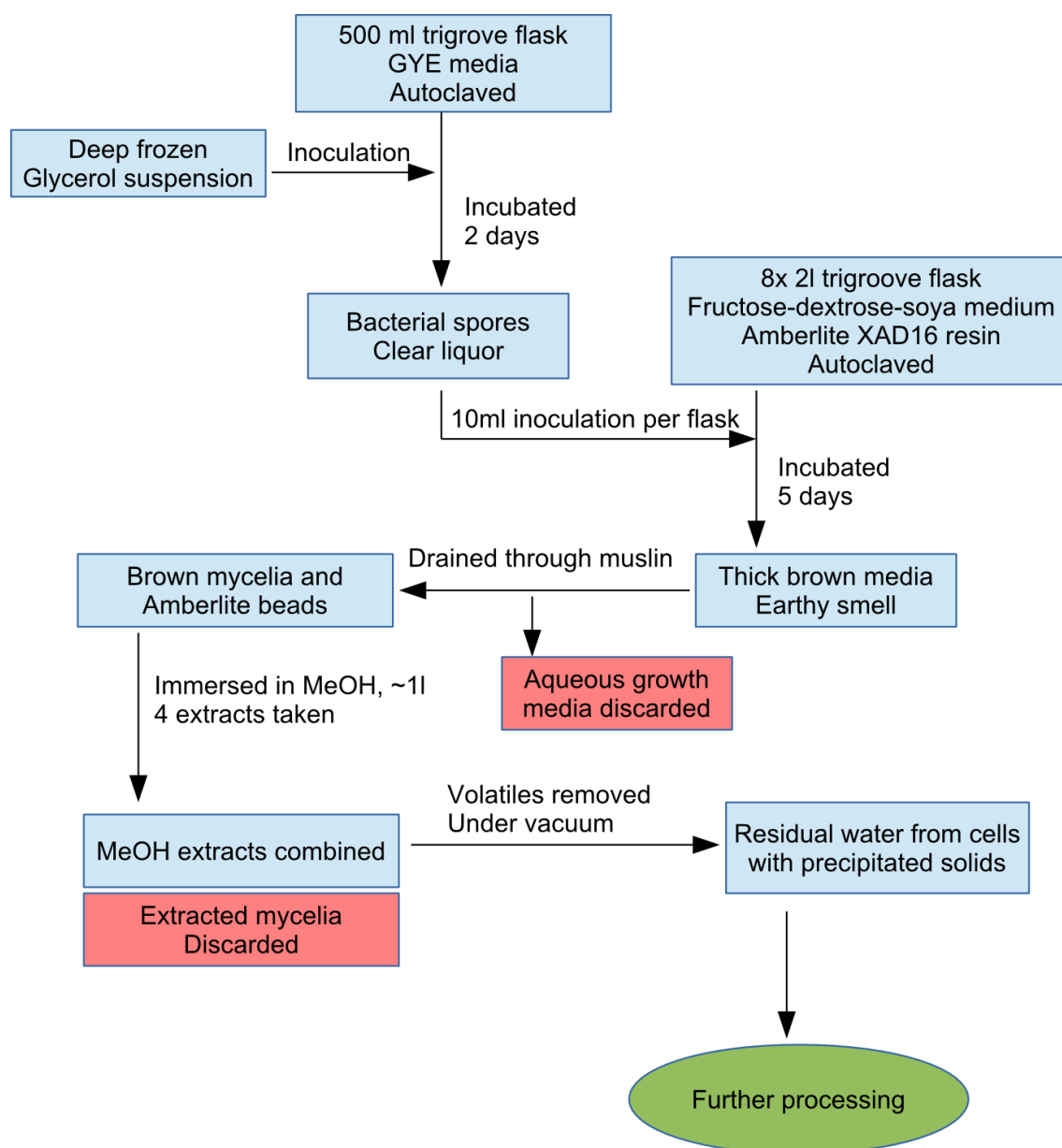
2.1 Attempted purification of AmNM (33) by existing method.

The first attempt here to isolate AmNM followed the method of a previous student, Bunmi Ibrahim (PhD student 2009-2013),¹⁹ to protect the NH₂ of the mycosyl sugar on AmNM with Fmoc-OSu and purify by column chromatography. Improvement to this method was desirable as yields of less than 5% were typical.

An eight-flask growth (Growth A) of AmNM was prepared to the standard recipe detailed in chapter 6, but with 12.5 g XAD16 resin (see section 2.5) as originally used by Ibrahim. The growth flasks were drained through muslin and the mycelia were extracted with methanol four times, the four extracts combined and the volatile methanol removed under vacuum leaving residual water resulting from the lysed cells; the aqueous sample was stored in the fridge until needed. This process is summarised in scheme 6.

The sample was centrifuged at 12,000 rpm for ten minutes. The supernatant was removed and retained, the precipitate resuspended in deionised water by sonication, and the sample centrifuged again at 12,000 rpm for ten minutes. The supernatant was again removed and retained.

Both aqueous supernatants were tested by UV/Vis spectroscopy, but showed very low (<1 mg) heptaene levels, so were discarded. The precipitate was resuspended in methanol, centrifuged, the supernatant retained, the precipitate resuspended in MeOH, centrifuged, the supernatant retained and the precipitate set aside. The MeOH supernatants were combined and evaporated to dryness to give a total crude product weight of 3.76 g. This crude product was tested by UV/Vis in methanol and found to contain 128 mg heptaene and 109 mg tetraene. The process is summarised in scheme 7.

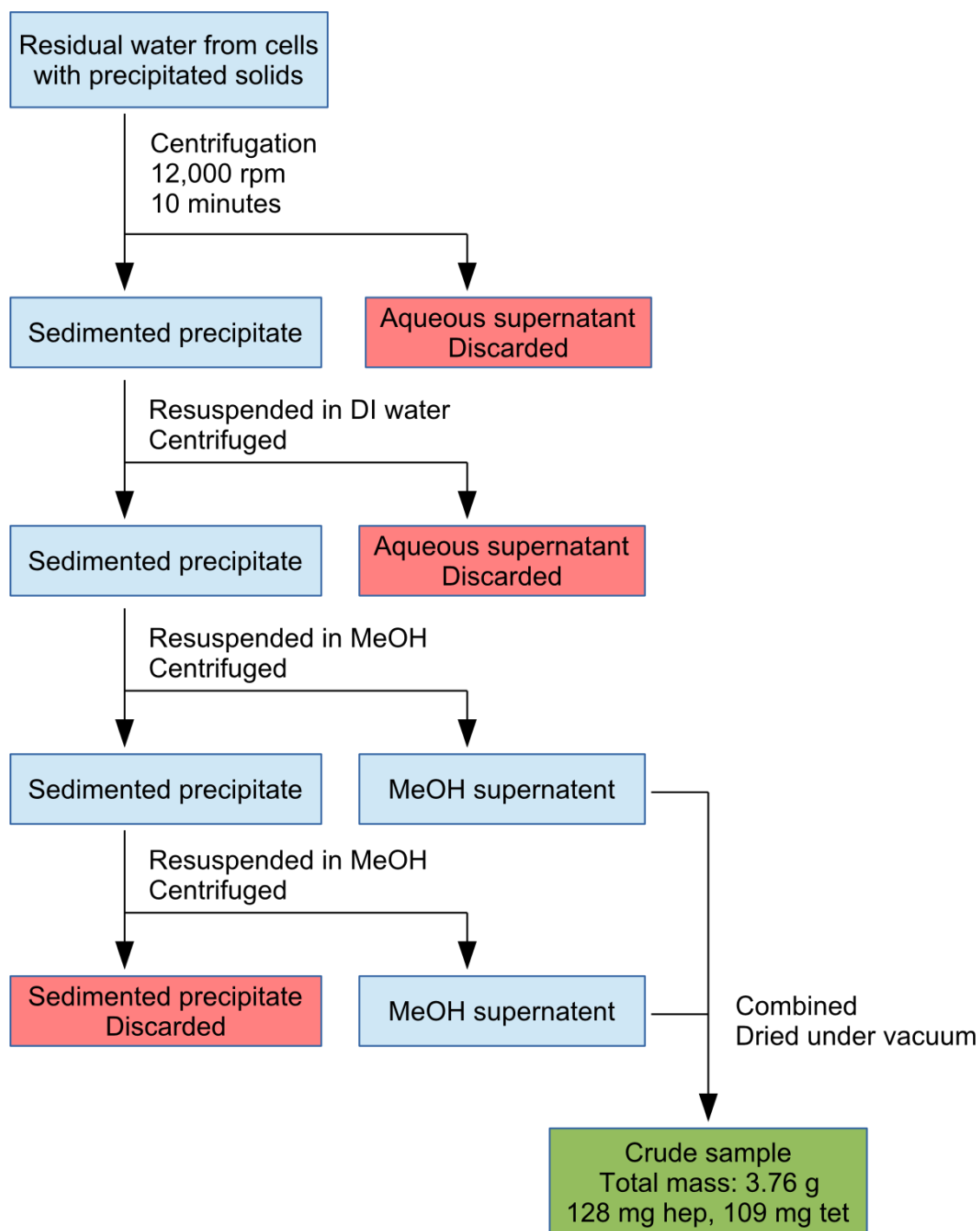


Scheme 6: Processing scheme for AmNM growth A

The dried crude sample was washed twice with ethyl acetate, the orange supernatants were tested by UV/Vis and found to contain the following.

EtOAc wash 1	7.1 mg Heptaene	24.1 mg Tetraene
EtOAc wash 2	0.3 mg Heptaene	0.8 mg Tetraene

Table 1: EtOAc washes of AmNM growth A



Scheme 7: Further processing for AmNM growth A

The precipitate remaining was 1.49g, showing that the ethyl acetate washes had removed 2.27 g of unwanted material.

Given that tetraene is more soluble than heptaene, it was thought possible that some tetraene could be removed by preferential dissolution. 2 ml MeOH was added to the sample, which was then sonicated and centrifuged. The supernatant and precipitate were separated and tested, results shown in table 2.

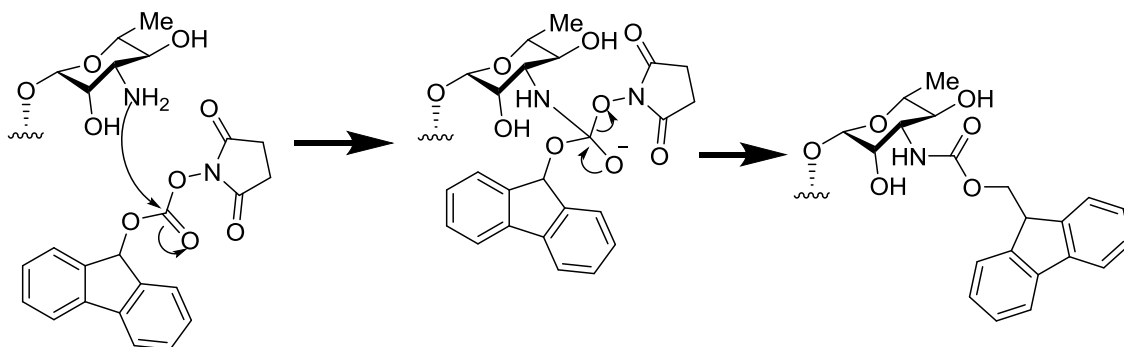
Supernatant	66.8 mg Heptaene	51.4 mg Tetraene
Precipitate	55.5 mg Heptaene	34.5 mg Tetraene

Table 2: Preferential dissolution of AmNM growth A

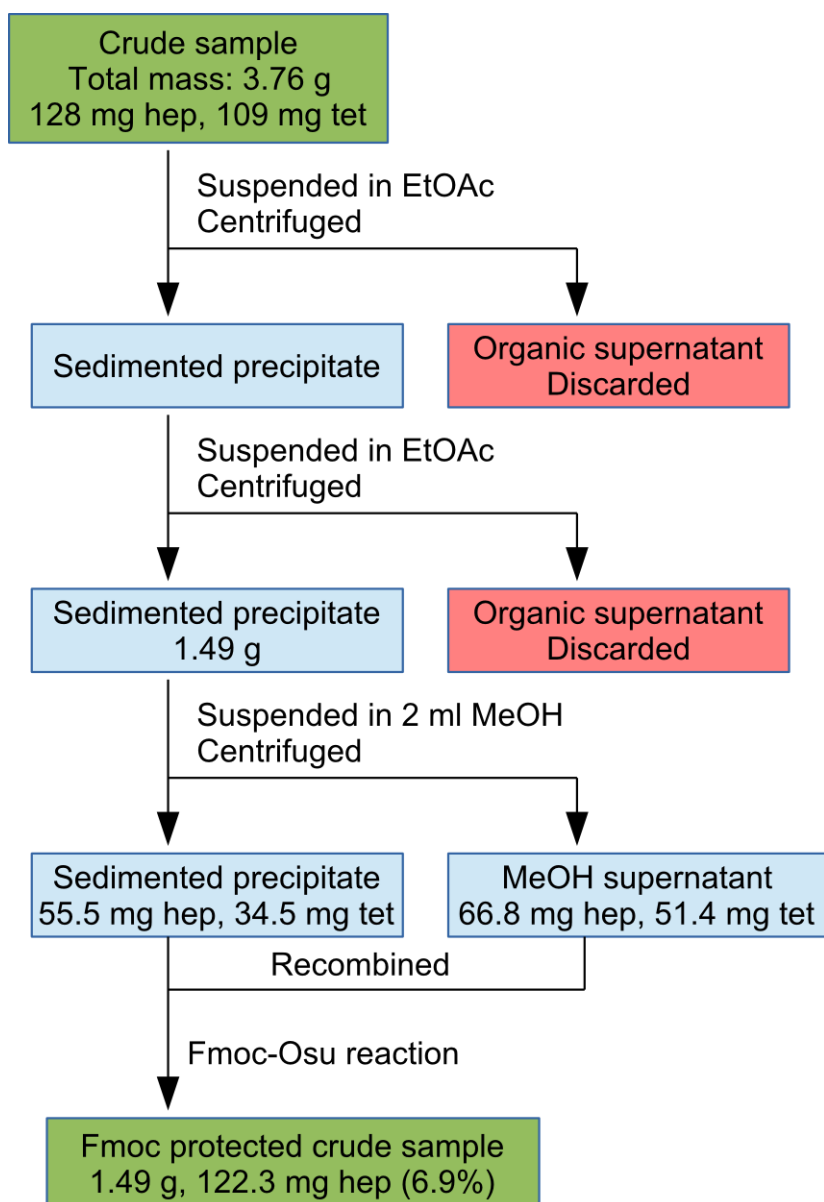
This was deemed to be a failure and they were recombined.

The amphotericin was reacted in the crude mixture with *N*-(9-fluorenylmethoxycarbonyloxy)succinimide (Fmoc-OSu), to protect the NH₂ group of the mycosyl sugar (see scheme 8), thus reducing the polarity and enabling some purification by flash column chromatography. This process is summarised in scheme 9.

The Fmoc-protected sample was loaded onto a 3 cm flash column containing silica gel 60. The column was eluted first with 250 ml ethyl acetate then with increasing percentages of methanol (also 250 ml). The fractions were collected, dried, and analysed by UV (table 3).



Scheme 8: Fmoc protection of mycosyl sugar



Scheme 9: Further processing of crude sample from scheme 7.

Fraction	Total weight	UV polyene weight
Ethyl acetate	370 mg	Hep: 47.5 mg (12%) Tet: 23.7 mg
5% methanol	260 mg	Hep: 4.8 mg (1.9%) Tet: 2.0 mg
10 % methanol	320 mg	Hep: 5.9 mg (1.9%) Tet: 6.3 mg
100 % methanol	320 mg	Hep: 21.0 mg (6.5%) Tet: 15.2 mg
	Total: 1.22g	Total hep: 79.2 mg Total tet: 47.2 mg

Table 3: First silica column of AmNM growth A

Given that the starting percentage of Heptaene before the Fmoc reaction in the sample was 6.9% by weight (122.3 mg in 1.49 g total), this method did not give a satisfactory increase in purity and resulted in the loss of over 35% of the heptaene (122.3 mg → 79.2 mg). It is possible that the lost heptaene was that which had not reacted with the Fmoc-OSu. Fmoc-OSu would react preferentially with the NH₂ group on the mycosyl sugar, but given long enough will also react with OH groups. The mixture in which the reaction was performed was very impure, containing many lipids and sugars also extracted from the mycelia. In the time necessary for the mycosyl amine to react, there is much opportunity for Fmoc to react with other cell products present, so even 2.5 equivalents may not have been enough.

All the fractions were recombined to give a sample of total weight 1.27 g and a heptaene content (by UV) of 83 mg. (6.53%).

This sample was loaded onto another silica gel column and eluted with the following: 500 ml 50% EtOAc:hexane, 500 ml 66% EtOAc:hexane, 250 ml 80% EtOAc:hexane, 250 ml EtOAc, 500 ml methanol. The fractions were collected in 100 ml aliquots and tested by UV. When >1 mg heptaene appeared in a fraction, the solvent was switched to 100% methanol. The fractions were monitored by UV/Vis and combined into those before and after the appearance of heptaene groups, dried and analysed by UV/Vis.

Fractions	Total weight	UV Polyene weight
pre-heptaene	280 mg	Hep: 4.72 mg (1.7%) Tet: 0.21 mg
post-heptaene	480 mg	Hep: 79 mg (16.5%) Tet: 13.4 mg

Table 4: Second column of AmNM growth A

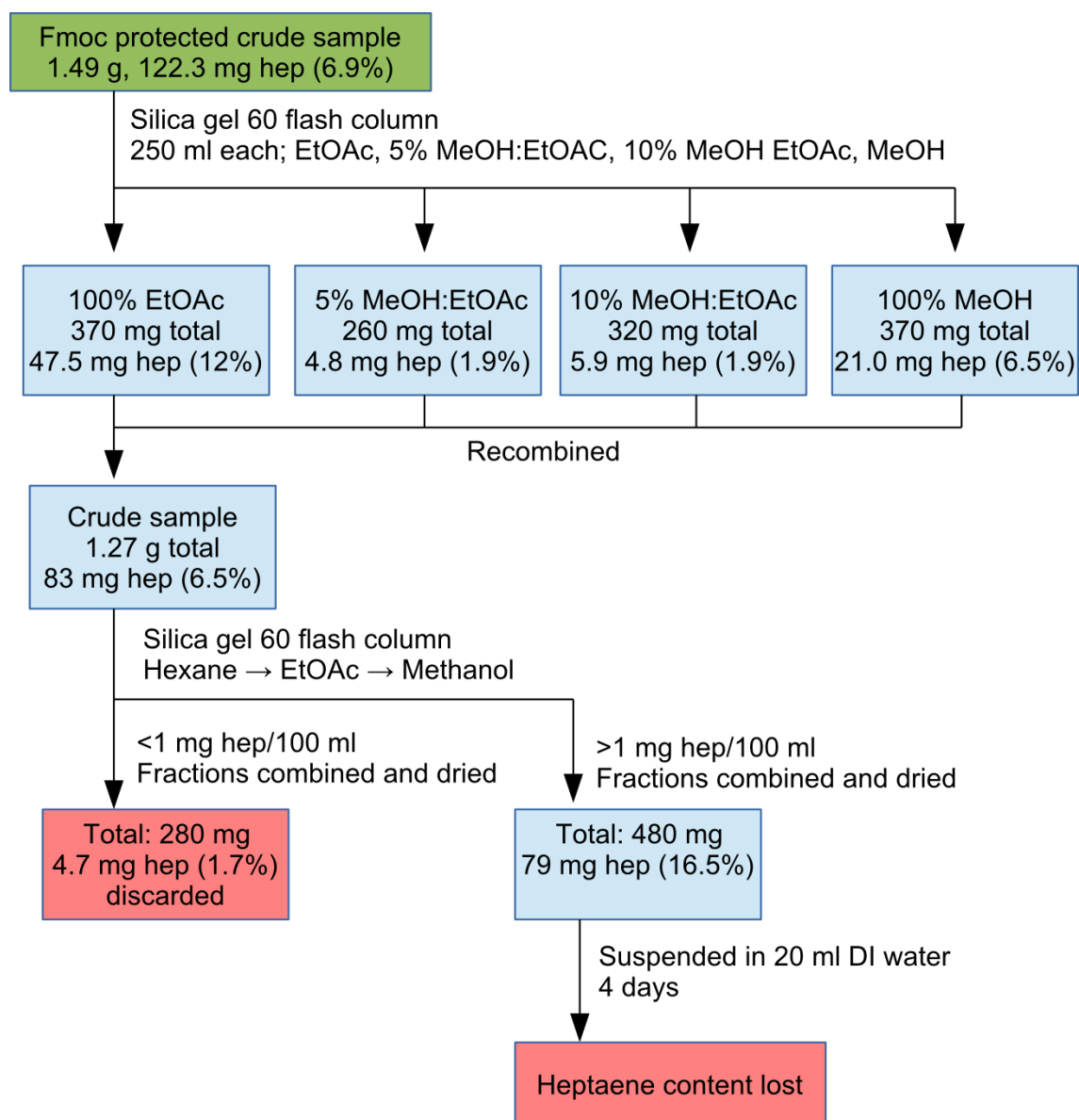
This was a much better increase in purity (6.53% → 16.5%) than before, over a third of the total mass has been removed with minimal loss of heptaenes.

The dried post-heptaene sample was then washed with water (20 ml) in an attempt to remove some of the sugars before further purification. The sample was suspended in water, and left in the fridge (4°C) over a long weekend (4 days). The sample was centrifuged and the supernatant removed. The precipitate was dissolved in methanol and both parts were tested by UV.

Supernatant	Hep: 4.1 mg Tet: 5.7 mg
Precipitate	Hep: 0.81 mg Tet: 0.57 mg

Table 5: AmNM growth A after 4 days standing

No explanation for this loss could be proven. It is possible that a sample tube may have been contaminated with a chemical that caused the breakdown of amphotericin, or that the deionised water may have been contaminated. A summary of this further processing is shown in scheme 10.



Scheme 10: Final processing of AmNM growth A

2.2 Second growth and improvements to method

A second growth (growth B) of sixteen flasks was prepared. This growth was drained then divided into two halves for ease of handling, these shall be referred to as B1 and B2. Both samples were extracted 4 times with methanol and separated from residual water after refrigeration as described previously in section 2.1.

Sample B1 (starting weight 3.64 g) was washed three times with ethyl acetate, removing 1.08 g of waste material. The remaining heptaene was measured by UV/Vis assay as 113 mg, and the Fmoc protection performed accordingly. The sample was dry loaded onto a 3 cm column and eluted with hexane → ethyl acetate until no more yellow colour was eluted, this eluent was retained. The column was then eluted with 250 ml 5% MeOH:EtOAc and 500 ml 10% MeOH:EtOAc. These methanol-containing fractions all contained heptaene (by UV/Vis) so were combined and dried, the combined sample was found to contain 79.4 mg Heptaene in 1.43 g total weight (5.6% w/w).

The hexane → EtOAc fractions were combined, dried, tested, and found to contain 30 mg Heptaene in 1.5 g total weight. These were used to test the effectiveness of diethyl ether as an eluent to remove unwanted material from the sample. The sample was loaded onto another column and eluted as follows. 250 ml Hexane, 250 ml 50% Et₂O:Hexane, 500 ml Et₂O, 500 ml 10% EtOAc:Et₂O, 250 ml EtOAc. The fractions were collected in 100 ml lots and tested for the appearance of Heptaene. The fractions were collated into those prior to a measurable heptaene UV/Vis signal, and those after.

Fractions	Total weight	UV Heptaene weight
Before heptaene appearance	1.2 g	1.7 mg (0.14%)
After heptaene appearance	210 mg	18.61 mg (8.86%)

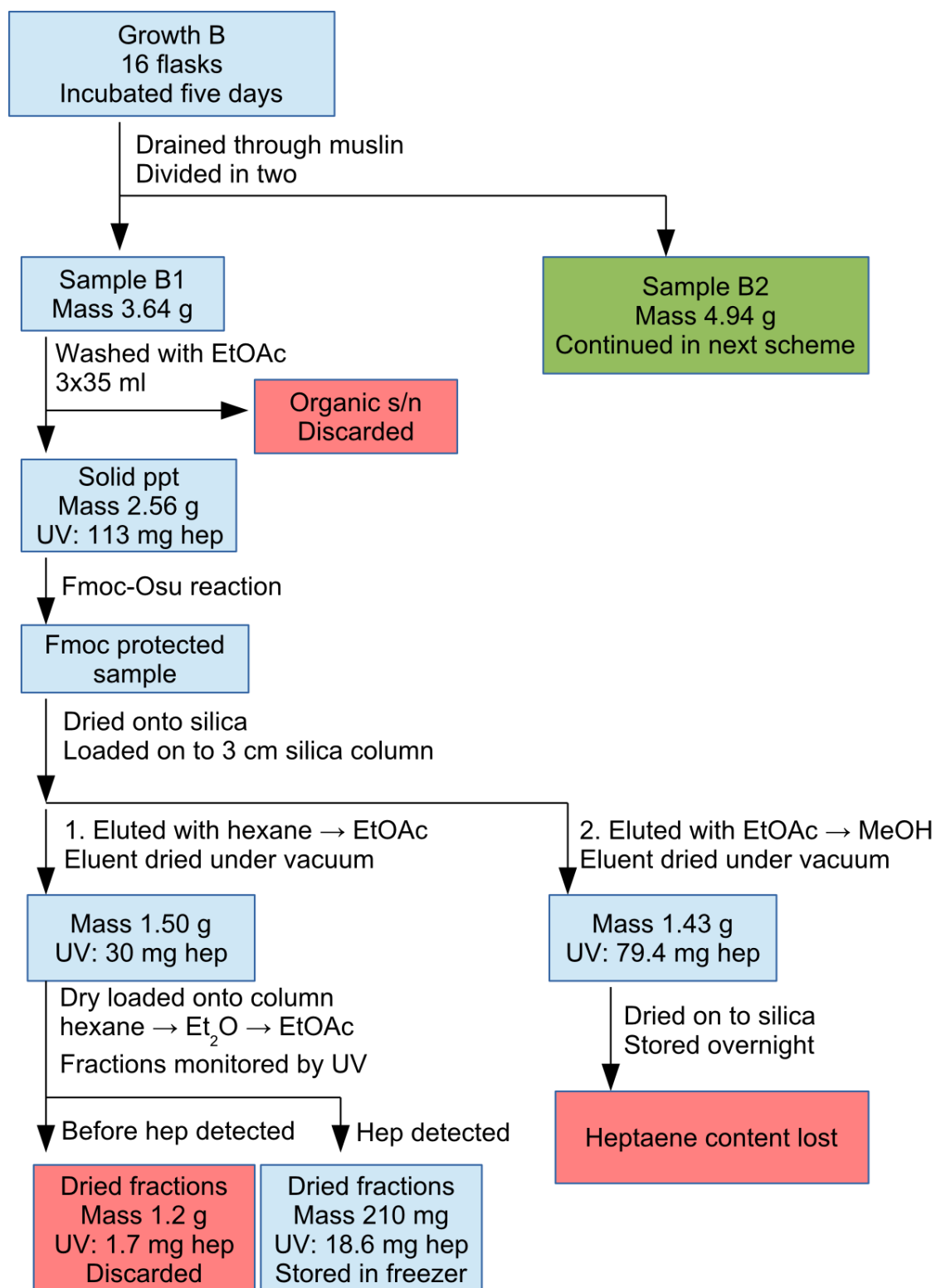
Table 6: First silica column of AmNM sample B1

This showed that diethyl ether is effective at removing unwanted material (lipids etc) without eluting heptaene.

The MeOH fractions from above were prepared for another column by drying the sample onto silica for dry loading. However, the column could not be run that day so the sample was stored in the fridge overnight. When the column was run next day,

starting with EtOAc, progressing up to 10% MeOH, UV analysis showed 1.4 mg heptaene in the EtOAc fractions and 2.3 mg in the MeOH fractions. A summary is shown in scheme 11. It is thought that the acidic silica may have caused the breakdown of amphotericin overnight. For this reason, it was decided to investigate whether sample B2 could be purified without the use of Fmoc or flash chromatography.

Sample B2 (starting weight 4.94 g) was washed (suspended then centrifuged) 7 times with water (30 ml), twice with Et₂O (30 ml) and once with EtOAc (30 ml). Water was used to remove sugars without dissolving the desired heptaene. The Et₂O and EtOAc together removed 0.807 g of material, the quantity of material removed by water was not recorded, though a UV/Vis assay was performed to check that no heptaene had been lost. The sample was then suspended in DCM and filtered, the filter paper collected an orange solid, which was rinsed into a clean flask with MeOH. The DCM filtrate was dried under vacuum to show it had removed 270 mg of material, a UV assay showed no heptaene. The dried orange precipitate (310 mg) was assayed to show 122 mg heptaene (39.4%). The heptaene from this sample was isolated by semi-prep HPLC (C8 column, see figure **36**) to yield 43.5 mg AmNM as a fluffy yellow powder (>95% purity by UV/Vis assay). This is summarised in scheme 12.



Scheme 11: Processing of AmNM growth B1

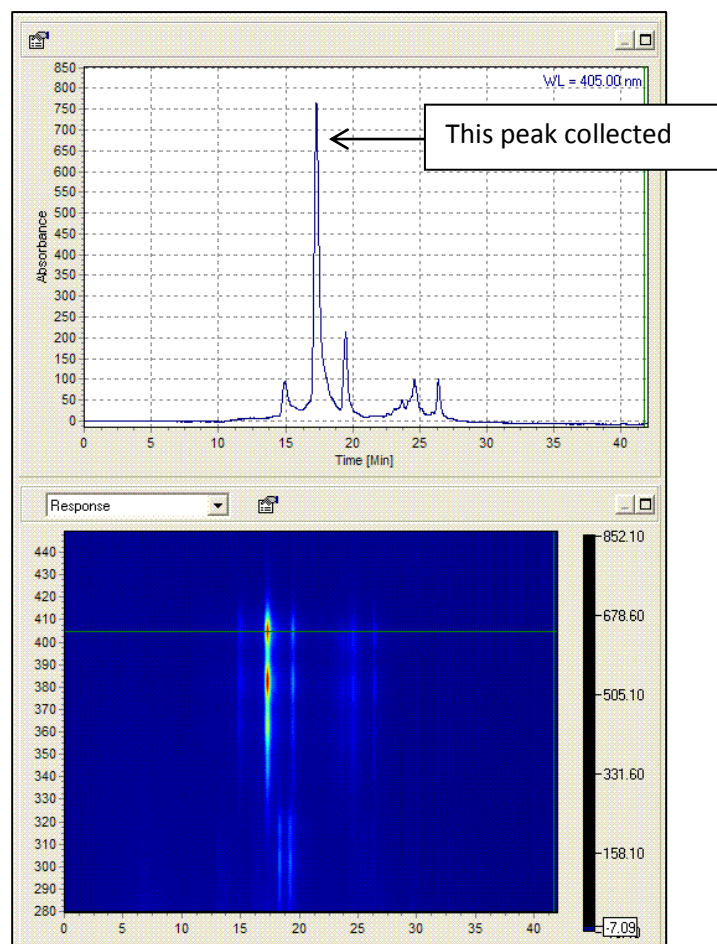
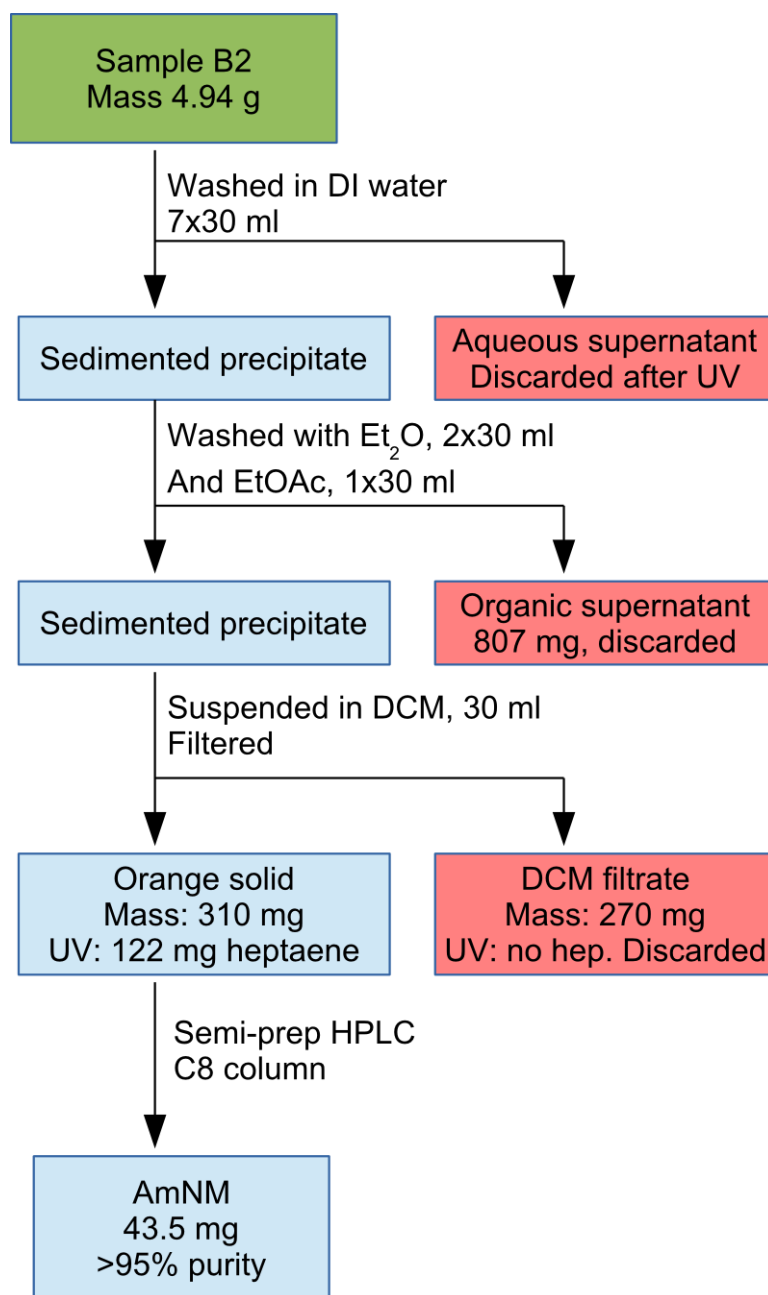


Figure 36: Semi-prep purification of sample B2 on C8 column.



Scheme 12: Processing of AmNM growth B2

2.3 Investigating necessity of XAD16 resin and variations on B2 method.

The Amberlite XAD16 beads are expensive, £116/kg in Jan 2013. They are added to the growth media because they were shown by Bunmi¹⁹ to improve the yield from a growth. However, the quantity used may not be necessary. If similar results could be achieved with a lower quantity of beads, this would be a significant cost reduction. To

investigate this, two sets of eight growth flasks were produced. Growth D contained 12.5 g XAD16 per flask while growth E contained 7.5 g XAD16 (growth C was not used due to contamination). All other ingredients were kept as standard. All sixteen flasks were inoculated from the same starter flask, and incubated for 5 days. They were drained and extracted, extracts being taken at the same time, the results are tabulated below.

Part of extract	Mass Heptaene (mg) by UV assay	
	Growth D (12.5 g XAD16)	Growth E (7.5 g XAD16)
MeOH flask rinse	25	11
Mycelia Extract 1	6	13
Mycelia Extract 2	14	25
Mycelia Extract 3	23	30
Mycelia Extract 4	25	15
Media ppt extract	7.5	4.8
<i>Total</i>	<i>100.5</i>	<i>98.8</i>

Table 7: MeOH extractions of AmNM growths D and E

A fifth mycelia extract was taken for each, but found to contain <2 mg Heptaene.

The drained growth media was also centrifuged, the precipitate suspended in MeOH, then filtered, dried and assayed. This was to determine if lessening the XAD16 resulted in more amphotericin remaining in the media, it did not.

Since roughly the same quantity of amphotericin was obtained from each growth, it appears that a lower quantity of amberlite per flask is still sufficient. A 40% reduction in resin represents a significant cost saving.

Growths D and E were each divided in two to produce four test samples. Each of these samples was washed with the solvents used to clean B2 (section 2.2), but with variations in the ordering and method to investigate which order is most efficient.

Growth D part 1 (sample D1, starting weight 6.46 g, 48 mg heptaene) was suspended in water (80 ml) and shaken with Et₂O (100 ml) then the mixture centrifuged. An orange solid formed at the boundary between the solvents, this solid was collected on a filter paper, then washed into a clean flask with methanol. The Et₂O and H₂O fraction were separated and retained. Each division was tested by HPLC (Et₂O sample was first dried then dissolved in MeOH).

Fraction	Dried weight	Observations
Et ₂ O	1.48 g	HPLC showed trace of tetraene, no heptaene
H ₂ O	Not measured	HPLC showed clear tetraene signal, trace heptaene UV/Vis showed 8 mg heptaene.
MeOH solution of boundary solid	90 mg	HPLC showed clear heptaene signal UV/Vis showed 35 mg heptaene

Table 8: Et₂O/H₂O wash of AmNM sample D1

The MeOH solution of the boundary solid contained 39% heptaene by weight, this was purified by semi-prep HPLC to yield 24.9 mg AmNM (>95% pure by UV/Vis)

To sample D2 (starting weight 6.33 g, approx. 52 mg Heptaene) was added 100 ml DCM and the mixture sonicated for 20 minutes, during this time much of the solid failed to dissolve. The liquid portion was poured through a filter, the small amount of solid on the paper was washed back into the flask with the undissolved solid using MeOH. The DCM filtrate was dried under vacuum (0.54 g) and tested by UV/Vis, which showed 2 mg heptaene, this was discarded. The undissolved sample was then washed twice with water (2x30 ml). The washes were examined by HPLC and showed very little heptaene so were discarded. The remaining sample was then washed with Et₂O (2x30 ml), UV/Vis of the washes showed no heptaene so they were also discarded. The sediment (660 mg) was then washed with EtOAc (2x10 ml) leaving 305 mg remaining. This was purified by semi-prep HPLC to yield 18 mg AmNM (>95%)

Sample E1 (starting weight 1.01g, 50 mg heptaene) was washed with water (3x30 ml), UV/Vis showed no heptaene in the first two water washes and a trace in the third. The remaining sample was then washed with Et₂O (2x30 ml) removing 620 mg but no heptaene, EtOAc (15 ml) removing 180 mg and only a trace of heptaene, and then suspended in 30 ml DCM, filtered by gravity, removing 110 mg, the filter paper was rinsed with MeOH to give 59 mg of crude sample. This was purified by semi-prep HPLC to give 25 mg pure AmNM.

Sample E2 (starting weight 1.21 g, 42 mg Heptaene) was washed with Et₂O (2x30 ml), then with water (30 ml), then with EtOAc (30 ml), and then with DCM (30 ml). This left 77 mg crude sample containing 36 mg heptaene. This was purified by semi-prep HPLC to give 28.6 mg pure AmNM.

These results are summarised in the following table:

Sample	D1	D2	E1	E2
Starting weight	6.42 g	6.33 g	1.01 g	1.21 g
Heptaene	45 mg	52 mg	50 mg	42 mg
Washes in order	H ₂ O/Et ₂ O	DCM (100 ml) H ₂ O (2x30 ml) Et ₂ O (2x30 ml) EtOAc (2x10 ml)	H ₂ O (3x30 ml) Et ₂ O (2x30 ml) EtOAc (15 ml) DCM (30 ml)	Et ₂ O (2x30 ml) H ₂ O (30 ml) EtOAc (30 ml) DCM (30 ml)
Pre HPLC mass	90 mg	305 mg	59 mg	77 mg
Hep (%)	35 mg (39%)	38 mg (12%)	30 mg (51%)	36 mg (47%)
HPLC yield	24.9 mg	18 mg	25 mg	28.6 mg
% hep recovery	55%	34%	50%	68%

Table 9: Summary of AmNM growths D and E

For future growths the method in E2 was used, as it gave the highest yield. It also had the advantage that by removing lipids and other low density (<1 g/ml) impurities using ether first, the precipitate from the water wash required less time (~3 minutes) to sediment than *vice versa* (~15 minutes), speeding up the procedure considerably.

2.4 Contamination of flasks

Growth F was prepared using the standard recipe with 7.5 g XAD16, however after a couple of day's growth it became clear that all eight flasks were contaminated. A good growth should be thick and dark yellow, with an earthy smell due to the geosmin produced, and spores can be seen to cling to the sides of the flask. If a growth turns milky, with a vinegar-like smell, this is a clear indication of contamination. The beads were also observed to turn bright orange rather than the dark brown expected. Such a growth produces no amphotericin and also runs straight through the muslin cloth so is usually discarded immediately. The flasks are also soaked in bleach before reuse to kill any contaminants left on the glass after normal washing.

If one or two flasks in a set become contaminated this indicates the foreign organism was probably either on the flask or incorporated during inoculation, if all flasks in a set become contaminated this probably indicates a contaminated starter flask. The sporulated bacteria in the starter flask should settle to the bottom leaving clear media above them, if the media appears cloudy this indicates the presence of an alien bacterium, yeast or fungus.

2.5 Further reduction in quantity used of XAD16

Two further growths of eight flasks were prepared, growth G contained 7.5 g XAD16 per flask, growth H contained 5 g XAD16 per flask. All sixteen were inoculated from the same starter flask. The flasks were incubated for five days then processed as describe in the previous section, the eight flasks from each growth being treated together. The results are summarised below.

	Growth G (7.5 g XAD16)	Growth H (5 g XAD16)
# MeOH extracts taken	4	4
Starting total weight	2.96 g	3.54 g
Starting Hep weight	35 mg	74 mg
Washes:	2x30 ml Et ₂ O 30 ml EtOAc 50 ml DCM	3x30 ml Et ₂ O 30 ml EtOAc 60 ml DCM
Hep weight before HPLC	26 mg	60 mg
Pure AmNM recovered	12 mg	18 mg
% recovery	34%	24%

Table 10: Summary of AmNM growths G and H

The Et₂O washes were repeated until the supernatant became colourless, indicating a lack of solute. Amphotericin is very insoluble in Et₂O so this wash may be repeated as often as necessary without losing product.

The starter flask used was a third generation flask, yields from flasks beyond second generation can become inconsistent as was also found by Ibrahim.¹⁹

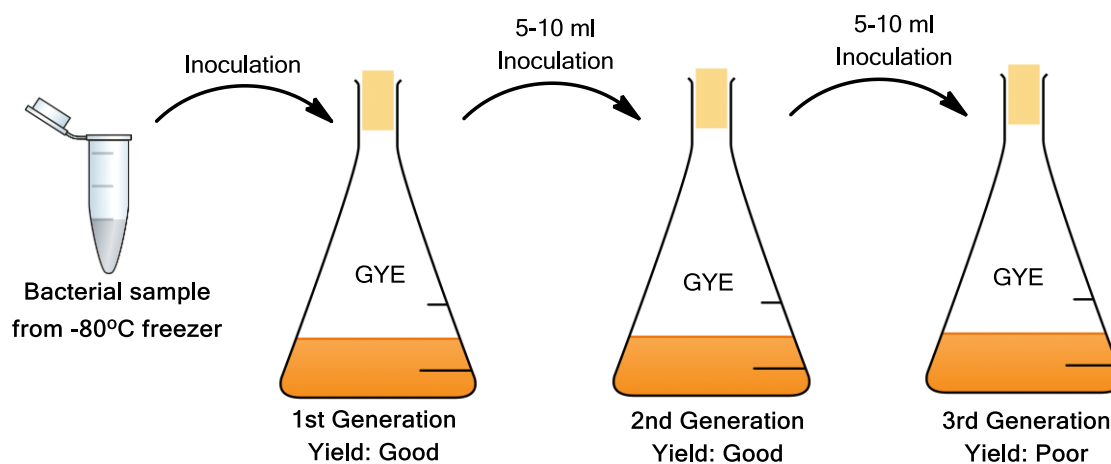


Figure 37: Generations of GYE medium flask

From this it was decided that all future growths would be made from 1st or 2nd generation flasks, from which a yield of ~100 mg AmNM per growth in standard media would be usual. It also appears that 5 g XAD16 is still sufficient, representing a 60% saving from the original quantity of 12.5 g. Both G and H contained significant quantities of aglycone which was removed in prep-HPLC, this accounts for the low yields of AmNM.

Further frozen Eppendorf samples can be made from 1st generation flasks. The flask is allowed to settle, then a 0.5 ml sample containing a high concentration of mycelia is transferred to a sterile Eppendorf tube, 0.5 ml sterile glycerol is added, and the tube vortexed to homogenise the media. This is then frozen at -80°C until needed.

2.6 Investigating use of Cottonseed flour

An alternative media⁷⁷ used to produce amphotericin B contains cottonseed flour. To investigate whether this would improve yields cottonseed flour was purchased from Sigma-Aldrich and two growths of eight flasks prepared. Growth J contained 7.5 g cottonseed flour in place of soybean, Growth K was made to the standard recipe, (letter I was not used to avoid labelling confusion). All sixteen flasks were inoculated from the same starter flask. The flasks were incubated for five days then processed in the usual way.

	Growth J (cottonseed)	Growth K (soybean)
MeOH extract 1	0.17 mg heptaene	16 mg heptaene
MeOH extract 2	5 mg heptaene	40 mg heptaene
MeOH extract 3	9.5 mg heptaene	30 mg heptaene
MeOH extract 4	8.5 mg heptaene	17.5 mg heptaene
Total crude weight (Heptaene)	2.216 g (23.17 mg)	2.79 g (103.5 mg)
Washes	2x30 ml Et ₂ O 10 ml H ₂ O	3x30 ml Et ₂ O 30 ml EtOAc 35 ml H ₂ O 35 ml DCM
Pre prep-HPLC weight	114.3 mg (21 mg hep, 18%)	413.7 mg (86 mg hep, 20%)
AmNM reclaimed	Molecule 1: 8.6 mg Molecule 2: 10 mg	45 mg (43% Yield)

Table 11: Summary of AmNM growths J and K

Analytical HPLC of the MeOH crude extracts of growth J showed two strong peaks (where normally one strong peak would be expected) indicating two heptaene containing molecules (possibly isomers) present. Molecule one at 23 minutes corresponded to the expected AmNM, molecule two at 26 minutes was an unknown less-polar Heptaene. The HPLC result is shown in figure 38 below.

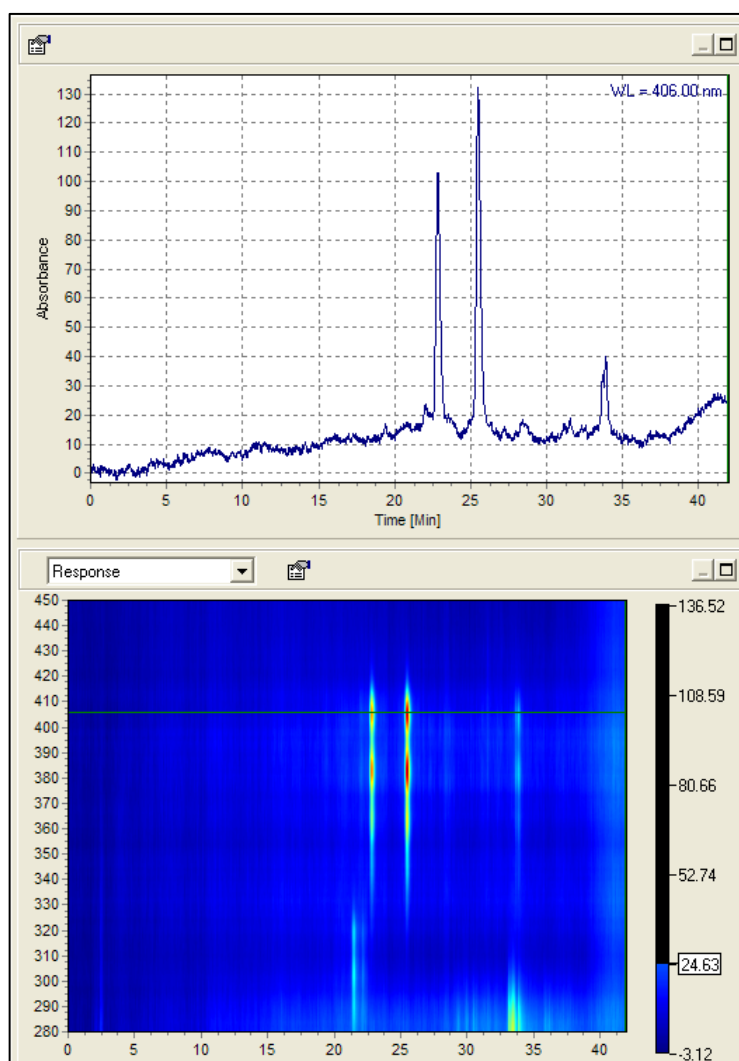


Figure 38: Analytical HPLC of Growth J showing two heptaene-containing molecules.

LCMS of the same sample showed molecule one to have a mass of 893, indicating it was the AmNM expected. Molecule two had a mass of 877, this corresponds to a deoxy form of AmNM, probably at the C8 position, as in figure 39 below.

It is proposed that **39** is the product produced because a missing hydroxyl from the aglycone structure implies an interruption to the PKS synthesis by Amph I or Amph J, which would result in no amphotericins being produced, and a missing hydroxyl from the mycosaminyl sugar synthesised by DII and DIII would likely inhibit recognition and attachment by DI, resulting in only aglycone being produced. Therefore, it appears that only the Amph L has being partially inhibited somehow by the changed media, resulting in coproduction of 8-deoxyAmNM. In retrospect, MS/MS should have been performed to gain more data about the structure of this molecule.

The two products were isolated by semi-prep HPLC. Product one (AmNM, >95%) was added to the AmNM collected from previous growths, Product two (8-deoxyAmNM (>95%)) was retained for later testing.

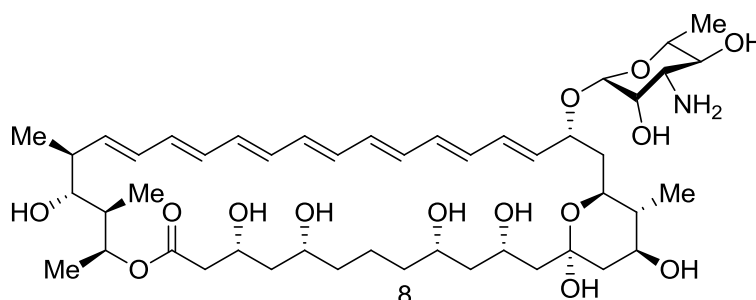


Figure 39: 8-deoxy-AmNM

2.7 Further production of AmNM.

Four more growths of eight flasks were produced to generate more AmNM for further experimentation. All flasks produced to the standard recipe. These growths are summarised in the following table:

	Growth L	Growth M	Growth N	Growth O
MeOH extracts	5	5	5	5
Total start weight	2.689 g	3.923 g	3.178 g	2.553 g
Heptaene weight	110.4 mg	67 mg	81 mg	75 mg
Washes	4x30 ml Et ₂ O 40 ml H ₂ O 40 ml EtOAc	4x35 ml Et ₂ O 25 ml H ₂ O 30 ml EtOAc	3x30 ml Et ₂ O 3x10 ml H ₂ O 35 ml EtOAc	3x35 ml Et ₂ O 30 ml EtOAc 2x10 ml H ₂ O
Pre-HPLC weight (Heptaene)	578.5 mg (84 mg, 15%)	744.2 mg (59 mg, 8%)	663.2 mg (61 mg, 9%)	300.2 mg (65 mg, 21%)
AmNM recovered	50.4 mg	32.2 mg	40 mg	38 mg
Yield	46%	48%	49%	51%

Table 12: Summary of AmNM growths L, M, N & O

Before prep-HPLC, samples M, N and O were dissolved in the minimum quantity of methanol and passed through a small plug of silica in a Pasteur pipette (figure 40). The silica in the pipette retains anything that adsorbs to silica strongly enough that methanol is unable to elute it, thus avoiding transfer of such contaminants to the prep-HPLC column. This small amount of silica did not appear to cause any measurable loss of heptaene, unlike the larger quantity required for chromatography which was ruled out in chapter 2.2 earlier. Once the sample had been filtered, the pipette was flushed with

methanol until the eluent ran colourless. Without this treatment, the semi-prep column would require cleaning by flushing with non-polar solvents (IPA, EtOAc, hexane) after every third or fourth injection, when peak shape is lost (see figure 41), whereas after this treatment the column lasted up to fifteen injections before requiring cleaning.

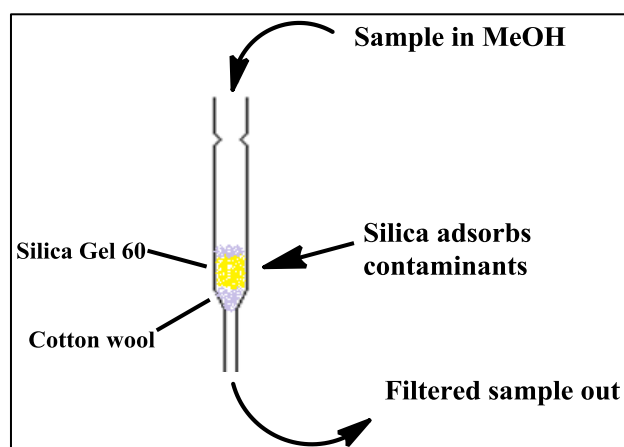


Figure 40: Pre-HPLC silica filtration of sample.

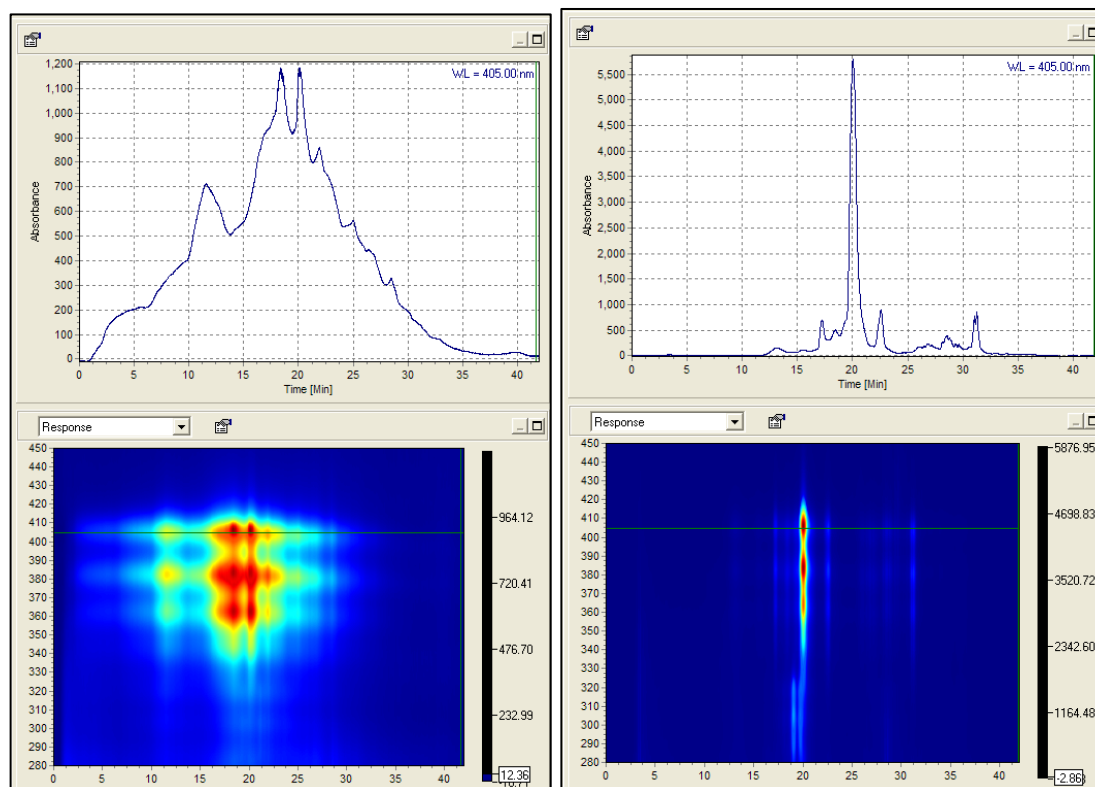


Figure 41: Examples of contaminated (left) and clean (right) prep column elution peaks.

2.8 Functionalisation of the amine group

A paper by Paquet and Carreira⁷⁸ describes how the mycosamine group of amphotericin B can be alkylated, leading to a 15-fold improvement of the antifungal activity. (MIC: **1** 0.3 μ M, **42** 0.02 μ M)

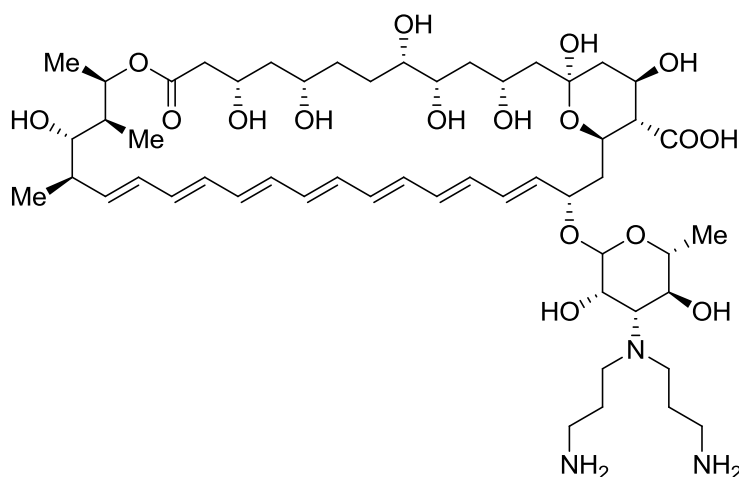


Figure 42: Bisalkylated AmB described by Paquet and Carreira.

Applying this technique to AmNM could result in a molecule with both reduced haemolytic activity and improved antifungal activity.

2.8.1 Oxidation of 3-(Fmoc-amino)-1-propanol

The alkylation of amphotericin requires the use of an aldehyde. The aldehyde used by Carreira was 3-(Fmoc-amino)-1-propanal, **43b**.

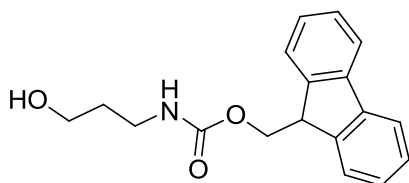


Figure 43a:

3-(Fmoc-amino)-1-propanol

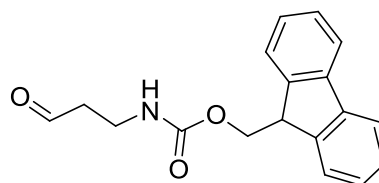


Figure 43b:

3-(Fmoc-amino)-1-propanal

The aldehyde is prepared from the alcohol **43a** (purchased from Sigma Aldrich) by oxidation with 2-iodoxybenzoic acid (IBX, **44**). This acid is highly explosive so is supplied by Sigma-Aldrich in a stabilised form (SIBX) mixed with isophthalic acid (**45**) and benzoic acid (**46**).

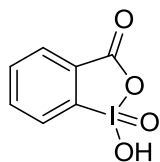


Figure 44:
2-Iodoxybenzoic acid

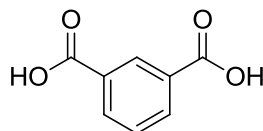


Figure 45:
Isophthalic acid

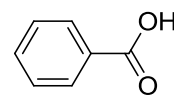
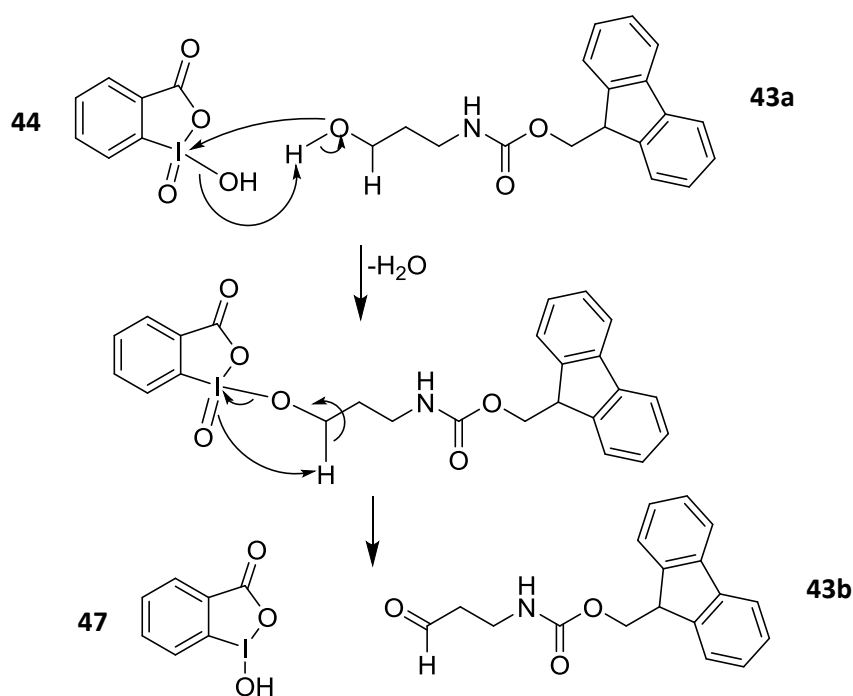


Figure 46:
Benzoic acid

The oxidation reaction is performed in EtOAc at reflux, taking 4 hours, the mechanism is shown in scheme 13. Whilst many different solvents will suffice, EtOAc was chosen because both IBX and the reduced form iodosobenzoic acid (IBA, **47**) are insoluble at room temperature, facilitating their removal by simply cooling and filtering the mixture. Isophthalic and benzoic acid are removed by washing the EtOAc with saturated aqueous NaHCO₃ solution, the EtOAc is then removed under vacuum giving a quantitative yield of **43b**.

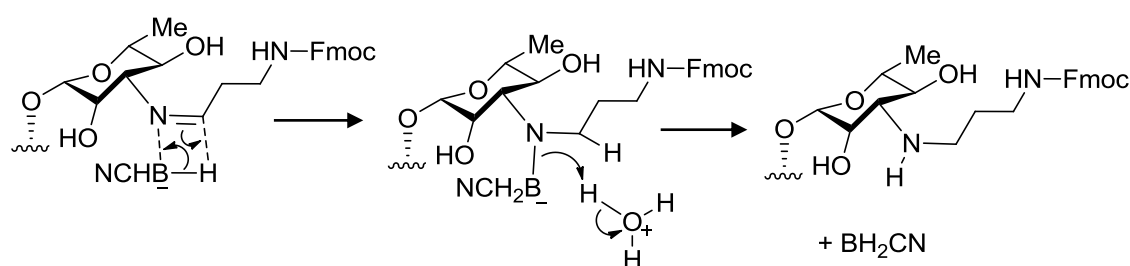


Scheme 13: Oxidation of 3-(Fmoc-amino)-1-propanol

2.8.2 Alkylation of mycosaminyl sugar amine

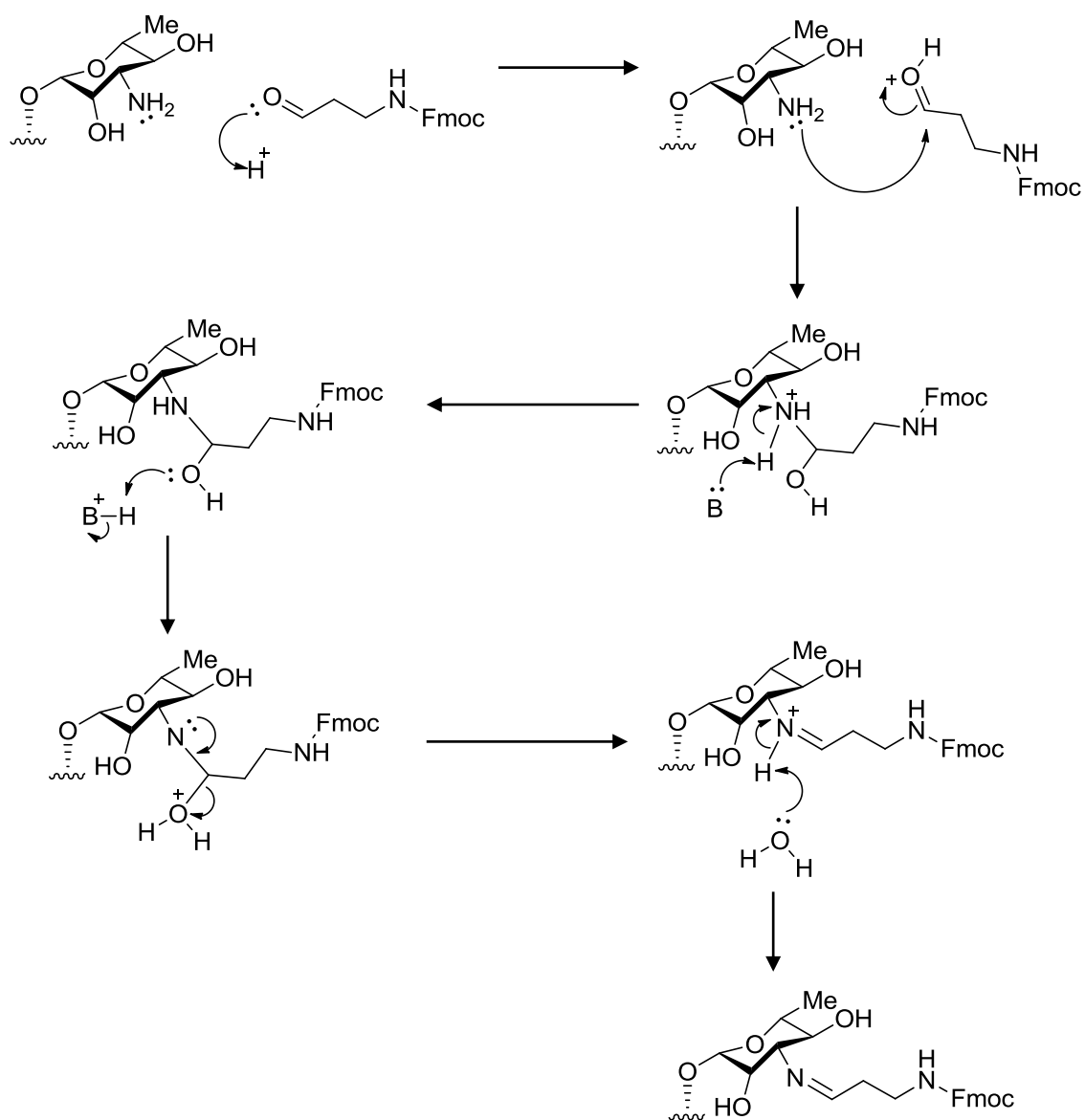
Amines can undergo nucleophilic addition with aldehydes and ketones, yielding carbinolamines which then undergo dehydration to yield substituted imines. The imine is then reduced to an amine allowing a second nucleophilic addition (scheme 14). These processes together are known as a reductive amination.

The mycosyl amine undergoes a nucleophilic addition with the 3-(Fmoc-amino)-1-propanal (**43b**) prepared above. The mechanism is illustrated in scheme 15. The aldehyde is added in excess, so the reaction proceeds twice to give a disubstituted tertiary amine.



Scheme 14: Reduction of imine with NaBH_3CN

The resultant imine is reduced to a secondary amine by sodium cyanoborohydride. The electron-withdrawing cyanide substituent makes NaCNBH_3 a much weaker reducing agent than sodium borohydride allowing this whole reaction to be performed in one mixture, because cyanoborohydride is too weak to reduce the aldehyde back to its original alcohol, as borohydride would.

Scheme 15: Nucleophilic addition of **43b** to mycosyl amine

The substitution was first tested with AmB. Carreira's method was performed in DMSO with the addition of one drop of conc. HCl. This gave an unsatisfactory yield, with around ~20% mono-substituted, ~15% di-substituted, and ~65% unreacted AmB. The analytical HPLC trace is shown in figure 48. A second attempt gave similar results.

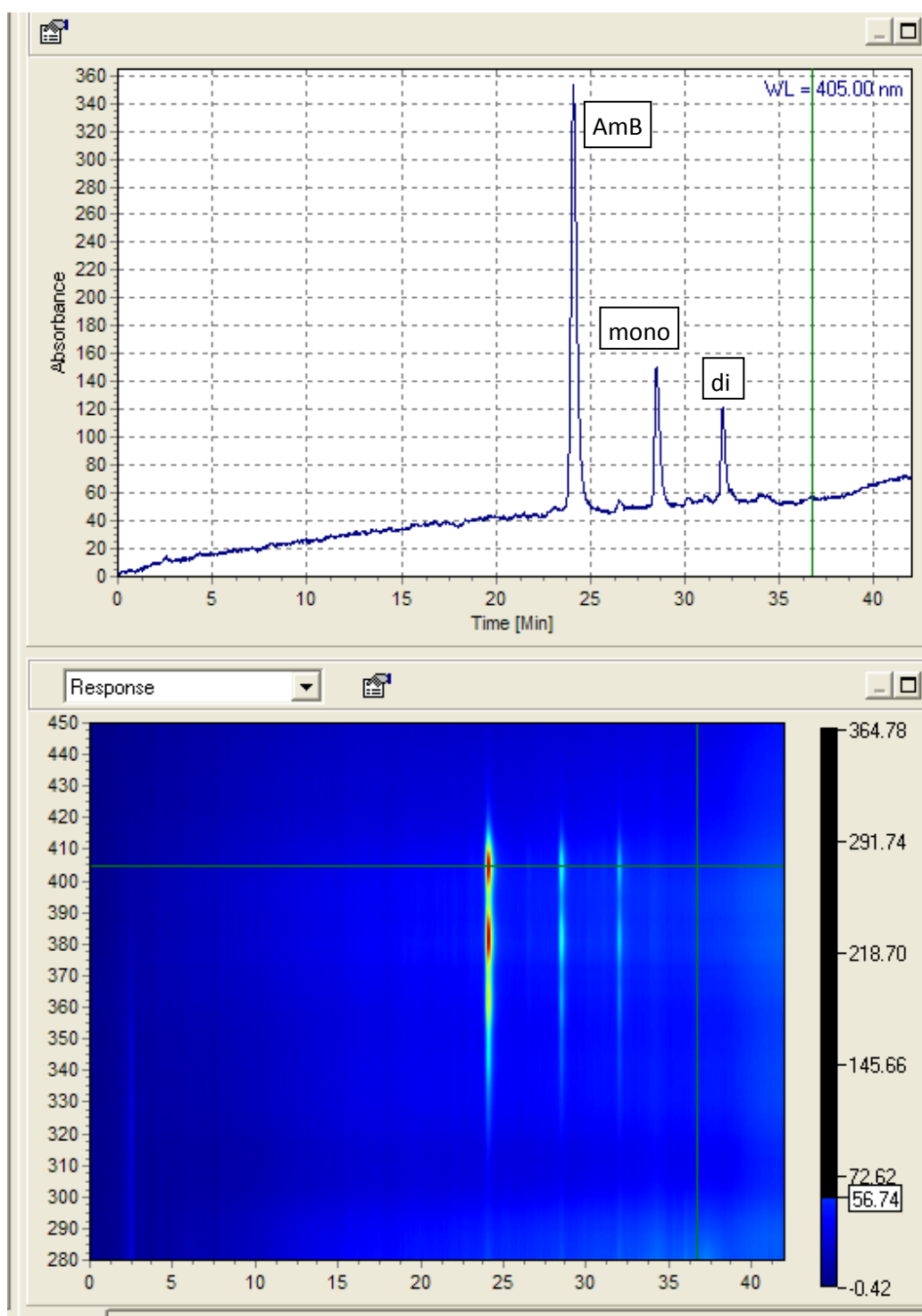


Figure 48: Analytical HPLC trace of AmB alkylation in DMSO

The reaction was tried a third time but in DMF omitting the HCL and was found to give a much better result, with ~40% mono-substituted and ~60% di-substituted. The reaction was repeated with AmNM and similar results obtained. An analytical HPLC trace of the NM substitution is shown in figure 49.

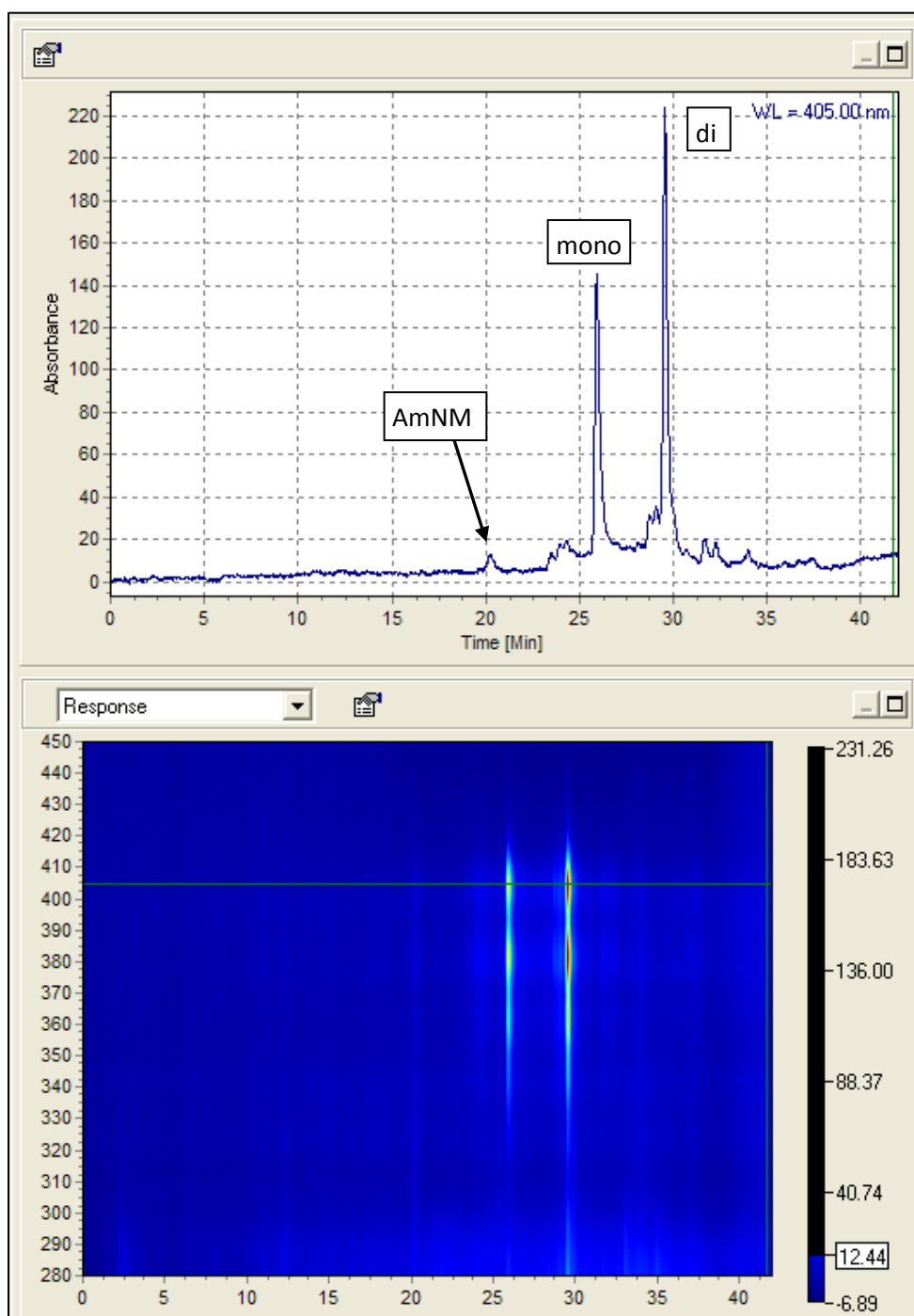


Figure 49: Analytical HPLC of AmNM alkylation in DMF.

DMF facilitates the reaction due to the trace presence of breakdown products formic acid and dimethylamine. The formic acid protonates the aldehyde carbonyl thus activating it and allowing attack by the neutral nucleophile nitrogen, this makes the addition of the concentrated HCl unnecessary, the dimethylamine is a weak base which aids the formation of the carbinolamine intermediate by neutralising the positive charge on the nitrogen.

The two products were isolated from the reaction by semi-prep HPLC. A yield of 31% **50** and 34% **51** was obtained. An NMR was taken to check for the presence and intensity of the Fmoc protecting groups to confirm the reaction had succeeded. Fmoc's characteristic signals were clearly visible at 7.37, 7.42, 7.66 and 7.83 ppm on the spectra, and those for **51** were approximately double the intensity of those for **50**.

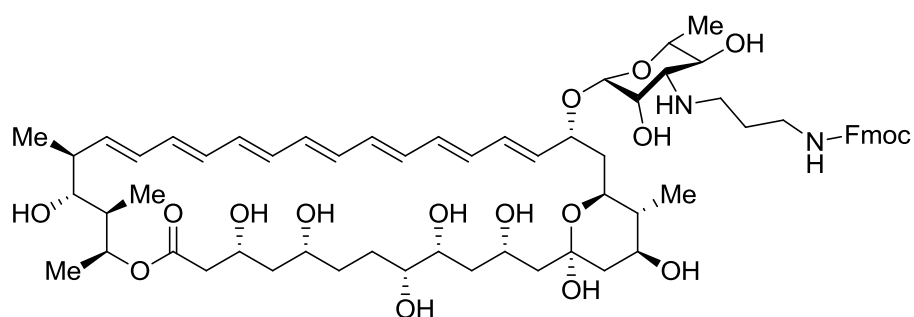


Figure 50: mono 3-(Fmoc-amino)-1-propanal substituted AmNM

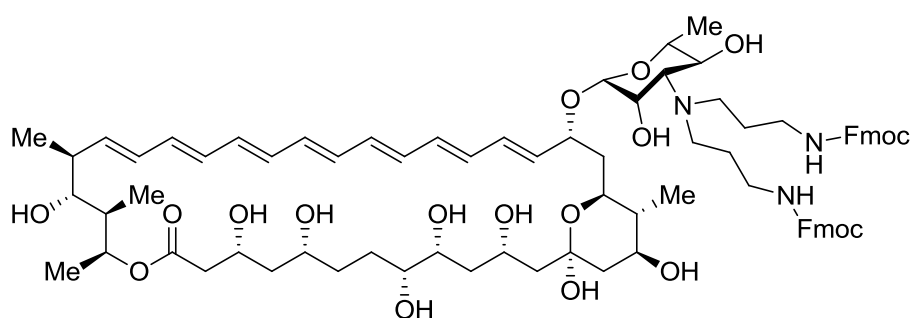


Figure 51: di 3-(Fmoc-amino)-1-propanal substituted AmNM

2.8.3 Fmoc deprotection of alkylated AmNM

After isolation **50** and **51** had their Fmoc protecting groups removed with 5% piperidine in DMSO at room temperature for two hours (see scheme 16). Diluting the mixture with Et₂O and collecting the precipitate by filtration gave the deprotected substituted AmNM in good yield (**50**→**52** 74%, **51**→**53** 77%) The NMR spectra collected, though not of very high quality, did show that the characteristic Fmoc signals had disappeared, thus confirming removal of the Fmoc protecting groups.

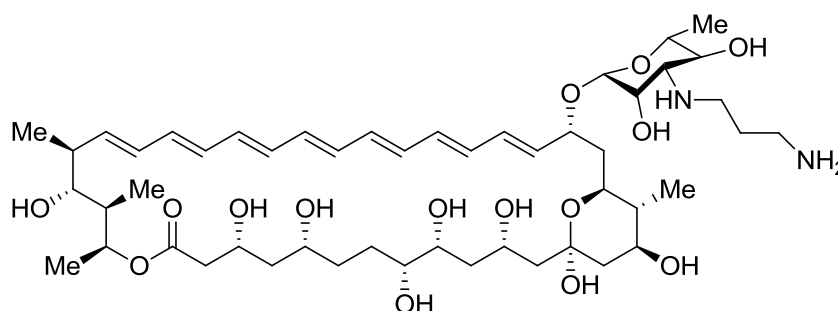


Figure 52: mono amino-propanyl substituted AmNM

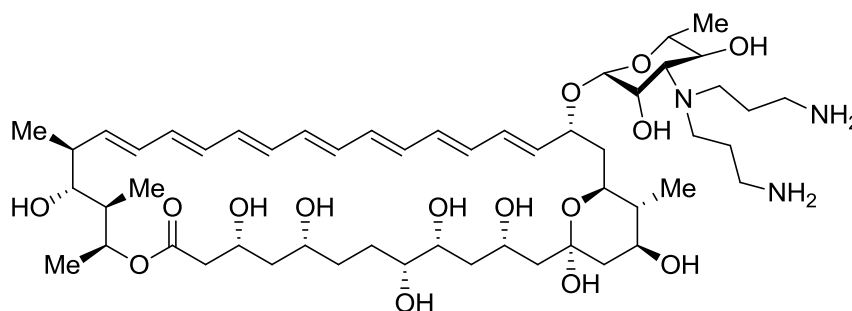
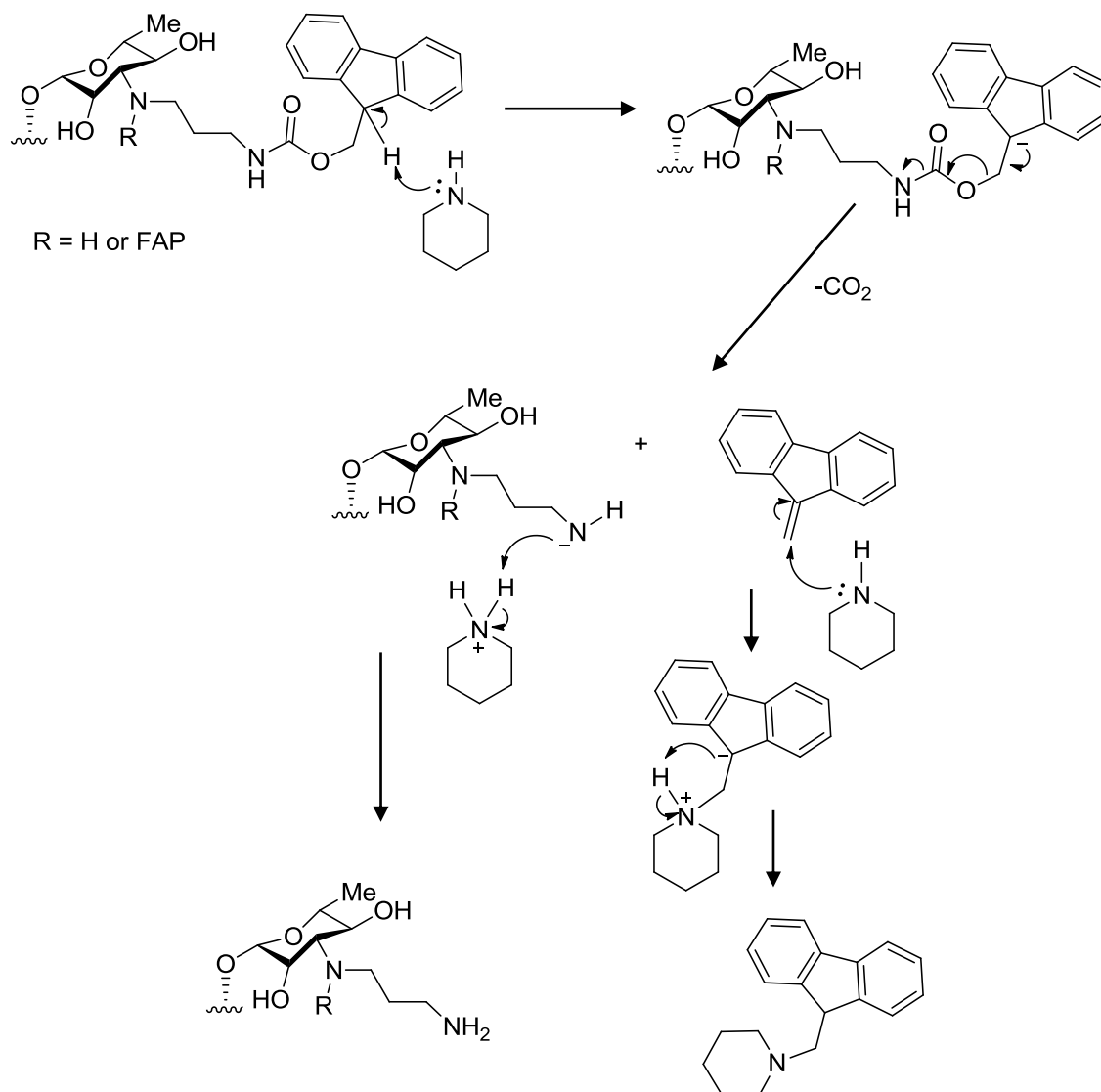


Figure 53: di amino-propanyl substituted AmNM



Scheme 16: Fmoc deprotection of substituted mycosyl

2.8.4 Alkylation with 2-(Fmoc-amino)-1-ethanol.

Fmoc-protected amino ethanol (**54a**) is another cheap and readily available starting material which could be oxidised to an aldehyde (**54b**) and used to substitute the amine group of the amphotericin. The oxidation reaction is similar to that shown in scheme 13.

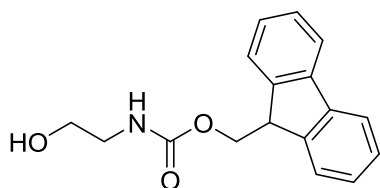


Figure 54a:
2-(Fmoc-amino)-1-ethanol

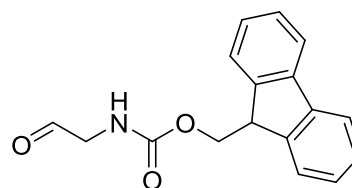


Figure 54b:
2-(Fmoc-amino)-1-ethanal

As before, the reaction was performed in EtOAc to facilitate removal of the spent IBX by cooling and filtering. A proton NMR was taken to confirm conversion of the alcohol into the aldehyde, evidence for this being the appearance of the aldehyde proton at 9.6 ppm and the disappearance of the CH_2OH signal at 3.3 ppm.

The produced aldehyde was reacted with AmNM in DMF under nitrogen, with sodium cyanoborohydride to reduce the imine formed and permit a second substitution. After six hours the reaction mixture was diluted with diethyl ether and the precipitate collected by centrifugation. However, analytical HPLC (figure 56) of the reaction showed only one major peak (mono-substituted, **55**), not the two that were expected (mono and di-substituted, such as figure 49).

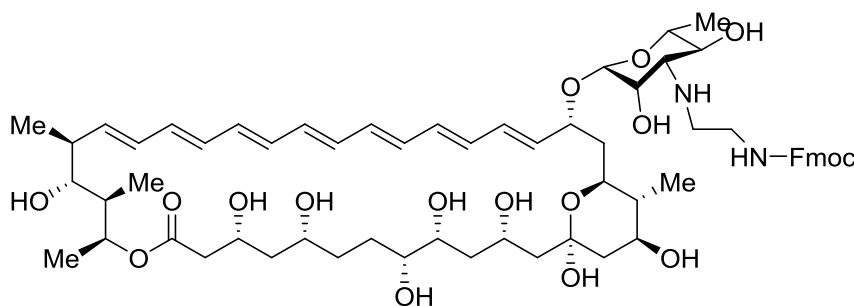


Figure 55: mono 2-(Fmoc-amino)-1-ethanol substituted AmNM

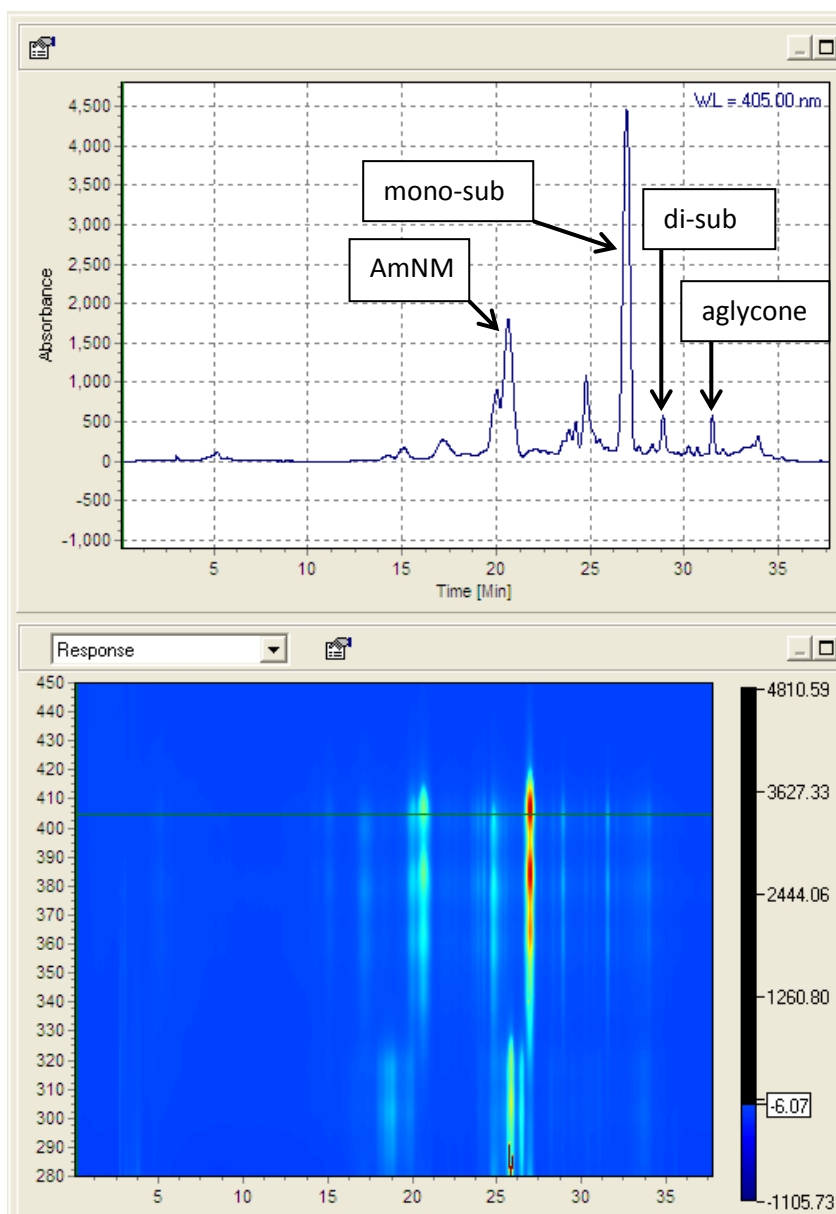


Figure 56: Analytical HPLC of first 54b derivatisation reaction.

The compounds present in each peak were confirmed by LCMS.

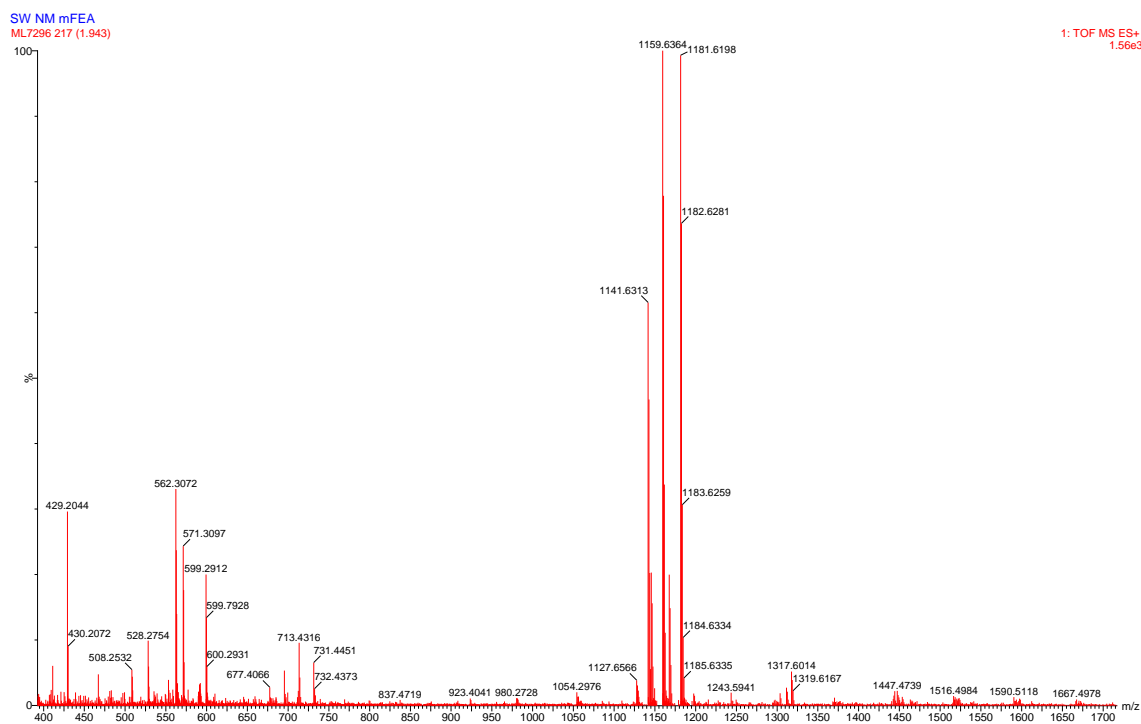


Figure 57: LCMS of 'mono-sub' peak in figure 56.

Elemental Composition Report: SW NM mFEA							
Elements Used:							
C: 64-64	H: 0-180	N: 0-30	O: 0-30				
Minimum:				-1.5			
Maximum:		5.0	5.0	80.0			
Mass	Calc. Mass	mDa	PPM	DBE	i-FIT	i-FIT	Formula
1159.6364	1159.6318	4.6	4.0	20.5	29.2	0.0	C64 H91 N2 O17

Figure 58: Elemental composition report of 1159 Da peak in figure 57.

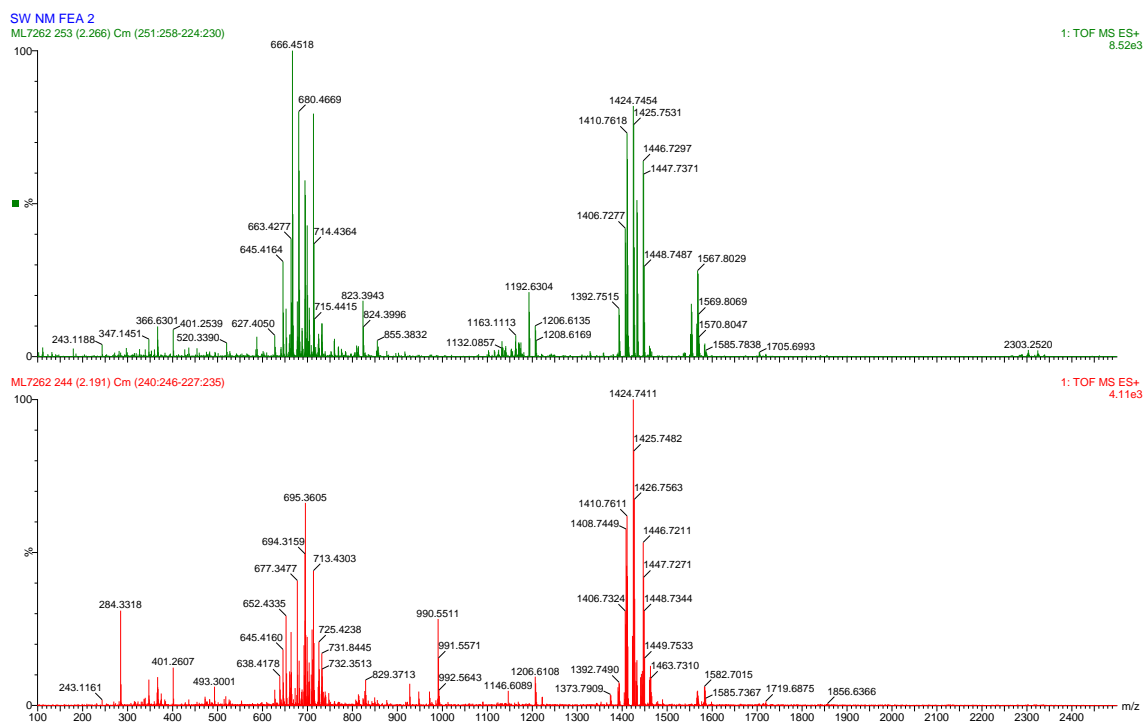


Figure 59: LCMS of di-sub peak in figure 56

Elemental Composition Report: SW NM FEA 2							
Elements Used:							
C:	81-81	H:	0-180	N:	3-3	O:	0-30
Minimum:							-1.5
Maximum:			5.0	5.0			80.0
Mass	Calc. Mass	mDa	PPM	DBE	i-FIT	i-FIT	Formula
1424.7411	1424.7421	-1.0	-0.7	30.5	53.5	0.0	C81 H106 N3 O19

Figure 60: Elemental composition report of 1424 Da peak in figure 59.

These data confirm that both mono and disubstituted forms were produced, however the HPLC trace shows that a far greater quantity of monosubstituted was produced.

The reaction was repeated and left to stir overnight. After 14 hours the mixture was diluted with ether as before and the products examined by analytical HPLC (figure 61).

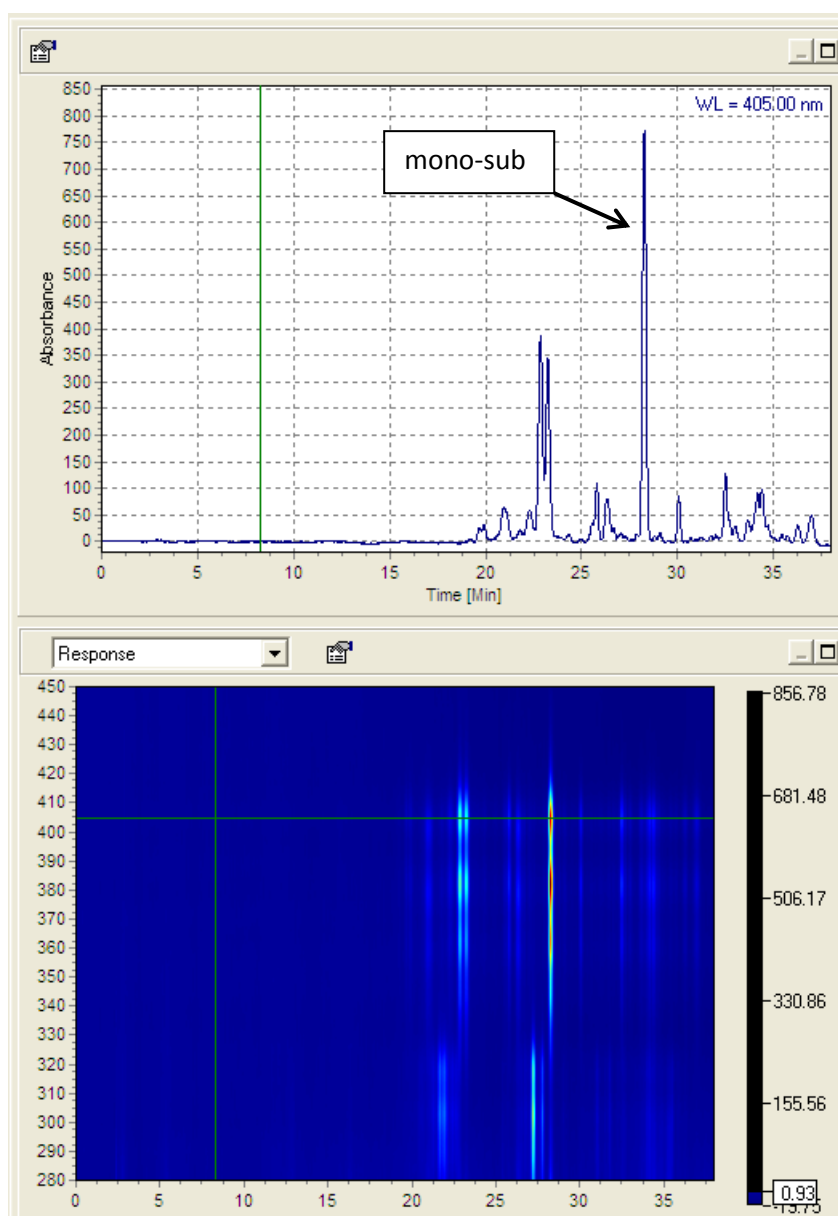


Figure 61: Analytical HPLC of second FAE substitution reaction.

From this it is clear that the longer reaction time did not have a significant impact on the ratio of mono to di substitution.

The monosubstituted AmNM from both reactions was isolated by preparative HPLC, its presence confirmed by accurate mass spec and a proton NMR recorded.

The Fmoc protecting group was removed in 5% piperidine/DMSO over two hours. The deprotected product was collected by dispersal of the reaction mixture in diethyl ether and filtering to collect the precipitate. A proton NMR showed that the characteristic Fmoc signals at 7.22, 7.30, 7.55 and 7.71 ppm visible on **55** had disappeared, confirming removal of the Fmoc group, and an accurate mass spectroscopy elemental composition report (figure **63**) confirmed the molecular formula of the product (**64**).

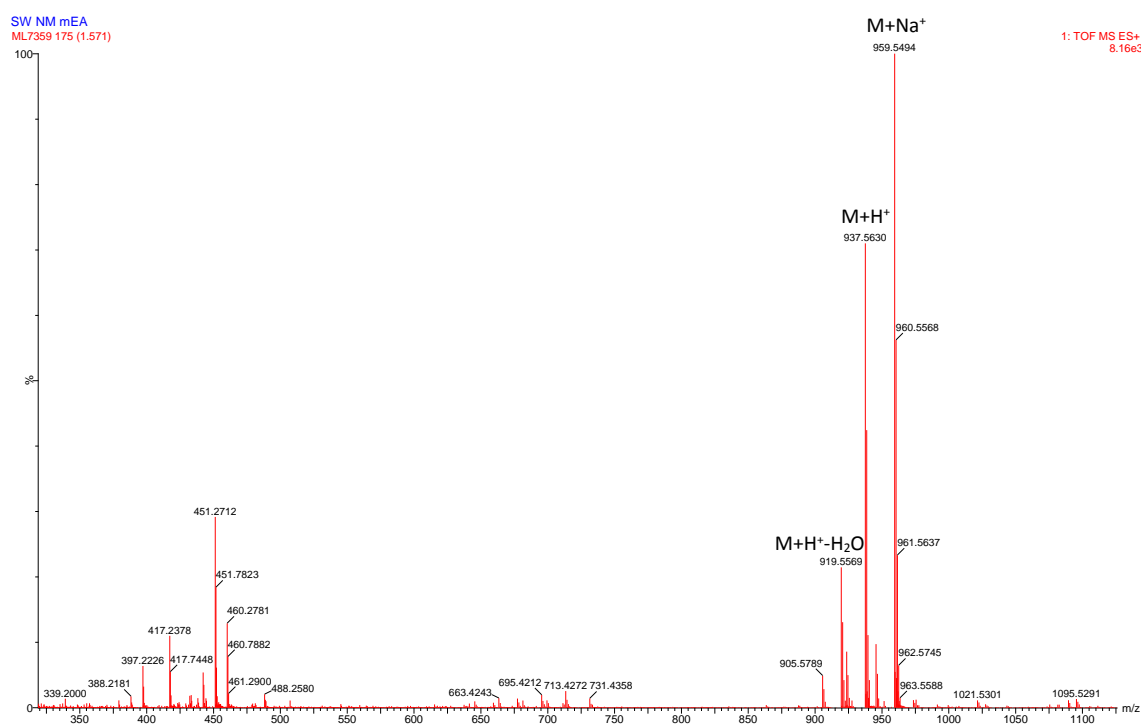


Figure **62**: LCMS of *N*-ethylaminoAmNM (**64**)

Elemental Composition Report: SW NM mEA							
Elements Used:							
C: 49-49	H: 0-180	N: 0-30	O: 0-30				
Minimum:				-1.5			
Maximum:		5.0	5.0	80.0			
Mass	Calc. Mass	mDa	PPM	DBE	i-FIT	i-FIT	Formula
937.5630	937.5637	-0.7	-0.7	10.5	52.6	0.0	C49 H81 N2 O15

Figure **63**: Elemental composition report of $M+H^+$ peak in figure **62**

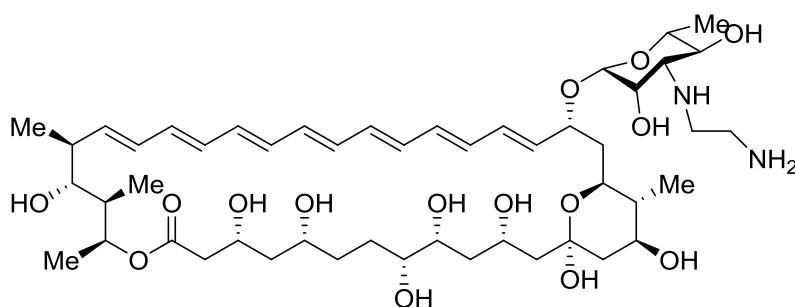


Figure 64: mono amino-ethanyl substituted AmNM

It is proposed that the reason 2-(Fmoc-amino)-1-ethanal only disubstitutes the AmNM in trace quantities is the steric hindrance caused by the Fmoc group once the first substitution has occurred. 3-(Fmoc-amino)-1-propanal, with an extra carbon in the chain, has the Fmoc group slightly further from the mycosaminyl sugar so the longer ‘tail’ on the molecule can reach the amino group to substitute it a second time.

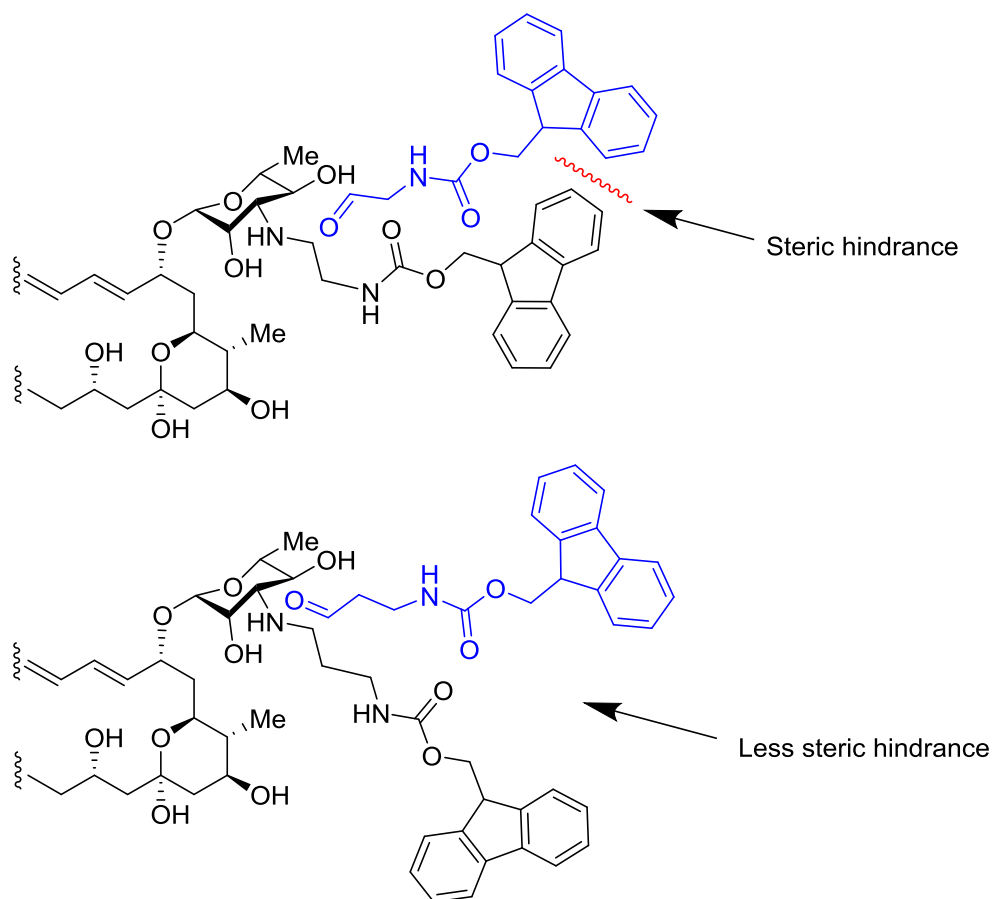


Figure 65: Steric hindrance difference between ethyl (top) and propyl (bottom) chains on Fmoc protected substrate.

2.8.5 Derivatisation with iodoacetic anhydride

In the first paper to publish a crystal structure of AmB, Ganis⁷⁹ described the iodoacetylation of AmB, as a heavy ion derivative (**66**) with which to perform X-ray diffraction.

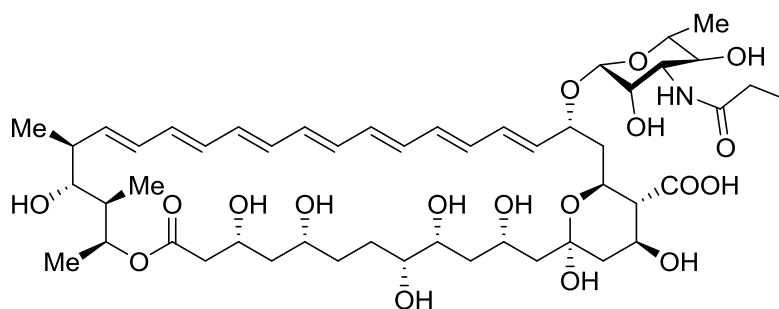


Figure 66: N-iodoacetylAmB

This derivative retains the biological activity of the parent compound.⁸⁰

It was investigated whether iodoacetylation of AmNM would produce a biologically active derivative which could also be used for crystallisation.

Following the method published by Ganis, AmNM was dissolved in a 50:50 mixture of DMSO and methanol, cooled to 0°C, then two equivalents of iodoacetic anhydride were added. The mixture was stirred for 15 minutes then precipitated in diethyl ether. Analytical HPLC of the collected yellow solid showed only unreacted AmNM starting material.

The reaction was repeated using DMF as the solvent because use of DMF in the alkylamino substitutions discussed earlier in this section had proved beneficial, this time analytical HPLC showed good conversion of the AmNM into a new product eluting at 34 minutes (see figure 67).

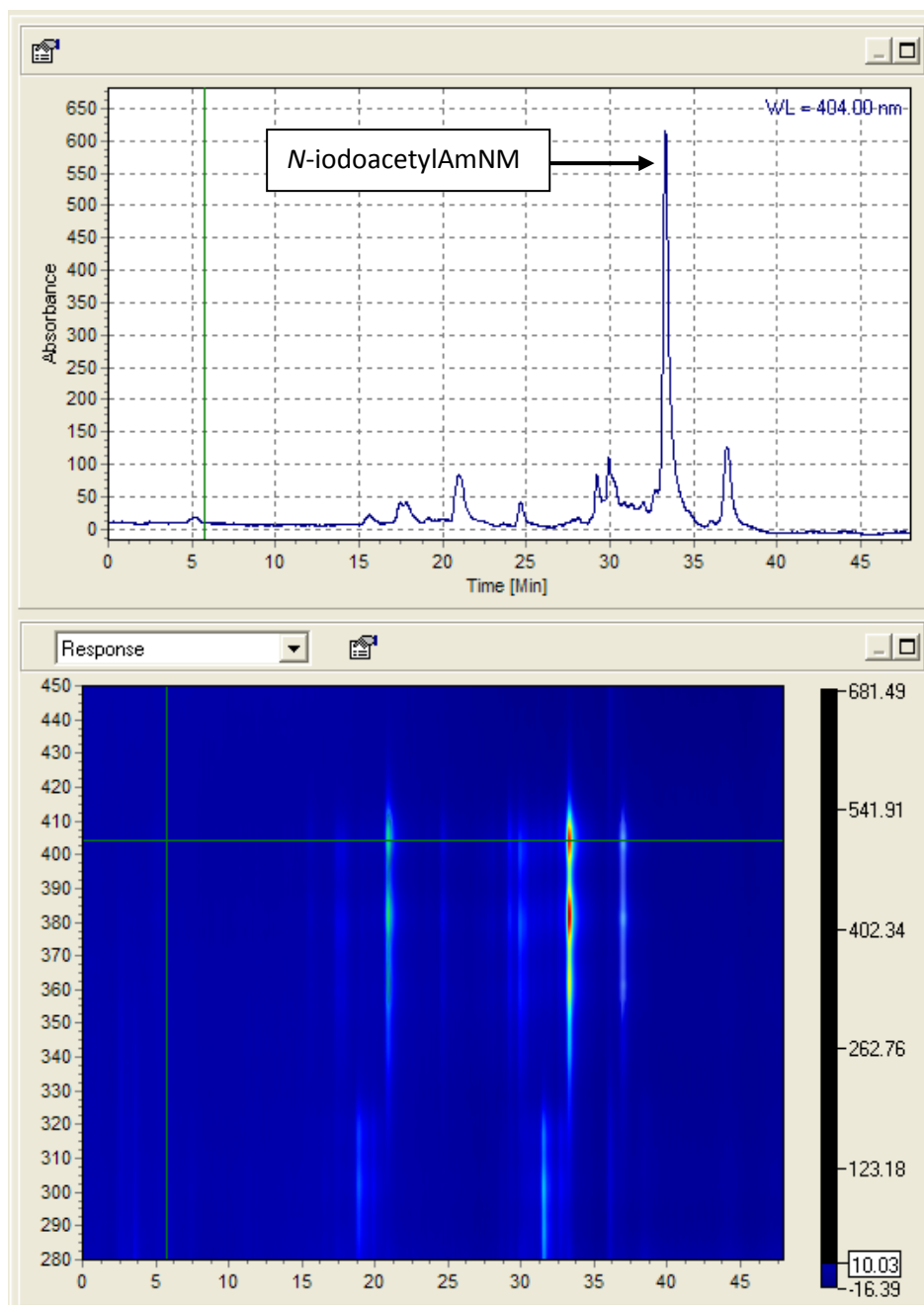


Figure 67: Analytical HPLC of iodoacetylation reaction.

LCMS of the collected yellow solid confirmed the presence of the expected molecular mass of *N*-iodoacetylAmNM (**68**) (1084.4033, $M+Na^+$). The product was purified by preparative HPLC to obtain a yield of 96%. A proton NMR was taken but the additional acetyl signal could not be identified.

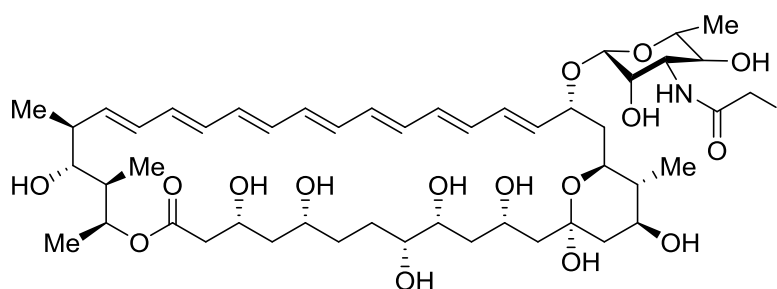
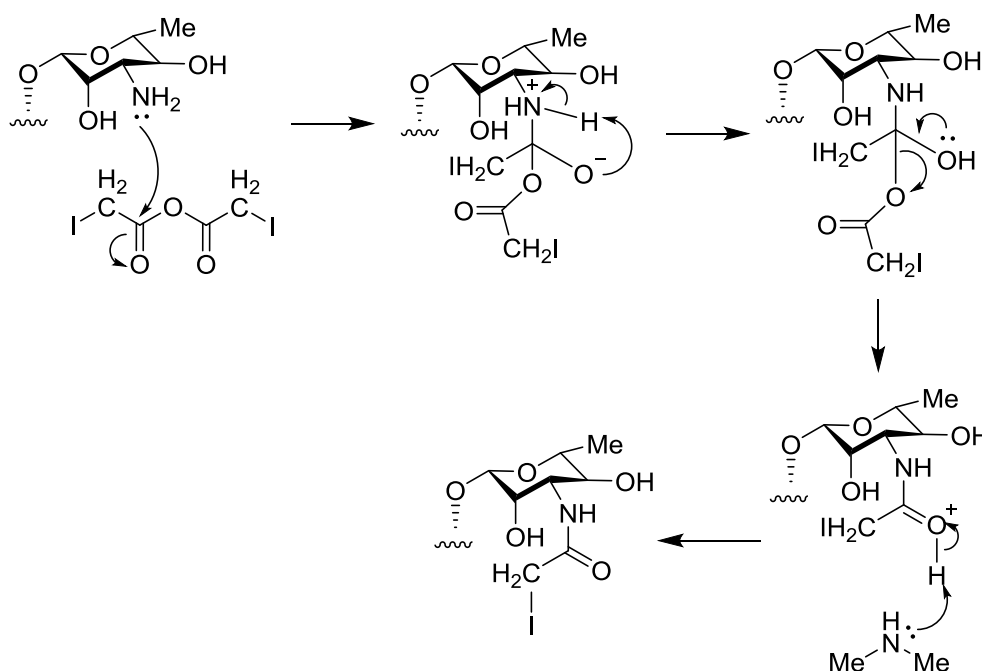


Figure 68: *N*-iodoacetylAmNM

Using their mixture of DMSO and methanol as solvent, Ganis' group claimed a reaction yield of 70%, although an attempt here with AmNM could not reproduce their method. Using DMF as the solvent, a reaction yield of >95% was recorded. Aprotic solvents such as DMF and DMSO are known to facilitate nucleophilic substitution reactions⁸¹, the reason that DMF facilitates the reaction better in this case may be due to the trace presence of formic acid and, in particular, dimethylamine (see scheme 17).



Scheme 17: Proposed iodination mechanism of amino group of mycosaminyl sugar.

2.8.6 Derivatisation with acetic anhydride

Acetic anhydride is a very common and cheaply available chemical reagent, despite being on the list of restricted drug precursors due to its use in the synthesis of heroin from morphine.

Following the successful iodoacetylation of AmNM a similar reaction was performed to produce *N*-acetylAmNM. AmNM was reacted with two equivalents of acetic anhydride in DMF under nitrogen. After 20 minutes the reaction mixture was dripped into diethyl ether and examined by analytical HPLC, which showed only partial (~10%) conversion into *N*-acetylAmNM.

The reaction was repeated but stirred for four hours, dripped into diethyl ether and examined by analytical HPLC, two new peaks were observed (figure **69**). An LCMS of the sample was performed, however only one major peak was observed at 405 nm, with a mass corresponding to the expected *N*-acetylAmNM (**70**) product (958.5168 Da, M+Na⁺).

The two peaks were isolated by preparative HPLC. The LCMS UV trace of each fraction showed one major peak at 405 nm, both corresponding to the molecular mass of the *N*-acetylAmNM product, however when each fraction was re-examined by analytical HPLC, the same two peaks as before were observed.

It is theorised that the slower speed of the acetylation reaction compared to the iodoacetylation is due to the absence of the large halogen (iodine) which, as a large substituent with non-bonding electrons, stabilises the charged intermediate.

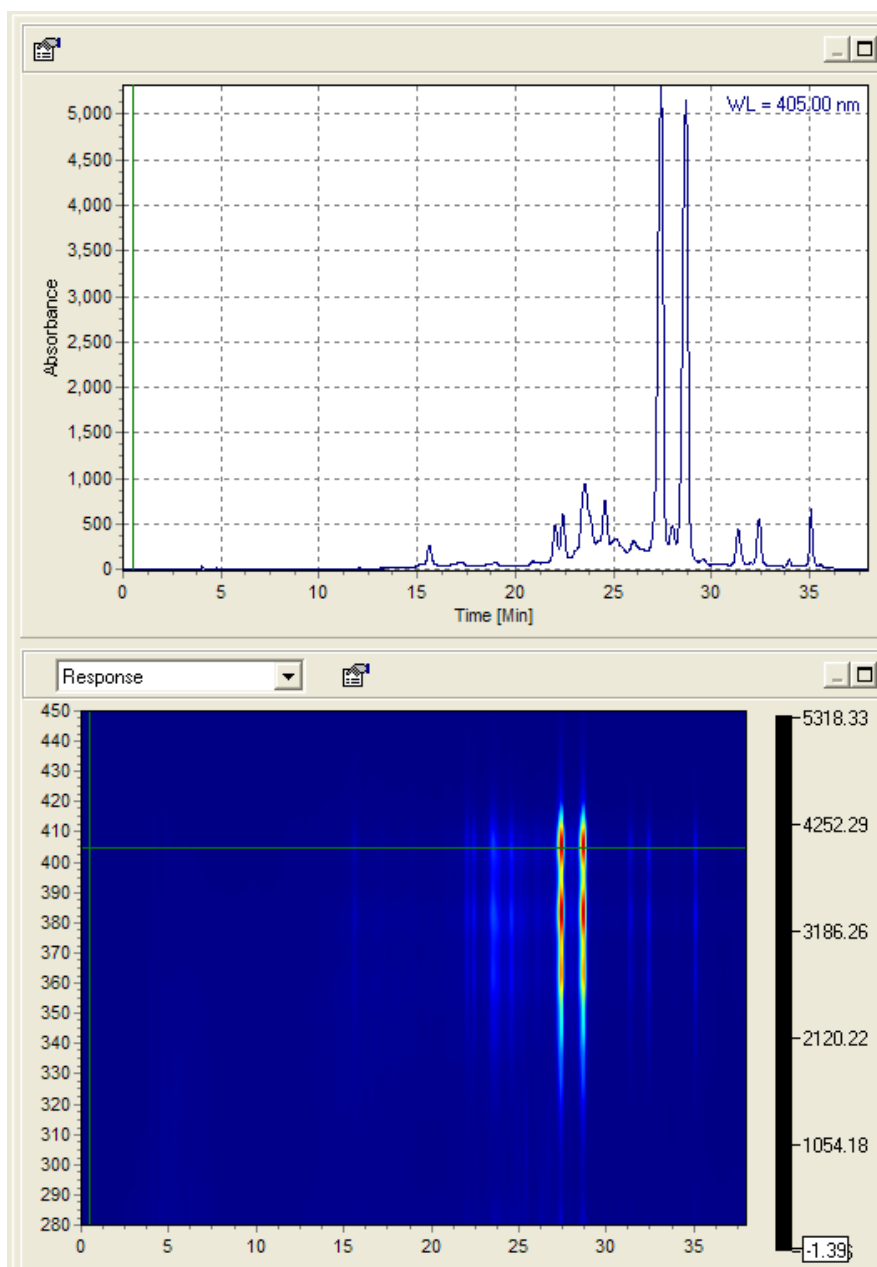


Figure 69: Analytical HPLC of four hour AmNM acetylation reaction.

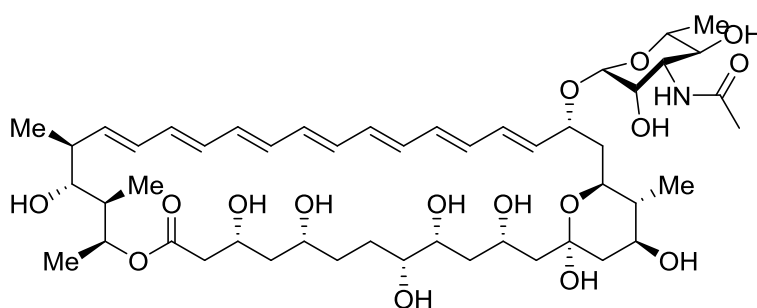


Figure 70: N-acetyl-AmNM

It is also proposed that the acetylated AmNM molecule exists as two isomers which readily interconvert (tautomers), which are likely the keto and enol forms of the carbonyl present on the acetyl group (figure 71). Such interconversion⁸² on other molecules containing acetyl groups is well known.⁸³

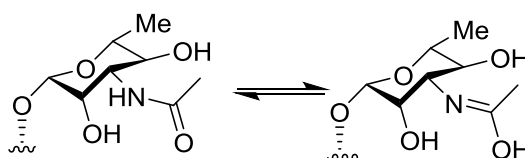


Figure 71: Keto (left) and enol (right) forms of acetylated mycosaminyl sugar

The hydrogen bonding potential of the solvent has a great effect on the keto-enol ratio.⁸⁴ This accounts for the difference in visibility between the LCMS and HPLC traces, because the LCMS was performed using a water:acetonitrile mix, whereas the HPLC was performed in a water:methanol mix. Acetonitrile weakens the hydrogen bonding present in an aqueous mix⁸⁵, whereas methanol (which is more polar than acetonitrile and is also capable of hydrogen bonding) does not.

Nearby groups also play a role on the keto-enol ratio.⁸⁶ In this case the acetyl group is proximate to hydrogen bond donors in the form of hydroxyl groups on the sugar, these will have the effect of stabilising the keto form (see figure 72)

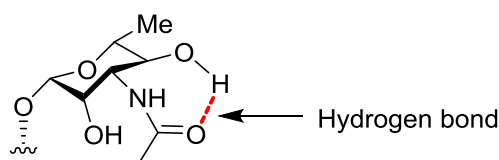


Figure 72: Example of hydrogen bonds stabilising the keto form

Putting all this together, it appears likely that when eluted in a solvent containing acetonitrile the acetylated product will be mostly in the keto form, whereas in the methanolic solvent a roughly 50/50 mix of the two isomers is present, as seen in figure 69.

2.9 Biological testing of AmNM derivatives.

The five synthesised derivatives (at >95% purity); mono (**52**) and di (**53**) *N*-aminopropyl, mono *N*-aminoethyl (**64**), *N*-iodoacetyl (**68**) and *N*-acetyl (**70**) AmNM, and also the collected 8-deoxyAmNM (**39**) resulting from experimentation with cottonseed flour, were tested for antifungal and haemolytic activity.

Antifungal activity⁸⁷ was tested using the standard broth dilution test M27-A2 as published⁷⁶ by NCCLS, with *Candida albicans* as the indicator organism. The broth dilution test involves a multi-welled plate containing the indicator organism and growth medium to which varying concentrations of the agent being tested are added. The plate is then incubated and checked for fungal cell growth. The minimum inhibitory concentration (MIC) is the lowest concentration at which no discernible fungal cell growth occurs.

Haemolytic activity was determined using horse blood erythrocytes⁶⁰. Serial two-fold dilutions were made of the polyene agent being tested. A 50 µl volume of each dilution was added to 250 µl of defibrinated* horse blood in phosphate buffered saline. These are incubated for one hour at 37°C, haemolysis is determined by sedimenting unlysed erythrocytes and measuring the absorbance of the supernatant at 545 nm. The minimum haemolytic concentration (MHC) is the lowest concentration resulting in complete haemolysis.

(*Defibrinated blood is blood which has had the plasma component fibrinogen removed, usually by clotting which converts the soluble fibrinogen to the insoluble fibrin, defibrinated plasma is also known as serum.)

2.9.1 Antifungal activity

The six derivatives were tested by Caffrey for antifungal activity against *Candida albicans* with AmB as the standard reference, the following MICs were found.

Polyene	MIC, μM
Amphotericin B	1.56
<i>N</i> -mono(propylamine)AmNM (52)	1.56
<i>N</i> -di(propylamine)AmNM (53)	1.56
<i>N</i> -ethylaminoAmNM (64)	1.56
<i>N</i> -iodoacetylAmNM (68)	>100
<i>N</i> -acetylAmNM (70)	100
8-deoxyAmNM (39)	50

Table 13: Antifungal activity of AmNM derivatives

This data shows that the three alkylamino derivatives (**52**, **53** & **64**) of AmNM retain equivalent antifungal activity to AmB, the 8-deoxy (**39**) and *N*-acetyl (**70**) forms have much diminished activity, and the *N*-iodoacetyl derivative (**68**) has such diminished antifungal activity as to be unmeasurable on this scale.

Notably, this varies from the findings of Carreira, who found that **42** had 15-fold improvement of antifungal activity (MIC: 0.02 μM) to the unalkylated AmB (MIC: 0.3 μM) against *Saccharomyces cerevisiae*.

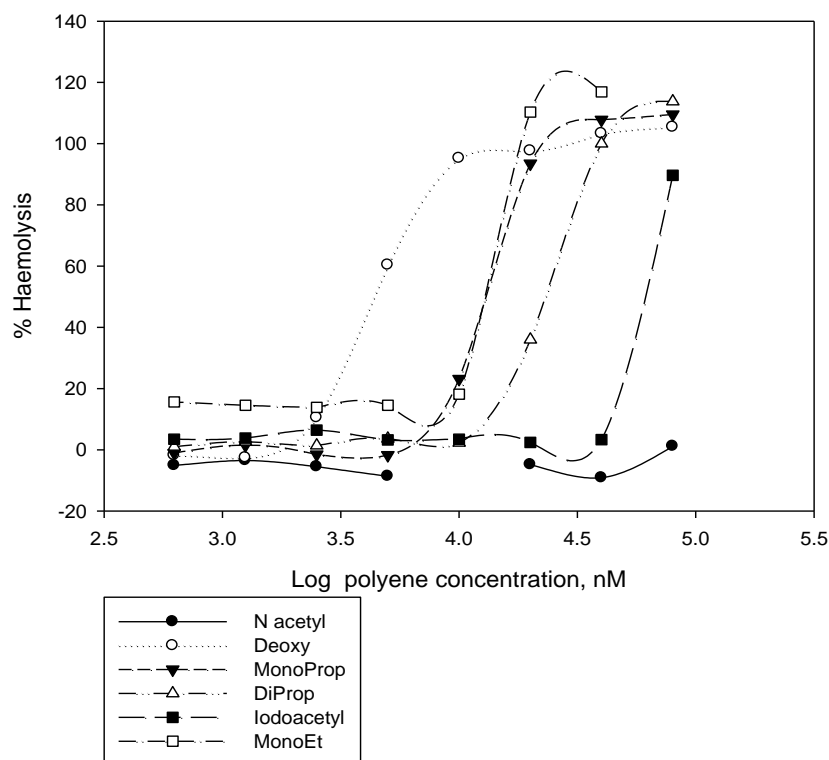
2.9.2 Haemolytic activity

The six derivatives were tested for haemolytic activity with AmB as the standard reference, the following MHCs were found.

Polyene	MHC ₀ , μM	MHC ₅₀ , μM	MHC ₁₀₀ , μM
Amphotericin B	1.26	2.00	5.01
<i>N</i> -mono(propylamine)AmNM (52)	7.9	12.59	25.12
<i>N</i> -di(propylamine)AmNM (53)	10	24.55	39.81
<i>N</i> -ethylamineAmNM (64)	9.12	12.59	19.5
<i>N</i> -iodoacetylAmNM (68)	40	50	>80
<i>N</i> -acetylAmNM (70)	>80	>80	>80
8-deoxyAmNM (39)	2.51	4.47	12.59

Table 14: Haemolytic activity of AmNM derivatives

Haemolytic assay 2



From this data it can be seen that of the derivatives showing antifungal activity, i.e. the three alkylamino derivatives, the disubstituted propylamino **53** has the lowest haemolytic activity, approximately one eighth that of AmB, followed by the monosubstituted **52** (one fifth) and the ethylamino **64** (one quarter). The trend here appears to be that the longer the alkyl chain attached to the amino group on the mycosaminyl sugar, the lower the haemolytic activity. Carreira found that **42** had a 2.5 fold reduction of haemolytic activity (10 μ M to AmB's 4 μ M). Importantly however, whilst all of the alkylamino derivatisations tested above retained the antifungal activity of AmNM, which itself retains that of AmB, the MHCs of all three were higher than that of AmNM, previously tested to be 50 μ M.

Suggested further work in this area would be to produce derivatives with longer chains (butyl, pentyl, hexyl, etc) to investigate whether the MHC can be improved beyond that of AmNM, and whether at any point the antifungal activity of the substituted derivatives is affected by the alkylamino chain.

2.10 Summary

Following on from the work of Ibrahim, where previously only very low (~5 mg) quantities of AmNM had been obtained, a procedure has been developed to allow decigram (>100 mg) quantities to be produced at a 50% overall yield. With these higher yields, further experimentation into simple chemical derivatives was possible, with the discovery that the addition of alkylamino chains to the amine of the mycosaminyl sugar altered the haemolytic activity without affecting the antifungal activity, though a significant improvement has not yet been achieved.

3. Amphotericin disaccharides

In this chapter will be discussed work done to grow, isolate and purify novel biosynthetic disaccharide derivatives of amphotericin B, the complications encountered, and biological testing to determine the effect of mannosylation on the antifungal and haemolytic activity of the molecule.

3.1 Introduction

Previous research has shown modifying the mycosaminyl sugar of AmB to be beneficial, such as the addition of two 3-aminopropyl groups to the amine which increases potency and reduces toxicity⁷⁸, and the MFAME semi-synthetic derivative with greater water solubility and decreased toxicity⁵⁴. This new process may make it possible to generate bacteria which produce disaccharide amphotericins *in vivo*, if successful, this could allow production of these potentially improved compounds in a cost effective and hopefully clinically affordable way, since expensive post-synthesis modification will not be required.

Conjugation with arabinogalactan polysaccharides converts amphotericin B to a water-soluble form,⁸⁸ In studies by Ehrenfreund-Kleinman arabinogalactan, a highly branched natural polysaccharide with high water solubility, was coupled to AmB via amine and imine bonds. The resulting conjugates were soluble in water and exhibited improved stability in water compared to unbound AmB. They also showed comparable antifungal activity to AmB tested against *Candida albicans* but 60 times lower haemolytic activity against sheep erythrocytes.

Pseudocardia autotrophica has been found to synthesise a tetraene known as NPP (Nystatin-line *Pseudocardia* Polyene, **73**), this compound is effectively a nystatin molecule with an *N*-acetyl glucosaminyl residue linked to the mycosaminyl sugar. In testing this compound was found to be 300 times more water soluble whilst retaining about half the antifungal activity of nystatin against *C. albicans*.⁸⁹

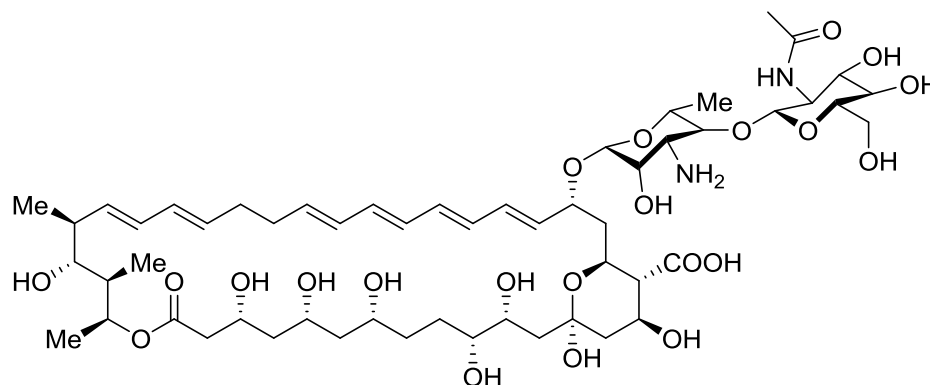


Figure 73: NPP

Another new nystatin-like molecule was discovered being produced by a *Pseudocardia* strain forming a tripartite mutualism, along with the fungus *Leucoagaricus gongylophorus*, in a colony of Attine ants, also known as leafcutter ants. The bacteria produce antifungal agents that defend the ants against fungal parasites such as *Escovopsis*.⁹⁰ The bacteria are thought to have co-evolved with the ants and are transmitted vertically by the queen, though more recent studies have indicated that the worker ants may also select suitable antibiotic-producing actinomycetes from the soil.⁹¹ The new antifungal molecule was a nystatin with a hexosyl residue attached to the mycosaminyl sugar. This compound, tentatively named nystatin P1 (figure 74), has not yet been tested for antifungal activity or had the identity of the additional sugar positively confirmed, but the NypY glycosyltransferase that adds the extra sugar was identified after genome sequencing.⁹²

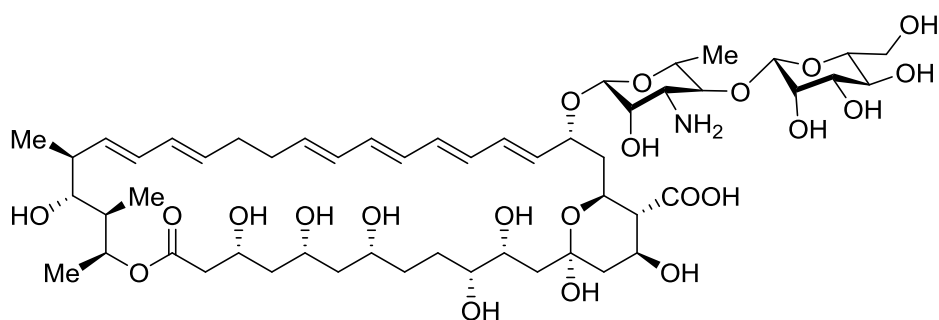


Figure 74: Putative nystatin P1

Actinoplanes caeruleus synthesises 67-121C, an aromatic heptaene with a mannosyl residue β -1,4 linked to the mycosamine sugar (figure 75).

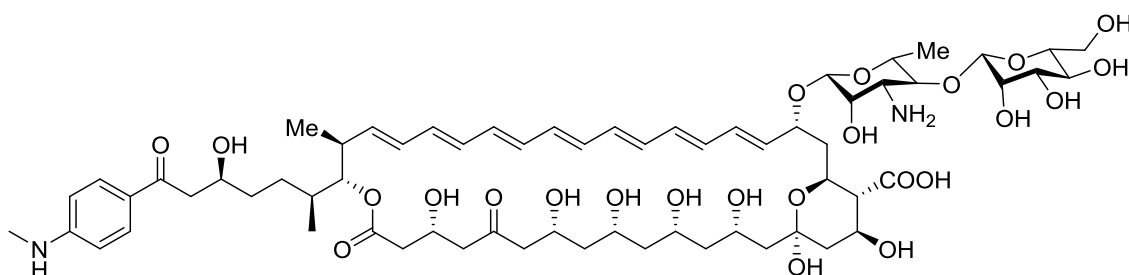


Figure 75: 67-121C

Research by Caffrey into draft genome sequencing of the above molecules has uncovered genes for two glycosyltransferases that catalyse mannosylation of mycosaminyl sugars on polyene macrolides⁹³. These are the *nypY* genes from the P1 strain of *Pseudonocardia*, and *pegA* from *Actinoplanes caeruleus*. This research also showed that expressing *PegA* in *S. nodosus* generated only trace quantities of mannosylated amphotericin,⁹³ though it was unclear whether this was due to the *PegA* not recognising the amphotericin, low quantities of GDP-D-mannose inside the cell, the amphotericin being exported from the cell before mannosylation could happen, or other unknown factors.

PegA and NypY have 51% sequence identity, indicating they both use GDP- α -D-mannose as the activated sugar donor. So it was investigated whether NypY will recognise amphotericins *in vivo*. A plasmid (pIAGO-nypY) was produced and transformed into *S. nodosus* (the plasmids are mixed with bacteria in antibiotic-free media, then grown on an agar plate containing antibiotic, this case thiostrepton, for which the plasmid contains a resistance gene, thus only those bacteria which have taken up the plasmid survive and reproduce) and the polyenes extracted and analysed.⁹⁴ HPLC analysis showed the presence of new heptaene and tetraene analogues which were identified by LCMS as corresponding to mannosylated amphotericin B (**76**), with a mass of 1086.6 Da ($M+H^+$), and mannosylated amphotericin A, with a mass of 1088.6 Da ($M+H^+$).

3.2 Mannosyl-amphotericin B

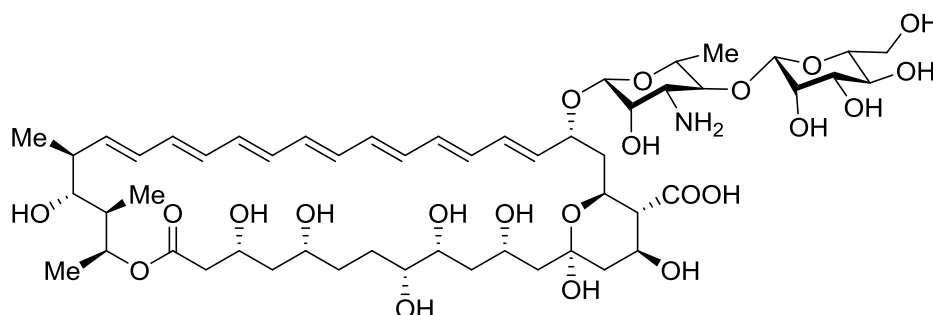


Figure 76: Mannosyl-amphotericin B

Previous work summarised above showed that it is possible to produce mannosylated amphotericins *in vivo*, however, to be feasible for use in the clinic it would be necessary from them to be produced in sufficient quantity to be extracted and purified at a clinically-affordable cost, this chapter describes the process therein.

First growth

Deep frozen samples of *S. nodosus* transformed with the pIAGO-nypY plasmid arrived as a glycerol suspension from Caffrey. Two autoclaved starter flasks were prepared containing 1 g glucose and 1 g yeast extract, adjusted to pH 7 with sodium hydroxide. One sample of *S. nodosus* was added to each under sterile conditions, with thiostrepton to a final concentration of 50 µg/ml. The flasks were incubated with shaking at 30°C for three days, after which could be seen mycelia growing in the otherwise clear liquid.

Eight 2l trigrooved Erlenmeyer flasks containing 250 ml of autoclaved growth medium were produced, each containing 5 g of Amberlite resin. 10 ml of starter culture was transferred to each from one flask under sterile conditions, and the flasks incubated for five days at 30°C with shaking. The contents of the flasks were centrifuged at 13,000 rpm for twenty minutes to separate mycelia from the aqueous growth media, which was tested by UV/Vis spectroscopy, found to contain no polyenes, and discarded.

The sedimented mycelia were lysed in methanol to extract polyenes. Six extracts were taken, the methanol removed under vacuum and the residual water refrigerated overnight. The precipitated solid was collected by centrifugation. A total weight of 5.21 g was collected, analysed by UV/Vis spectroscopy to contain 104 mg of heptaene. The HPLC analysis showed a large peak corresponding to the expected presence of amphotericin B, with a smaller peak eluting slightly ahead (see figure 77 below). The sample was too impure to achieve good separation by LCMS to identify this new peak.

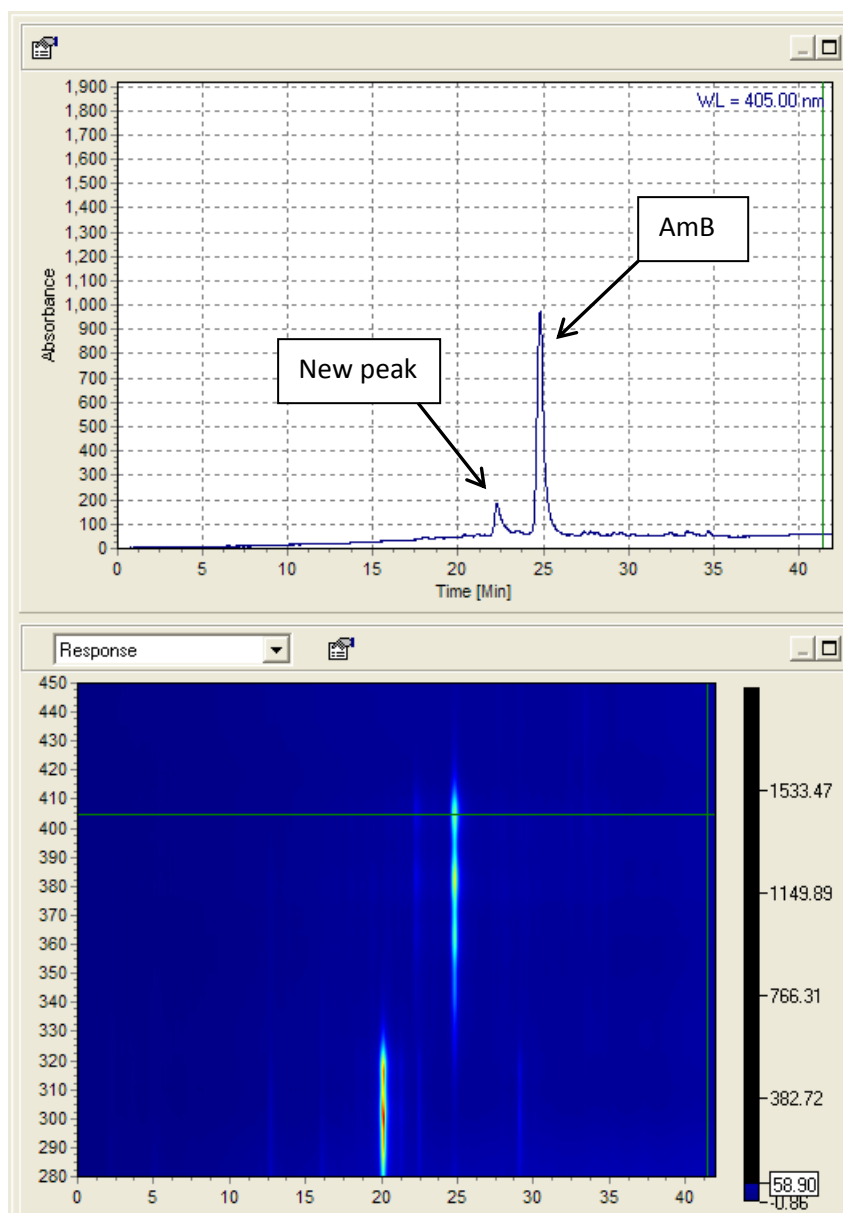


Figure 77: Analytical HPLC analysis of first NypY modified growth

The extract was washed (suspended then centrifuged) with diethyl ether (3x40 ml), removing 2 g of impurities, then with water (1x40 ml) leaving 600 mg of impure sample, then with DCM (2x40 ml) leaving 554 mg of impure sample. The sample was not treated further to avoid accidentally breaking down any desired product.

The small peak was collected by preparative HPLC (Supelco Acentis C18 21.2x250 mm column), the methanol was removed under vacuum and the water

removed by lyophilisation. A total mass of 13.5 mg was collected, UV/Vis analysis showed a mass of 1.43 mg heptaene and 1.52 mg tetraene.

Analysis by LCMS of the collected sample showed only a mass of 924 Da ($M+H^+$), with none of the expected 1086 Da ($M+H^+$) of the disaccharide.

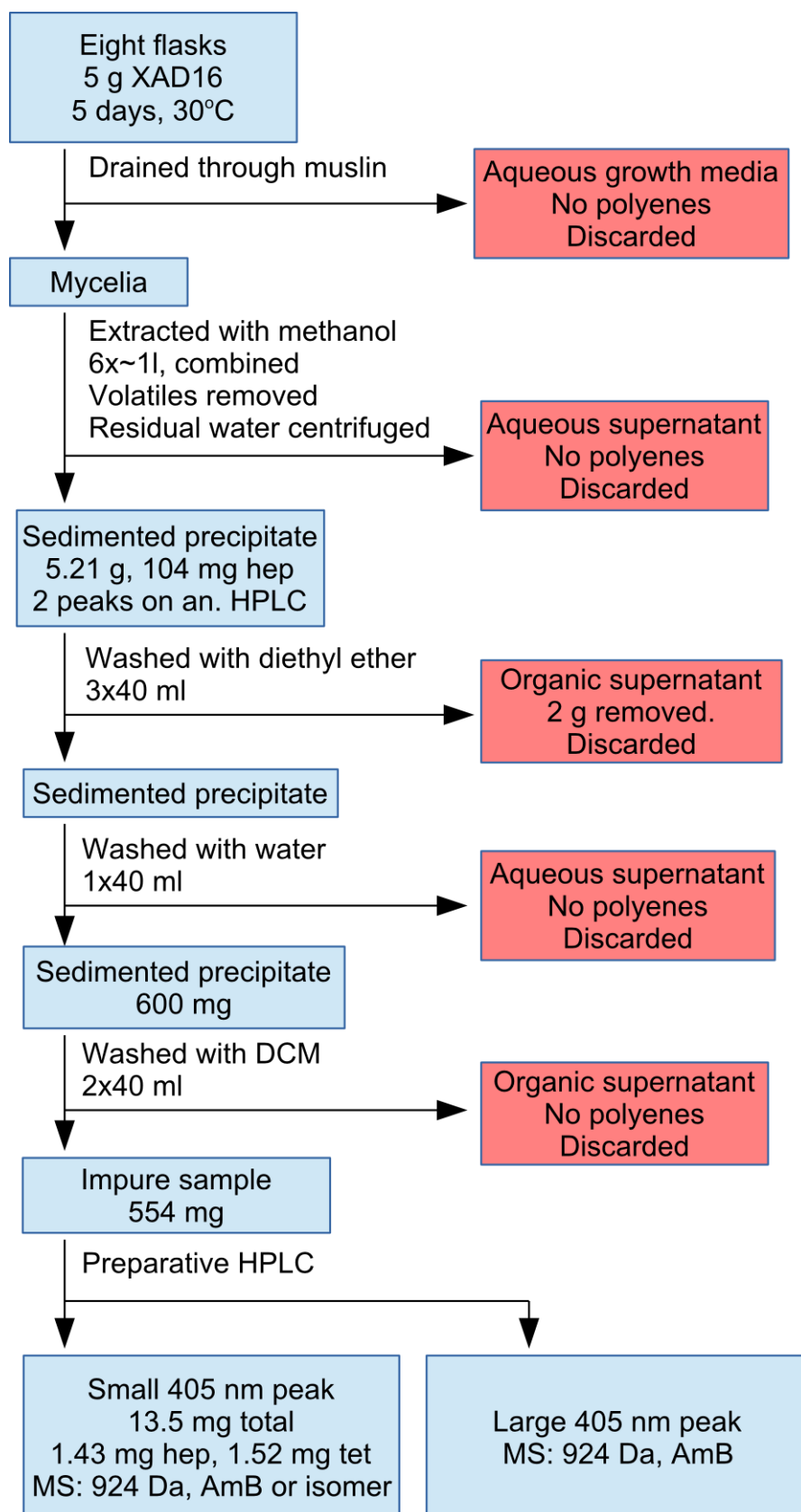
The processing of this growth is summarised in scheme 18.

Second growth

A second growth was prepared as before, but consisting of 16 flasks of fructose-dextrose-soya media. These were incubated for 6 days, drained through muslin cloth, and the mycelia lysed in methanol to extract cell contents and desorbed polyenes from Amberlite beads.

The drained media water was analysed by UV/Vis spectroscopy and found to contain polyenes, it was therefore shaken with butan-1-ol and allowed to separate. The organic layer was extracted and dried under vacuum. Since butanol does not easily evaporate at low temperatures, and temperatures above 40°C risk causing breakdown of the products, 15% of water was added to form an azeotrope and facilitate solvent removal. The dried extract was analysed by UV-Vis spectroscopy to contain 27.5 mg heptaene and 27.7 mg tetraene.

The first six methanolic extracts and the butanol extract were combined to give an extract with a total mass of 14.96 g and a heptaene content of 300 mg.



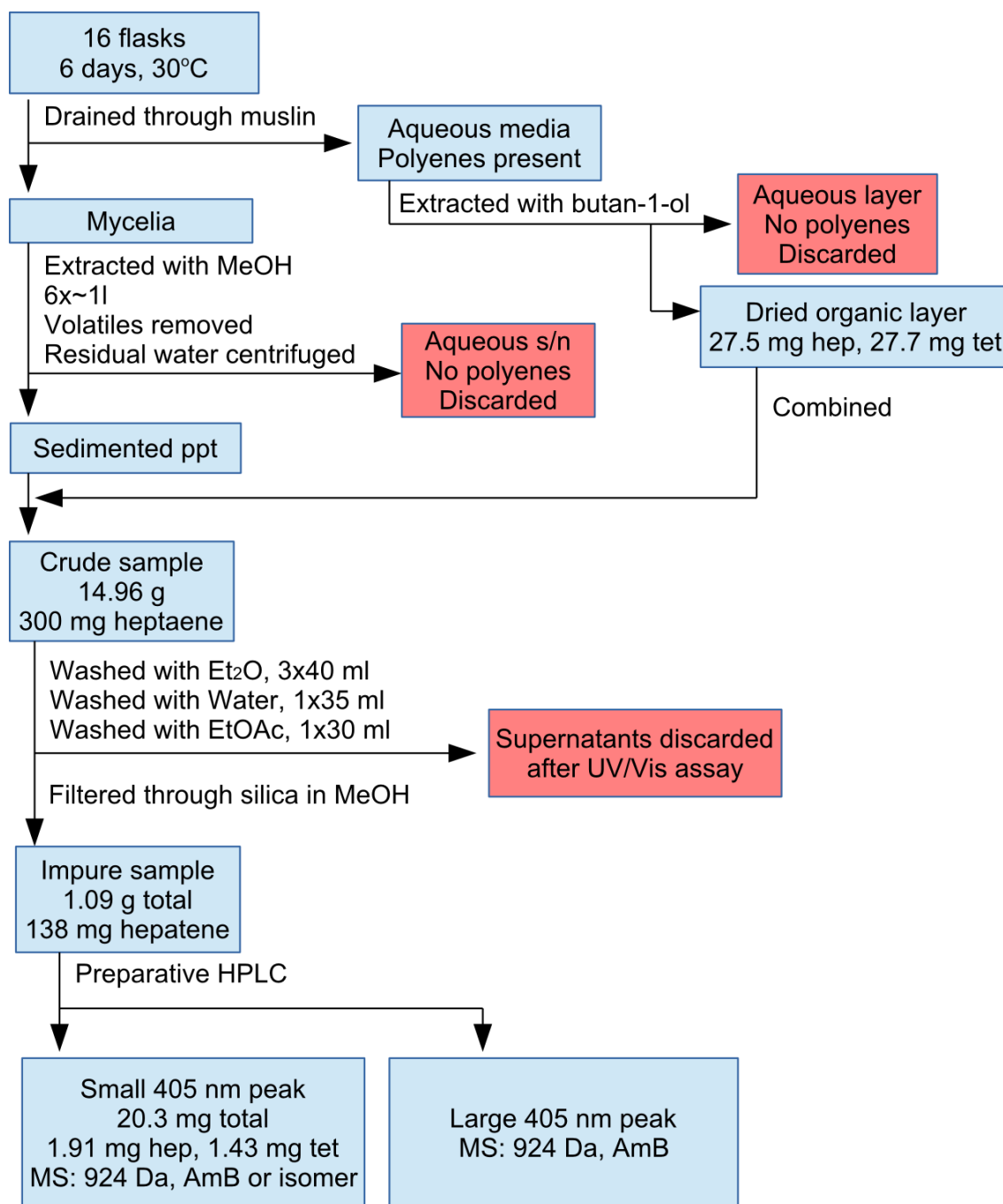
Scheme 18: Processing of first NypY modified growth

The extract was washed with diethyl ether (3x40 ml), water (1x35 ml), and ethyl acetate (1x30 ml), leaving a total mass of 1.2859 g. The extract was dissolved in a large volume of methanol (200 ml) and filtered through a plug of silica as had proved successful in earlier studies at removing impurities which would otherwise foul the HPLC column. The methanol was removed under vacuum to leave an impure sample with a total mass of 1.09 g and a heptaene content by UV/Vis of 138 mg. This loss of over half the mass of heptaene was unexpected, as all wash solutions were inspected by UV/Vis before being discarded and none had been found to contain above trace quantities of heptaene. The silica plug was rinsed with further methanol in case product had stuck to it but analysis of the rinsing showed no further heptaene.

Analytical HPLC showed one large peak of AmB and a much smaller peak ahead of it as before. The small peak was collected by prep-HPLC and dried, giving a total weight of 20.3 mg, 1.91 mg of heptaene and 1.43 mg of tetraene. Analysis by LCMS again showed only one peak in the 405 nm wavelength, with a mass of 924 Da ($M+H^+$).

Processing of this second growth is shown in scheme 19

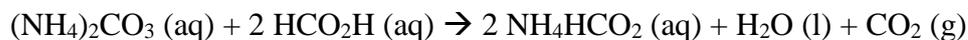
It was hypothesised that the formic acid present in the HPLC solvent may be causing breakdown of the product, which due to the large number of runs required to avoid overloading the column was only present in very dilute quantities. Removal of the formic acid from the solvent resulted in very poor separation of all products, and the concentration (0.01%) has already been proved to be the minimum quantity required for effective separation. It was therefore investigated whether immediately neutralising the formic acid upon each fraction's emergence from the collecting arm would be effective in countering this problem.



Scheme 19: Processing of second NypY modified growth

Ammonium carbonate was chosen to neutralise the acid. Other work in the lab by a masters student using sodium carbonate to neutralise an acidic reaction had shown that the resulting sodium formate was very difficult to remove from the amphotericin afterwards. Using ammonium carbonate would produce ammonium formate which is

volatile so easily removed during the lyophilisation process necessary to remove the water.



A saturated solution of ammonium carbonate was prepared and tested upon fraction tubes containing 5 ml of prep-HPLC eluent. The pH was monitored by tricolour pH paper.

Tube number	NH ₄ CO ₃ solution added (μl)	Resultant pH
1	0	4
2	50	7
3	100	8
4	30	6.5
5	40	7
6	35	7

Table 15: Testing quantities of ammonium carbonate to neutralise HPLC fractions

From this it appears that 35 μl of sat. NH₄CO₃ solution adequately neutralises the residual formic acid in each tube.

Methanol extracts 7 to 14 from growth 2 were combined, giving a total weight of 2.038 g, containing 130 mg heptaene and 74.8 mg tetraene. The sample was washed with diethyl ether (3x40 ml), water (1x35 ml) and ethyl acetate (1x35 ml), all washings were carefully examined by UV/Vis spectroscopy, only the water contained heptaene (0.98 mg), along with tetraene (7.62 mg). The ethyl acetate contained no heptaene and

12.7 mg of tetraene. The remaining 352.2 mg of impure sample contained 110 mg heptaene and 38.2 mg tetraene by UV/Vis. Analytical HPLC showed the large AmB peak with the smaller peak before it, but LCMS showed that both peaks only contained a species with a mass of 924 Da ($M+H^+$).

Four further growths were produced, under similar conditions, from new deep frozen samples each time. All growths exhibited the same pattern of a smaller peak ahead of the large one. LCMS analyses showed the small peak in all samples to have the same mass (924 Da $M+H^+$) as the larger one. It is hypothesised that this small peak is an isomer of amphotericin B, for example a reversed chiral centre. If the chiral centre contained a hydroxyl group being shifted to a new configuration, this could account for the small increase in polarity resulting in the isomer's shorter retention time on the reverse-phase chromatography column. An NMR of the product collected from the smaller fraction was taken, but a difference from normal AmB could not be determined, as the changed signal could be hidden under others in a cluttered region.

Seventh growth

Since the plasmid upon which the new DNA was transferred to the bacteria also contains a thiostrepton (**78**) resistance gene, this being the method by which those bacteria which have not taken up the plasmid are suppressed, it was investigated whether increasing the concentration of thiostrepton in the growth media might permit production of the desired disaccharide analogue.

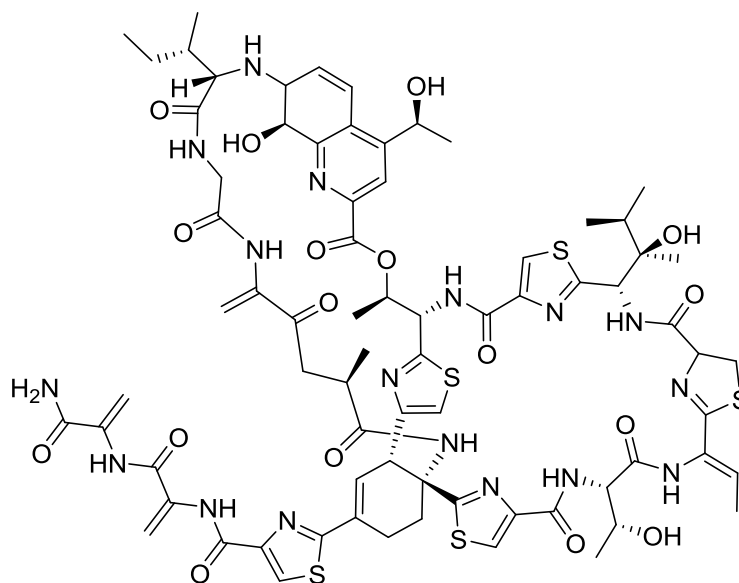


Figure 78: Thiostrepton

A starter flask was prepared containing the glucose and yeast solution as before. A fresh deep-frozen bacteria sample was added, and thiostrepton to a concentration of 100 $\mu\text{g/ml}$ (double that of previously). After incubating for three days, bacterial spores were observed in clear liquid as usual. Eight flasks of fructose-dextrose-soya medium were prepared, inoculated with 10 ml of starter culture under sterile conditions, and thiostrepton added to a concentration of 70 $\mu\text{g/ml}$.

The flasks were incubated with shaking at 30°C, four of the flasks had their contents drained and lysed after five days, the other four after seven days. This was to establish whether an extra two days in the incubator would affect yields, or whether it would be necessary to give the bacteria extra time to grow in the media when it contained a higher concentration of thiostrepton.

The five-day mycelia was extracted with methanol five times. to give a total sample weight of 6.12 g containing by UV/Vis 168 mg heptaene and 61 mg tetraene.

The seven-day mycelia were also extracted with methanol five times, to give a total weight of 5.47 g containing 184 mg heptaene and 52 mg tetraene. This is a slightly

higher yield of heptaene from the flasks that were incubated two days longer but it is thought this is not a large enough difference to be significant and can be accounted for by the normal variability between any two flasks of a growth.

Both samples were washed with diethyl ether (3x40 ml) and examined by analytical HPLC. Both samples only showed one large peak corresponding to AmB with no evidence of the smaller peak observed in previous growths. The mass was confirmed by LCMS as 924 Da ($M+H^+$), with no evidence of a species of mass 1086 Da ($M+H^+$) present in either extract.

Eighth growth

To investigate whether the temperature of incubation might be affecting the stability of the disaccharide during the growth period, eight flasks of fructose-dextrose-soya medium were prepared, inoculated with 10 ml of starter culture and thiostrepton to a concentration of 50 $\mu\text{g/ml}$ (back to the usual concentration, since thiostrepton is expensive), and incubated with shaking for 6 days at 25°C. The hypothesis being that the new glycosidic bond formed could be vulnerable to hydrolysis by enzymes or other reactive species that may be present in the bacterial cell or the aqueous growth medium, for example digestive enzymes sequestered by the bacteria into their environment.

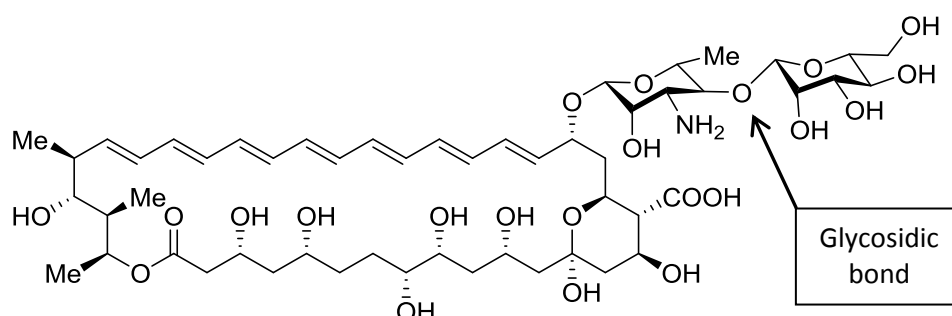


Figure 76a: mannosyl-amphotericin B

After six days the flask contents were drained and lysed in methanol. Six extracts were taken, giving a total mass of 4.25 g containing by UV/Vis 25.0 mg heptaene and 5.7 mg tetraene. The extract was washed with diethyl ether (2x35 ml) and examined by analytical HPLC, only one peak at 405 nm was observed conforming to AmB, the mass was confirmed as 924 Da ($M+H^+$) by LCMS.

The low yield from this growth also confirmed that an incubation temperature of $\sim 30^\circ\text{C}$ is necessary for efficient production of AmB.

Ninth Growth

Further to the hypothesis that disaccharide amphotericins might not be stable enough to survive long incubation periods, this growth was incubated for a short period then all extraction done as quickly as possible, to minimise the time that the amphotericins were exposed to destructive factors.

Eight flasks of fructose-dextrose-soya medium were prepared, inoculated with 10 ml of starter culture and incubated at 30°C with shaking. Four of the flasks were incubated for 1.5 days (part a), the other four for 2.5 days (part b). Upon harvesting, the mycelia were separated from the aqueous growth media by centrifugation at 13,000 rpm for 20 minutes, the supernatant being retained, and the cell mass was extracted six times with methanol in an ultrasonic bath in one day. The ultrasound helping to lyse the cell contents as quickly as possible.

The aqueous growth media supernatant was found by UV/Vis to contain heptaenes and tetraenes, so the liquid (~ 1 litre) was shaken with butan-1-ol (~ 300 ml) and allowed to separate. The organic layer was isolated and dried under vacuum, with the addition of ~ 100 ml of water to form an azeotrope to facilitate evaporation.

The methanolic extracts were combined, the volatile solvent removed under vacuum and the aqueous component refrigerated to precipitate polyenes, which were collected by centrifugation at 6,000 rpm for 15 minutes. The aqueous layer was found by UV/Vis to contain no polyenes and was discarded. The results are summarised in the table below.

Sample	Methanolic extract	Butanolic extract
Part a	943 mg total, 1.8 mg heptaene	1.943 g total, 37 mg heptaene
Part b	599 mg total, 12.6 mg heptaene	737 mg total, 35 mg heptaene

Table 16: Extracts of mannosyl-AmB growth 9.

All extracts were examined by analytical HPLC and LCMS. Both butanolic extracts contained only one peak on HPLC, identified as 924 Da ($M+H^+$) by LCMS. The methanolic extract from part a also contained only AmB, however part b showed two peaks at 405 nm on analytical HPLC (see figure **79** below). The sample was washed with ether (1x35 ml) to remove lipids then preparative HPLC was performed to isolate these two peaks which were then analysed by LCMS. The new peak (marked) was found by LCMS to contain a species with a mass of 1086 Da ($M+H^+$). (See figures **80** and **81** below) However, upon drying this fraction was found to have a mass of 0.6 mg and, as can be seen from the LCMS, contained roughly equal quantities of 924 Da ($M+H^+$) and 1086 Da ($M+H^+$) species. 1H NMR was attempted, but the mass was too low to give acceptable resolution.

From this, it is deduced that the plasmid-modified bacteria do appear to produce mannosylated-AmB, but in very small quantities, and these small quantities do not survive the incubation environment long enough to be isolated and purified. If such a compound were ever to be clinically useful, far more efficient production by the bacteria would be required.

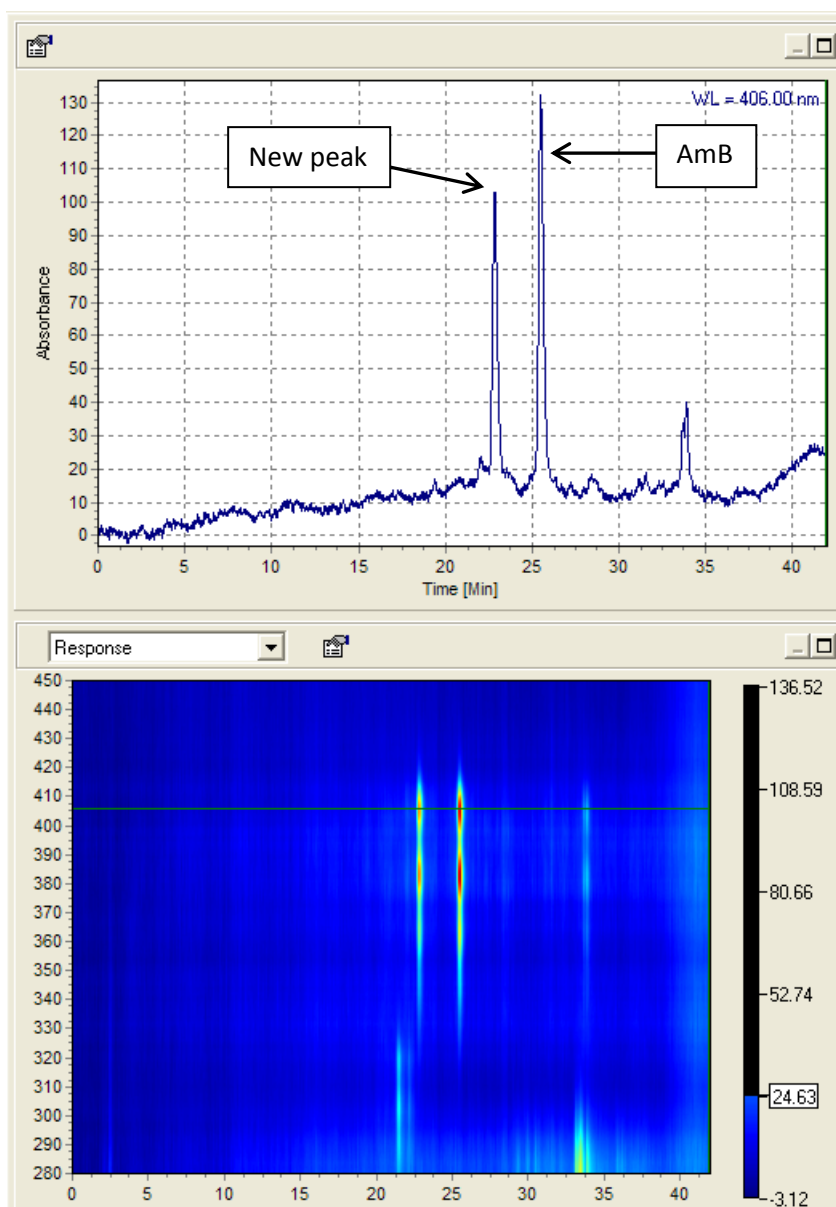


Figure 79: Analytical HPLC of 9b methanolic extract.

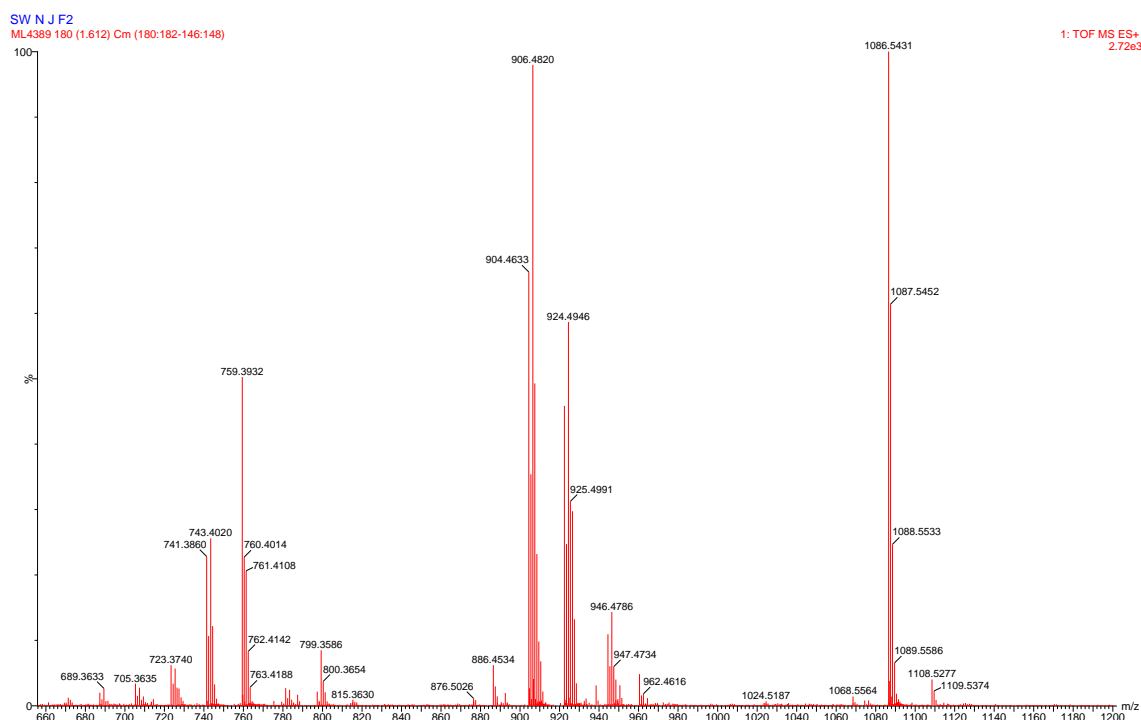


Figure 80: LCMS of analytical HPLC fraction containing putative mannosyl-AmB

Elemental Composition Report: SW N J F2							
Elements Used:							
C: 53-53		H: 0-180		N: 0-50		O: 0-50	
Minimum:				-1.5			
Maximum:				5.0	6.0	80.0	
Mass	Calc. Mass	mDa	PPM	DBE	i-FIT	i-FIT	Formula
1086.5431	1086.5485	-5.4	-5.0	12.5	53.0	0.2	C53 H84 N O22

Figure 81: Elemental composition report of putative mannosyl-AmB

To summarise:

Growth 1 followed the standard eight-flask recipe as used in chapter 2, no mannosylated products could be identified.

Growth 2 comprised 16 flasks, but was otherwise unchanged, a new small peak was observed by HPLC, but was shown by LCMS to have an equal mass to AmB.

Growths 3-6 used fresh deep frozen samples in the starter flasks, and the HPLC fractions neutralised by ammonium carbonate, enough of the smaller HPLC peak was collected to perform a proton NMR, but no difference from AmB could be identified.

Growth 7 used an increased (doubled) concentration of the thiostrepton antibiotic, this had no discernible effect on the products from the bacteria.

Growth 8 investigated the effect of growing bacteria at a lower temperature (25°C), a much lower yield of AmB was obtained showing that 30°C is required for efficient production, no mannosylated product was detected.

Growth 9 used a short growth time and rapid extraction to minimise the possible time for breakdown of any mannosylated molecules that may have formed. A very small quantity of putative mannosyl-AmB (or a mass corresponding to such on LCMS) was detected by LCMS but could not be isolated.

In conclusion, this bacterium does produce a molecule with a mass corresponding to mannosyl-AmB (**76**), but only at levels too low for the molecule to be isolated and definitively characterised.

3.3 Mannosyl-7-oxo-amphotericin B (**82**)

Since mannosylated AmB was deemed to not be viable, Caffrey also transfected the pLAGO-nypY plasmid into the KR16 mutant *S. nodosus* strain⁹⁴. This strain has had the keto-reductase module 16 genes knocked out and usually produces 7-oxo-amphotericin B (**29**).

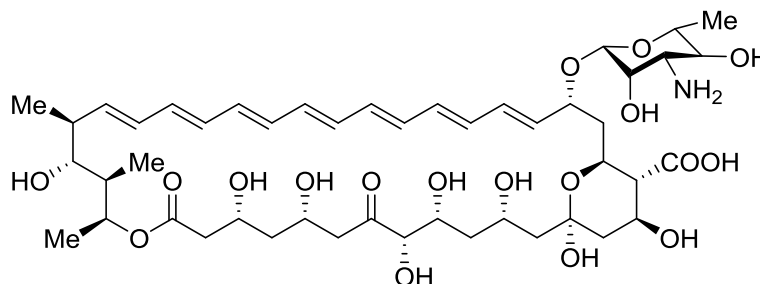


Figure 29: 7-oxo-amphotericin B

The carbonyl group on carbon-7 would normally be reduced twice to leave a CH₂ in that position on the aglycone, which would then be functionalised by further PKS genes as discussed in section 1.8. However, Caffrey found that by knocking out these genes⁶⁹ the keto group remains on the aglycone but this molecule is still functionalised by the same PKS genes, which are not specific enough to reject this altered substrate.

The additional carbonyl group is located remotely from the mycosaminyl moiety so the function of the *nypY* genes to add the mannosyl group should not be affected.

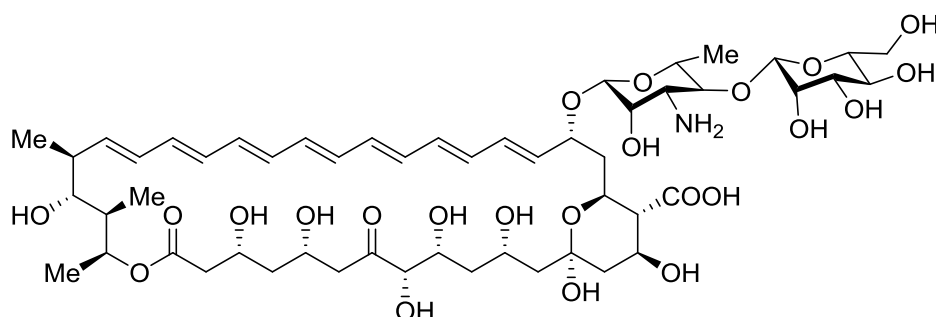


Figure 82: mannosyl-7-oxo-amphotericin B

Growth 1

2 starter flasks of GYE media, neutralised to pH 7 with sodium hydroxide, were prepared, and inoculated with deep-frozen bacteria samples from Caffrey. After two days incubation with shaking, bacteria spores in clear liquid were observed.

8 flasks of fructose-dextrose-soya medium were prepared, inoculated with 10 ml of starter culture from one flask and thiostrepton to a concentration of 50 µg/ml, and incubated for 4 days at 30°C with shaking. The mycelia were separated by centrifugation at 13,000 rpm for 20 minutes. UV/Vis showed no polyenes in the aqueous layer which was discarded.

The mycelia were lysed in methanol. The methanolic extract had the volatiles removed under vacuum and the residual water was refrigerated overnight. The yellow

precipitate was collected by centrifugation at 6,000 rpm for 15 minutes. A total weight of 1.42 g was collected with a polyene content by UV/Vis of 34.5 mg heptaene and 10.2 mg tetraene.

Analytical HPLC analysis showed the presence of heptaene in the aqueous supernatant, the absorbance at 405 nm was a broad peak so at this stage it cannot be determined how many different species of heptaene were present, but the supernatant was retained for further study.

The mycelia were extracted four times with methanol, in each case after centrifugation of residual water HPLC showed the presence of heptaenes in the aqueous supernatant so they were also retained, the precipitates are tabulated below.

Extract	Total mass	Heptaene	Tetraene
1	1.42 g	34.5 mg	10.2 mg
2	1.92 g	20.7 mg	5 mg
3	1.14 g	12.3 mg	1.6 mg
4	1.03 g	<1 mg	trace

Table 17: Extracts of mannosyl-7-oxo-AmB growth 1

The precipitate from extract 4 was discarded. The four combined aqueous supernatants were found by UV/Vis to contain 27.3 mg heptaene and 18.4 mg tetraene. It appears that the addition of a carbonyl group in this amphotericin makes it considerably more water soluble than previous variants studied. This aqueous sample was extracted twice with butan-1-ol and the organic layer dried to give a mass of 220 mg. Multiple peaks at 405 nm appeared on the analytical HPLC trace (see figure **83** below) so the sample was separated by preparative HPLC. The higher concentration of compound used in prep-HPLC meant that only three distinct peaks were observed. These three fractions were collected and examined by LCMS. Fraction 1 (mass 25 mg) contained only 938 Da, fraction 2 (figures **84** and **85**) (mass 7 mg) contained both 938

and 1100 Da ($M+H^+$), fraction 3 (the largest peak, mass 51.8 mg) contained only 938 Da ($M+H^+$), corresponding to 7-oxo-amphotericin B.

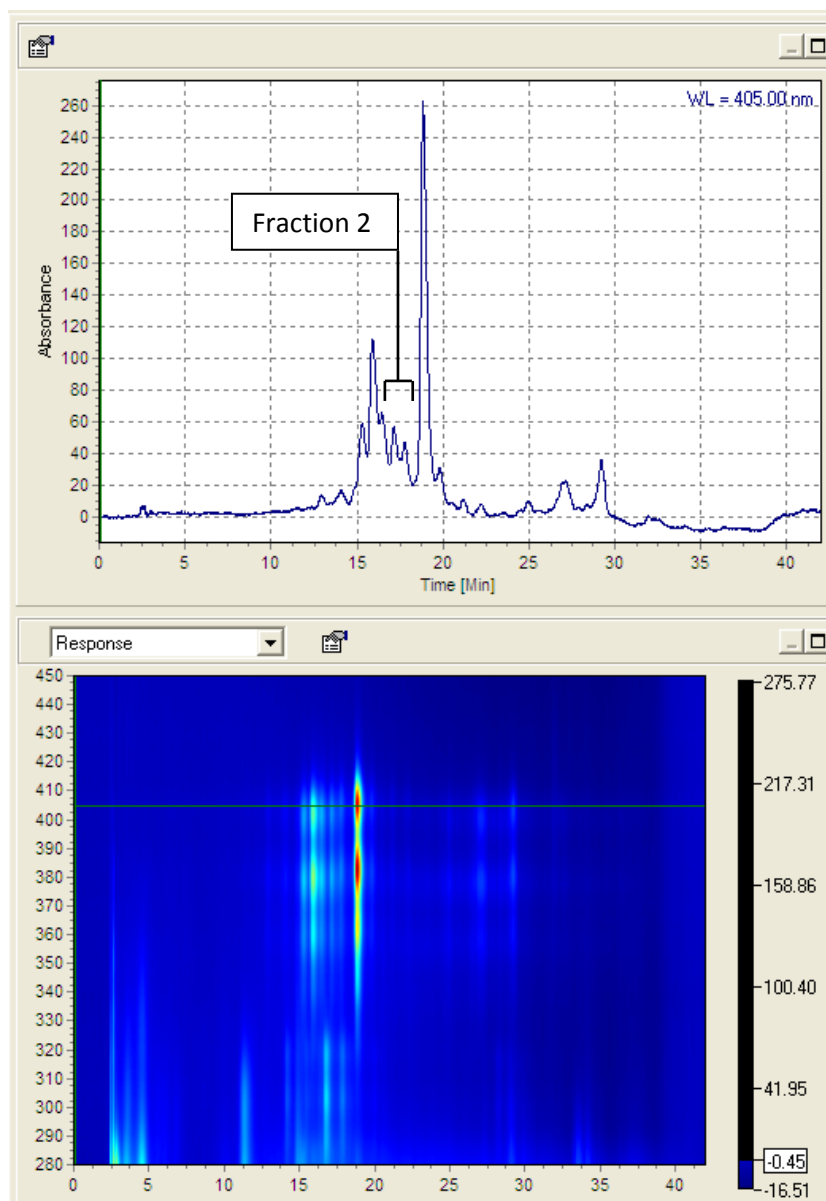


Figure 83: Analytical HPLC of growth 1 aqueous supernatant butanol extraction.

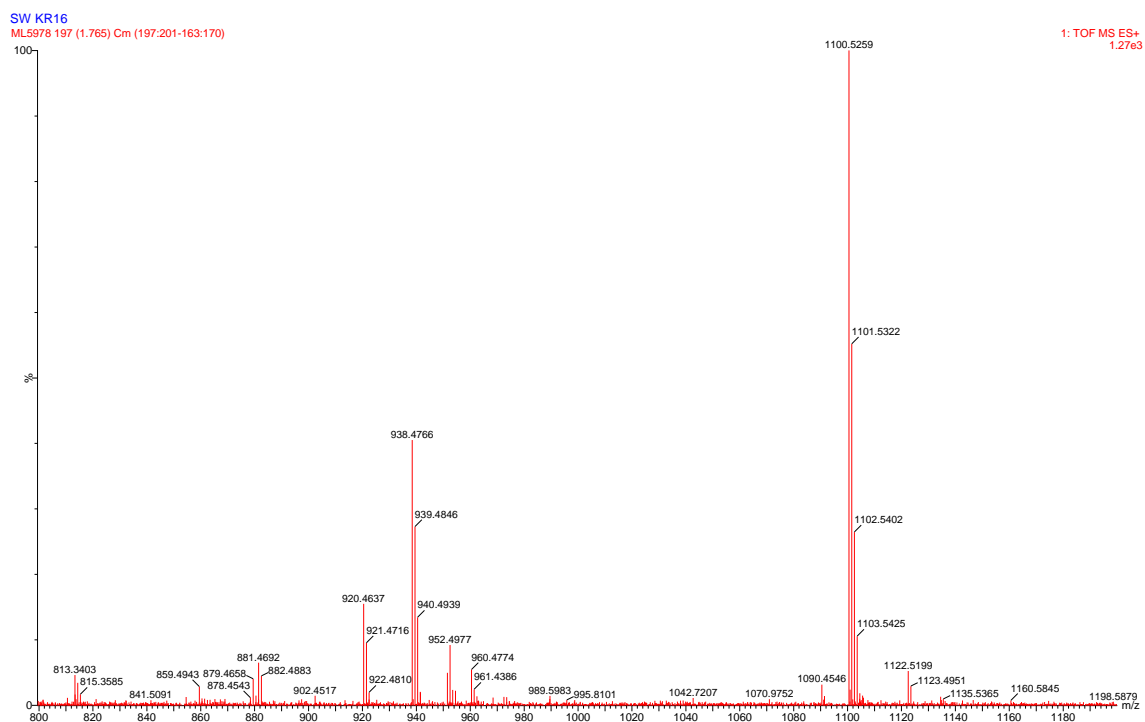


Figure 84: LCMS of Fraction 2 in figure 83

Elemental Composition Report: SW KR16							
Elements Used:							
C: 53-53 H: 0-180 N: 0-20 O: 0-30							
Minimum: -1.5							
Maximum: 5.0 5.0 80.0							
Mass	Calc. Mass	mDa	PPM	DBE	i-FIT	i-FIT	Formula
1100.5259	1100.5278	-1.9	-1.7	13.5	50.3	0.0	C53 H82 N O23

Figure 85: Elemental composition report of 1100 Da peak in figure 84.

After the volatile methanol had been removed from fraction 3 under vacuum, the aqueous component was stored in the refrigerator overnight due to the lyophiliser being temporarily unavailable. The following day crystals were observed to have formed, however upon X-ray diffraction they were discovered to be ammonium formate.

The precipitates from extracts 1-3 were combined to give a total weight of 4.48 g. This sample was washed with diethyl ether (3x40 ml) leaving 2.86 g, ethyl acetate (1x35 ml) leaving 2.50 g, and DCM (60 ml) leaving 2.23 g. The sample was then

washed once with cold water (10 ml) leaving 435 mg. This small volume of very cold water was to minimise losses of heptaene which was known to be potentially water soluble. The supernatant was tested by UV/Vis to contain 0.843 mg of heptaene and by analytical HPLC where only one peak appeared corresponding to 7-oxo-amphotericin B, it was concluded that no mannosylated form had been lost.

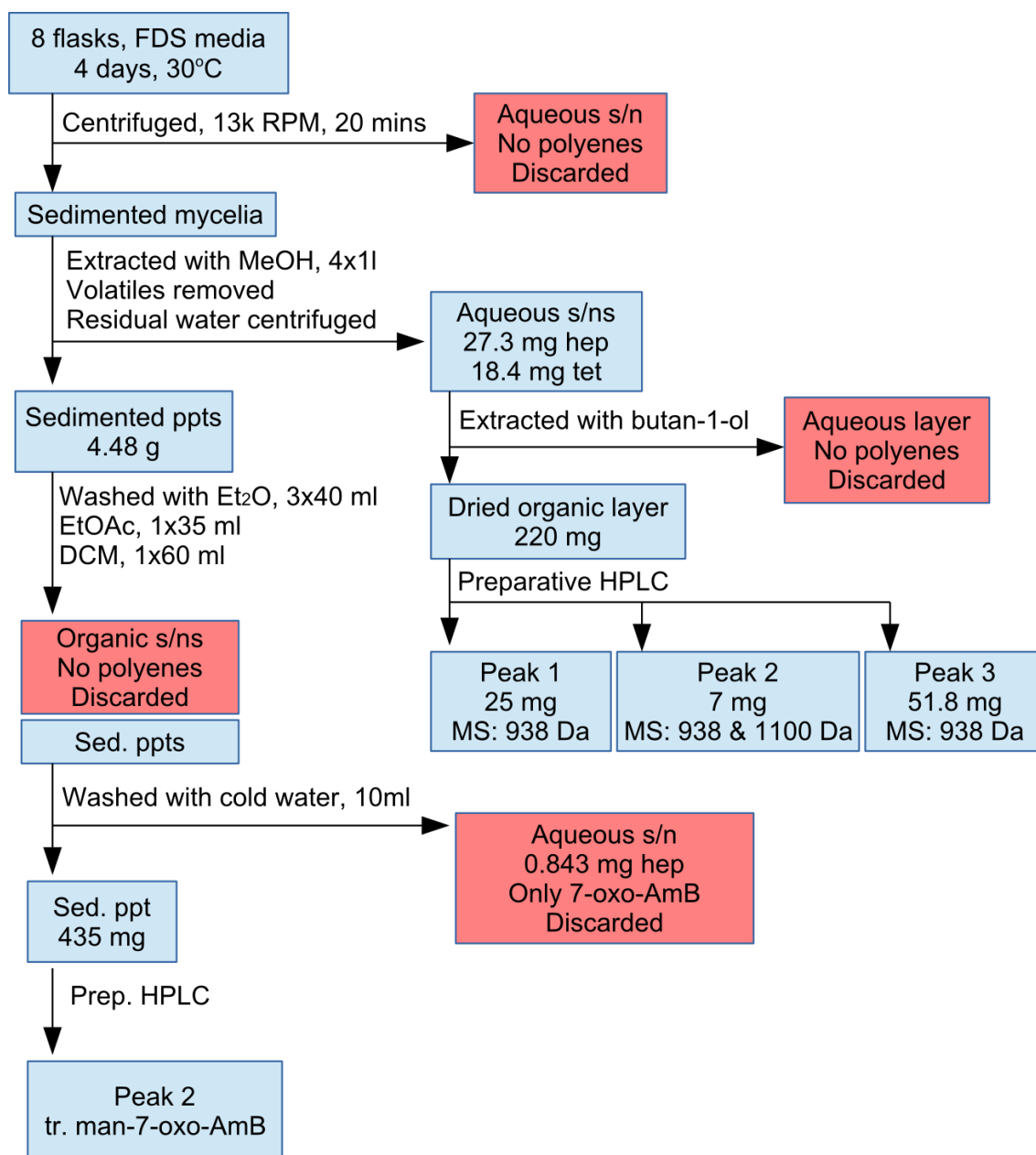
The washed sample was purified by preparative HPLC, the fractions tested by LCMS and again fraction 2 was found to contain a potentially mannosylated species. From this it is appears that mannosyl-7-oxo-amphotericin B was produced, though still only in very small quantities.

Processing of this growth is shown in scheme 20.

Growth 2

8 flasks of fructose-dextrose-soya medium were prepared, inoculated with 10 ml of starter culture under sterile conditions and thiostrepton to a final concentration of 50 µg/ml. The flasks were incubated for 6 days at 30°C with shaking. The media was strained through muslin cloth to collect mycelia which were extracted in methanol five times. The first extract was lost due to a cracked erlenmyer flask. Each subsequent extract had the volatiles removed and the precipitates collected. The aqueous supernatants contained polyenes by UV/Vis so were extracted with butan-1-ol, the results are shown in table 18 below.

The butanol extracts were combined to give a total weight of 1.19 g, the sample was washed with diethyl ether (40 ml) and ethyl acetate (35 ml) and separated by preparative HPLC to give four fractions (table 19).



Scheme 20: Processing of first KR16 NypY growth

Extract	Precipitate	Butanol
2	615 mg total 22 mg heptaene	451 mg total 33 mg heptaene
3	562 mg total 21 mg heptaene	340 mg total 11 mg heptaene, 4.2 mg tetraene
4	400 mg total 15.6 mg heptaene	283 mg total 18 mg heptaene
5	237 mg total 2.6 mg heptaene	271 mg total 12.2 mg heptaene

Table 18: Mycelia MeOH extracts of mannosyl-7-oxo-AmB growth 2.

Fraction	Total mass	Mol. masses present	Conclusions
1	38.5 mg	938	Isomer of 7-oxo-AmB
2	27.1 mg	938 + 1100	7-oxo-AmB + mannosyl form
3	45.4 mg	938	7-oxo-AmB
4	171.6 mg	749	7-oxo-aglycone

Table 19: prep-HPLC fractions of mannosyl-7-oxo-AmB growth 2

The combined precipitate samples, total mass 1.73 g, were washed with diethyl ether (3x35 ml), and a liquid/liquid extraction performed with water and butan-1-ol. This method was used in lieu of a water wash to prevent loss of heptaene which would otherwise dissolve in the water. The aqueous layer was examined by analytical HPLC and UV/Vis spectroscopy, and found to contain 0.68 mg heptaene, all of it 7-oxo-amphotericin B.

The organic layer was dried, total mass 402 mg, and was separated by preparative HPLC into two fractions. Fraction 1, total mass 38.9 mg, was shown by LCMS to contain both 7-oxo-amphotericin B and the putative mannosylated form. Fraction 2, total weight 119.9 mg, contained only 7-oxo-amphotericin B.

Growth 3

8 flasks of fructose-dextrose-soya medium were inoculated with 10 ml of starter culture and 50 µg/ml of thiostrepton and incubated with shaking at 30°C for 6 days. The mycelia were collected by straining through muslin cloth and the aqueous media extracted with butan-1-ol. The organic layer was dried to give a total mass of 4.56 g, this was washed with diethyl ether (3x35 ml) to leave 3.73 g.

The mycelia were extracted five times in methanol, in each case the methanol being removed under vacuum and the residual water refrigerated to precipitate polyenes. The precipitate was collected by centrifugation and the aqueous supernatant was extracted with butanol-1-ol. The results are tabulated below.

Extract	Precipitate	Butanol extract
1	366 mg total 4.3 mg heptaene	286 mg total 5.4 mg heptaene
2	593 mg total 18.2 mg heptaene	306 mg total 14.5 mg heptaene
3	299 mg total 4.5 mg heptaene	226 mg total 6.4 mg heptaene
4	470 mg total 12 mg heptaene	228 mg total 5.4 mg heptaene
5	119 mg total 1.8 mg heptaene	142 mg total 2.3 mg heptaene

Table 20: MeOH mycelia extractions of mannosyl-7-oxo-AmB growth 3

The butanol extracts were combined, total mass 983 mg, washed with diethyl ether (2x35 ml), filtered through silica and separated by preparative HPLC, three fractions were obtained.

Fraction	Total mass	Molecular masses by LCMS (M+H⁺)
1	79.4 mg	938
2	13 mg	938 + 1100
3	82.3 mg	938

Table 21: prep-HPLC fractions of mannosyl-7-oxo-AmB growth 3 water/butanol extracts

The precipitates were combined, total mass 1.75 g, washed with diethyl ether (3x35 ml), filtered through silica and separated by preparative HPLC, three fractions were obtained.

Fraction	Total mass	Molecular masses by LCMS
1	Not measured	No UV active compounds, discarded
2	18.4 mg	938 + 1100
3	22.9 mg	938

Table 22: prep-HPLC fractions of mannosyl-7-oxo-AmB growth 3 water precipitates

A liquid/liquid water/butanol extraction was performed on the media extract. The organic layer was dried, total weight 214 mg, and separated by preparative HPLC. Two fractions were obtained.

Fraction	Total mass	Molecular masses by LCMS
1	13.5 mg	938 + 1100
2	80 mg	938

Table 23: prep-HPLC fractions of mannosyl-7-oxo-AmB growth 3 media butanol extraction

All fractions containing amphotericins were retained for further study.

Growth 4

8 flasks of fructose-dextrose-soya medium were prepared, inoculated with 10 ml of starter culture and 50 µg/ml of thiostrepton and incubated with shaking at 30°C for 6 days. The mycelia were collected by straining through muslin cloth and the growth media extracted with butan-1-ol twice.

The butanol extracts were dried to give a total mass of 11.16 g, this was washed with water (35 ml) and diethyl ether (35 ml).

The drained flasks were rinsed with methanol to remove mycelia stuck to the sides, the rinsings allowed to lyse for a few hours then filtered. The methanol was removed under vacuum and the water refrigerated to precipitate polyenes. The precipitate was collected by centrifugation and found to have a total mass of 862 mg containing 6 mg of heptaene, which was shown by analytical HPLC to be only 7-oxo-amphotericin B (one 405 nm peak), this was discarded.

Five methanol extracts were taken of the mycelia, each having the volatiles removed under vacuum, the water refrigerated overnight then centrifuged, and the supernatants extracted with butan-1-ol. The results are tabulated below.

Extract	MeOH precipitate	BuOH extract
1	1.05 g total 22 mg heptaene	670 mg total 11 mg heptaene, 32 mg tetraene
2	927 mg total 42 mg heptaene	853 mg total 13 mg heptaene, 36 mg tetraene
3	461 mg total 24.7 mg heptaene	544 mg total 11 mg heptaene, 25 mg tetraene
4	376 mg total 4.5 mg heptaene	251 mg total 6.5 mg heptaene, 12.5 mg tetraene
5	274 mg total 1.2 mg heptaene	163 mg total 3.6 mg heptaene, 4 mg tetraene

Table 24: mannosyl-7-oxo-AmB growth 4 mycelia MeOH extractions

The precipitates were combined to give a total mass of 3.44 g, and a heptaene content by UV/Vis of 78 mg. The butanol extracts were combined to give a total mass of 2.28 g and by UV/Vis a heptaene content of 45 mg and a tetraene content of 109 mg.

The precipitate sample was washed with diethyl ether (3x35 ml), dissolved in methanol and filtered through a plug of silica 60. It was separated by preparative HPLC to give three fractions of mass 86.8 mg, 43.1 mg and 202.4 mg. The fractions were analysed by LCMS and the first was found to contain a mass of 1100 Da ($M+H^+$) corresponding to putative mannosyl-7-oxo-amphotericin B.

The butanol sample was washed with diethyl ether (1x125 ml) and filtered through a plug of silica 60 in methanol. A test run of preparative HPLC showed poor separation of peaks, so a liquid/liquid water/butanol extraction was performed. The aqueous layer was shown by analytical HPLC to contain a very small quantity of only 7-oxo-amphotericin B so was discarded. The organic layer was dried to give a total mass of 1.316 g containing by UV/Vis 38 mg heptaene and 102 mg tetraene. This was separated by preparative HPLC to give three samples of mass 95 mg, 57 mg and 93.7 mg. Analysis by LCMS showed putative mannosylated compound in the first fraction.

Growth 5

Since earlier experimentation attempting to extract mannosylated amphotericin B appeared to show that even if the disaccharide form were produced, it did not survive the five day incubation period; and that the only trace of the compound was discovered by growing the bacteria for a shorter time and processing the mycelia quickly, a similar attempt was made for this mannosyl-7-oxo-amphotericin B to investigate whether higher yields of mannosyl-7-oxo-amphotericin B might be obtained.

Eight flasks of fructose-dextrose-soya medium were prepared, inoculated with 10 ml of starter culture and 50 µg/ml thiostrepton and incubated with shaking for 60 hours. The mycelia were collected by centrifugation at 13,000 rpm for 20 minutes. The mycelia were extracted six times in methanol with sonication, the volatiles were removed under vacuum and the water chilled and centrifuged at 6,000 rpm for 15 minutes to give a total mass of 1.16 g, analysed by UV/Vis to show 1.3 mg of heptaene and 2 mg of tetraene.

The aqueous supernatant was extracted with butan-1-ol (2x50 ml), which was dried to give a total mass of 1.42 g, analysed by UV/Vis to show no heptaene and 4.2 mg tetraene.

The aqueous media supernatant was extracted with butan-1-ol (2x300 ml) which was dried, the solid suspended in methanol (200 ml), filtered and dried to give a total mass of 3.06 g, analysed by UV/Vis to show no polyenes.

Analytical HPLC of the precipitate sample showed only heptaene and tetraene aglycones, and of the supernatant butanol extraction sample showed only tetraene aglycone.

From this it was concluded that 7-oxo-amphotericin requires the full incubation period to be produced.

Collation of Prep-HPLC fractions

So far preparative HPLC had separated the putative mannosyl-7-oxo-amphotericin B from the bulk of the impurities but not all, LCMS analyses showed the continued presence of tetraenes and some 7-oxo-AmB in gathered fractions. All fractions that had been shown by LCMS to contain a mass corresponding to mannosyl-7-oxo-AmB were

combined to give one sample with a total mass of 403 mg. This was isolated by preparative HPLC to give three fractions, each corresponding to a peak in the 405 nm wavelength.

Fraction	total mass	LCMS (M+H ⁺)	UV/Vis
1	22.6 mg	938 Da	
2	2.1 mg	938 + 1100 Da	0.9 mg heptaene
3	37.6 mg	938 Da	

Table 25: prep-HPLC fractions of collated prep-HPLC fractions of mannosyl-7-oxo-AmB

A proton NMR of fraction 2 in methanol-d₄ was attempted, but the purity was too low for acceptable resolution to be obtained. Accurate mass analysis by LCMS however, did confirm the compound present to have the expected atomic makeup of mannosyl-7-oxo-AmB (figures 86 and 87).

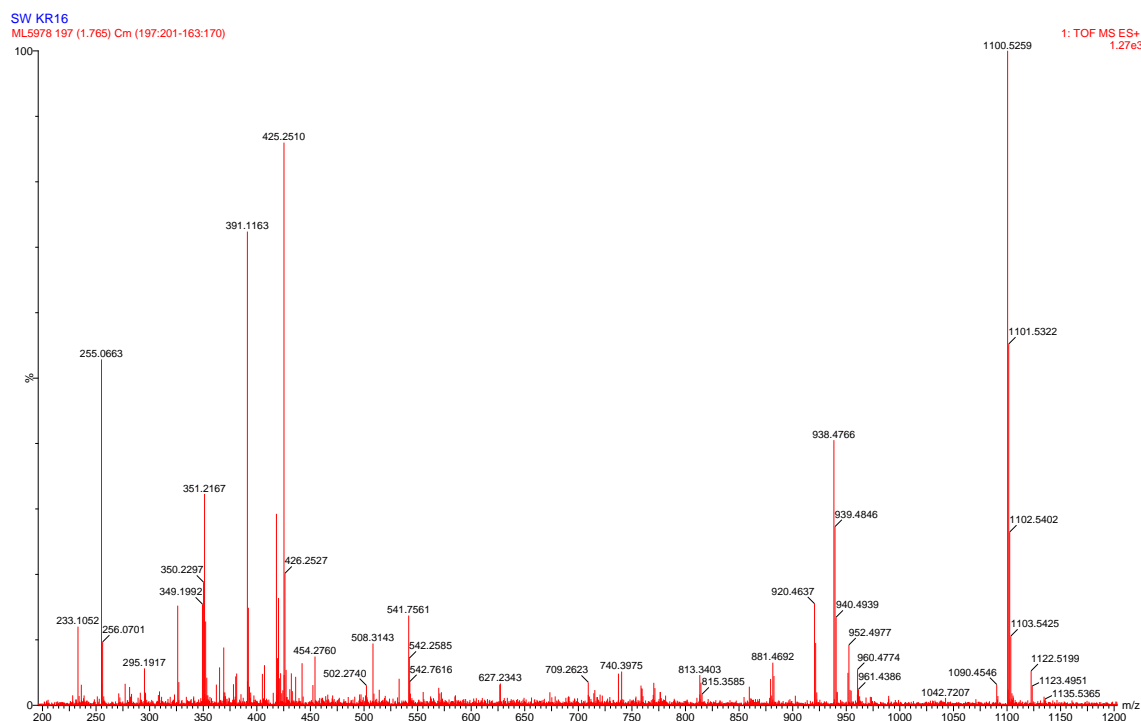


Figure 86: LCMS of fraction 2 from table 25

Elemental Composition Report: SW KR16							
647 formula(e) evaluated with 1 results within limits (all results (up to 1000) for each mass)							
Elements Used:							
C: 53-53 H: 0-180 N: 0-20 O: 0-30							
Minimum: -1.5							
Maximum: 5.0 5.0 80.0							
Mass	Calc. Mass	mDa	PPM	DBE	i-FIT	i-FIT (Norm)	Formula
1100.5259	1100.5278	-1.9	-1.7	13.5	50.3	0.0	C53 H82 N O23

Figure 87: Elemental composition report of 1100 Da peak in figure 86

Summary

Five bacterial growths of putative mannosyl-7-oxo-AmB only resulted in enough product to perform an LCMS, which confirmed that a molecule with the expected mass of 1100 Da ($M+H^+$) was produced but in too small a quantity to be isolated, purified and tested.

An attempted short growth produced only aglycones showing that the full incubation period was required for 7-oxo-AmB production.

3.4 Mannosyl-8-deoxy-amphotericin B

Caffrey also transfected the pIAGO-nypY plasmid into the *amphL* mutant, which normally produces 8-deoxyamphotericin B (**27**) due to having had the PKS module *amphL* knocked out so the carbon at position 8 remains unhydroxylated.

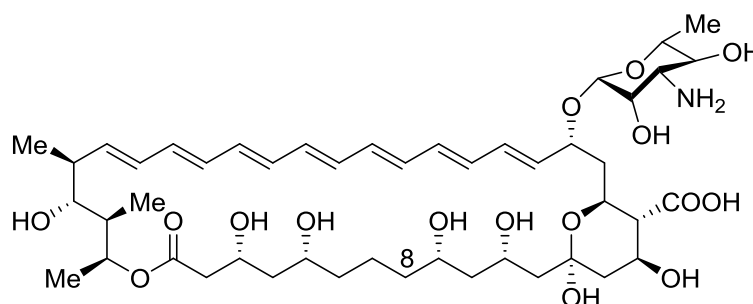


Figure 27: 8-deoxyAmB

This mutant also contains a hygromycin (**88**) resistance gene, so cultures are grown in media containing both thiostrepton and hygromycin, at concentrations of 50 µg/ml each.

Starter flasks containing 100 ml autoclaved GYE media were inoculated under sterile conditions with deep-frozen glycerol suspensions of bacteria supplied by Caffrey, thiostrepton and hygromycin to concentrations of 50 µg/ml were also introduced at this time, the flasks were incubated with shaking for two days at 30°C. If the media remained clear when the flask was allowed to settle then it was deemed fit for further use, if the media was cloudy then it had become contaminated by other bacteria and was discarded.

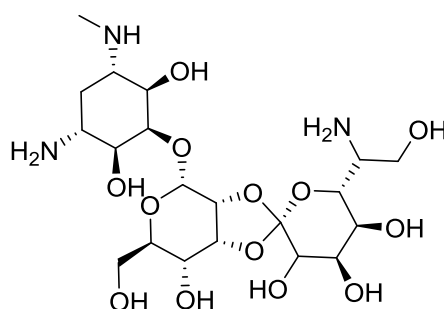


Figure 88: Hygromycin

Growth 1

Sixteen flasks of autoclaved fructose-dextrose-soya medium were inoculated with 10 ml of starter culture, thiostrepton and hygromycin were added to a concentration of 50 µg/ml. The flasks were incubated with shaking for 6 days at 30°C.

Ten of the flasks became thick and brown and smelt earthy, six of the flasks turned thin and pink and smelt of vinegar, these six had become contaminated and were discarded.

The ten good flasks were strained through muslin to separate the mycelia from the aqueous media, the media was tested by analytical HPLC and UV/Vis and found to contain no polyenes so was discarded. The mycelia were immersed in methanol to lyse cells and desorb polyenes from the amberlite beads. 19 methanol extractions were taken due to the apparent low solubility of the products in methanol. Each extract had the volatiles removed under vacuum, the residual water refrigerated, the precipitate collected by centrifugation at 6,000 rpm for 15 minutes. The solid was then analysed by UV/Vis spectroscopy in methanol, the results are tabulated below.

Extract	Precipitate	Extract	Precipitate
1	727 mg total 8.1 mg hep, 14.1 mg tet	11	673 mg total 20.6 mg hep, 8.8 mg tet
2	446 mg total 2.3 mg hep, 25.7 mg tet	12	672 mg total 18.7 mg hep, 5 mg tet
3	411 mg total 3.1 mg hep, 28.5 mg tet	13	412 mg total 26.7 mg hep, 3.3 mg tet
4	406 mg total 7.6 mg hep, 38.2 mg tet	14	836 mg total 15.6 mg hep, 21.4 mg tet
5	400 mg total 10.2 mg hep, 38.7 mg tet	15	463 mg total 33.2 mg hep, trace tet
6	327 mg total 12.2 mg hep, 28.9 mg tet	16	323 mg total 18.6 mg hep, trace tet
7	409 mg total 12.7 mg hep, 23.9 mg tet	17	192 mg total 20.2 mg hep
8	366 mg total 10.5 mg hep, 12.6 mg tet	18	102 mg total 10.5 mg hep
9	373 mg total 15 mg hep, 4.9 mg tet	19	155 mg total 8.1 mg hep
10	218 mg total 11.5 mg hep, 2.6 mg tet		

Table 26: MeOH mycelia extractions of mannosyl-8-deoxy-AmB growth 1

Extractions were stopped at 19 because analytical HPLC analysis of the extracts showed that the small peak thought to correspond to the mannosylated form had ceased to appear.

The extracts were combined to give a total weight of 6.64 g (278 mg hep, 242 mg tet), this was washed with diethyl ether (3x35 ml) removing 4.51 g of unwanted material. This was analysed by UV/Vis spectroscopy and found to contain no polyenes so was discarded.

The sample was washed with water (2x30 ml), these were also analysed by UV/Vis and found to contain 4.5 mg of heptaene and 25.6 mg of tetraene. Analytical HPLC showed these to be aglycones so the washings were discarded.

The remaining sample was dissolved in a large (~300 ml) volume of methanol and passed through a 3 cm column of silica gel 60. This was effectively using the silica as a filter aid to remove any components that adsorb strongly to silica and so prevent heavy fouling of the preparative HPLC column.

The solution before columning was a dark orange colour, the first ~200 ml of methanol to pass out of the column was a yellow colour (part 1), this was collected separately from the remaining ~100 ml of methanol (part 2) which was also orange. Finally 100 ml of methanol was run through the dry column to rinse through any remaining polyenes (part 3). See table 27

The three collected fractions were dried under vacuum and analysed.

	Total mass	UV heptaene	UV tetraene
Part 1	916 mg	141 mg	137 mg
Part 2	483 mg	23 mg	59.4 mg
Part 3	113 mg	36 mg	none

Table 27: Fractions of silica column of mannosyl-8-deoxy-AmB growth 1

This does not reveal any significant advantage in collecting multiple fractions from such a column.

Each of the component parts was separated by preparative HPLC, two fractions were collected in each case, the small earlier peak thought to correspond to the mannosylated heptaene (fraction 1), and the large later peak corresponding to the unmannosylated 8-deoxyAmB (fraction 2). Each collected fraction had the volatiles removed under vacuum and the water removed by lyophilisation. The results are tabulated below.

		Total mass	UV heptaene
Part 1	Fraction 1	20.2 mg	6.2 mg
	Fraction 2	83.9 mg	
Part 2	Fraction 1	33 mg	3.8 mg
	Fraction 2	117.7 mg	
Part 3	Fraction 1	44.6 mg	1.9 mg
	Fraction 2	36.8 mg	

Table 28: prep-HPLC fractions of mannosyl-8-deoxy-AmB growth 1

All fractions were dried then stored at -20°C for further investigation later.

Growth 2

A second growth was prepared. Eight flasks of autoclaved fructose-dextrose-soya medium were inoculated with 10 ml of starter culture, and thiostrepton and hygromycin to final concentrations of 50 µg/ml, incubated for five days and harvested by draining through muslin cloth. No flasks had to be discarded due to contamination. The aqueous media was examined by UV/Vis spectroscopy, found to be polyene free and discarded. The mycelia were lysed in methanol to extract polyenes. At first, four extracts were taken, tabulated below.

	Total mass	UV heptaene	UV tetraene
Extract 1	540 mg	1.8 mg	7 mg
Extract 2	548 mg	3.1 mg	10.7 mg
Extract 3	1.25 g	6.9 mg	18.2 mg
Extract 4	774 mg	9.5 mg	11 mg

Table 29: First MeOH mycelia extractions of mannosyl-8-deoxy-AmB growth 2

To prevent an inconveniently large number of extractions being required again, an alternative method was desirable.

Sodium thiocyanate (NaSCN) is a well known chaotropic agent. A chaotropic agent disrupts hydrogen bonding in solvents, usually water, thus affecting the native state of molecules in solution and decreasing the hydrophobic effect. Since amphotericin B is a fairly hydrophobic molecule and the 8-deoxy form even more so, it was theorised that the addition of sodium thiocyanate would increase the molecule's solubility in a polar solvent, in this case methanol.

A saturated solution of NaSCN in methanol was prepared and used to take a fifth extraction of the mycelia. When the solvent was removed under vacuum a large mass of oily yellow residue appeared in the flask. To this 100 ml of water was added and the solution centrifuged at 10,000 rpm at 1°C for 20 minutes. The supernatant was separated from the precipitate (mass 9.83 g) and both were examined by UV/Vis spectroscopy.

	UV heptaene	UV tetraene
Supernatant	6 mg	12.8 mg
Precipitate	48.4 mg	15.3 mg

Table 30: MeOH mycelia extraction number 5 of mannosyl-8-deoxy-AmB growth 2

Due to the presence of NaSCN, it was not possible to obtain analytical HPLC results for either the supernatant or the precipitate. The precipitate was washed with water (30 ml), the supernatant containing 3.1 mg heptaene by UV/Vis, to leave a total mass of 2.28 g.

Four more mycelia extractions were taken using methanol saturated with NaSCN.

Extract 6 had the volatiles removed leaving a thick orange oily mass with suspended white solids, to this 100 ml of water was added and centrifuged at 10,000 rpm and 1°C for 20 minutes. The precipitate was resuspended in another 100 ml of water and centrifuged again leaving a precipitate of mass 36.57 g.

The first aqueous supernatant showed 72.1 mg heptaene by UV/Vis, the second showed 13.7 mg heptaene. These two were combined and an extraction with butan-1-ol was attempted. However, probably due to the presence of NaSCN, the two solvents did not separate into two layers but formed a mixture. This mixture was reduced to approx half the volume under vacuum whereupon a precipitate was observed in suspension. The mixture was centrifuged to attempt to collect the precipitate with only partial success, much of the solid remained in suspension even after centrifugation at 13,000 rpm for 30 minutes. The sample was filtered to collect the yellow solid (16.66 g) and the filtrate examined by UV/Vis spectroscopy (3.5 mg heptaene, 2.7 mg tetraene).

The precipitate was suspended in ~100 ml THF and filtered leaving a white solid on the filter paper. This was to examine whether THF would dissolve the polyenes but not the NaSCN. The THF filtrate was dried to give a yellow solid of mass 16.405 g.

Extract 7 had the volatiles removed under vacuum and the remaining water was refrigerated overnight. The yellow solid formed was collected by centrifugation, the supernatant was examined by UV/Vis spectroscopy and found to contain 37.2 mg heptaene. This aqueous supernatant was dried on a rotary evaporator under very high vacuum to give a solid of mass 17.88 g. Lyophilisation was first attempted but found to be impracticable because the sample melted too quickly.

The precipitate was suspended in dry THF (~200 ml) and filtered leaving a white powder on the filter paper, the filtrate was dried to give a mass of 40.02 g, this was repeated to give a mass of 20.60 g, and again to leave a mass of 13.09 g. The dried supernatant was suspended in THF and filtered, the filtrate was dried to give a mass of 10.97 g.

So far it has been observed that while NaSCN does indeed help to extract polyenes from the mycelia, the NaSCN is subsequently very difficult to remove from the polyene sample due to its altering not only the solvation properties of the solvent but also the solvent's miscibility with other solvents (for example butan-1-ol and water).

Extract 8 was dried completely to give a yellow powder which was suspended in dry THF and filtered, leaving a white powder on the filter paper and an orange filtrate, which was dried to give a mass of 31.73 g, this was re-extracted with THF to give a mass of 15.49 g. UV/Vis analysis showed approx 51 mg heptaene.

Extract 9 was also dried and extracted with THF twice, mass 23.07 g, UV/Vis 32 mg heptaene.

Extracts 6 to 9 were combined, extracted twice with THF to give a mass of 16.29 g and a content of 84.3 mg heptaene by UV/Vis, this sample was stored at -20°C to await a better method of purification.

The first four extracts were combined, washed with ether (2x35 ml) and water (1x30 ml), and filtered through a plug of silica to give a total mass of 910 mg. This was separated by preparative HPLC to give two fractions. Fraction 1 (containing disaccharide) total mass 13.9 mg, heptaene by UV/Vis 3.72 mg. Fraction 2 (8-deoxyAmB) total mass 68.4 mg.

Growth 3

Eight flasks of fructose-dextrose-soya were prepared, autoclaved, and inoculated with 10 ml of starter culture, hygromycin and thiostrepton were added to final concentrations of 50 µg/ml. After incubating at 30°C for six days, the mycelia were collected by draining through muslin cloth. The media was examined by UV/Vis spectroscopy and found to contain polyenes so was extracted with butan-1-ol. The drained flasks were rinsed with methanol, the rinsings were filtered, the filtrate had the volatiles removed under vacuum and was refrigerated overnight to precipitate polyenes which were collected by centrifugation at 6,000 rpm for ten minutes. The mycelia were lysed once in pure methanol which was similarly treated. The results are tabulated below.

	Total mass	UV/Vis analysis
Butanol extraction	2.68 g	4.5 mg heptaene 5.1 mg tetraene
Flask rinsings	3.73 g	8.9 mg heptaene
Extract 1	1.04 g	1.1 mg heptaene 7.6 mg tetraene

Table 31: First extractions of mannosyl-8-deoxy-AmB growth 3

The three samples were combined (total mass 6.91 g), washed with diethyl ether (2x35 ml) and water (1x30 ml), remaining sample mass 811 mg, and separated by preparative HPLC to give two fractions. Fraction 1 (disaccharide) mass 7 mg, UV/Vis: 0.9 mg heptaene. Fraction 2 (8-deoxyAmB) mass 15.8 mg.

Five further extractions of the mycelia were taken using methanol saturated with NaSCN. Each extract was dried fully, resuspended in THF (~200 ml) and filtered, each filtrate then being reduced to approximately half the volume under vacuum, and filtered again to remove the white powder. all five filtrates were combined and the volatiles removed to leave a thick brown oil. Diethyl ether (100 ml) was added to attempt to remove some lipids from the mixture however nothing from the oil dissolved and the diethyl ether remained clear so the ether was poured off and 100 ml of ethyl acetate added. Upon sonication the solvent turned orange. The suspended solid was compacted by centrifugation and the orange supernatant collected and dried, total mass 9.31 g, UV/Vis 26.6 mg heptaene, 16.6 mg tetraene. The solid was suspended again in 200 ml EtOAc, centrifuged and the supernatant collected and dried, total mass 10.64 g, UV/Vis 5.7 mg heptaene. The solid was resuspended in 100 ml methanol to form a cloudy solution, which was filtered. The filtrate was dried under vacuum, total mass 10.65 g, UV/Vis 66.7mg heptaene 30.3 mg tetraene. The collected solid had a mass of 1.29 g, but no polyene content by UV/Vis so was discarded.

From this it has been discovered that NaSCN makes amphotericins soluble in EtOAc, and prevents cell debris and other by-products from dissolving in diethyl ether, thus making any effective separation or purification using these two solvents impracticable.

It was also discovered that the presence of NaSCN in the solution made any separation by HPLC impossible because all components were eluted straight away without any retention on the column, and the column itself required flushing with 100% water for ~20 column volumes before separation was restored for subsequent samples.

All remaining samples containing heptaenes from the above were combined, dried, and the resultant solid divided approximately in half. One half was loaded onto a chromatography column (3 cm diameter) containing silica gel 60 and eluted with 20:6:1 chloroform:methanol:water (250 ml), 10:6:1 chloroform:methanol:water (250 ml) and methanol (125 ml). Fractions were collected in 10 ml increments. The fractions were examined by UV/Vis spectroscopy, the UV/Vis readings for heptaene (blue) and tetraene (red) in mg per fraction are graphed below (figure 89).

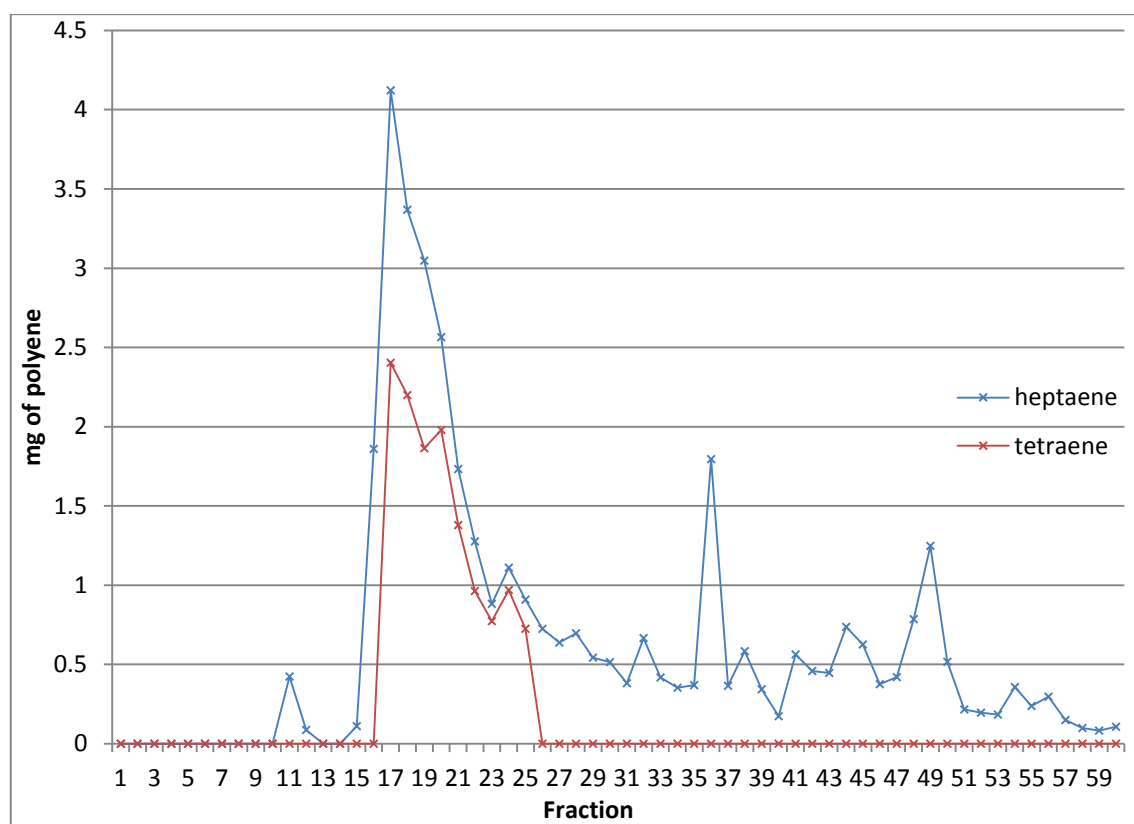


Figure 89: UV/Vis readings for first chromatography column

Another column was performed with the other half of the sample and the same solvent system, with the addition of 200 ml pure chloroform at the start, to test whether any extra unwanted material would elute first.

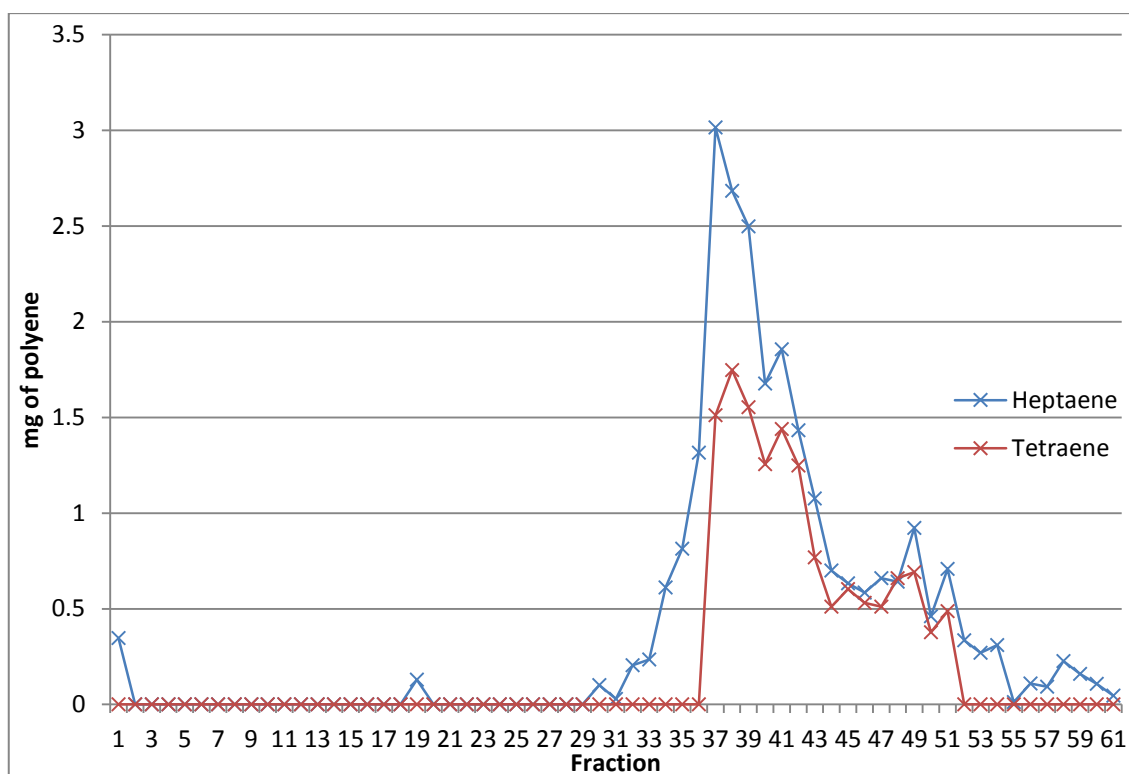


Figure 90: UV/Vis readings for second chromatography column

The following fractions were collated and dried:

Column	Fractions	Total mass
1	16-24	1.62 g
	25-50	8.71 g
	50-60	3.17 g
2	34-40	3.57 g
	41-46	3.42 g
	47-60	5.09 g

Table 32: Collation of column fractions

All six parts were examined by LCMS. A mass corresponding to the putative mannosylated product was found in the third part (coloured red in table 32) from each column. These two were suspended in water (10 ml) and centrifuged, the supernatant and precipitate were both found to contain polyenes by UV.

Other work done in the lab by a masters student (unpublished) investigated the possibility of using custom designed polymers to extract amphotericins from crude solutions. To investigate whether a similar process might be performed using silica gel, the aqueous supernatant from column 1 part 3 was passed through a chromatography column containing a small amount of silica gel 60, the column was then eluted with 10 ml of clean water and 20 ml of methanol. Examination of all three samples by UV/Vis spectroscopy showed no polyenes in either of the aqueous samples but that 12.5 mg heptaene was present in the methanolic sample. This was examined by analytical HPLC to contain two peaks, one corresponding to the putative mannosylated product and one to 8-deoxyAmB. The success of the analytical HPLC also showed that there was no or very little NaSCN present in the sample. The precipitate from column 1 part 3 and the whole from column 2 part 3 were also passed through a column of silica gel, which was washed with water (10 ml) and eluted with methanol (20 ml), no polyenes being detected in the aqueous samples, the heptaene containing methanolic samples were separated by preparative HPLC into two fractions of mass 34.2 mg (disaccharide by LCMS) and 72.1 mg (8-deoxyAmB by LCMS). The first sample contained 2.1 mg heptaene by UV/Vis spectroscopy.

From this it was learned that passing an aqueous solution containing NaSCN and the target polyenes through a chromatography column of silica gel 60 allows the silica to retain the polyenes whilst the NaSCN is flushed through with water, the polyenes can then be eluted from the column using methanol to give a crude sample which can be further purified by preparative HPLC, HPLC not being possible for a sample containing NaSCN.

The sample set aside from growth 2 above was suspended in water (40 ml) and passed through a column of silica gel, which was washed with water and eluted with methanol (20 ml), the methanolic extract was separated by preparative HPLC to give two fractions. Fraction 1 (disaccharide) total mass 13.3 mg, UV heptaene content 3.1 mg. Fraction 2 (8-deoxyAmB) total mass 122.2 mg.

Growth 4

Eight flasks of autoclaved fructose-dextrose-soya medium were inoculated with 10 ml of starter culture and thiostrepton and hygromycin added to a concentration of 50 µg/ml. The flasks were incubated for five days before the mycelia were collected in muslin cloth.

The aqueous media contained polyenes by UV/Vis so was extracted with butan-1-ol. The organic layer was dried to give a yellow solid of mass 2.76 g. This was washed with water (10 ml) to leave 1.42 g, which was separated by preparative HPLC into two fractions. Fraction 1 (disaccharide) total mass 2.9 mg, UV/Vis 0.9 mg heptaene. Fraction 2 (8-deoxyAmB) total mass 86.4 mg, UV/Vis 18.5 mg heptaene.

Six extractions of the mycelia were performed using methanol containing NaSCN. Each extract was dried completely, suspended in THF (~100 ml) and filtered.

After the Fmoc deprotection (performed in DMSO) of amphotericin derivatives discussed earlier, the reaction mixture is dripped into diethyl ether to disperse the DMSO and precipitate the product. It was examined whether a similar process could be used here to remove some unwanted material from the crude mixture. The dried solid from extract 2 was dissolved in 60 ml DMSO (the minimum volume) and dripped into 1 litre of diethyl ether. However, the orange DMSO solution did not disperse into the ether which remained clear and colourless. The ether was poured off and the DMSO solution diluted in water (200 ml), this solution was passed through a column of silica gel, which was then eluted with 100 ml of water and 100 ml of methanol. Examination by UV/Vis showed no polyenes in the aqueous eluents but 21.2 mg of heptaene in the methanolic eluent, which was dried under vacuum to give a mass of 1.72 g.

The other five extractions were dissolved in 300 ml water and passed through a silica column, which was washed with 100 ml water and eluted with 200 ml methanol. Again, UV/Vis showed no polyenes in the aqueous eluents but 64 mg heptaene in the methanol eluent, which was dried under vacuum to give a mass of 12.63 g. This was washed with diethyl ether (3x35 ml) to leave 3.73 g.

Both samples were then separated by preparative HPLC to give two fractions. Fraction 1 (disaccharide) total mass 7 mg, UV/Vis 2.1 mg heptaene. Fraction 2 (8-deoxyAmB) total mass 64.2 mg.

Growth 5

Eight flasks of autoclaved fructose-dextrose-soya medium were inoculated with 10 ml of starter culture and thiostrepton and hygromycin to concentrations of 50 µg/ml. After incubation with shaking for six days, the mycelia were collected by draining through muslin cloth.

The mycelia were lysed by soaking in methanol, the first extract was taken using clean methanol, subsequent extractions were taken using methanol containing NaSCN, however, instead of being saturated with NaSCN as previously, this was diluted by mixing 1 part saturated to 2 parts clean methanol, to investigate whether lower levels of NaSCN also facilitate easier extraction without causing so many problems with purifying the desired product. Ten extractions were taken, each extract had the volatiles removed under vacuum and the residual water refrigerated overnight to precipitate polyenes. The precipitate was collected by centrifugation at 6,000 rpm for 15 minutes. The precipitate and aqueous supernatant were then examined by UV/Vis spectroscopy, the results are tabulated below.

Extract	ppt mass	ppt UV/Vis	s/n UV/vis
1	1.45 g	3.4 mg heptaene	no polyenes
2	9.87 g	9.5 mg heptaene 14.2 mg tetraene	no polyenes
3	6.25 g	15.8 mg heptaene 27.0 mg tetraene	3.0 mg heptaene 25.4 mg tetraene
4	3.73 g	25.6 mg heptaene	3.1 mg heptaene 15.1 mg tetraene
5	7.65 g	20.1 mg heptaene	6.6 mg heptaene 2.1 mg tetraene
6	5.25 g	23.2 mg heptaene	9.96 mg heptaene 3.9 mg tetraene
7	12.02 g	52.3 mg heptaene	3 mg heptaene
8	13.47 g	23.2 mg heptaene	13 mg heptaene
9	12.90 g	38.2 mg heptaene	28.5 mg heptaene
10	9.24 g	3.1 mg heptaene	47.5 mg heptaene

Table 33: MeOH/NaSCN extractions of mannosyl-8-deoxy-AmB growth 5

Analytical HPLC of extract 10 supernatant showed it to be all 8-deoxyAmB, with none (or an undetectable level) of the disaccharide, so extractions were stopped.

The drained aqueous media was extracted with butan-1-ol, the organic layer separated and dried, mass 2.57 g, analytical HPLC showed this to also contain only 8-deoxyAmB.

The supernatants from extracts 3, 4 and 5 were combined and passed through a column of silica 60, the column was rinsed with 100 ml water then eluted with 100 ml methanol, the methanol was dried to give a brown solid of mass 896 mg.

The supernatants from extracts 6-9 were combined (total volume 320 ml) and passed through a column of silica 60, the column was rinsed with 100 ml water then eluted with MeOH until the eluent ran clear, the solvent was removed to give an orange solid of mass 1.17 g.

Both methanol elutions were combined and then separated by preparative HPLC, three peak fractions were collected: Peak 1, total mass 21.1 mg, LCMS showed molecular mass of 908 ($M+H^+$) therefore 8-deoxyAmB or an isomer. Peak 2, total mass 11.4 mg, LCMS showed molecular mass of 1070 ($M+H^+$) therefore putative mannosyl-8-deoxyAmB, UV/Vis showed 1.7 mg heptaene. Peak 3, total mass 105.9 mg, 8-deoxyAmB.

The extract precipitates were combined and washed with water (3x30 ml), the centrifuged supernatants were examined by UV/Vis and found to contain 24.5 mg heptaene, 3.6 mg heptaene and 4.6 mg heptaene. They were combined, passed through a column of silica 60 as above, and the methanol eluent separated by preparative HPLC into two fractions. Fraction 1, total mass 5.2 mg, UV/Vis 3.4 mg heptaene, LCMS shows mannosylated product. Fraction 2, total mass 21.6 mg, UV/Vis 19.4 mg heptaene, 8-deoxyAmB.

The centrifuged precipitates were dissolved in water (100 ml) and extracted by silica 60 column. The methanol eluent was dried to give a yellow solid of mass 184 mg, which was separated by preparative HPLC into two fractions. Fraction 1, total mass 2.2 mg, UV/Vis 0.4 mg heptaene, mannosyl-8-deoxyAmB. Fraction 2, total mass 22 mg, 8-deoxyAmB.

From this it was learned that using a chromatography column of silica gel 60, the crude polyenes can be extracted from an aqueous mixture containing NaSCN. Once the NaSCN has been removed the crude mixture can be purified by preparative HPLC.

Final purification of mannosyl-8-deoxyAmB

All HPLC fractions from above containing mannosyl-8-deoxyAmB (**93**) were collated into one sample. This sample contained ~17 mg of heptaene by UV/Vis in ~1 g total weight. This is because, due to the very impure nature of the crude sample injected into the machine, some sugars and other unwanted cell byproducts pass through the column into the 'pure' fractions.

This collated sample was washed with ice cold water (6x1 ml) with centrifugation at 13,000 rpm for ten minutes, then with ethyl acetate (2x1 ml), and then with methanol at -80°C (1 ml), the methanol was kept extremely cold to minimise the solubility of amphotericin. The resultant yellow solid was suspended in water (1 ml) and lyophilised to give a fluffy yellow powder with a total mass of 25.1 mg and a heptaene content (by UV/Vis) of 13 mg, therefore ~50% purity by mass, which was sufficient for biological testing.

LCMS showed the sample to contain only one UV active compound with a molecular mass of 1070 Da. Crucially, therefore, the amphotericin present in the sample is only the mannosyl-8-deoxyAmB form, all unmannosylated amphotericin and aglycone has been successfully removed (see figures **91** and **92**).

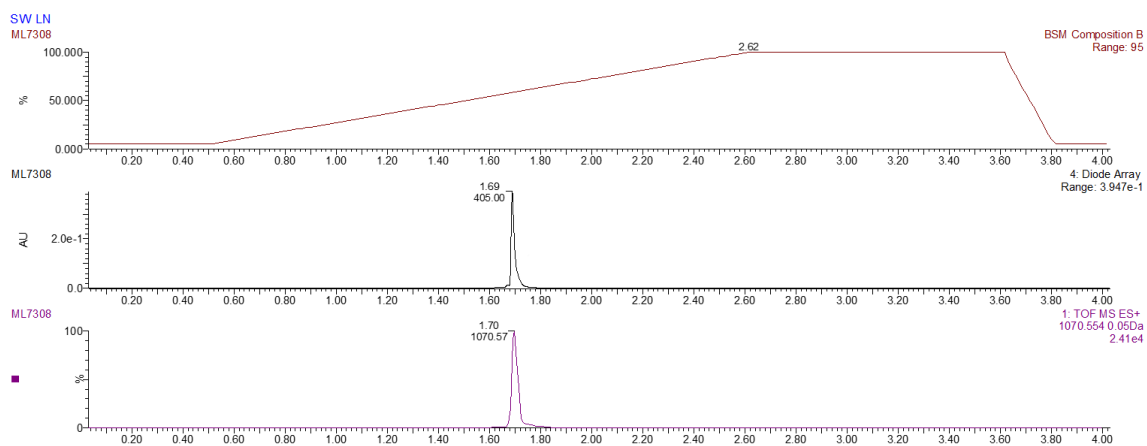


Figure 91: LCMS UV trace of final mannosyl-8-deoxyAmB sample

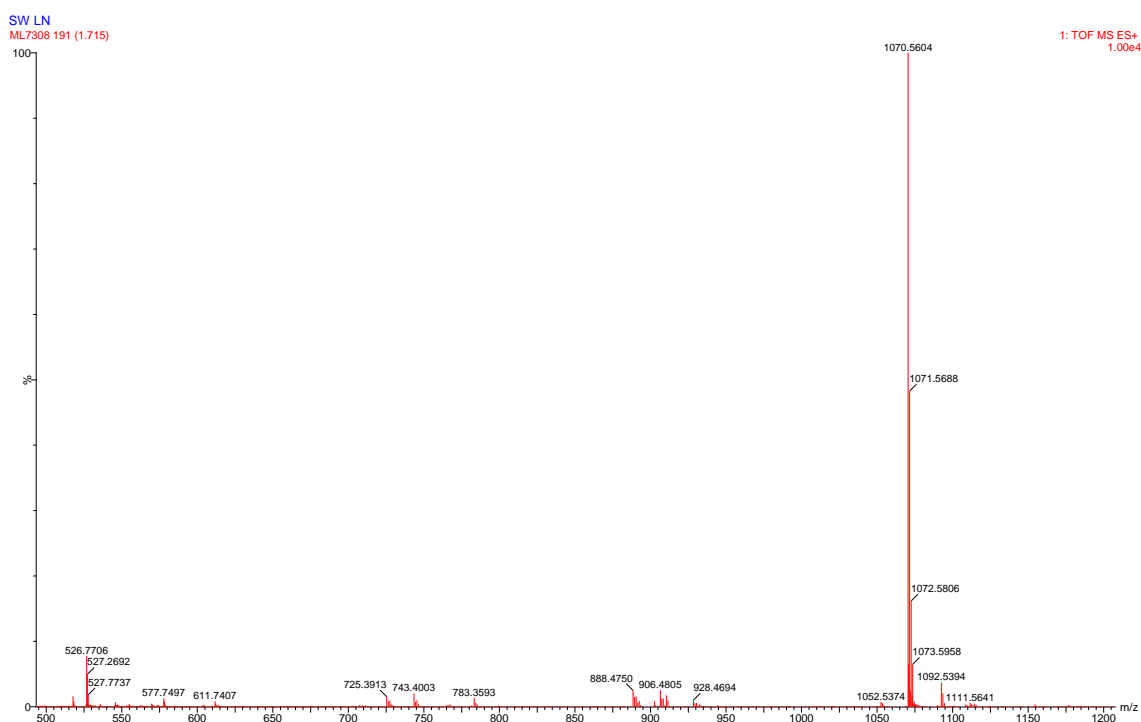


Figure 92: Reading from single peak in figure 91.

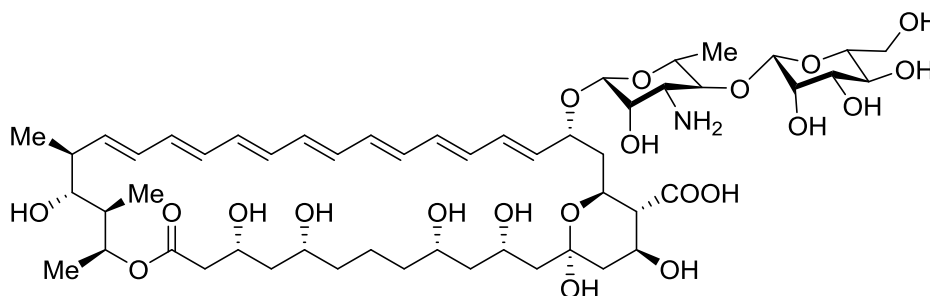


Figure 93: mannosyl-8-deoxyAmB

It was also noted that at no point was a mass corresponding to mannosylated-8-deoxy-aglycone observed, this is highly suggestive of a mycosamine-mannose disaccharide, rather than a separate mannosyl sugar attachment elsewhere on the aglycone structure. If the mannose were to attach to one of the hydroxyl groups in red in figure 94, we might expect to see a mass of 925 Da ($M+H^+$) appear either from fragmentation in the mass spectrometer, or failure of the mycosamine to attach.

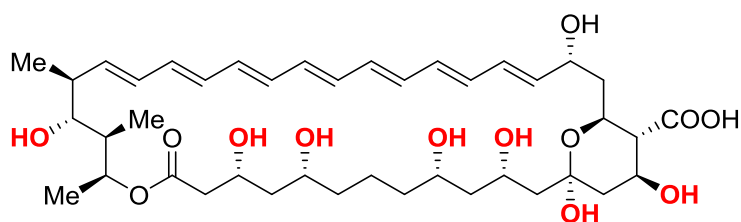


Figure 94: 8-deoxy-aglycone

^1H NMR was performed in methanol- d_4 , although since the mannosyl-8-deoxyAmB is poorly soluble in this solvent the resultant NMR data is not of very high quality. However, the following differences from a ^1H NMR of 8-deoxyAmB were observed:

(DMSO- d_6 could have been used to obtain greater resolution, however amphotericin has proved very difficult to remove from DMSO so this solvent was not used in order to preserve the isolated mannosyl-8-deoxyAmB for biological testing.)

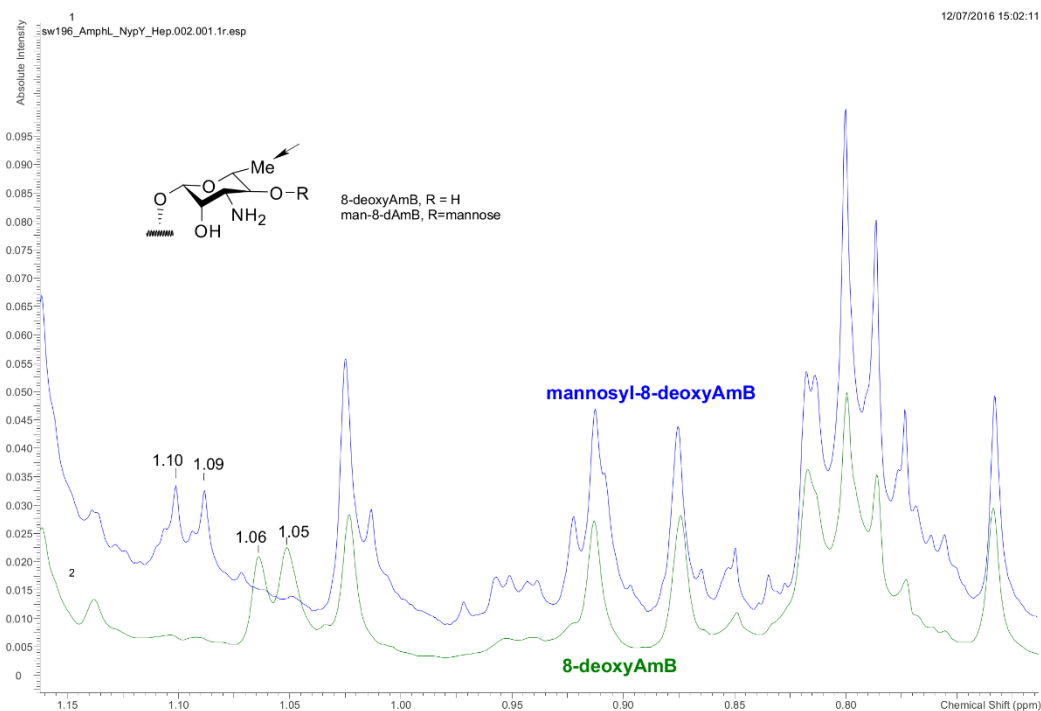


Figure 95: Shifted methyl doublet on mannosyl-8-deoxyAmB

The doublet from the methyl group on the mycosaminyl sugar is shifted slightly downfield on the mannosylated product, providing evidence of a substitution on the nearby 4'-OH (figure 95).

The methyl group shows correlation on the COSY NMR spectrum to the hydrogens on the mycosamine sugar at around 5.25 ppm (figure 96).

An additional doublet at 3.96 was observed, corresponding to the CH₂ of the mannosyl moiety. At higher purity a doublet of doublets might be observed, due to geminal and vicinal coupling. (figure 97)

The additional signal at 4.26 on mannosylated product appears to be a doublet as would be the expected splitting due to one adjacent hydrogen, the singlet visible on the 8-deoxyAmB spectrum may be hidden beneath this stronger peak.

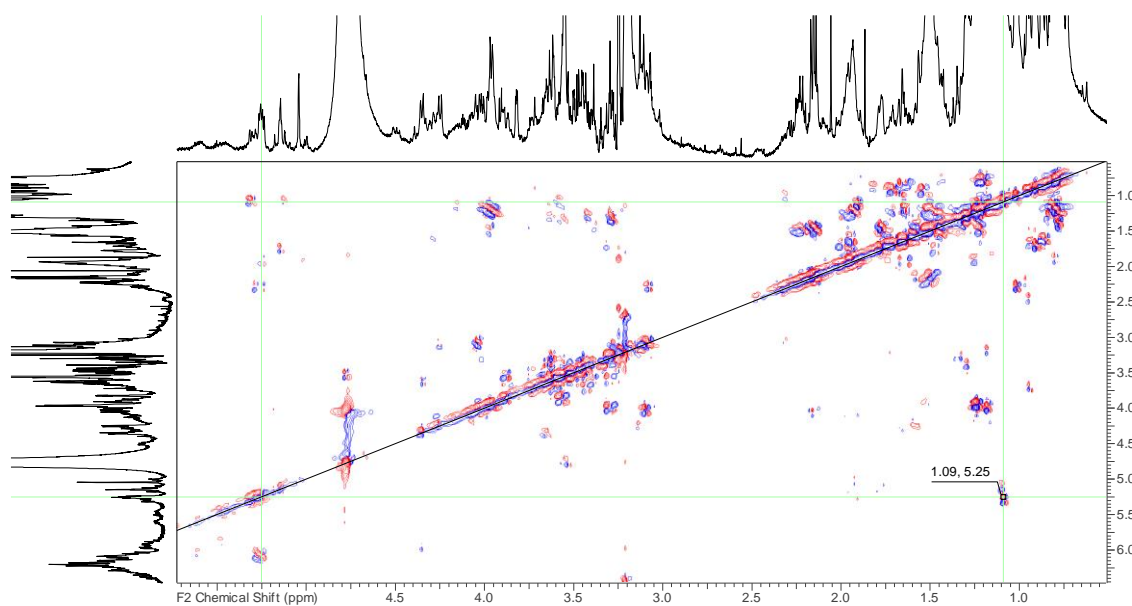


Figure 96: Zoomed COSY of mannosyl-8-deoxyAmB

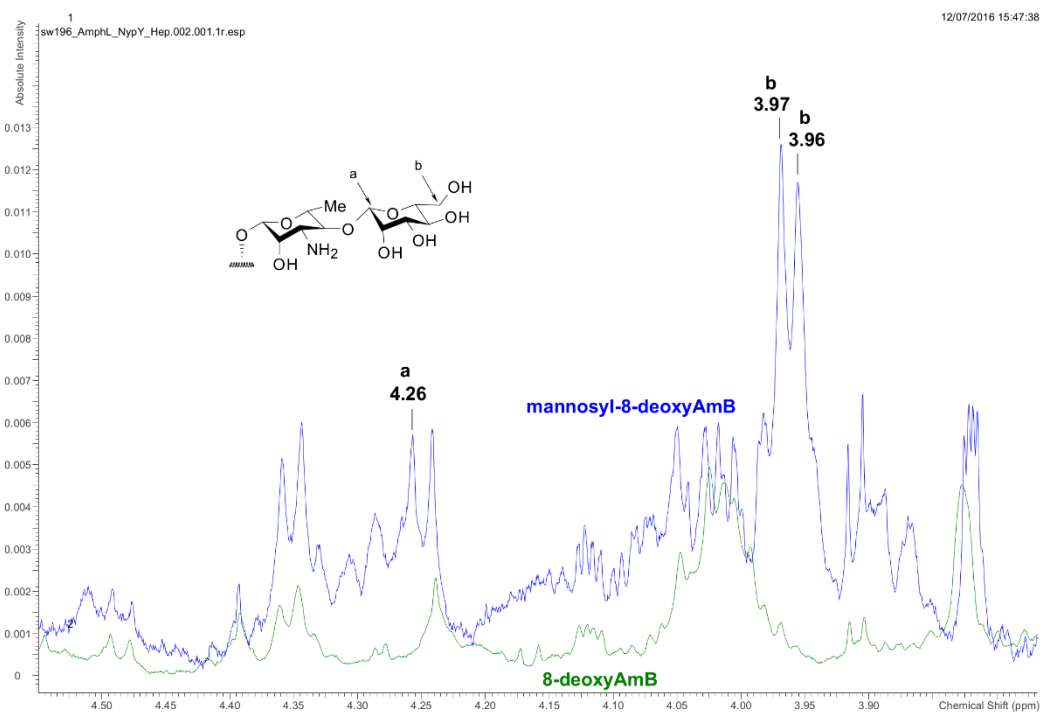


Figure 97: Additional peaks on mannosyl-8-deoxyAmB

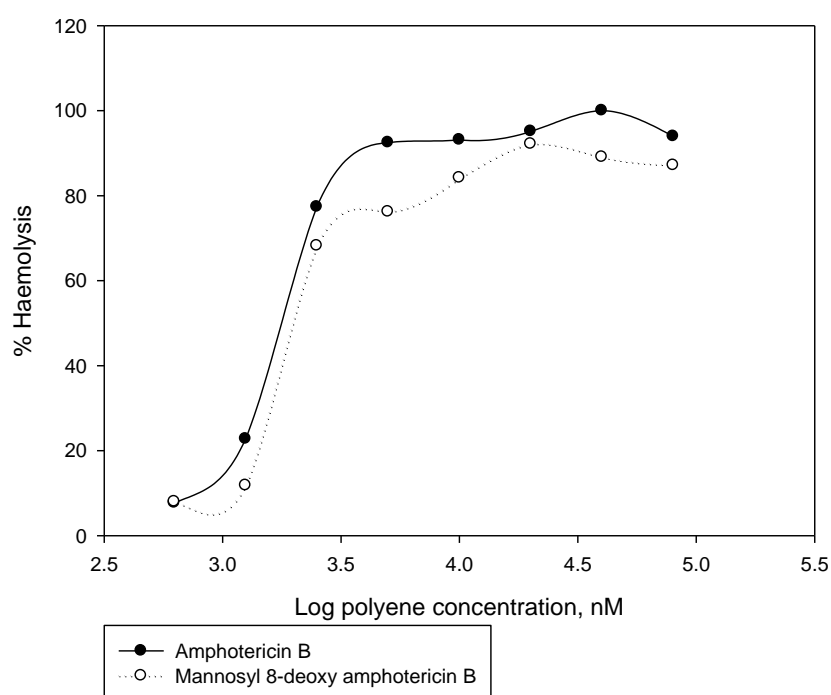
3.5 Biological testing of mannosyl-8-deoxyAmB

Mannosyl-8-deoxyAmB was tested for antifungal and haemolytic activity by Caffery, using AmB as the reference (as in section 2.9).

Polyene	MIC, μM	MHC ₀ , μM	MHC ₅₀ , μM	MHC ₁₀₀ , μM
AmB	1.56	0.631	1.585	3.162
Mannosyl-8-deoxyAmB	1.56	1.0	2.512	7.943

Table 34: Results of mannosyl-8-deoxy-AmB biological testing

Haemolytic assay 1



From this it appears that mannosylation gives a reduction in haemolytic activity to approximately half that of AmB, with antifungal activity remaining unaffected.

A paper on this work has been prepared and published.⁹⁵

Chapter 4: Crystallisation.

So far several analytical techniques have been used in this work to gather data about AmB and the derivatives produced. However, each of these techniques is limited in their own way, mass spec for example provides a measure of the molecular mass of each compound but little data as to structure, proton NMR shows the presence and neighbours of different hydrogen atoms, but for a large molecule such as AmB the data is hard to analyse and prone to misinterpretation. X-ray crystallography, whereby a high-powered x-ray beam is directed through a crystal of a compound onto a CCD (charge-coupled device, similar to that found within a digital camera) detector and the resulting diffraction pattern analysed by a computer, not only provides data showing the position of each atom in the compound, but also shows the configuration and shape of the molecule, and how it might interact with its neighbours, information which is very hard or impossible to garner by other means.

However, while some compounds naturally form crystals very easily, for example salts and sugars; AmB, with its large number of different environments (hydrophilic hydroxyls, hydrophobic heptaene backbone, and a sugar moiety containing an amine group) does not normally crystallise willingly. In this chapter, the previous work done on AmB will be discussed, along with attempts towards producing a crystal of some of the derivatives previously mentioned.

4.1 Previous work

A crystal structure of amphotericin B was first published in 1970 by Ganis *et al*⁷⁹. After failing to crystallise amphotericin B in its usual form, they focused upon a biologically active heavy atom derivative, *N*-iodoacetyl-amphotericin B (AmB-I, **66**).

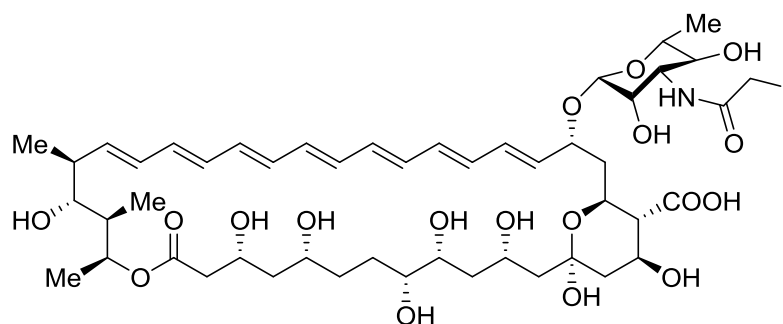


Figure 66: *N*-iodoacetyl-amphotericin B

Their elucidated structure showed for the first time the stereochemical features of the macrolactone ring, namely that most of the hydroxyl groups were axial with respect to the plane of the lactone ring, and towards one side together with the mycosaminyl moiety.

A later paper⁹⁶ by Jarzemska *et al* confirmed this, and also noted the presence of two water molecules in the crystal lattice, one interacting with the hydroxyl group on carbon-8, the other with the hydroxyl group on carbon-13 of one molecule and the hydroxyl group on carbon-2' (on the mycosaminyl sugar) of an adjacent molecule (figure 98)

A notable problem in both of these papers is that by derivatising the amine group on the mycosaminyl sugar, the amine's interaction with the proximate carboxyl group cannot be observed, so the zwitterion configuration of amphotericin B thought to be important for its biological activity cannot be studied or confirmed.

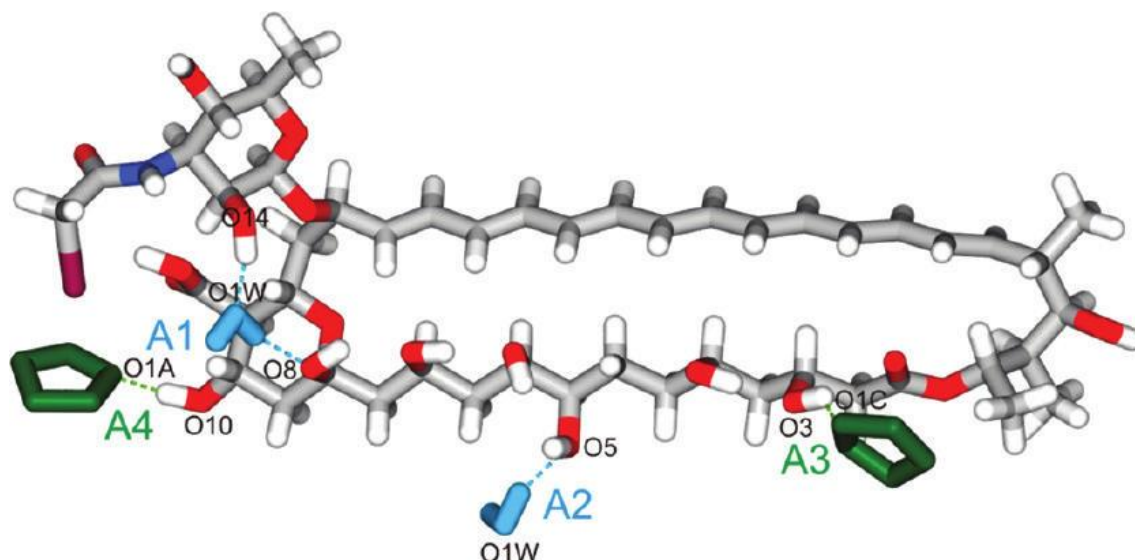


Figure 98: Solvent interactions of AmB-I molecule from Jarzemska paper

Detailed spectroscopic analysis⁹⁷ performed by Gagoś *et al* of the variations between crystalline and amorphous AmB-I allowed the molecular organisation of AmB-I in the crystalline stage to be examined. Using FTIR and Raman spectroscopy, they found particular differences in the bands associated with C=O and C-C-H groups, in addition to C=C-C stretching vibrations. An increase in absorbance at 1010 cm^{-1} in the crystal structure, compared to a very low level in the amorphous phase, is accounted for by the rigid conformation resulting from molecular interactions between the heptaene regions of adjacent molecules. The shift from a broad band at 1725 cm^{-1} in the amorphous phase to the sharp band at 1710 cm^{-1} in the crystalline state indicates that a carbonyl group has formed a hydrogen bond to an adjacent hydrogen atom. They conclude that the intensity of the absorption band at 1010 cm^{-1} can be used as a measure of the degree of crystallisation present in the sample.

4.2 Crystal-growing methods

There are many known techniques used for growing crystals, some more applicable to certain types of compound. The methods considered were:

1. Evaporation. This is the simplest of crystallisation techniques. A strong solution of the compound is prepared in a suitable solvent. This solution is placed into a clean container and covered loosely, over time solvent will evaporate, causing the solution to become saturated and then over more time, some of the compound to slowly come out of solution. If the rate of evaporation is slow enough the precipitated compound may form into a crystal, it is not uncommon to crystals to form in NMR tubes that have been left undisturbed (for example in a fridge) as many of the usual lids fitted to NMR tubes are not gas tight.

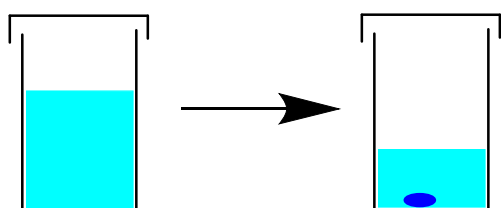


Figure 99: Crystal growing by evaporation

2. Cooling. This technique uses the fact that the warmer the solvent, the greater the quantity of compound that can dissolve in it. A hot solution is prepared and allowed to cool, as the solubility decreases, the excess solute comes out of solution. This is the principle behind the common lab purification technique of recrystallisation.

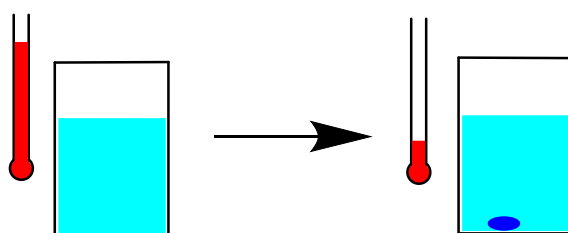


Figure 100: Crystal growing by cooling

3. Solvent layering. This method uses two miscible solvents, where the compound is soluble in only one. A solution is prepared in the solvent which will dissolve the compound, placed in a container, and the second solvent (precipitant) is very carefully layered on top. This technique works best if the solvents have sufficiently varying properties to allow an interface to form. Then, as the second solvent diffuses into the first, the compound is slowly forced out of solution.

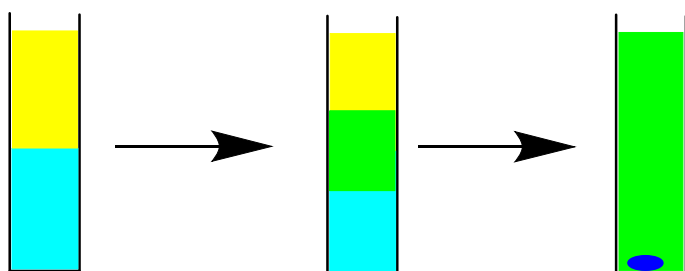


Figure 101: Crystal growing by solvent layering

4. Vapour diffusion. Similar to the former, this technique again requires two miscible solvents of which the compound is soluble in only one, ideally the second solvent will be more volatile than the first. A solution of compound is prepared and placed into a small container, which is then placed inside a larger vessel containing the precipitant, the whole unit then being sealed. As the precipitant diffuses into the solution, the compound will be slowly forced out.

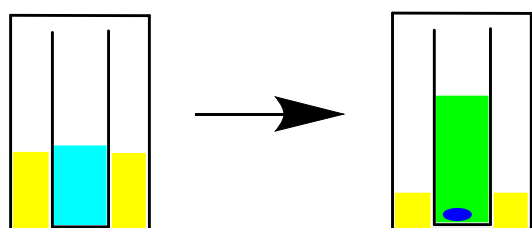


Figure 102: Crystal growing by vapour diffusion

5. Sublimation. This technique is unusual for not requiring solvent. The compound is heated in the bottom of a container under reduced pressure, the compound vapour then deposits upon a cooler area of the container; sometimes the walls, or if the compound sublimes close to room temperature a cold finger may be added. This technique can provide very good crystals but is not suitable for many compounds.

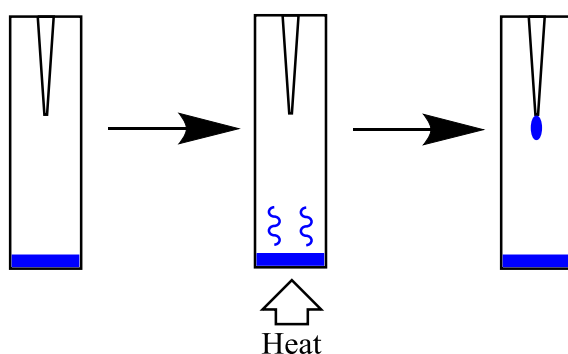


Figure 103: Crystal growing by sublimation

Since AmB is known to decompose at temperatures much above 40°C, sublimation and cooling were decided to not be appropriate techniques. Solvent layering was attempted but a sufficient separation interface could not be formed. Therefore, evaporation and vapour diffusion were the methods investigated.

4.3 Pure AmNM

AmNM has very low or no solubility in most common solvents. The common solvents in which it shows good solubility are methanol, ethanol, isopropyl alcohol (IPA), butanol-1-ol and tetrahydrofuran (THF). AmNM has excellent solubility in DMF and DMSO, however these solvents were deemed unsuitable for crystal growing, because the formic acid present in DMF would degrade the AmNM, and DMSO is very difficult to remove. Both solvents also have very low volatility.

Crystal-growing was first attempted at room temperature. Close to saturated

solutions (~10 ml) of AmNM in the above mentioned alcohols and THF were prepared. Each solution was pipetted in 1 ml aliquots into clean 12x50 mm glass sample tubes, which were capped with plastic lids into which a very small hole had been punctured. The tubes were placed away from light and disturbance and observed periodically over the following weeks.

After one month, the tubes were examined, most of the methanol, ethanol and THF had evaporated, approximately half of the IPA and very little of the butanol. Yellow powder had precipitated in all the tubes. Examination of the tubes under a microscope showed no crystalline material.

4.4 Iodoacetyl derivatisation

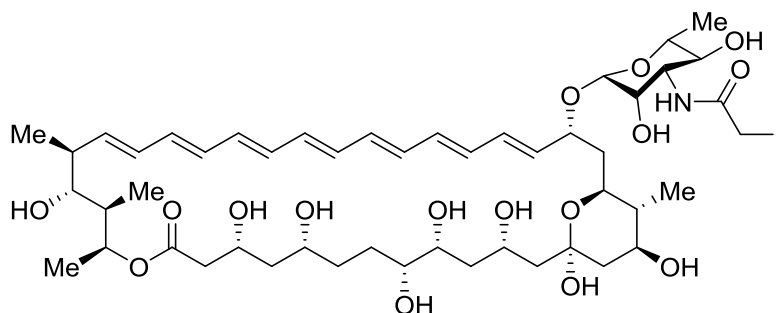


Figure 68: *N*-iodoacetyl-AmNM

Previous published papers^{79, 96-97} used AmB with an iodoacetyl group on the amine to grow crystals. The reaction to derivatise amphotericin is described in chapter 2.8.5 above.

A 2 mg/ml solution of *N*-iodoacetylAmNM in MeOH was prepared. This was pipetted in 0.5 ml aliquots into 15 12x50 mm clean glass sample tubes, which were then placed inside 25x50 mm sample tubes containing 2 ml of diethyl ether. The larger tube was sealed, ensuring a gap remained at the top of the smaller tube to allow diffusion of vapour. The tubes were placed away from light and left undisturbed for one week. After

this week they were examined, and the inner tube found to contain yellow powder, no crystalline material was observed under a microscope.

The experiment was repeated, using THF in place of methanol. These tubes were observed to contain yellow powder after two days. A weaker solution (1 mg/ml) was produced in THF and the tubes prepared again. Again, yellow powder was observed after two days.

It appeared that the ether was diffusing into the THF very quickly. The tubes were prepared again and placed in a cold room at 4°C. However, these tubes again failed to produce any crystals, although it took longer (approx. 1 week) for powder to form.

Another solution of 1 mg/ml was prepared in THF and pipetted into clean 12x50 mm sample tubes, capped with punctured lids and left at room temperature to evaporate. After three weeks when most of the THF had evaporated and yellow powder formed once again, the contents of the tubes were examined by UV/Vis spectroscopy and it was discovered that nearly all the heptaene content had broken down, either through being left at room temperature or exposed to oxygen for long periods. The experiment was repeated with the tubes being left in the cold room, after six weeks, only powder had formed again, though examination of the contents by UV/Vis showed ~90% of the heptaene content remained.

The table of hydrogen bonds⁹⁶ within the structure published by Jarzemska *et al* shows a strong bond between the –OH on the carboxyl group of one molecule and a nearby –OH of the mycosaminyl sugar on the adjacent molecule. The absence of a carboxyl group on AmNM provides a reason why the molecules may not form a stable crystal lattice.

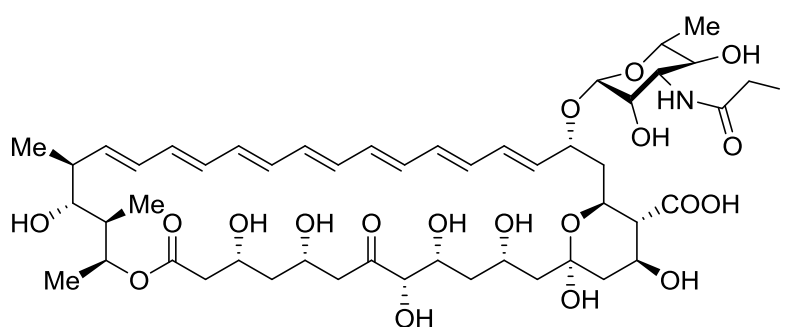
4.5 7-oxo-AmB N-iodoacetyl

Figure 104: *N*-iodoacetyl-7-oxo-amphotericin B

Further attempts at crystallisation were made using the 7-oxo-AmB formed as a by-product of attempting to produce the disaccharide NypY variant as described in chapter 3.3. The 7-oxo-amphotericin B was derivatised with an iodoacetyl group by the same method as previously described. 68 mg (0.073 mmol) of 7-oxo-amphotericin B and 77 mg Iodoacetic anhydride (3 eq.) produced 74.5 mg *N*-iodoacetyl-7-oxo-amphotericin B (**104**).

A small peak corresponding to a mass of 988 Da ($M+H^+$) was observed by LCMS. An explanation for this increase in mass of 50 Da has not been found.

80 12x50 mm tubes of 1 mg/ml solution in THF were prepared, sealed with a punctured lid, placed in the cold room at 4°C and covered to foil to achieve a very slow rate of evaporation. After three months, microscopic examinations of the tubes revealed only amorphous powder had been produced.

Vapour diffusion with both MeOH and THF as solvent and diethyl ether as precipitant was also attempted, without success.

4.6 8-deoxy-AmB N-iodoacetyl

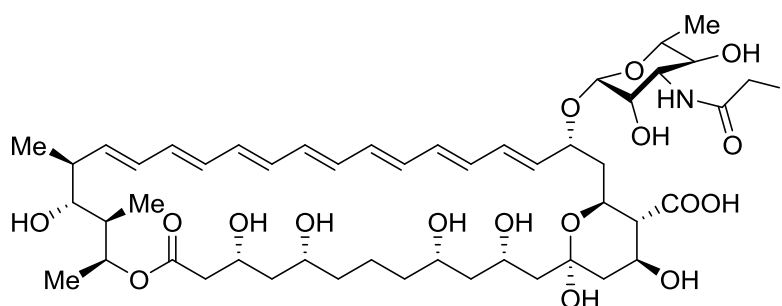


Figure 105: *N*-iodoacetyl-8-deoxy-amphotericin B

The leftover 8-deoxyamphotericin B acquired during chapter 3.4 was also used. 104 mg (0.12 mmol) 8-deoxyAmB and 121 mg iodoacetic anhydride (3 eq.) formed 120.1 mg *N*-iodoacetyl-8-deoxyAmB (**105**). A peak corresponding to a mass of 958 Da ($M+H^+$) was also identified by HPLC and LCMS, this appears to be a similar by-product to the 988 Da peak observed in the KR16 reaction above.

50 tubes were prepared containing a solution (~1 mg/ml) of *N*-iodoacetyl-8-deoxyAmB in THF, capped with punctured lids and left undisturbed in the cold room at 4°C. After 3 months, no crystalline material was observed.

Vapour diffusion with MeOH, EtOH and THF as solvents and diethyl ether as precipitant was also unsuccessful.

4.7 Amphotericin DI-DII-NM

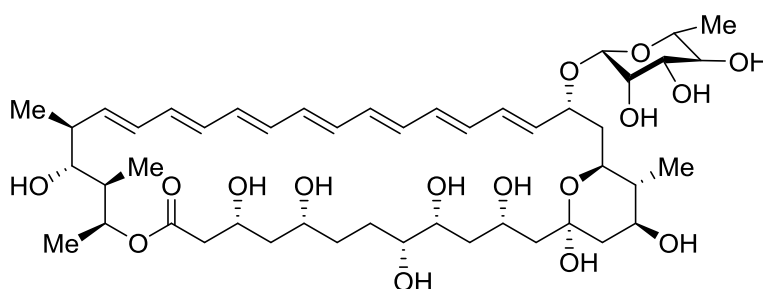


Figure 106: 16-descarboxy-16-methyl-19-rhamnosyl-amphoterinolide B

Caffrey *et al* found that deletion of both the *amphN* and *amphDII* genes gave **106** and its tetraene form⁶², lacking the exocyclic carboxyl group and glycosylated with a 6-deoxyhexose (probably rhamnose), that is presumed to be a shunt product from reduction of the 4-keto or 3-keto sugar intermediate by an as yet unknown enzyme. The stereochemistry of this sugar has never been positively identified. A crystal structure of this analogue would provide proof of both the identity of the sugar attached and its stereochemistry.

The bacteria were grown in fructose-dextrose-soya medium as described earlier, addition of antibiotics such as thiostrepton is not necessary in this case. The mycelia were harvested after five days and lysed in methanol. The crude extracts were washed in water and ether to remove cellular debris. This left a crude mixture containing ~15% **106** by UV/Vis, this was purified to 92% **106** by UV/Vis on a column of silica gel 60 eluted with 10:6:1 CHCl₃:MeOH:H₂O. The molecular weight of the analogue was checked by LCMS and found to be the expected 895.50 Da (M+H⁺)

The Amph DI-DII-NM variant produced does not have an amine group to derivatise, so crystallisation was attempted on the molecule with no modifications. It was observed that the product was more soluble in THF than the derivatives attempted above, in addition, 1% of water was added to the THF because examination of a previous paper⁹⁶ by Jarzemska *et al* showed that the crystal structure of *N*-iodoacetylAmB included water molecules.

60 tubes containing 1 ml of a 3 mg/ml solution of product in wet THF were prepared, sealed with punctured lids and foil and left in the cold room at 4°C for four months.

After this period, examination of the tubes by microscope showed no crystalline material in most, however, in ten of the tubes, very small crystals with amorphous strings attached could be seen, similar in appearance to a pollen grain. These crystals were unfortunately too small to be used for XRD.

4.8 Co-crystallisation

AmB *in vivo* is known to form complex structures with the steroid ergosterol. It was investigated whether this property could be used *in vitro* to form a crystalline structure suitable for use in XRD, which would also provide data showing the interactions between the two molecules which could be compared to existing models for the formation of the barrel-stave tube. Ten 12x50 mm tubes were prepared containing 10.4 mg of AmNM (0.012 mmol) and 4.7 mg ergosterol (0.012 mmol) in 2 ml THF and 0.5 ml DI water. It is observed that the addition of ergosterol to the solution appears to make amphotericin much more soluble than it would be alone. The tubes were placed inside 25x50 mm tubes containing water, and sealed with lids pierced with a needle protruding into the outer chamber, this was ensure that hydration levels remained high as the THF evaporated. The tubes were placed in the cold room at 4°C.

After three weeks, amorphous solid began to appear at the base of the tubes.

After four weeks, a thick layer of solid had formed in all tubes, they were examined by microscope, and found to contain no crystalline material.

5. Summary and future work

The purification method for AmNM has been improved allowing a far greater quantity of product to be isolated from a growth of bacteria (45-51% of crude heptaene mass recovered at >95% purity.) The quantity of XAD16 resin required per growth flask has been reduced by 60% allowing a significant cost saving. Cottonseed flour has been tested as an alternative growth media ingredient and found to be inferior to soybean flour, although a novel analogue of amphotericin B was discovered.

A substitution method for the mycosyl amine on AmNM has been developed allowing novel analogues to be produced in a few synthetic steps. Biological testing of the alkylamino derivatives showed their antifungal activity had been maintained whilst their haemolytic activity had been altered, still lower than AmB but higher than AmNM. Suggested future work would be produce more derivatives with different lengths of alkyl chain to identify a correlation between the alkyl chain and the resultant biological activity and attempt to produce an alkylated AmNM with lower haemolytic activity than the parent compound.

The mannosylated derivative of the 8-deoxy analogue has been isolated and tested, it was found to have equal antifungal activity to AmB but reduced haemolytic activity. Mannosylated AmB and 7-oxoAmB were also detected but at too low levels to be successfully isolated and purified. Future work would be to investigate means of improving the yield of mannosyl-8-deoxyAmB and also produce mannosylated derivatives of other AmB analogues, such as mannosyl-AmNM.

Crystallisation of several analogues for XRD has been attempted without success, although the rhamnosyl analogue did produce microscopic crystals these were too small to diffract.

6. Experimental

Equipment used

UV/Vis assays were performed on a Shimadzu UV-2401PC spectrophotometer and analysed by Shimadzu's UVProbe software, version 2.21.

HPLC was performed on a Varian ProStar with two model 210 solvent delivery modules, equipped with a model 335 LC detector and a model 701 fraction collector. Columns available were all Supelco Ascentis, 25 cm x 4.6 mm with 5 µm pore C18 for analytical HPLC, 25 cm x 21.2 mm with 5 µm pore C8 for semi-prep and 25 cm x 21.2 mm with 5 µm pore C18 also for semi-prep. The software used for control and analysis was Galaxie Chromatography Workstation version 1.9.3.2.

NMR samples were prepared in Norell 508UP tubes and spectra recorded on Bruker AV500, DPX300 and DRX400 spectrometers. Chemical shifts are quoted in ppm. Deuterated solvents were supplied by Cambridge Isotope Laboratories Inc.

Centrifuges available were a Du Pont Instruments Sorvall RC-5B Refrigerated Superspeed Centrifuge with GSA (up to 13,000 rpm) and SS-34 (up to 20,000 rpm) rotors, a MSE Centaur 2 (up to 4,200 rpm) and a Centurion 1000 Series (up to 6,000 rpm).

Incubators available were a New Brunswick Scientific Co. Series 25 and two Gallenkamp Orbi-Safe TS.

Bacterial Preculture

Bacterial cultures were initially grown in a Glucose and Yeast Extract (GYE) medium. This medium was prepared in a 500 ml trigrooved conical flask, glucose (1 g) and yeast extract (1 g) were dissolved in deionised water (100 ml), to which either NaOH (2M aq, 0.25 ml) or CaCO₃ (1 g) was added as a pH buffer. The flask was sealed with a polyurethane foam stopper and autoclaved at 125°C for 20 minutes.

When cooled to RT, a bacteria sample was inoculated into the flask using aseptic techniques, the flask was then incubated (30°C) with shaking (124 rpm) for 2 days.

Bacterial Growth Medium

The growth medium was prepared in 2000 ml trigrooved conical flasks. Normally, eight flasks were prepared at a time. The standard recipe was as follows, any deviations were noted in the appropriate section, fructose (5 g), soybean flour (Type I, not roasted, 7.5 g), calcium carbonate (2.5 g), dextrin (type II, 15 g), Amberlite XAD16 resin (5 g) and deionised water (250 ml). This mixture was autoclaved at 125°C for 20 minutes.

When cooled to RT, a preculture aliquot (10 ml) was added to each flask under aseptic conditions. The flasks were then incubated (30°C) with shaking (124 rpm) for 4-6 days.

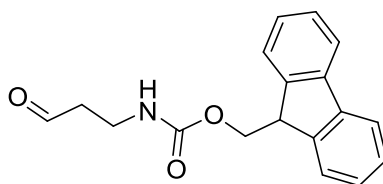
Mycelial extraction

After incubation, the contents of the growth media flasks were strained through muslin to separate the mycelia and XAD16 resin from the aqueous medium. Any residue stuck to the flasks was loosed with deionised water and added to the draining mixture. The solids were allowed to drain overnight, then the muslin fastened to form a bundle and immersed in methanol (~1500 ml). The bundle was allowed to infuse overnight to lyse bacterial cells and desorb polyenes from the resin. The yellow methanolic solution was collected with gravity filtration. This extraction was repeated as necessary with new methanol.

The methanolic extract was concentrated by rotary evaporation to remove the volatile solvent leaving a dark orange/brown suspension in residual water. This was refrigerated overnight (4°C). The precipitate was compacted by centrifugation. The supernatant was poured off, the precipitate resuspended in methanol, and filtered to remove insoluble impurities. The solution was evaporated to dryness to give a crude product mixture.

Washing of crude mycelial extract sample

The sample was suspended in ~35 ml of the washing solvent by sonication, then centrifuged to compact the insoluble precipitate. The supernatant was poured off and the wash repeated until the supernatant was clear, or UV/Vis showed that the supernatant was beginning to retain heptaene. The solid sample was dried under high vacuum to remove traces of solvent before washing with a new solvent.

Formation of 3-(Fmoc-amino)-1-propanal (**43b**)

3-(Fmoc-amino)-1-propanol (30 mg, 0.1 mmol) and SIBX (80 mg, 3 eq.) were added to 2 ml EtOAc and refluxed for 4.5 hours. The reaction was monitored by TLC. After completion the mixture was allowed to cool to RT and filtered, the filter cake was washed with EtOAc (2x3 ml). The combined EtOAc extracts were washed with sat. aq. NaHCO₃ (2x5 ml) and deionised water (5 ml). The EtOAc was removed under vacuum to give 3-(Fmoc-amino)-1-propanal as a yellow solid (25.3 mg, 85% yield).

¹H NMR (400 MHz, CDCl₃, TMS): 2.73 (2H, t, CH₂CH₂NH, *J*4.2Hz) 3.47 (2H, t, CH₂CH₂NH, *J*5.3Hz) 4.19 (1H, t, CHCH₂O, *J*4.3Hz) 4.54 (2H, d, CHCH₂O, *J*7.3Hz) 7.25 (1H, s, NH) 7.31 (2H, t, CHCH=CH, *J*7.3Hz) 7.38 (2H, t, CHCH=CH, *J*7.3Hz) 7.56 (2H, d, C=CHCH, *J*7.3Hz) 7.74 (2H, d, C=CHCH, *J*7.3Hz) 9.80 (1H, s, CHO)

¹³C NMR (100 MHz, CDCl₃): 34.5 (NHCH₂) 44.0 (CH) 47.3 (CH₂CHO) 66.7 (OCH₂) 120.0 125.0 127.0 127.7 141.3 143.9 (Fmoc) 156.3 (NHC=O) 201.1 (CHO)

HRMS: Calculated for C₁₈H₁₈NO₃ [M+H⁺]: 296.1287, Found: 296.1282

Formation of *N*-di(3-(Fmoc-amino)-1-propanyl)-AmNM (**51**)

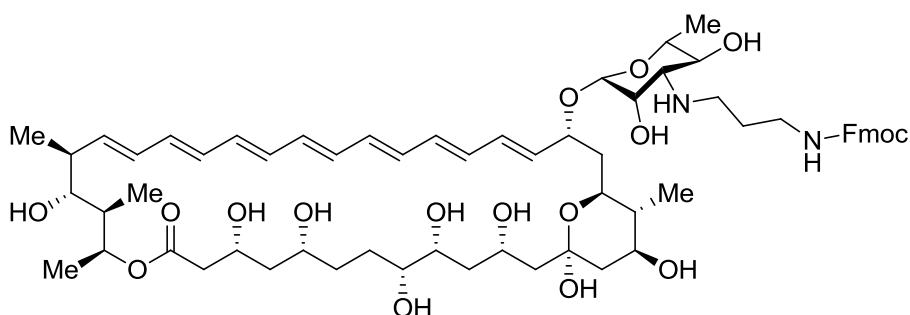


Figure 50: mono 3-(Fmoc-amino)-1-propanyl substituted AmNM

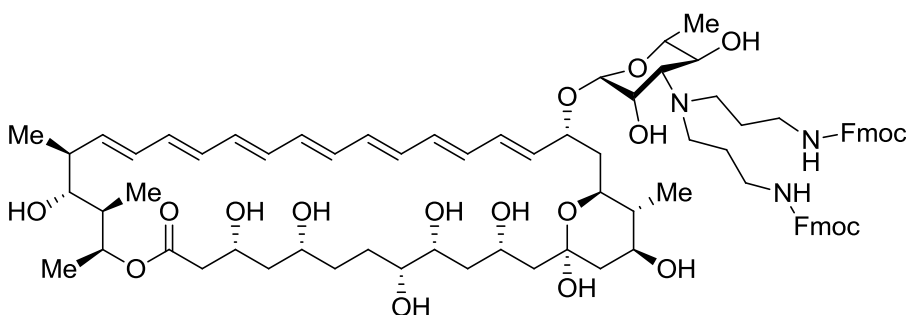


Figure 51: di 3-(Fmoc-amino)-1-propanyl substituted AmNM

3-(Fmoc-amino)-1-propanal (25 mg, 0.085 mmol, 3 eq.), NaCNBH₃ (1 mg) and 25 mg (0.028 mmol) AmNM were combined in 0.5 ml dry DMF. The mixture was stirred under nitrogen for 8 hours, after which further 3-(Fmoc-amino)-1-propanal (25 mg) and NaCNBH₃ (1 mg) were added and the reaction left to stir overnight. The contents of the reaction vessel were diluted with Et₂O, the yellow precipitate collected by filtration and washed with Et₂O to give a mixture of mono and di substituted AmNM (32.9 mg).

The products were isolated by prep HPLC to give *N*-mono(3-(Fmoc-amino)-1-propanyl)-AmNM (**50**, 10.2 mg, 0.0087 mmol, 31% yield) and *N*-di(3-(Fmoc-amino)-1-propanyl)-AmNM (**51**, 14.1 mg, 0.0097 mmol, 34% yield).

50: ¹H NMR (500MHz, methanol-d₄, TMS): 1.03 (8H, t, *J*7Hz) 1.14 (4H, d, *J*6Hz) 1.22 (5H, d, *J*6Hz) 1.31 (8H, t, *J*8Hz) 1.47-2.34 (17H, m) 3.14-3.30 (11H, m) 3.74 (1H, t, *J*10Hz) 3.98 (1H, t, *J*9Hz) 4.04 (1H, s) 4.20 (1H, t, *J*7Hz) 4.24 (1H, t, *J*7Hz)

4.34 (1H, t, $J_{10\text{Hz}}$, CHCH_2O) 4.43 (2H, d, $J_{7\text{Hz}}$, CHCH_2O) 4.61 (6H, s) 5.40 (2H, dd, $J_{10\text{Hz}}, 14\text{Hz}$) 6.02 (1H, dd, $J_{9\text{Hz}}, 15\text{Hz}$) 6.15-6.51 (14H, m, heptaene) 7.37 (4H, t, $J_{7\text{Hz}}$) 7.42 (4H, t, $J_{7\text{Hz}}$) 7.66 (4H, d, $J_{7\text{Hz}}$) 7.83 (4H, d, $J_{7\text{Hz}}$) 8.47 (1H, br s, NH)

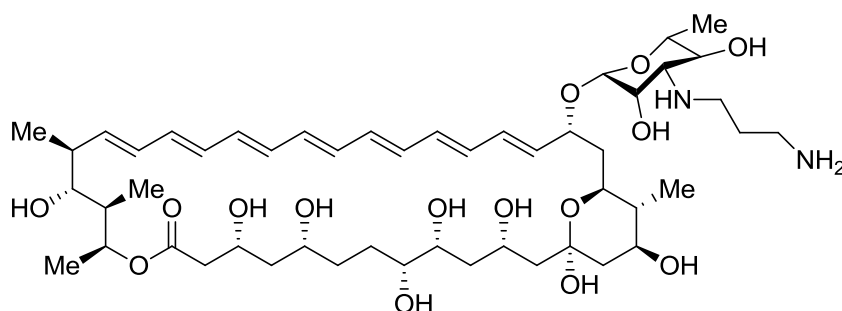
HRMS: Calculated for $\text{C}_{65}\text{H}_{93}\text{N}_2\text{O}_{17}$ [$\text{M}+\text{H}^+$] 1173.6474, Found: 1173.6453

51: ^1H NMR (500 MHz, methanol- d_4 , TMS) 4.19 (2H, t, $J_{6\text{Hz}}$, CHCH_2O) 4.35 (4H, d, $J_{6\text{Hz}}$, CHCH_2O) 5.97-6.53 (16H, m, heptaene) 7.31 (8H, t, $J_{7\text{Hz}}$) 7.39 (8H, t, $J_{7\text{Hz}}$) 7.63 (8H, d, $J_{7\text{Hz}}$) 7.80 (8H, d, $J_{7\text{Hz}}$) 8.46 (2H, br s, NH)

(This was a poor quality NMR)

HRMS: Calculated for $\text{C}_{83}\text{H}_{108}\text{N}_3\text{O}_{21}$ [$\text{M}+\text{H}^+$] 1482.7475, Found: 1482.7457

Deprotection of **50** to *N*-mono(3-amino-1-propanyl)-AmNM (**52**)



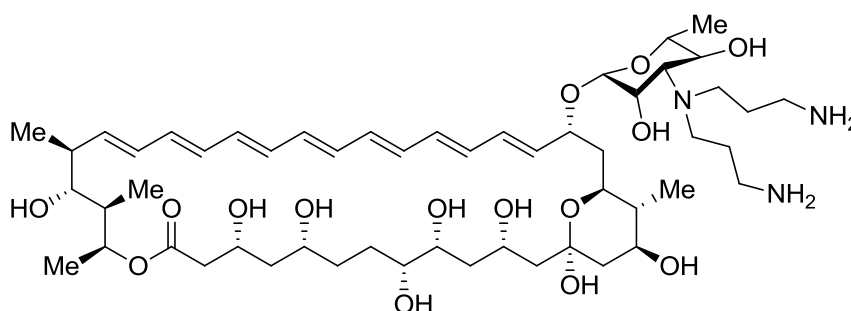
N-mono(3-(Fmoc-amino)-1-propanyl)-AmNM (10.2 mg, 0.0087 mmol) was dissolved in 5% piperidine/DMSO (2ml) and stirred for 2 hours. The mixture was diluted with Et_2O (50 ml), the yellow precipitate was collected by filtration and washed with Et_2O to give *N*-mono(3-amino-1-propanyl)-AmNM as a yellow solid (**52**, 6.1 mg, 0.0064 mmol, 74% yield).

^1H NMR (500 MHz, $\text{DMSO}-d_6$) δ ppm 0.86 (3H, t, $J_{6.4\text{Hz}}$) 0.91 (6H, t, $J_{8.2\text{Hz}}$) 0.99 (2H, br dd, $J_{15.2}, 7.7\text{Hz}$) 1.05 (3H, br d, $J_{6.4\text{Hz}}$) 1.12 (6H, br d, $J_{6.2\text{Hz}}$) 1.15 (3H, br d, $J_{6.2\text{Hz}}$) 1.24 (8H, s) 1.34 (1H, t, $J_{3.7\text{Hz}}$) 1.36 (1H, br s) 1.40 (3H, dd, $J_{13.5}, 5.5\text{Hz}$) 1.54 (5H, t, $J_{8.0\text{Hz}}$) 1.73 (2H, br d, $J_{6.9\text{Hz}}$) 1.84 (1H, br d, $J_{7.8\text{Hz}}$) 1.88

(1H, s) 2.08 (1H, s) 2.09 (1H, s) 2.17 (1H, d, J 6.0Hz) 2.31 (1H, s) 2.37 (1H, t, J 1.1Hz) 2.41 (1H, s) 2.64 (1H, t, J 1.3Hz) 2.68 (1H, s) 2.89 (2H, br s) 3.81 (1H, t, J 8.0Hz) 4.07 (1H, t, J 6.0Hz) 4.43 (1H, s) 5.44 (1H, dd, J 2.9,1.5Hz) 5.96 (1H, br dd, J 15.5,9.0Hz) 6.04 - 6.49 (14H, m, heptaene) 8.45 (1H, br s)

HRMS: Calculated for $C_{50}H_{83}N_2O_{15}$ [$M+H^+$] 951.5793, Found: 951.5792

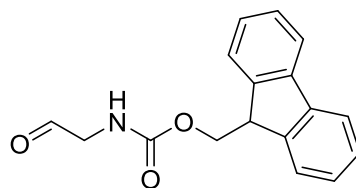
Deprotection of **51** to *N*-di(3-amino-1-propanyl)-AmNM (**54**)



N-di(3-(Fmoc-amino)-1-propanyl)-AmNM (14.1 mg, 0.0097 mmol) was dissolved in 5% piperidine/DMSO (2ml) and stirred for 2 hours. The mixture was diluted with Et₂O (50 ml), the yellow precipitate was collected by filtration and washed with Et₂O to give *N*-di(3-amino-1-propanyl)-AmNM as a yellow solid (**53**, 7.4 mg, 0.0073 mmol, 77% yield).

¹H NMR (500 MHz, DMSO-*d*₆) δ ppm 0.86 (1H, t, J 7.1Hz) 0.91 (1H, dd, J 10.1,6.9Hz) 1.04 (1H, br d, J 6.4Hz) 1.12 (2H, br d, J 5.7Hz) 1.19 (1H, t, J 8.9Hz) 1.24 (1H, br s) 1.39 (1H, t, J 13.3Hz) 1.54 (1H, t, J 12.6Hz) 1.67-1.92 (2H, m) 2.17 (1H, br d, J 6.0Hz) 2.33 (1H, s) 2.37 (1H, t, J 1.8Hz) 2.41 (1H, s) 2.65 (1H, t, J 1.6Hz) 2.68 (1H, s) 3.00 (1H, s) 3.17 (1H, s) 3.20 (1H, br s) 3.52 (1H, s) 4.07 (1H, t, J 7.3Hz) 4.41 (1H, br s) 5.21 (1H, br d, J 4.4Hz) 5.46 (1H, br s) 5.96 (1H, t, J 6.2Hz) 6.01 - 6.50 (14h, m, heptaene) 6.13 (1H, br s) 8.49 (1H, br s)

HRMS: Calculated for $C_{53}H_{90}N_3O_{15}$ [$M+H^+$] 1008.6372, Found: 1008.6412

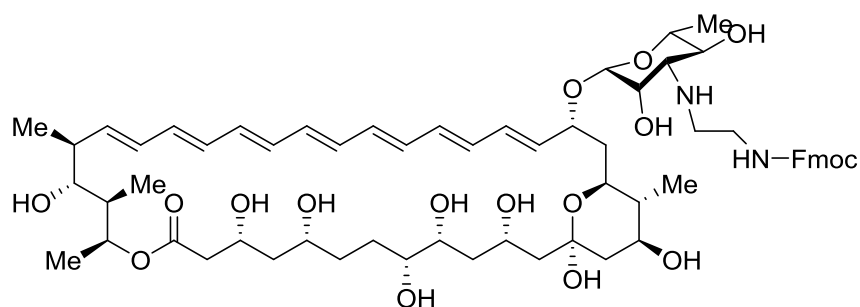
Formation of 2-(Fmoc-amino)-1-ethanal (**54b**)

2-(Fmoc-amino)-1-ethanol (80 mg, 0.282 mmol) and SIBX (240 mg, 3 eq.) were dissolved in 15 ml EtOAc and refluxed for five hours. The reaction was monitored by TLC. Upon completion the mixture was cooled to RT and filtered, the filter cake was washed with EtOAc (2x3 ml). The EtOAc extracts were washed with sat. aq. NaHCO₃ (5 ml) and deionised water (5 ml). The EtOAc was dried over magnesium sulphate and the solvent removed under vacuum to give 2-(Fmoc-amino)-1-ethanal as a light yellow solid (44 mg, 0.157 mmol, 55% yield).

¹H NMR (300 MHz, CDCl₃, TMS): 4.13 (2H, d, *J*5.3Hz) 4.22 (1H t, *J*1.7Hz) 4.42 (2H, d, *J*7Hz) 7.31 (2H, t, *J*7.3Hz) 7.39 (2H, t, *J*7.3Hz) 7.59 (2H, d, *J*7.3Hz) 7.75 (2H, d, *J*7.3Hz) 9.63 (1H, s)

¹³C NMR (75 MHz, CDCl₃): 47.1 (CH) 51.7 (CH₂CHO) 67.2 (OCH₂) 120.0 125.0 127.1 127.8 141.3 143.7 (Fmoc) 156.3 (NHC=O) 196.5 (CHO)

HRMS: Calculated for C₁₇H₁₆NO₃ [M+H⁺] 282.1130, Found: 282.1129

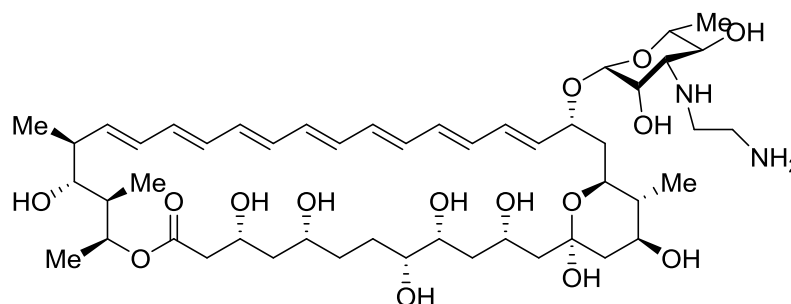
Formation of *N*-(2-(Fmoc-amino)-1-ethanyl)-AmNM (**55**)

AmNM (47 mg, 0.052 mmol) was dissolved in 2 ml dry DMF. The solution was degassed under nitrogen for 30 minutes. 2-(Fmoc-amino)-1-ethanal (22 mg, 1.5 eq.) and NaCNBH₃ (7.5 mg) were added and the mixture stirred under nitrogen for three hours. 2-(Fmoc-amino)-1-ethanal (22 mg, 1.5 eq.) and NaCNBH₃ (7.5 mg) were added again and the mixture stirred for a further three hours. The reaction mixture was diluted with Et₂O (80 ml), the yellow precipitate collected by filtration, washed with Et₂O, and purified by preparative HPLC to give *N*-(2-(Fmoc-amino)-1-ethanyl)-AmNM as a yellow solid (51.9 mg, 0.045 mmol, 86% yield.)

¹H NMR (400 MHz, methanol-d₄) 0.91 (8H, td, *J*6.5Hz,1.5Hz) 1.02 (3H, d, *J*6.5Hz) 1.10 (3H, d, *J*6.5Hz) 1.18 (3H, d, *J*6.5Hz) 1.29-1.74 (16H, m) 1.87 (2H, dd, *J*2.3Hz) 2.06 (1H, s) 2.10 (3H, br dd, *J*16.9Hz,2.8Hz) 2.19 (2H, br dd, *J*2.4Hz) 2.24 - 2.35 (2H, m) 3.09 (4H, t, *J*2.8Hz) 3.41-3.56 (4H, m) 3.80-3.94 (3H, m) 3.99-4.16 (3H, m) 4.22 (1H, t, *J*2.3Hz) 4.32 (2H, d, *J*6.5Hz) 5.28 (2H, t, *J*2.8Hz) 5.91 (1H, dd, *J*4.4Hz) 5.99-6.42 (14H, m, heptaene) 7.22 (2H, t, *J*7.5Hz) 7.30 (2H, t, *J*7.5Hz) 7.55 (2H, d, *J*7.5Hz) 7.71 (2H, d, *J*7.5Hz) 8.40 (1H, br s, *NH*)

HRMS: Calculated for C₆₄H₉₁N₂O₁₇ [M+H⁺] 1159.6318, Found: 1159.6364

Deprotection of **55** to *N*-(2-amino-1-ethanyl)-AmNM (**64**)

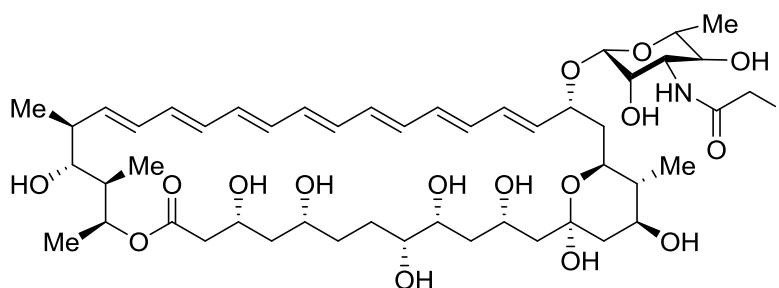


60 mg (0.052 mmol) of *N*-(2-(Fmoc-amino)-1-ethyl)-AmNM was dissolved in 2.5 ml 5% piperidine:DMSO and stirred under nitrogen for 2 hours. The reaction mixture was dripped into 200 ml diethyl ether and the precipitate collected by filtration to give *N*-ethylaminoAmNM as a yellow solid. (**64**, 28.1 mg, 0.030 mmol, 58% yield)

¹H NMR (500 MHz, methanol-*d*₄) δ ppm 0.73 (1H, s) 0.80 (2H, t, *J*5.0Hz) 0.82 (1H, s) 0.87 (3H, br t, *J*5.0Hz) 0.92 (6H, d, *J*7.1Hz) 0.95 (1H, br d, *J*6.4Hz) 1.02 (3H, d, *J*6.2Hz) 1.10 (3H, d, *J*6.4Hz) 1.17 (7H, br dd, *J*9.6,3.7Hz) 1.21 (1H, br s) 1.30 (1H, br t, *J*3.1Hz) 1.33 (1H, br s) 1.35 (1H, s) 1.37 (1H, br d, *J*4.8Hz) 1.48 (1H, d, *J*1.8Hz) 1.50 (1H, br s) 1.59 (1H, s) 1.61 (1H, d, *J*3.7Hz) 1.64 (1H, d, *J*2.3Hz) 1.64 (1H, br s) 1.71 (1H, dt, *J*4.9,2.3Hz) 1.77 (1H, d, *J*3.4Hz) 1.88 (1H, dd, *J*12.1,4.6Hz) 2.09 (1H, d, *J*2.8Hz) 2.12 (1H, d, *J*2.8Hz) 2.19 (1H, dd, *J*17.0,9.6Hz) 2.29 (1H, d, *J*6.6Hz) 2.33 (1H, t, *J*6.6Hz) 3.00 (1H, q, *J*5.0Hz) 3.03 (1H, d, *J*1.6Hz) 3.05 (1H, s) 3.07 (1H, br s) 3.10 (1H, br s) 3.14 (1H, t, *J*3.0Hz) 3.30 (1H, d, *J*2.8Hz) 3.50 (2H, t, *J*11.1Hz) 3.55 (1H, s) 3.62 (2H, t, *J*6.2Hz) 3.77 (1H, d, *J*2.5Hz) 3.82 (1H, dd, *J*3.3,1.7Hz) 3.88 (1H, t, *J*8.5Hz) 4.08 (1H, tt, *J*9.7,3.0Hz) 4.23 (1H, br t, *J*10.2Hz) 4.34 (1H, t, *J*7.8Hz) 4.45 (1H, s) 5.15 (1H, t, *J*3.2Hz) 5.28 (2H, t, *J*10.8Hz) 5.93 (1H, dd, *J*15.1,8.5Hz) 6.02 - 6.40 (14H, m, heptaene) 7.88 (1H, s)

HRMS: Calculated for C₄₉H₈₁N₂O₁₅I [M+H⁺] 937.5637, Found: 937.5630

Formation of *N*-iodoacetylAmNM (**68**)

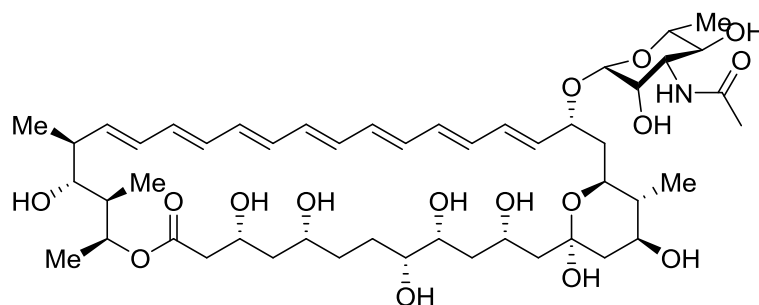


AmNM (8 mg, 0.009 mmol) was dissolved in 1 ml dry DMF, cooled to 0°C and degassed under nitrogen with stirring. Iodoacetic anhydride (7 mg, 2 eq.) was added and the mixture stirred for 20 minutes at 0°C. The mixture was added dropwise to 40 ml diethyl ether, and the precipitate collected by filtration to give *N*-iodoacetylAmNM (**68**) as a yellow solid (10.5 mg), which was purified by preparative HPLC (9.2 mg, 0.0087 mmol, 96% yield)

¹H NMR (500 MHz, methanol-d₄) 1.04 (6H, dd, *J*6.7,2.6 Hz,) 1.14 (3H, d, *J*6.4 Hz) 1.22 (3H, d, *J*6.4 Hz) 1.31 (3H, d, *J*1.0Hz) 1.35 (1H, s) 1.37-1.43 (4H, m) 1.46-1.55 (3H, m) 1.61 (2H, br d, *J*12.4Hz) 1.74 (4H, q, *J*1.0Hz) 1.83 (1H, dt, *J*7.2,2.2Hz) 1.99 (1H, br dd, *J*12.4,4.7Hz) 2.06 (1H, dd, *J*1.0Hz) 2.10 (1H, t, *J*2.9Hz) 2.14 (1H, d, *J*2.1Hz) 2.18 (1H, s) 2.20 (1H, d, *J*2.7Hz) 2.24 (1H, d, *J*2.6Hz) 2.31 (1H, dd, *J*1.0Hz) 2.41 (1H, q, *J*1.0Hz) 3.22 (2H, t, *J*1.0Hz) 3.59 (1H, dd, *J*10.5,4.3Hz) 3.64 (1H, br d, *J*10.7Hz) 3.74 (1H, t, *J*9.5Hz) 3.82 (4H, q, *J*1.0Hz) 3.99 (1H, t, *J*1.0Hz) 4.15 (1H, d, *J*2.0Hz) 4.20 (1H, tt, *J*9.7,2.9Hz) 4.36 (1H, br t, *J*9.6Hz) 4.45 (1H, t, *J*1.0Hz) 4.63 (1H, d, *J*8.1Hz) 5.40 (1H, dd, *J*1.0Hz) 6.04 (1H, dd, *J*15.0,8.8Hz) 6.16 - 6.52 (m, 14H, heptaene) 8.00 (1H, s, NH)

HRMS: Calculated for C₄₉H₇₆NO₁₆INa [M+Na⁺] 1084.4107, Found: 1084.4033

Formation of *N*-acetylAmNM (**70**)

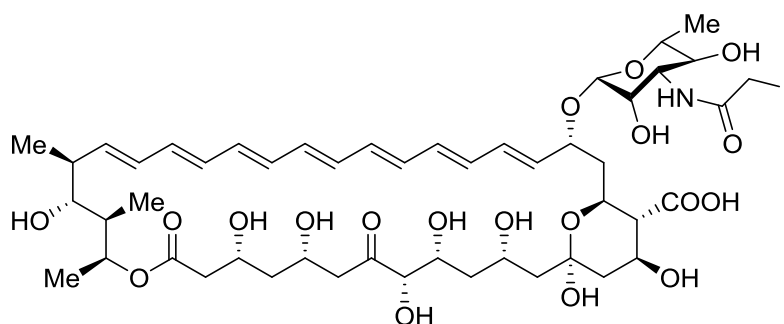


AmNM (30 mg, 0.033 mmol) was dissolved in 4 ml dry DMF, cooled to 0°C and degassed under nitrogen with stirring. Acetic anhydride (7 µl, 2 eq.) was added and the mixture stirred for four hours. The mixture was added dropwise to 80 ml diethyl ether and the precipitate collected by centrifugation to give *N*-acetylAmNM as a yellow solid (28.8 mg, 0.031 mmol, 92% yield)

¹H NMR (500 MHz, methanol-d₄) 0.92 (6H, t, *J*1.0Hz) 1.02 (3H, d, *J*6.4Hz) 1.10 (3H, d, *J*6.4Hz) 1.18 (3H, d, *J*5.7) 1.28-1.35 (4H, m) 1.38 (1H, d, *J*1.0Hz) 1.44 (1H, br d, *J*14.9Hz) 1.49 (1H, br dd, *J*14.0,1.8Hz) 1.55-1.64 (2H, m) 1.73 (1H, dt, *J*7.1, 2.9Hz) 1.79 (1H, br dd, *J*14.9,9.4Hz) 1.90-1.92 (3H, m) 1.99 (1H, dd, *J*1.0Hz) 2.11 (1H, d, *J*3.0Hz) 2.14 (1H, d, *J*3.2Hz) 2.16-2.23 (1H, m) 2.29 (1H, q, *J*1.0Hz) 3.07 (2H, s) 3.12 (1H, br d, *J*11.2Hz) 3.16 (1H, br d, *J*7.8Hz) 3.41 (1H, dd, *J*10.6,4.2Hz) 3.43-3.51 (2H, m) 3.61 (1H, br t, *J*9.4Hz) 3.71 (2H, ddd, *J*1.0Hz) 3.81 (1H, td, *J*8.6,4.1Hz) 4.07 (1H, tt, *J*9.4,3.2Hz) 4.24 (1H, br t, *J*10.1Hz) 4.33 (1H, t, *J*1.0Hz) 4.39 (1H, td, *J*8.1,2.4Hz) 4.51 (1H, d, *J*1.0Hz) 5.18 (1H, br dd, *J*6.3,3.1Hz) 5.33 (1H, dq, *J*1.0Hz) 5.74 (1H, dd, *J*1.0Hz) 5.92 (1H, dd, *J*1.0Hz) 6.03-6.42 (14H, m, heptaene) 8.42 (1H, br s, NH)

HRMS: Calculated for C₄₉H₇₇NO₁₆Na [M+Na⁺] 958.5140, Found: 958.5168

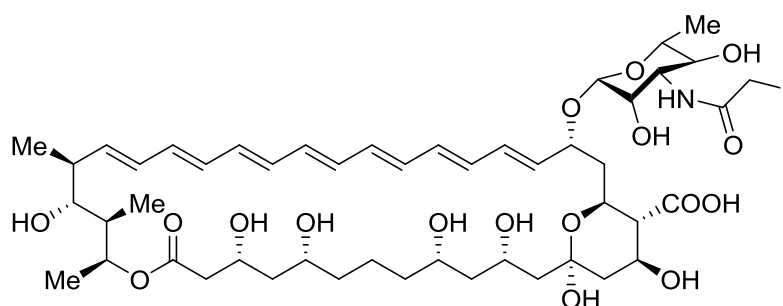
Formation of *N*-iodoacetyl-7-oxoAmB (104)



7-oxoAmB (68 mg, 0.073 mmol) was dissolved in 8 ml dry DMF, cooled to 0°C and degassed under nitrogen with stirring. Iodoacetic anhydride (77 mg, 3 eq.) was added and the mixture stirred for 30 minutes at 0°C. The mixture was added dropwise to 200 ml diethyl ether, and the precipitate collected by filtration to give *N*-iodoacetyl-7-oxoAmB as a yellow solid (74.5 mg, 0.067 mmol, 93% yield)

HRMS: Calculated for C₄₉H₇₂NO₁₉INa [M+Na⁺] 1128.3757, Found: 1128.3801

Formation of *N*-iodoacetyl-8-deoxyAmB (105)

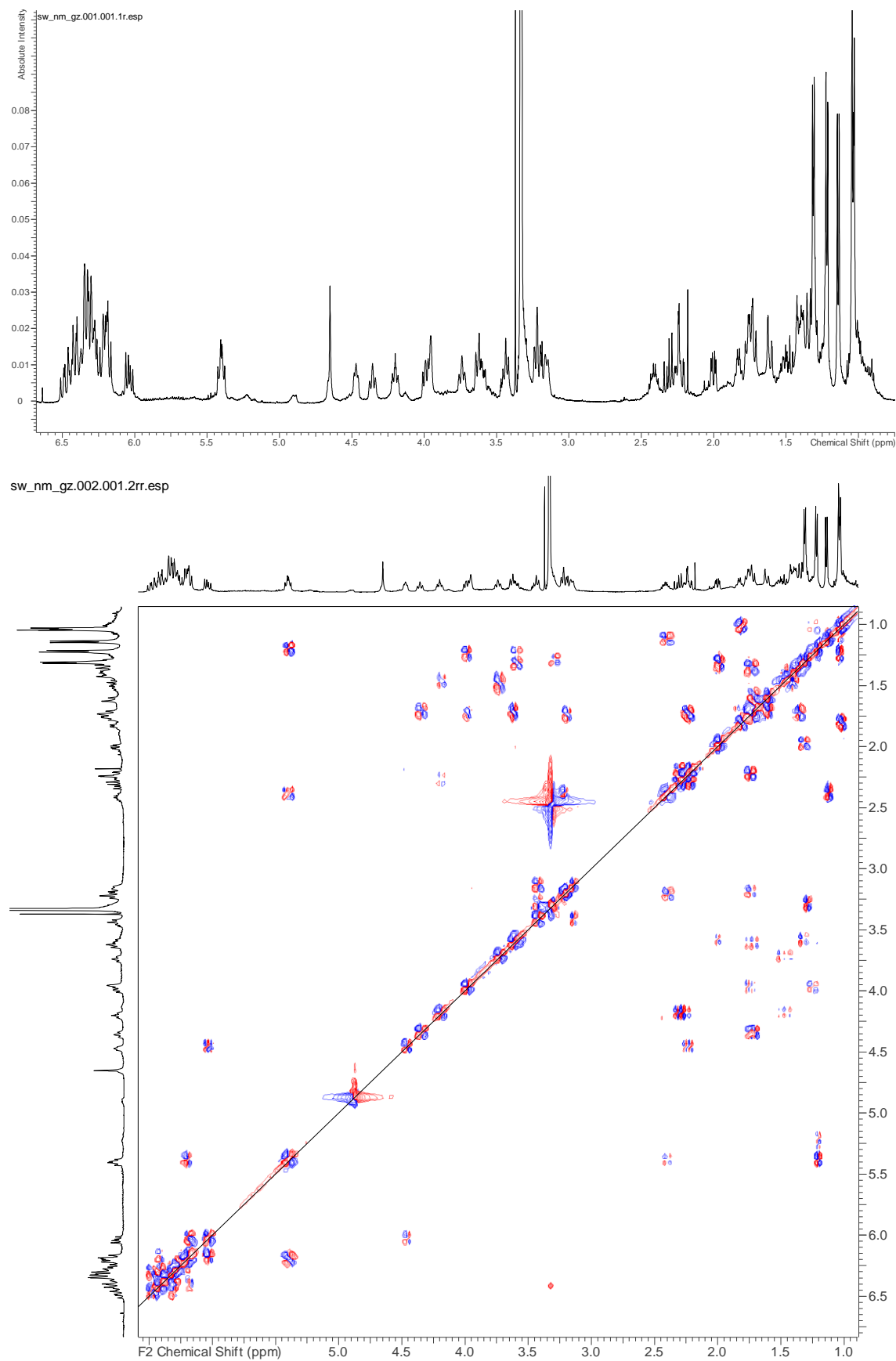


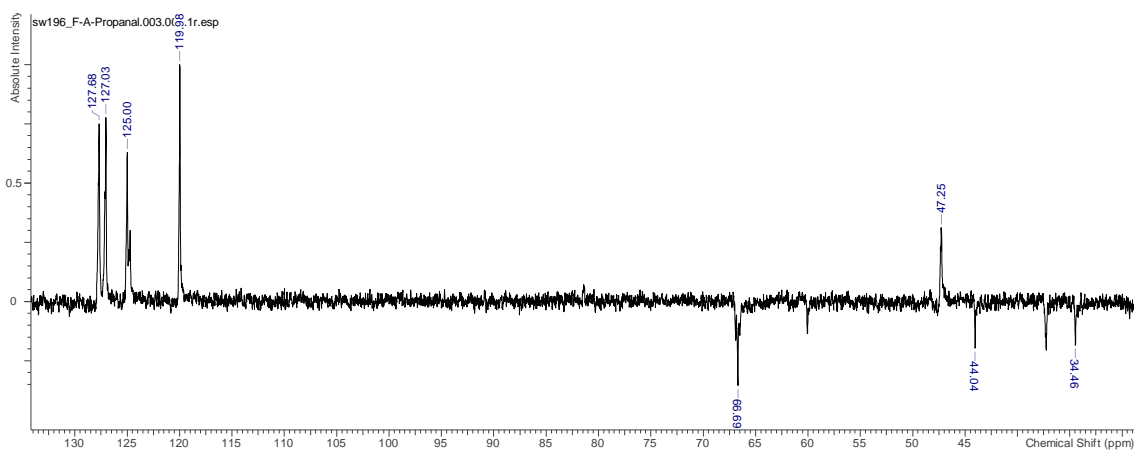
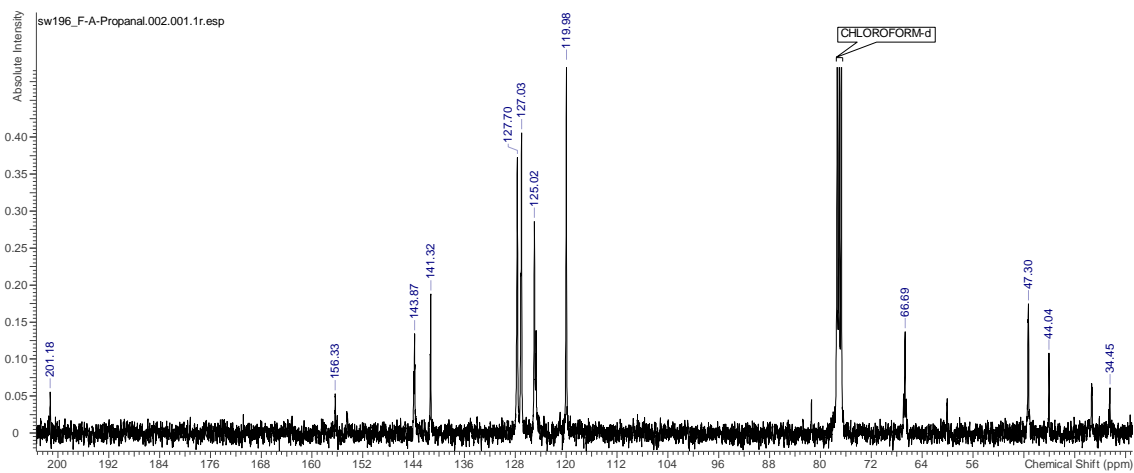
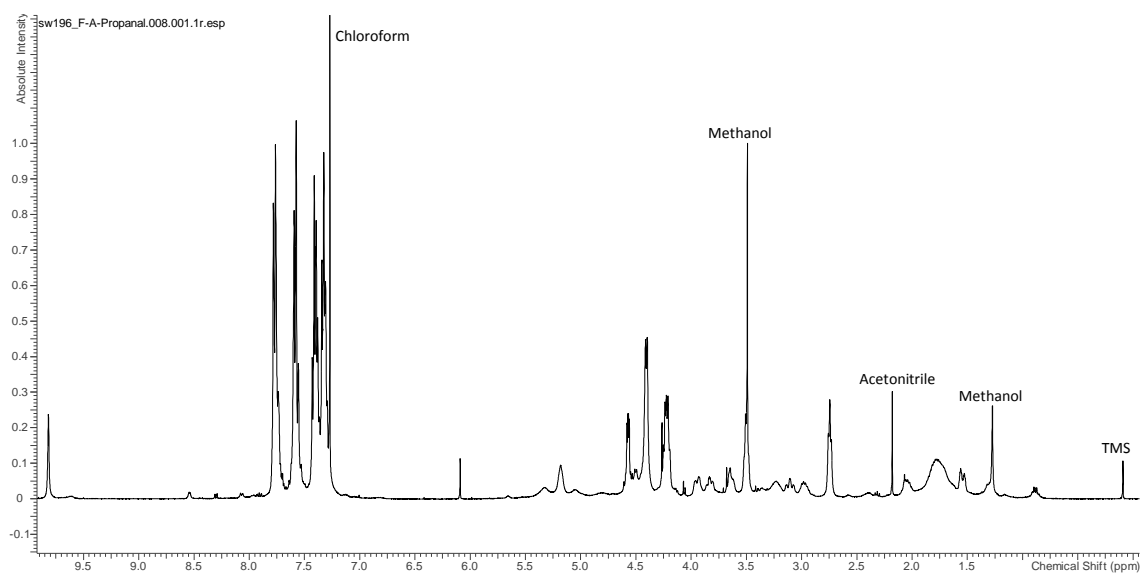
8-deoxyAmB (104 mg, 0.115 mmol) was dissolved in 8 ml dry DMF, cooled to 0°C and degassed under nitrogen with stirring. Iodoacetic anhydride (121 mg, 3 eq.) was added and the mixture stirred for 30 minutes at 0°C. The mixture was added dropwise to 200 ml diethyl ether, and the precipitate collected by filtration to give *N*-iodoacetyl-8-deoxyAmB as a yellow solid (120.1 mg, 0.112 mmol, 98% yield)

HRMS: Calculated for C₄₉H₇₄NO₁₇INa [M+Na⁺] 1098.4011, Found: 1098.3979

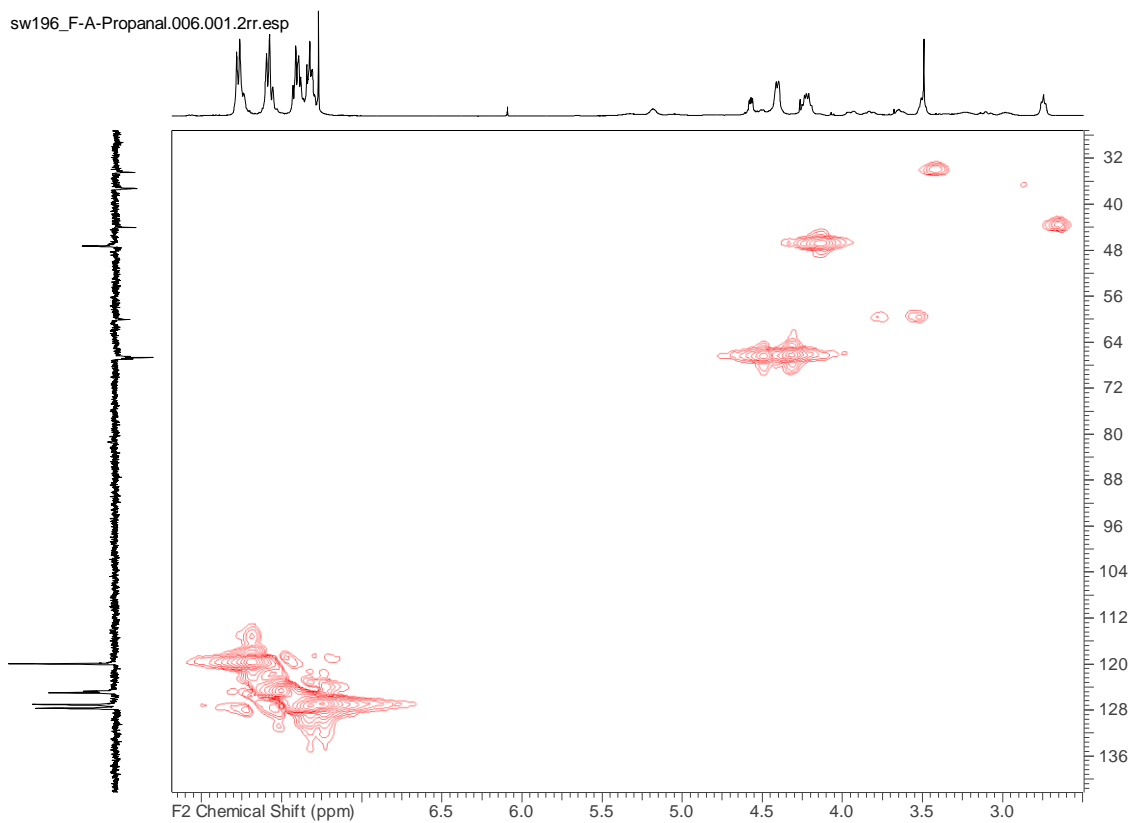
7. Appendix – NMR Spectra

16-descarboxyl-16-methyl-amphotericin B (AmNM, 33)

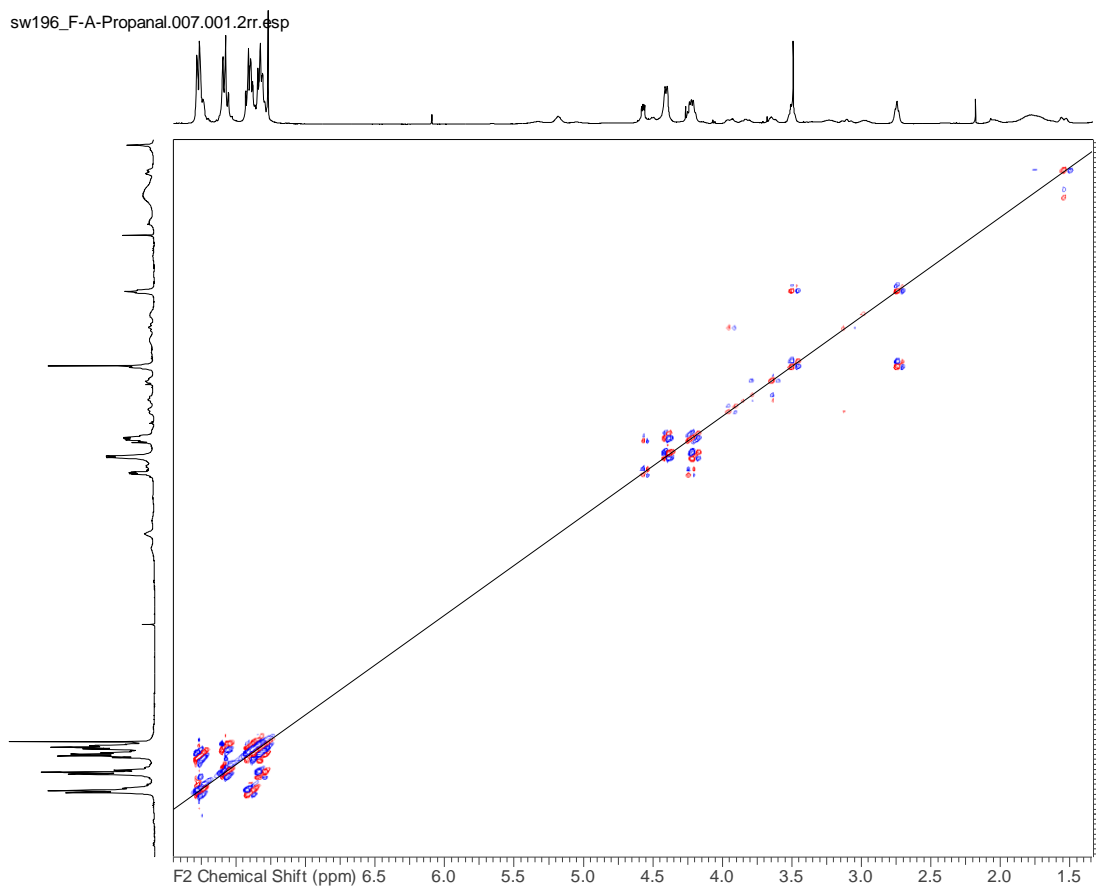


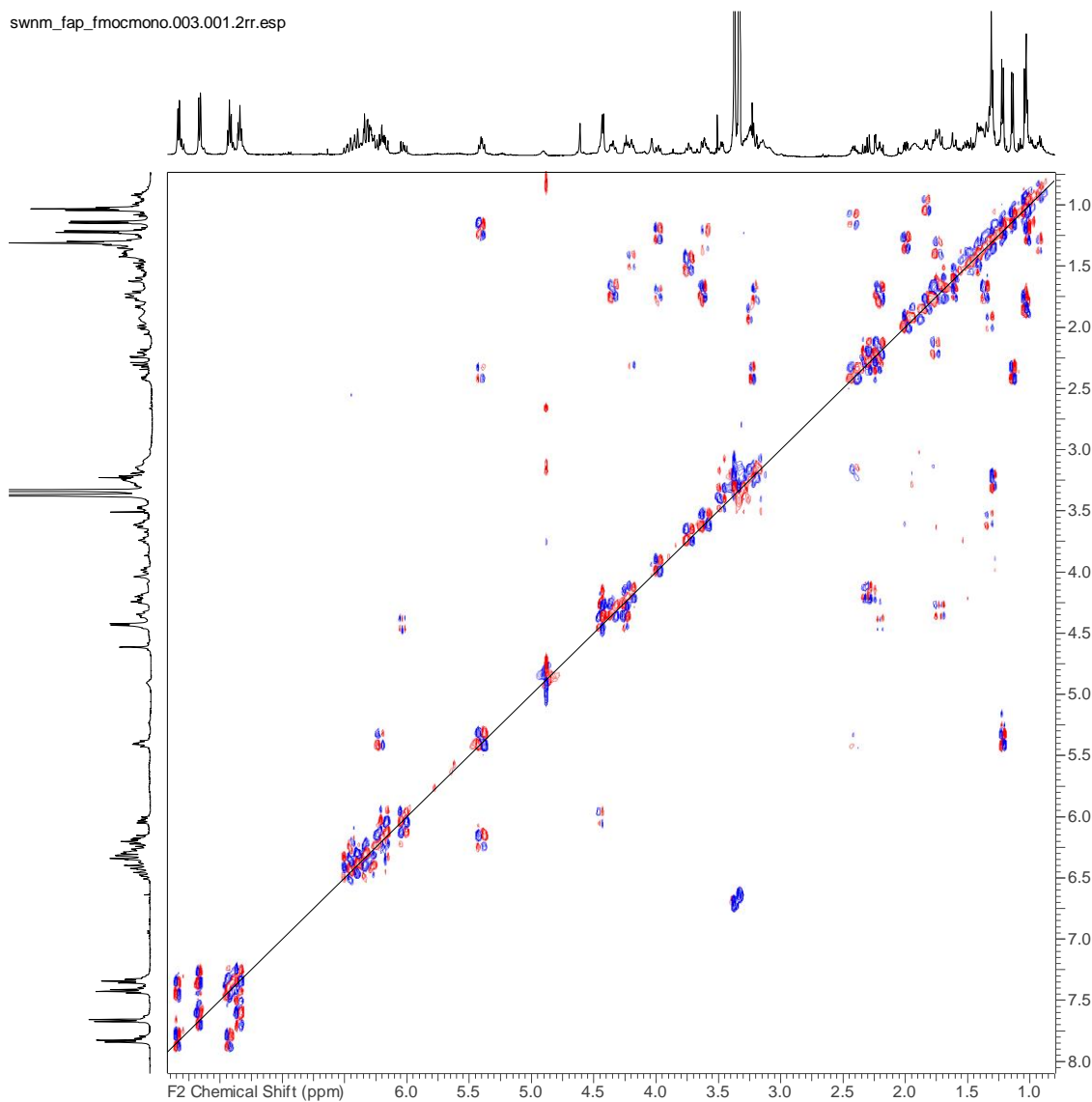
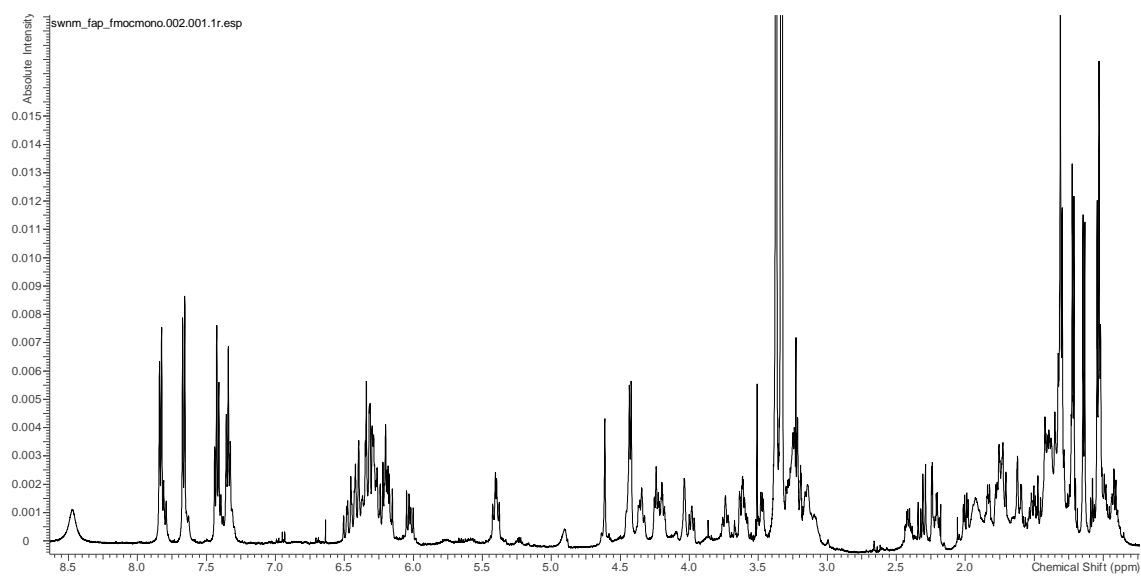
3-(Fmoc-amino)-1-propanal (43b)

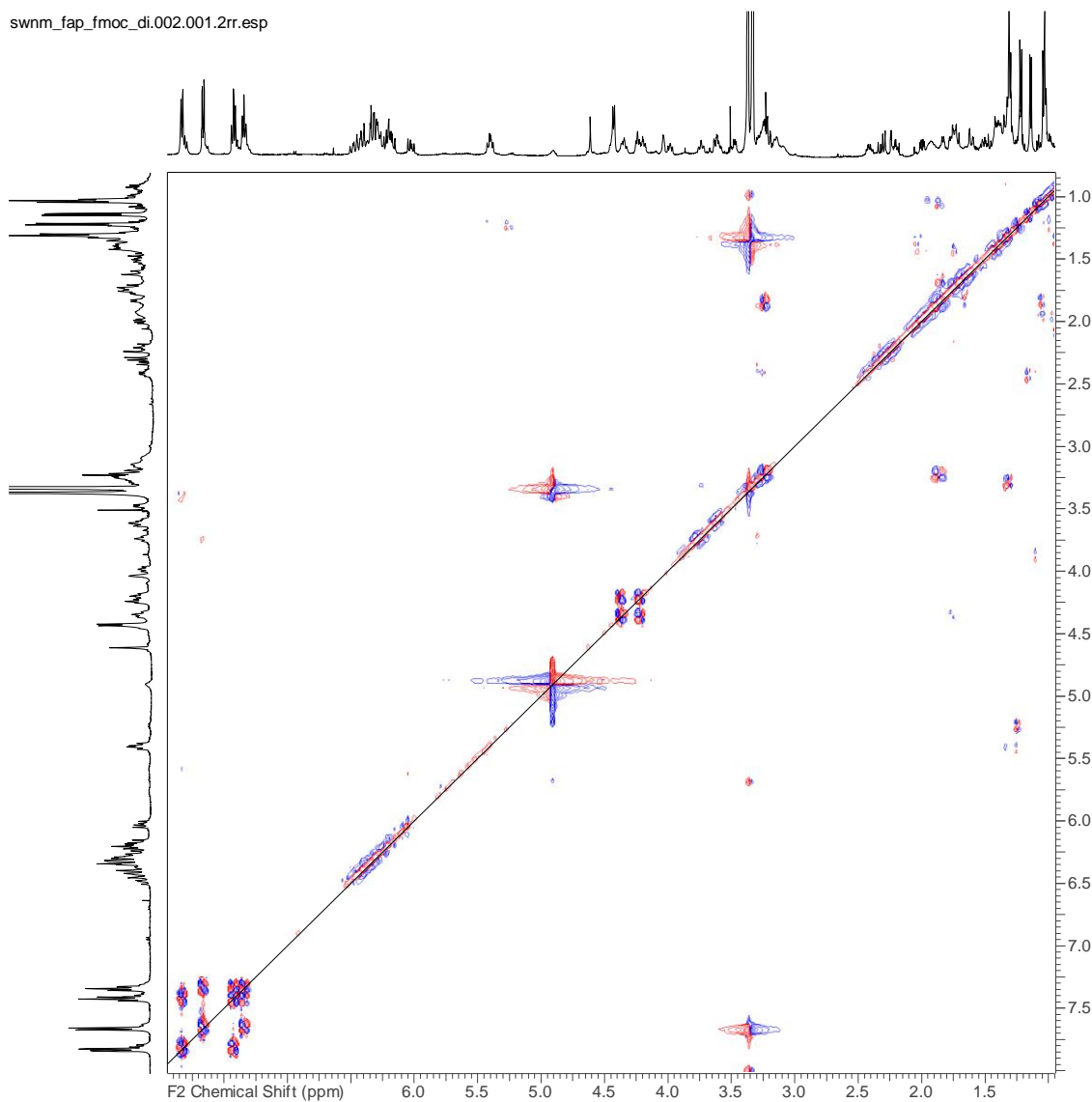
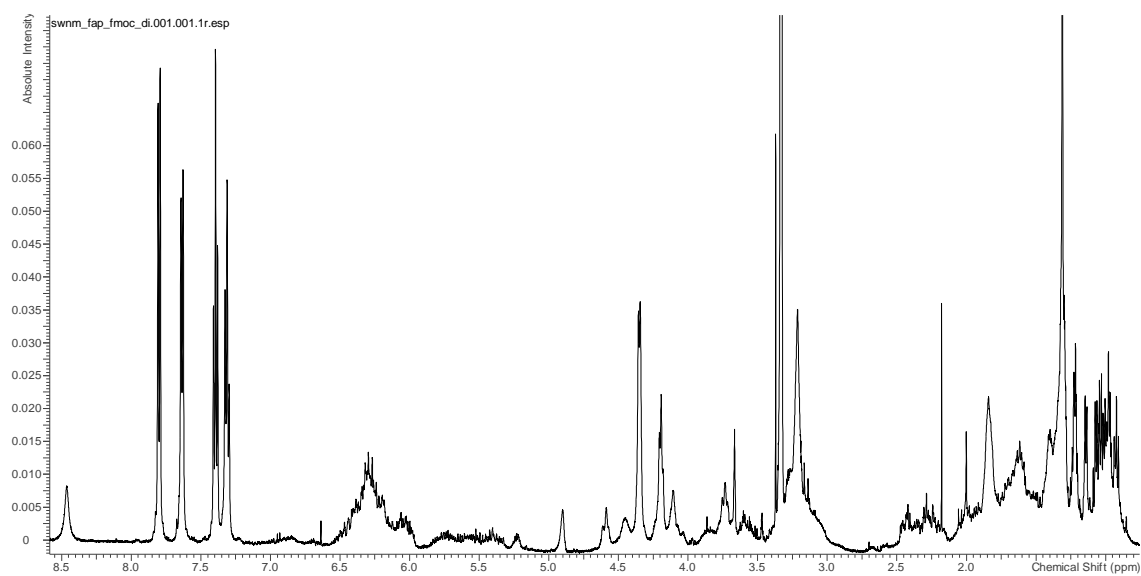
sw196_F-A-Propanal.006.001.2rr.esp

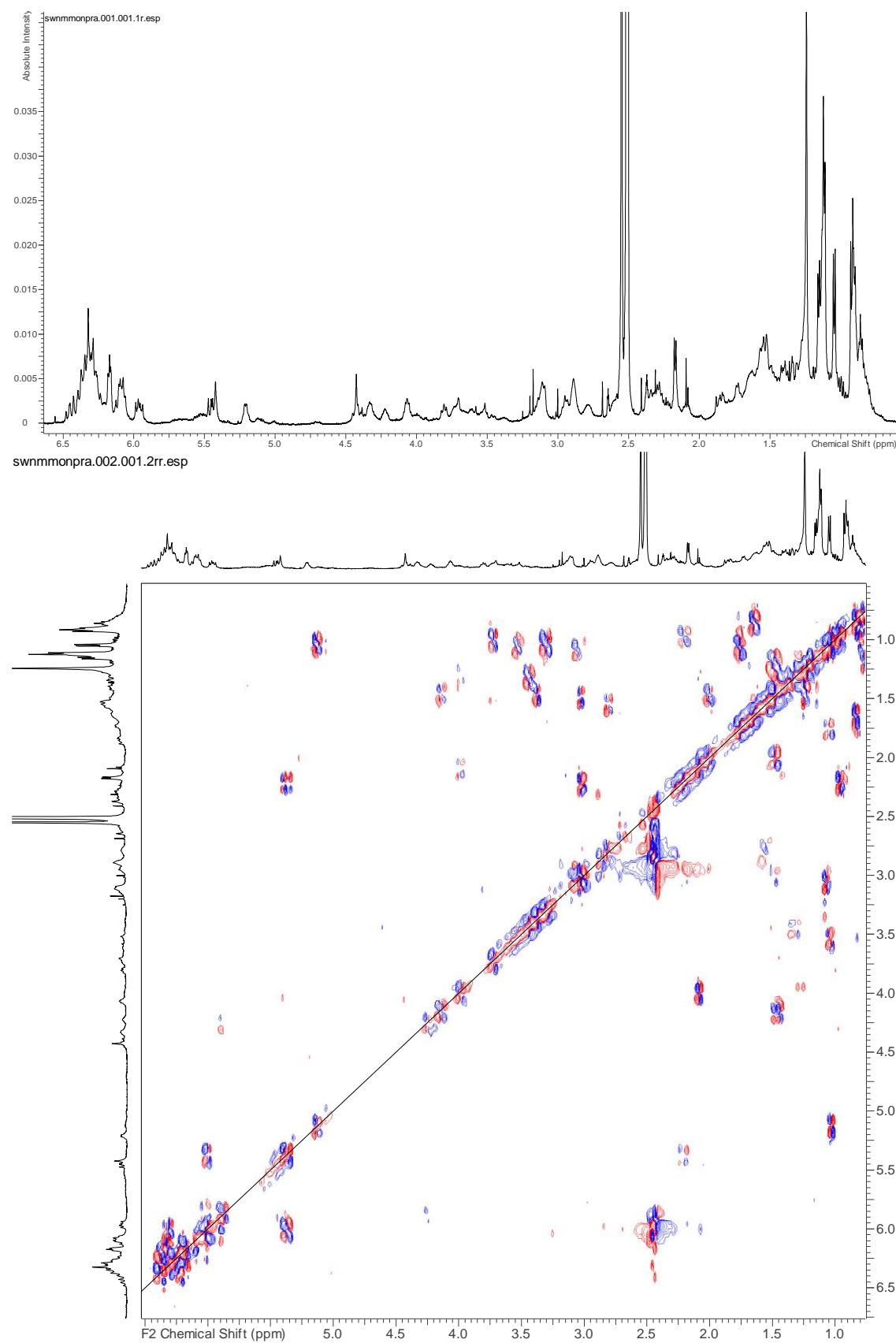


sw196_F-A-Propanal.007.001.2rr.esp

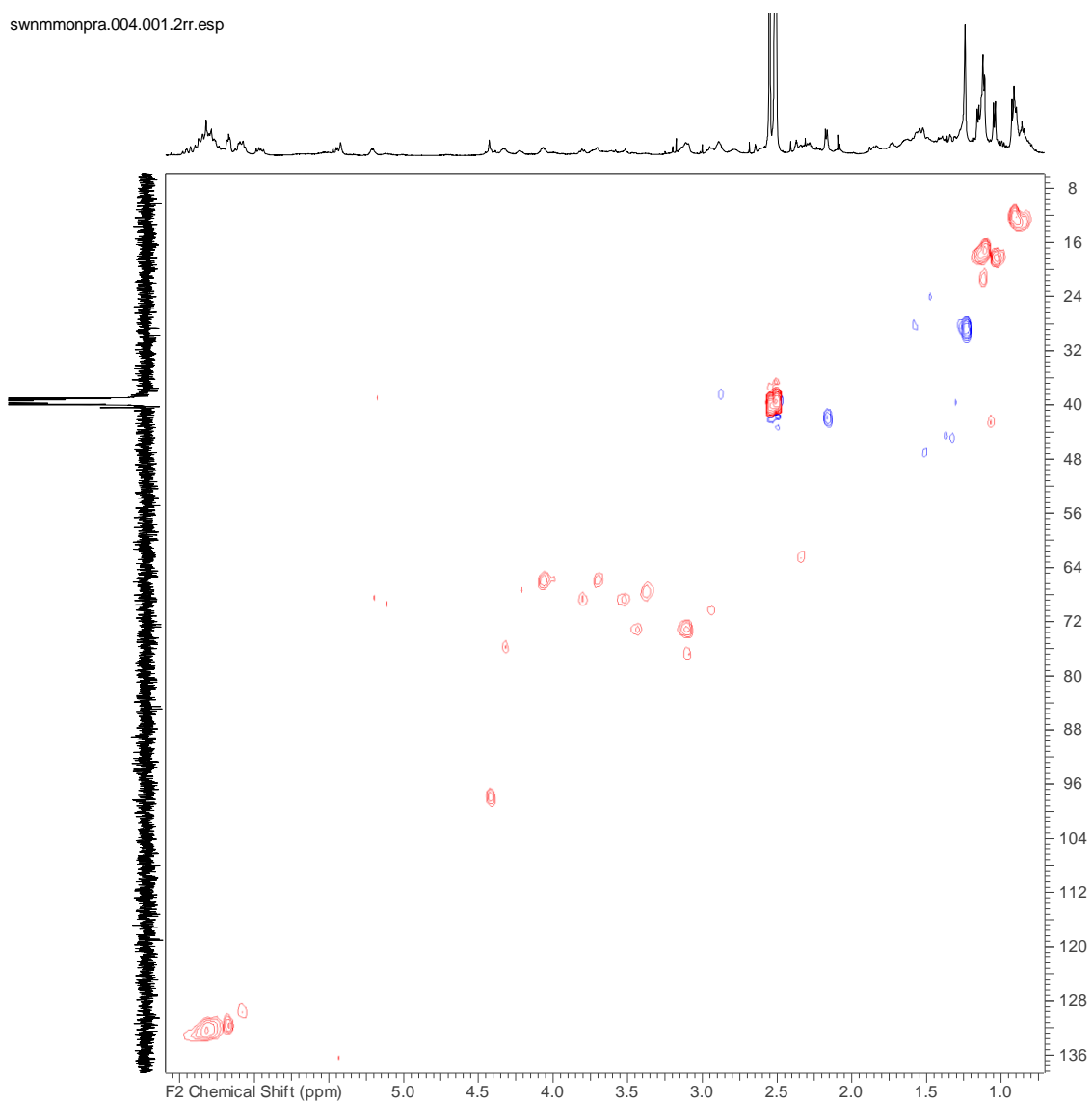


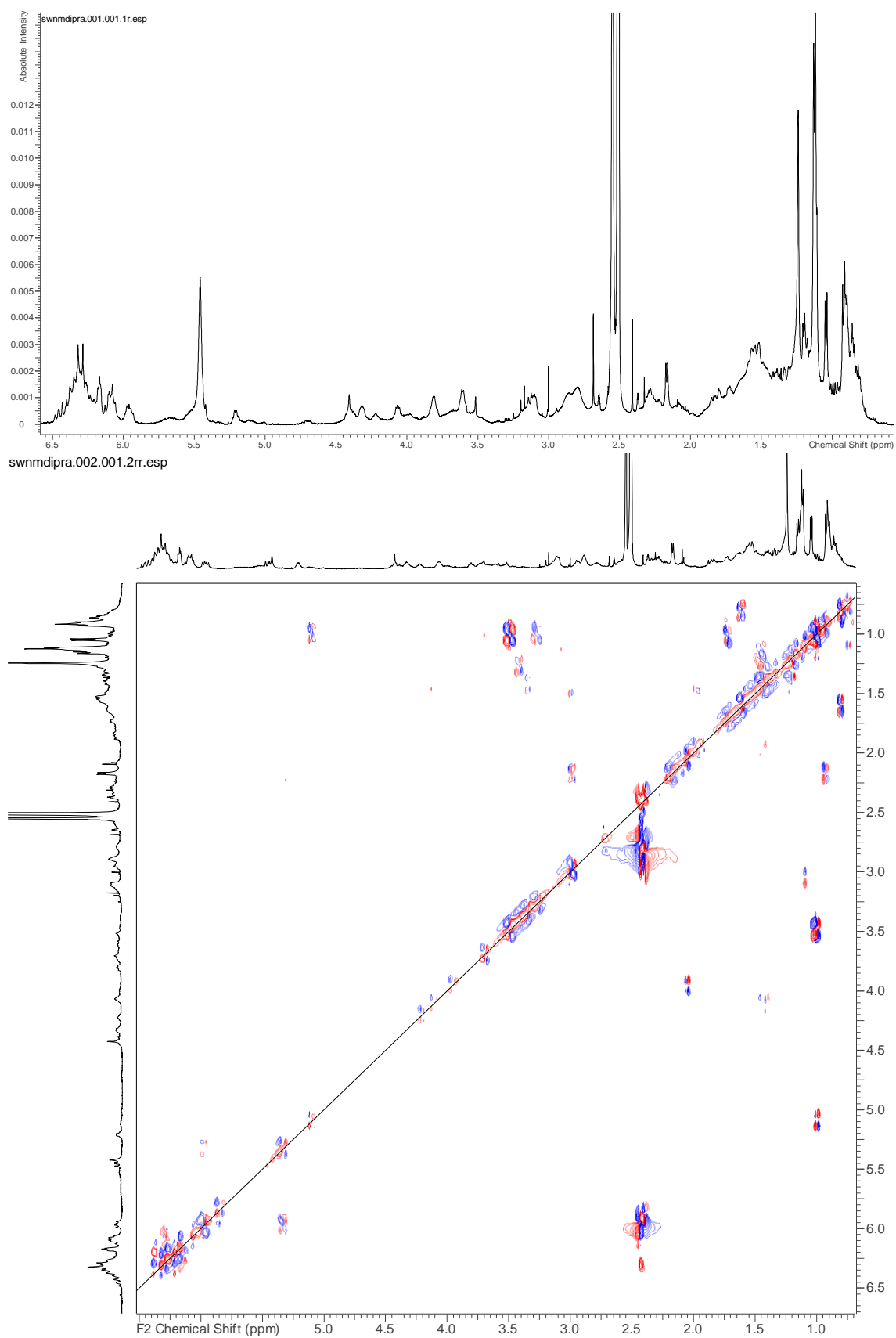
N-mono(3-(Fmoc-amino)propanyl)-AmNM (50)

N-di(3-(Fmoc-amino)propanyl)-AmNM (51)

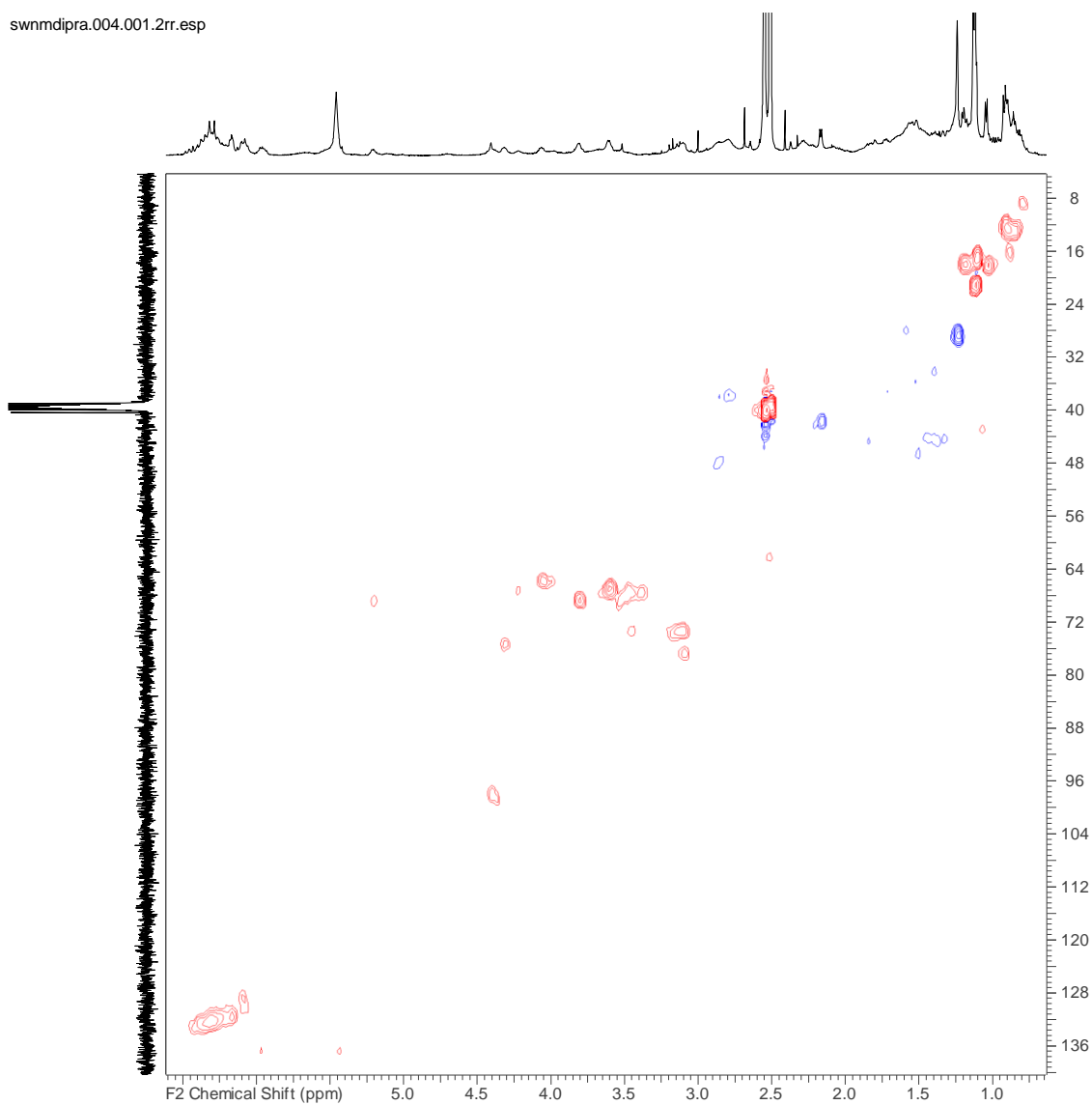
N-mono(3-aminopropanyl)-AmNM (52)

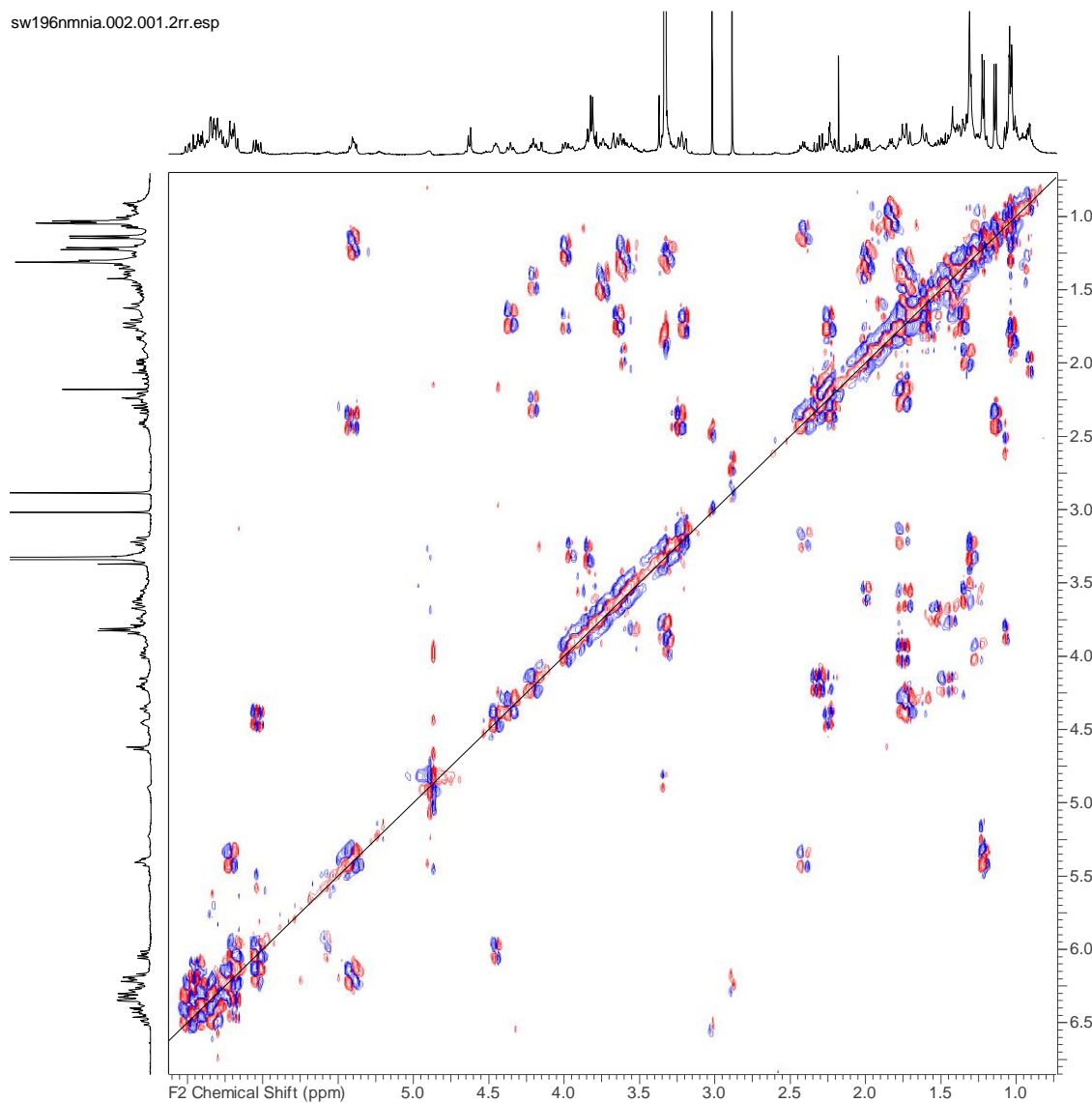
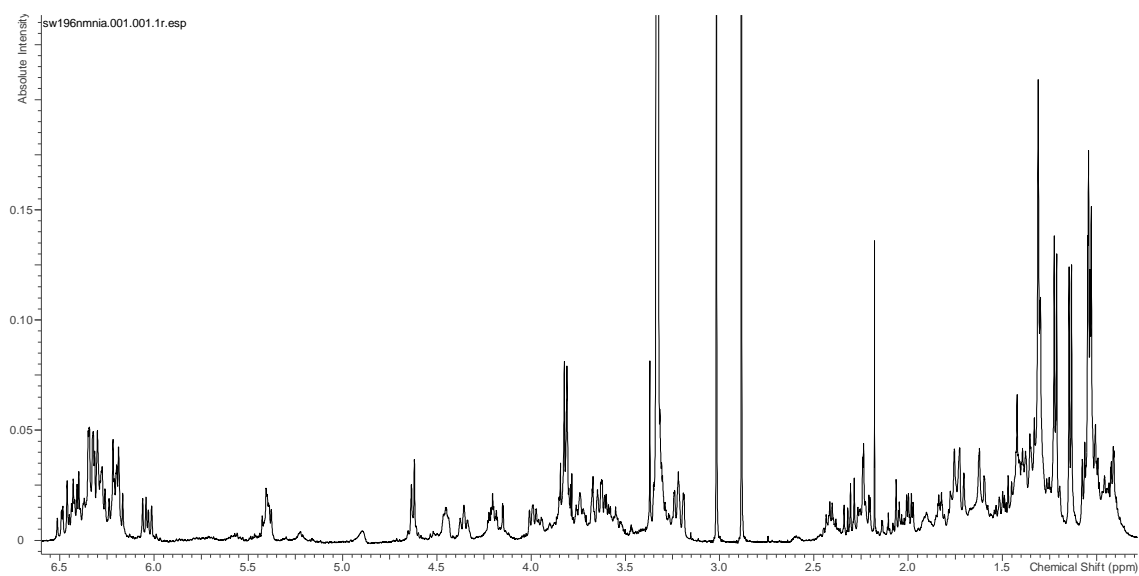
swnmmonpra.004.001.2rr.esp

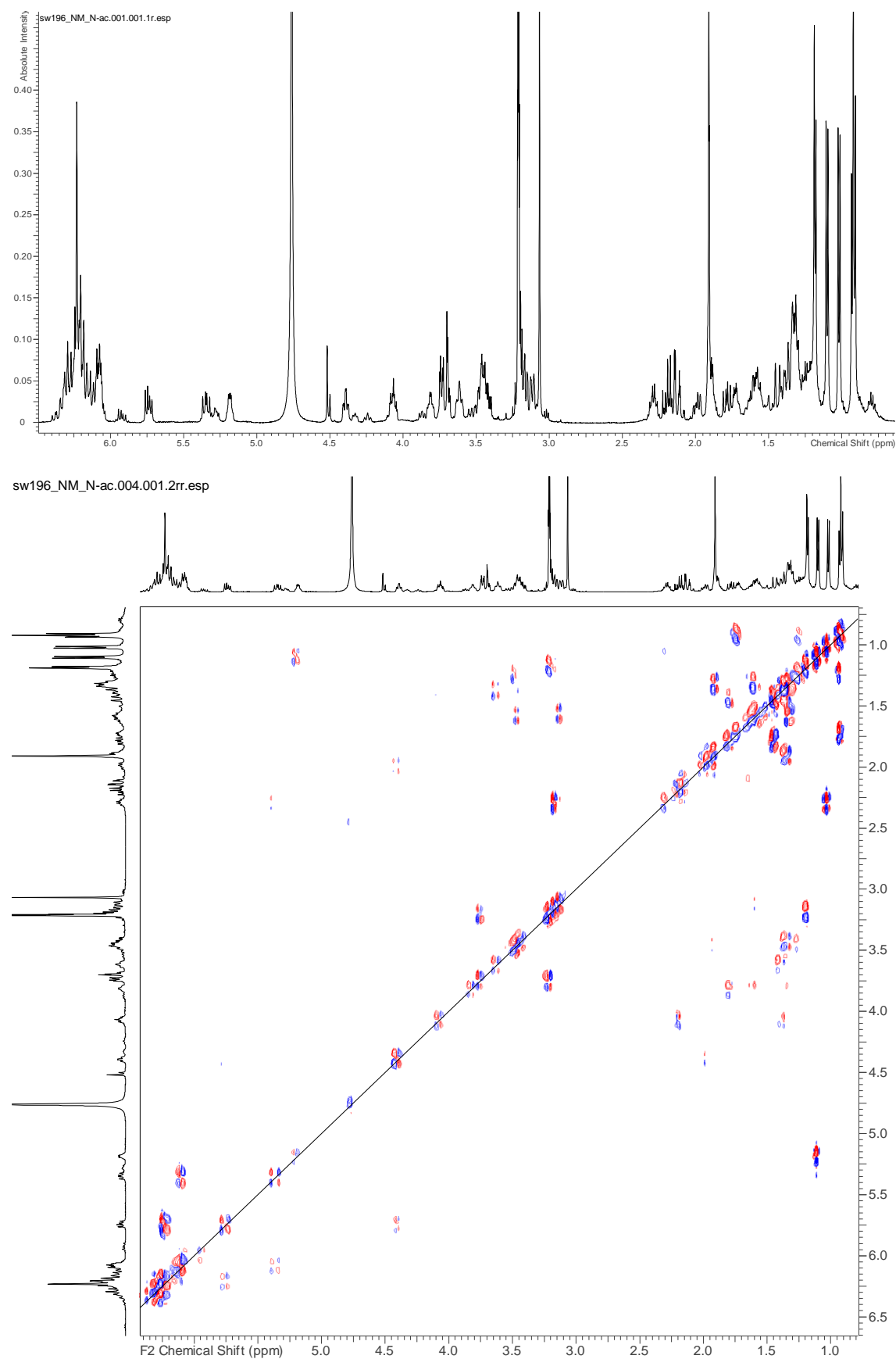


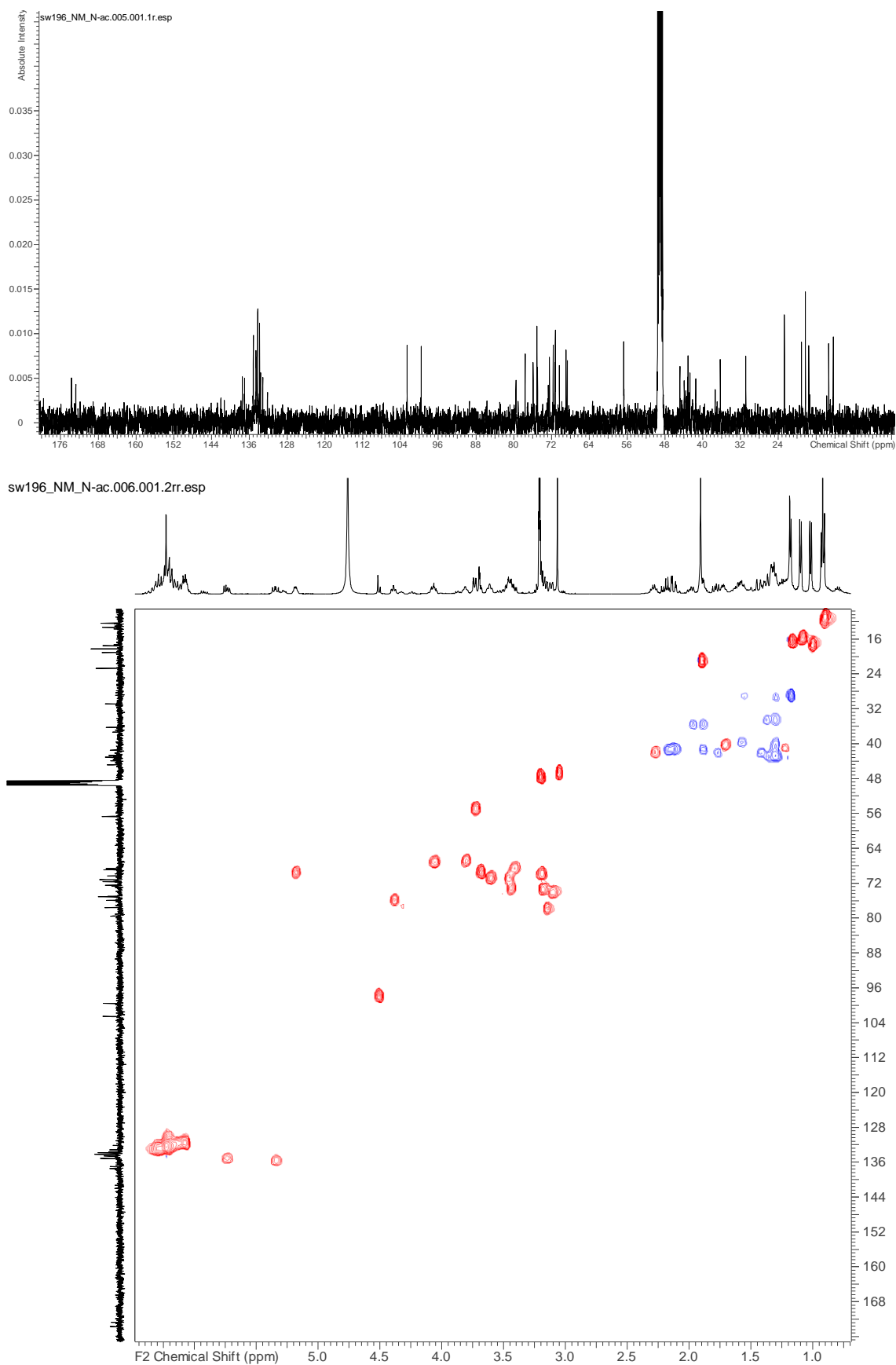
N-di(3-aminopropyl)-AmNM (53)

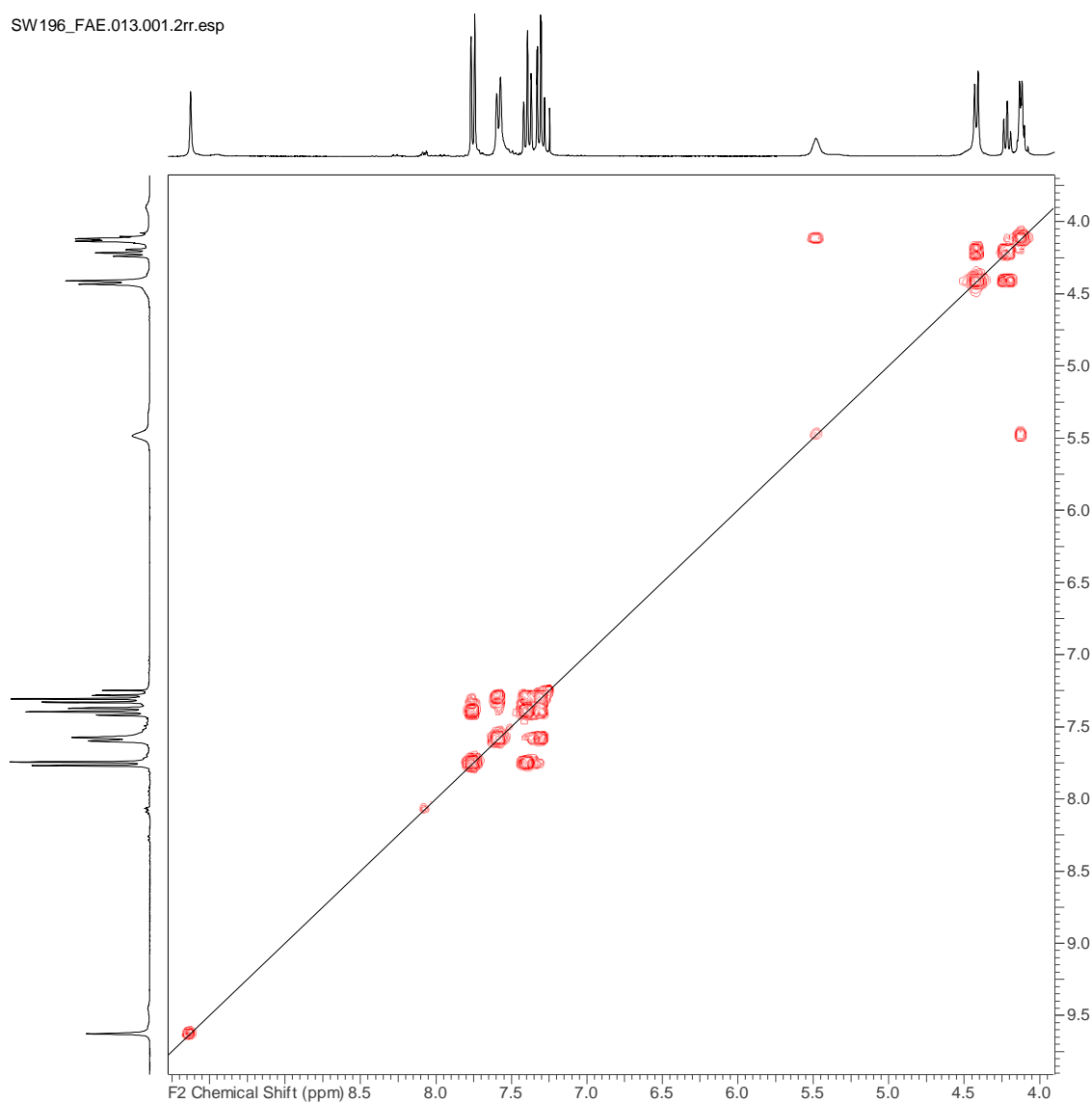
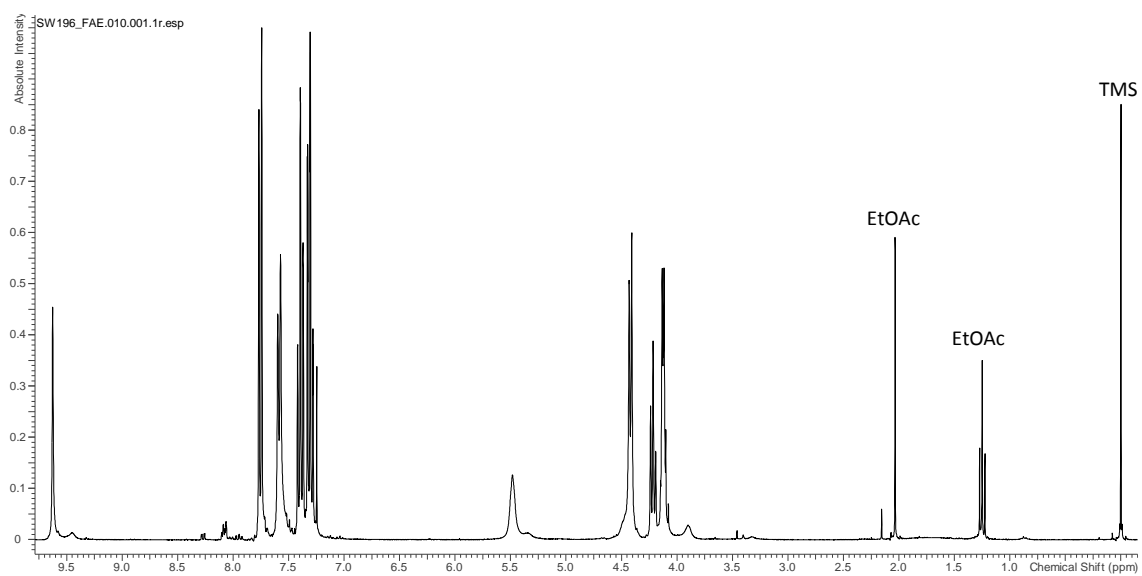
swnmdipra.004.001.2rr.esp

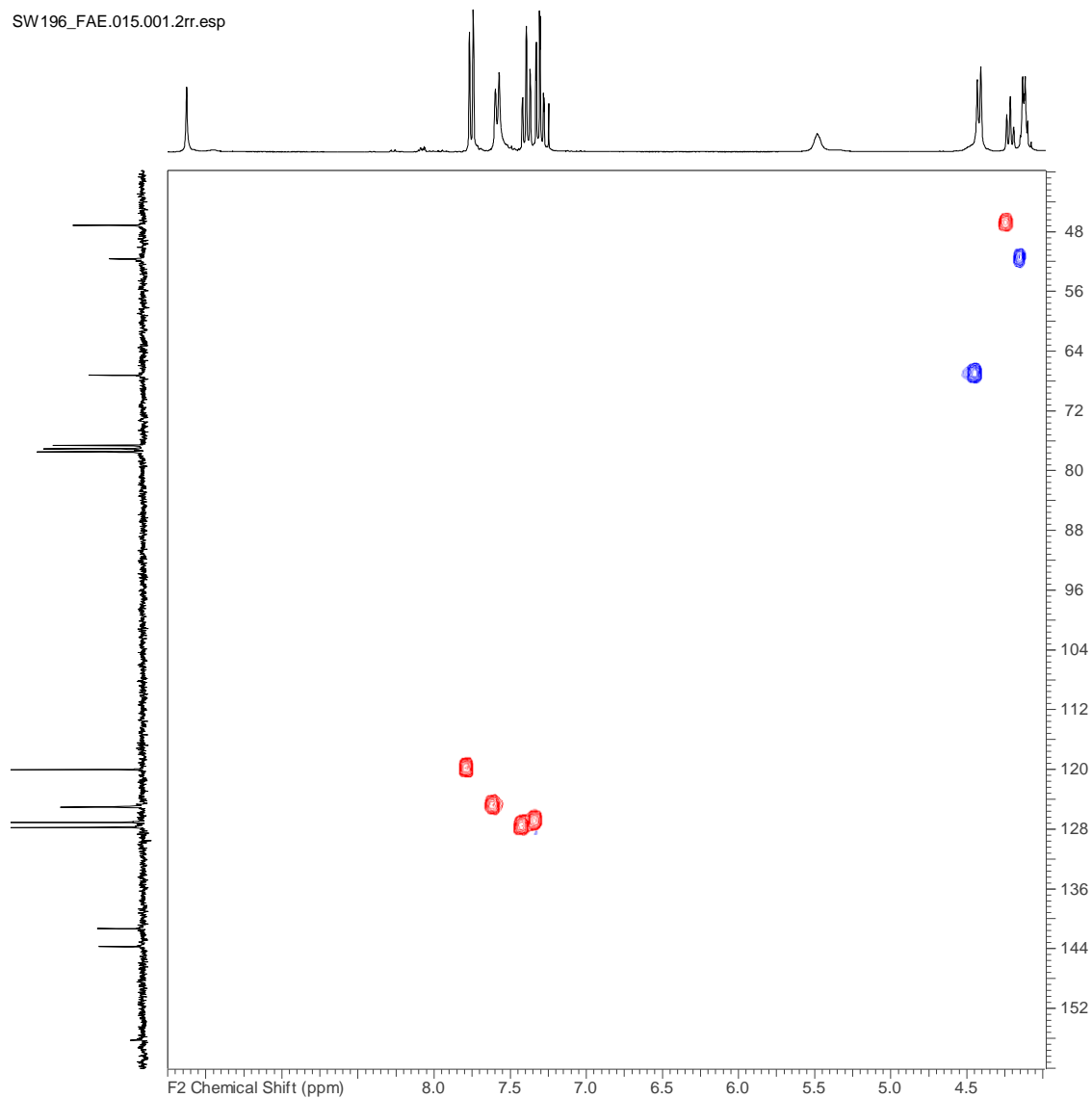
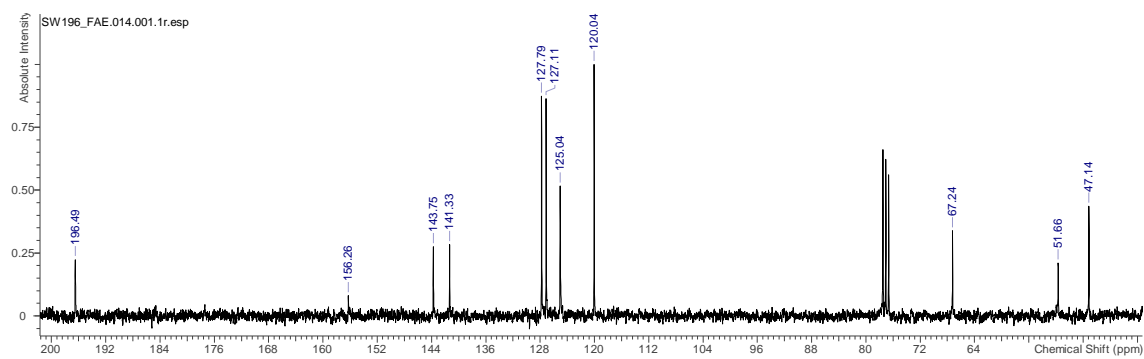


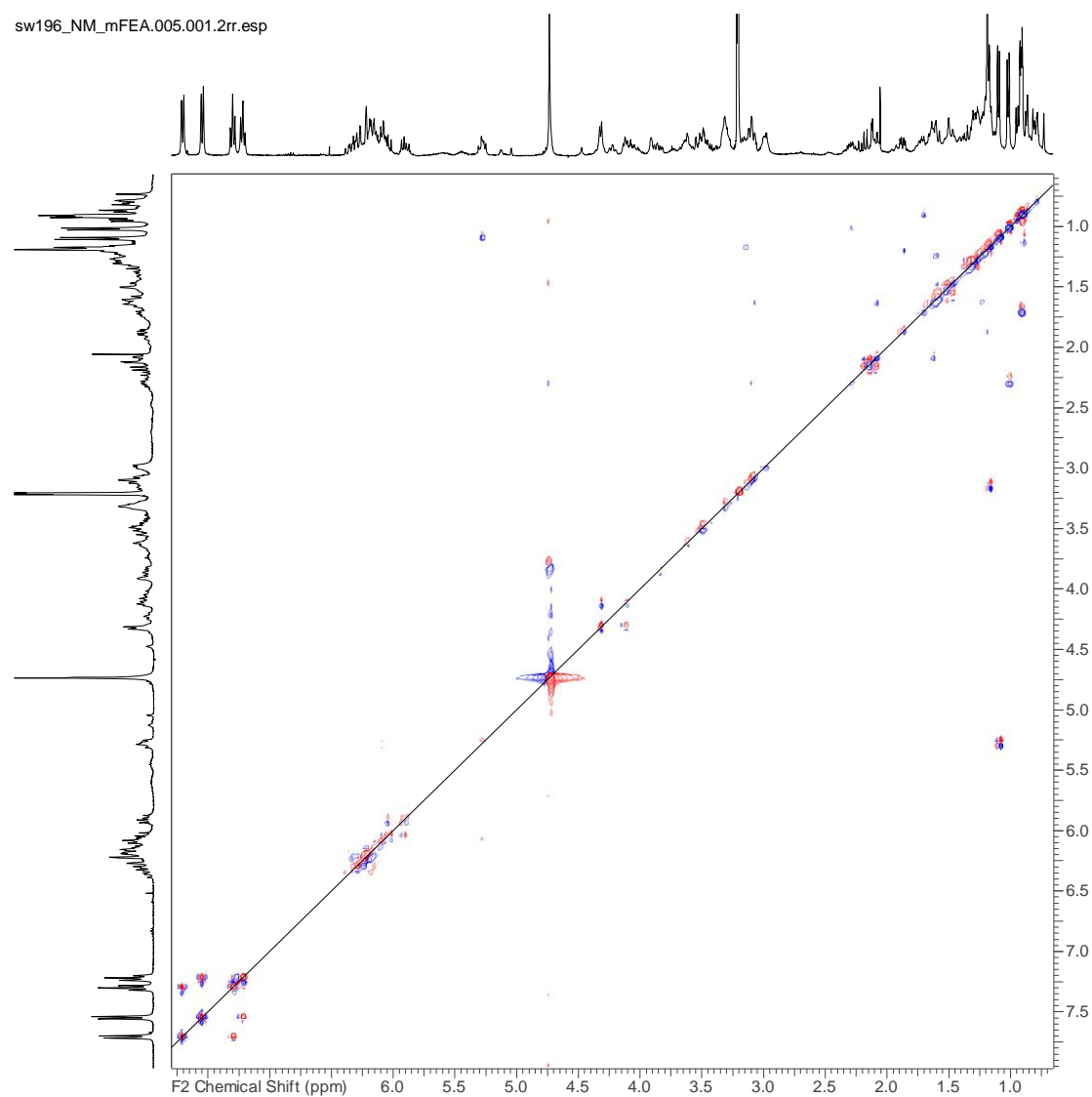
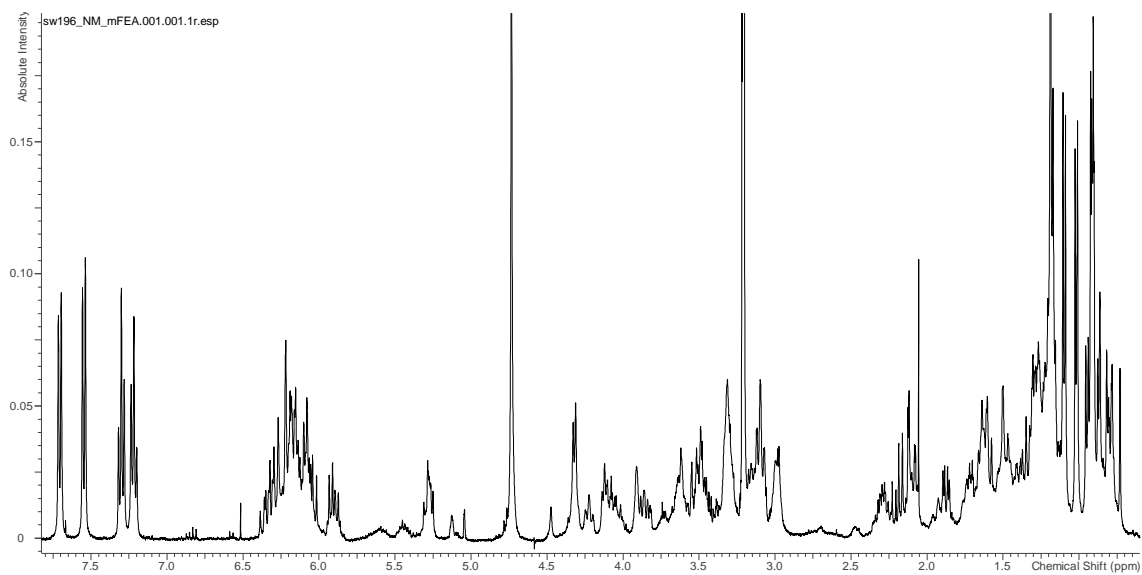
N-iodoacetyl-AmNM (68)

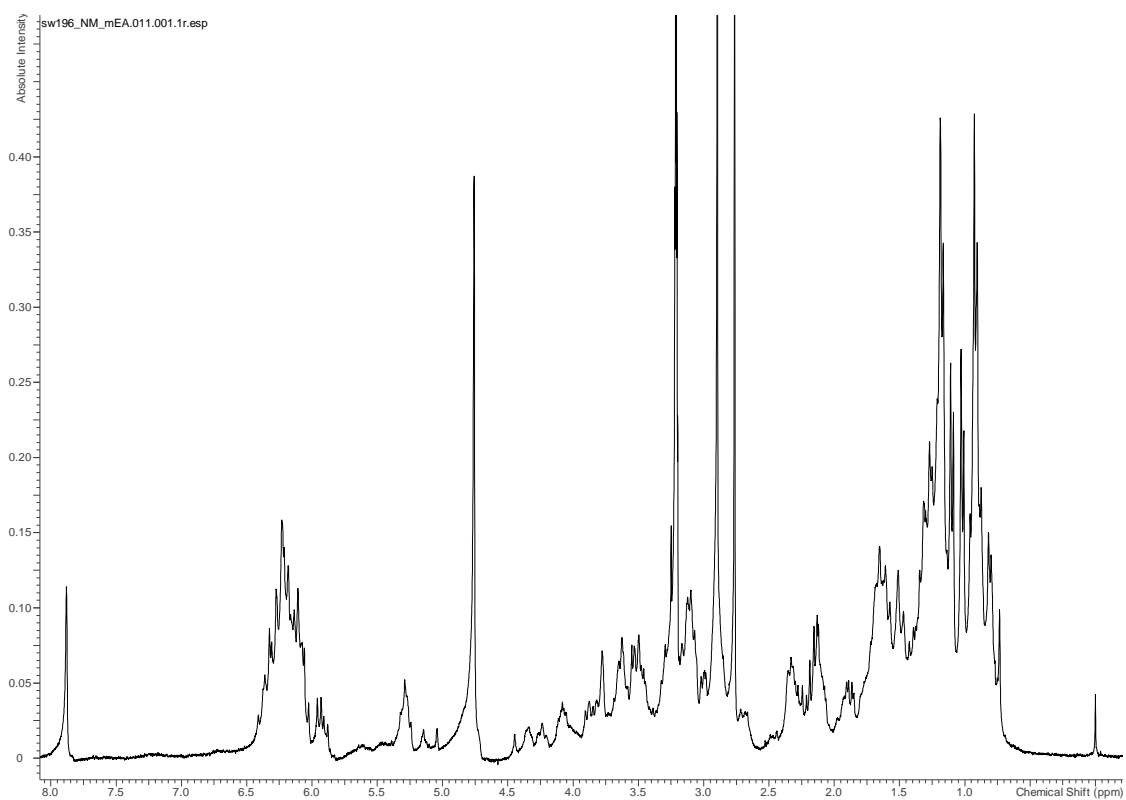
N-acetyl-AmNM (70)



2-(Fmoc-amino)-1-ethanal (54b)



N-(2-(Fmoc-amino)-1-ethyl)-AmNM (**55**)

N-(2-amino-1-ethanyl)-AmNM (64)

8. References

1. Vandeputte, I.; Wachtel, J.; Stiller, E., Antibiotics Annual 1955-1956. *Medical Encyclopedia, New York* **1956**, 587.
2. Dutcher, J. D., The Discovery and Development of Amphotericin B. *Diseases of the Chest* **1968**, *54, Supplement 1*, 296-298.
3. Payne, G. F.; Delacruz, N.; Coppella, S. J., Improved Production of Heterologous Protein from *Streptomyces-Lividans*. *Appl. Microbiol. Biotechnol.* **1990**, *33 (4)*, 395-400.
4. Gold, W.; Stout, H.; Pagano, J.; Donovan, R.; Welch, H.; Marti-Ibanez, F., Antibiotics Annual 1955–1956. *Medical Encyclopedia. New York.* p **1956**, 579-86.
5. Aszalos, A.; Bax, A.; Burlinson, N.; Roller, P.; McNeal, C., Physico-chemical and microbiological comparison of nystatin, amphotericin A and amphotericin B, and structure of amphotericin A. *The Journal of antibiotics* **1985**, *38 (12)*, 1699-1713.
6. Lewis, R. E.; Kontoyiannis, D. P.; Darouiche, R. O.; Raad, I. I.; Prince, R. A., Antifungal Activity of Amphotericin B, Fluconazole, and Voriconazole in an In Vitro Model of Candida Catheter-Related Bloodstream Infection. *Antimicrobial Agents and Chemotherapy* **2002**, *46 (11)*, 3499-3505.
7. Nadjm, B.; Behrens, R. H., Malaria: An Update for Physicians. *Infect. Dis. Clin. North Am.* **2012**, *26 (2)*, 243.
8. Lozano, R.; Naghavi, M.; Foreman, K.; Lim, S.; Shibuya, K.; Aboyans, V.; Abraham, J.; Adair, T., Global and regional mortality from 235 causes of death for 20 age groups in 1990 and 2010: a systematic analysis for the Global Burden of Disease Study 2010. *Lancet* **2012**, *380 (9859)*, 2095-2128.
9. Cheng, M., World Health Organization action in Afghanistan aims to control debilitating Leishmaniasis. *WHO Bulletin* **10th August 2004**.
10. Reithinger, R.; Mohsen, M.; Aadil, K.; Sidiqi, M.; Erasmus, P.; Coleman, P. G., Anthroponotic Cutaneous Leishmaniasis, Kabul, Afghanistan. *Emerging Infectious Diseases* **2003**, *9 (6)*, 727-729.

11. WHO Leishmaniasis. http://www.who.int/leishmaniasis/disease_epidemiology/en/.
12. Australian Society for Parasitology. <http://parasite.org.au/blog/an-unexpected-visitor-leishmaniasis-in-australia/>.
13. Gathany, J., Phlebotomine In *Public Health Image Library*, Center for Disease Control and Prevention, 2006.
14. PLoS Pathogens Issue Image | Vol. 5(8) August 2009. *PLOS Pathogens* **2009**, 5 (8), ev05.i08.
15. Cox, F. E. G., History of human parasitology. *Clin. Microbiol. Rev.* **2002**, 15 (4), 595.
16. Soto, J.; Toledo, J. T., Oral miltefosine to treat new world cutaneous leishmaniasis. *Lancet Infect. Dis.* **2007**, 7 (1), 7.
17. Coulombe, A.; Schanne, O. F.; Reisin, I.; Ruiz-Ceretti, E., Effects of amphotericin B on the electrical properties and electrolyte content of frog sartorius muscle. *Canadian Journal of Physiology and Pharmacology* **1980**, 58 (9), 1138-1141.
18. Kumar Saha, A.; Mukherjee, T.; Bhaduri, A., Mechanism of action of amphotericin B on *Leishmania donovani* promastigotes. *Molecular and Biochemical Parasitology* **1986**, 19 (3), 195-200.
19. Ibrahim, O. O. Studies towards the efficient isolation and purification of analogues of amphotericin B from *Streptomyces nodosus*. University of Leicester, 2013.
20. Matsumori, N.; Sawada, Y.; Murata, M., Mycosamine orientation of amphotericin B controlling interaction with ergosterol: Sterol-dependent activity of conformation-restricted derivatives with an amino-carbonyl bridge. *J. Am. Chem. Soc.* **2005**, 127 (30), 10667-10675.
21. Szpilman, A. M.; Manthorpe, J. M.; Carreira, E. M., Synthesis and biological studies of 35-deoxy amphotericin B methyl ester. *Angew. Chem.-Int. Edit.* **2008**, 47 (23), 4339-4342.
22. Gray, K. C.; Palacios, D. S.; Dailey, I.; Endo, M. M.; Uno, B. E.; Wilcock, B. C.; Burke, M. D., Amphotericin primarily kills yeast by simply binding ergosterol. *Proceedings of the National Academy of Sciences* **2012**, 109 (7), 2234-2239.

23. Chen, W. C.; Chou, D.-L.; Feingold, D. S., Dissociation Between Ion Permeability and the Lethal Action of Polyene Antibiotics on *Candida albicans*. *Antimicrobial Agents and Chemotherapy* **1978**, *13* (6), 914-917.
24. te Welscher, Y. M.; Jones, L.; van Leeuwen, M. R.; Dijksterhuis, J.; de Kruijff, B.; Eitzen, G.; Breukink, E., Natamycin Inhibits Vacuole Fusion at the Priming Phase via a Specific Interaction with Ergosterol. *Antimicrobial Agents and Chemotherapy* **2010**, *54* (6), 2618-2625.
25. Zhang, Y.-Q.; Gamarra, S.; Garcia-Effron, G.; Park, S.; Perlin, D. S.; Rao, R., Requirement for ergosterol in V-ATPase function underlies antifungal activity of azole drugs. *PLoS pathogens* **2010**, *6* (6), e1000939.
26. Klose, C.; Ejsing, C. S.; García-Sáez, A. J.; Kaiser, H.-J.; Sampaio, J. L.; Surma, M. A.; Shevchenko, A.; Schwille, P.; Simons, K., Yeast Lipids Can Phase-separate into Micrometer-scale Membrane Domains. *J. Biol. Chem.* **2010**, *285* (39), 30224-30232.
27. Jin, H.; McCaffery, J. M.; Grote, E., Ergosterol promotes pheromone signaling and plasma membrane fusion in mating yeast. *The Journal of Cell Biology* **2008**, *180* (4), 813.
28. Heese-Peck, A.; Pichler, H.; Zanolari, B.; Watanabe, R.; Daum, G.; Riezman, H., Multiple Functions of Sterols in Yeast Endocytosis. *Molecular Biology of the Cell* **2002**, *13* (8), 2664-2680.
29. Kato, M.; Wickner, W., Ergosterol is required for the Sec18/ATP-dependent priming step of homotypic vacuole fusion. *The EMBO Journal* **2001**, *20* (15), 4035-4040.
30. Welscher, Y. M. T.; Ten Napel, H. H.; Balague, M. M.; Souza, C. M.; Riezman, H.; De Kruijff, B.; Breukink, E., Natamycin blocks fungal growth by binding specifically to ergosterol without permeabilizing the membrane. *J. Biol. Chem.* **2008**, *283* (10), 6393-6401.
31. Saka, Y.; Mita, T., Interaction of amphotericin B with cholesterol in monolayers, aqueous solutions, and phospholipid bilayers. *J. Biochem.* **1998**, *123* (5), 798-805.
32. Deray, G.; Mercadal, L.; Bagnis, C., Amphotericin B nephrotoxicity. *Nephrologie* **2002**, *23* (3), 119-122.
33. Thakur, C. P.; Sinha, G. P.; Barat, D.; Singh, R. K., Are Incremental Doses of Amphotericin B required for the Treatment of Visceral Leishmaniasis. *Ann. Trop. Med. Parasitol.* **1994**, *88* (4), 365-370.

34. Baginski, M.; Resat, H.; McCammon, J. A., Molecular properties of amphotericin B membrane channel: A molecular dynamics simulation. *Mol. Pharmacol.* **1997**, *52* (4), 560-570.
35. Matsumori, N.; Sawada, Y.; Murata, M., Large molecular assembly of amphotericin B formed in ergosterol-containing membrane evidenced by solid-state NMR of intramolecular bridged derivative. *J. Am. Chem. Soc.* **2006**, *128* (36), 11977-11984.
36. Baron, S., *Medical Microbiology 4th Edition*. University of Texas, 1996.
37. Espinel-Ingroff, A. V., *Medical Mycology in the United States: A Historical Analysis (1894-1996)*. Springer Science: 2003.
38. Kelly, K., *Medicine becomes a Science 1840-1999*. Facts On File Inc.: 2010.
39. Nystatin (Oral Route).
<https://www.ncbi.nlm.nih.gov/pubmedhealth/PMH0044680/#DDIC601025>.
40. Mehta, R. T.; Hopfer, R. L.; Gunner, L. A.; Juliano, R. L.; Lopezberestein, G., Formulation, Toxicity and Antifungal Activity In Vitro of Liposome-Encapsulated Nystatin as Therapeutic Agent for Systemic Candidiasis. *Antimicrobial Agents and Chemotherapy* **1987**, *31* (12), 1897-1900.
41. Laskowni, Z.; Pasyk, K.; Porebska, A.; Zemburow, K., Pimaricin (Natamycin) in Treatment of Superficial Fungal Infections in Children. *Acta Paediatrica Scandinavica* **1971**, *60* (4), 456-&.
42. F. Aguilar, U. R. C., B. Dusemund, P. Galtier, J. Gilbert, D.M. Gott, S. Grilli, R. Guertler, J. Koenig, C. Lambré, J-C. Larsen, J-C. Leblanc, A. Mortensen, D. Parent-Massin, I. Pratt, I.M.C.M. Rietjens, I. Stankovic, P. Tobback, T. Verguieva, R.A. Woutersen, Scientific Opinion on the use of natamycin (E 235) as a food additive. *EFSA Journal* **2009**, *7* (12), 1412-n/a.
43. Oostendorp, J. G., Natamycin(R). *Antonie van Leeuwenhoek* **1981**, *47* (2), 170-171.
44. Borowski, E. S. C. P., Lechevalier H. and Schwartz B. S., *Perimycin, a novel type of heptaene antifungal antibiotic*. Plenum Press: New York, 1961.
45. Tadeusz Korzybski, Z. K.-G., Włodzimierz Kurylowicz, *Antibiotics: Origin, Nature and Properties*. Pergamon Press Ltd: 1967.

46. Tu, E. Y.; Joslin, C. E.; Nijm, L. M.; Feder, R. S.; Jain, S.; Shoff, M. E., Polymicrobial Keratitis: Acanthamoeba and Infectious Crystalline Keratopathy. *American Journal of Ophthalmology* **2009**, *148* (1), 13-19.e2.
47. Kotler-Brajtburg, J.; Medoff, G.; Kobayashi, G. S.; Boggs, S.; Schlessinger, D.; Pandey, R. C.; Rinehart, K. L., Classification of Polyene Antibiotics According to Chemical Structure and Biological Effects. *Antimicrobial Agents and Chemotherapy* **1979**, *15* (5), 716-722.
48. Thirumalachar, M. J. N., M. J., *Hamycin: twenty years and the future. Recent trends in the discovery, development and evaluation of antifungal agents*. Prous Science: 1987.
49. Mehta, R. T.; McQueen, T. J.; Keyhani, A.; Lopezberestein, G., Liposomal Hamycin - Reduced Toxicity and Improved Antifungal Efficacy In Vitro and In Vivo. *J. Infect. Dis.* **1991**, *164* (5), 1003-1006.
50. Balasegaram, M.; Ritmeijer, K.; Lima, M. A.; Burza, S.; Genovese, G. O.; Milani, B.; Gaspani, S.; Potet, J.; Chappuis, F., Liposomal amphotericin B as a treatment for human leishmaniasis. *Expert Opin Emerg. Drugs* **2012**, *17* (4), 493-510.
51. Ahmed, A.; Brocchini, S.; Croft, S. L., Recent advances in development of amphotericin B formulations for the treatment of visceral leishmaniasis. *Curr. Opin. Infect. Dis.* **2012**, *25* (6), 695-702.
52. Volmer, A. A.; Szpilman, A. M.; Carreira, E. M., Synthesis and biological evaluation of amphotericin B derivatives. *Nat. Prod. Rep.* **2010**, *27* (9), 1329-1349.
53. Caffrey, P.; Lynch, S.; Flood, E.; Finnan, S.; Oliynyk, M., Amphotericin biosynthesis in *Streptomyces nodosus*: deductions from analysis of polyketide synthase and late genes. *Chem. Biol.* **2001**, *8* (7), 713-723.
54. Szlinder-Richert, J.; Cybulska, B.; Grzybowska, J.; Borowski, E.; Prasad, R., Comparative studies on cell stimulatory, permeabilizing and toxic effects induced in sensitive and multidrug resistant fungal strains by amphotericin B (AMB) and N-methyl-N-D-fructosyl amphotericin B methyl ester (MFAME). *Acta Biochim. Pol.* **2000**, *47* (1), 133-140.
55. Falkowski, L.; Golik, J.; Kołodziejczyk, P.; Pawlak, J.; Zieliński, J.; Zimiński, T.; Borowski, E., N-glycosyl derivatives of polyene macrolide antibiotics. *Journal of Antibiotics* **1975**, *28* (3), 244-245.

56. Grzybowska, J.; Sowiński, P.; Gumieniak, J.; Zieniawa, T.; Borowski, E., N-methyl-N-D-fructopyranosylamphotericin B methyl ester, new amphotericin B derivative of low toxicity. *Journal of Antibiotics* **1997**, *50* (8), 709-711.
57. Aparicio, J. F.; Caffrey, P.; Gil, J. A.; Zotchev, S. B., Polyene antibiotic biosynthesis gene clusters. *Appl. Microbiol. Biotechnol.* **2003**, *61* (3), 179-188.
58. Bruheim, P.; Borgos, S. E. F.; Tsan, P.; Sletta, H.; Ellingsen, T. E.; Lancelin, J.-M.; Zotchev, S. B., Chemical Diversity of Polyene Macrolides Produced by *Streptomyces noursei* ATCC 11455 and Recombinant Strain ERD44 with Genetically Altered Polyketide Synthase NysC. *Antimicrobial Agents and Chemotherapy* **2004**, *48* (11), 4120-4129.
59. Brautaset, T.; Sekurova, O. N.; Sletta, H.; Ellingsen, T. E.; Strøm, A. R.; Valla, S.; Zotchev, S. B., Biosynthesis of the polyene antifungal antibiotic nystatin in *Streptomyces noursei* ATCC 11455: analysis of the gene cluster and deduction of the biosynthetic pathway. *Chem. Biol.* **2000**, *7* (6), 395-403.
60. Carmody, M.; Murphy, B.; Byrne, B.; Power, P.; Rai, D.; Rawlings, B.; Caffrey, P., Biosynthesis of amphotericin derivatives lacking exocyclic carboxyl groups. *J. Biol. Chem.* **2005**, *280* (41), 34420-34426.
61. Murphy, B.; Anderson, K.; Borissow, C.; Caffrey, P.; Griffith, G.; Hearn, J.; Ibrahim, O.; Khan, N.; Lamburn, N.; Lee, M.; Pugh, K.; Rawlings, B., Isolation and characterisation of amphotericin B analogues and truncated polyketide intermediates produced by genetic engineering of *Streptomyces nodosus*. *Org. Biomol. Chem.* **2010**, *8* (16), 3758-3770.
62. Hutchinson, E.; Murphy, B.; Dunne, T.; Breen, C.; Rawlings, B.; Caffrey, P., Redesign of Polyene Macrolide Glycosylation: Engineered Biosynthesis of 19-(O)-Perosaminyl-Amphoteronolide B. *Chem. Biol.* **2010**, *17* (2), 174-182.
63. Sullivan, F. X.; Kumar, R.; Kriz, R.; Stahl, M.; Xu, G.-Y.; Rouse, J.; Chang, X.-j.; Boodhoo, A.; Potvin, B.; Cumming, D. A., Molecular Cloning of Human GDP-mannose 4,6-Dehydratase and Reconstitution of GDP-fucose Biosynthesis in Vitro. *J. Biol. Chem.* **1998**, *273* (14), 8193-8202.
64. Nedal, A.; Sletta, H.; Brautaset, T.; Borgos, S. E. F.; Sekurova, O. N.; Ellingsen, T. E.; Zotchev, S. B., Analysis of the Mycosamine Biosynthesis and Attachment Genes in

- the Nystatin Biosynthetic Gene Cluster of *Streptomyces noursei* ATCC 11455. *Appl. Environ. Microbiol.* **2007**, *73* (22), 7400-7407.
65. Zhang, C.; Moretti, R.; Jiang, J.; Thorson, J. S., The in vitro Characterization of Polyene Glycosyltransferases AmphDI and NysDI. *ChemBioChem* **2008**, *9* (15), 2506-2514.
66. Mendes, M. V.; Recio, E.; Fouces, R.; Luiten, R.; Martin, J. F.; Aparicio, J. F., Engineered biosynthesis of novel polyenes: a pimaricin derivative produced by targeted gene disruption in *Streptomyces natalensis*. *Chem. Biol.* **2001**, *8* (7), 635-644.
67. Carmody, M.; Byrne, B.; Murphy, B.; Breen, C.; Lynch, S.; Flood, E.; Finnan, S.; Caffrey, P., Analysis and manipulation of amphotericin biosynthetic genes by means of modified phage KC515 transduction techniques. *Gene* **2004**, *343* (1), 107-115.
68. Chéron, M.; Cybulska, B.; Mazerski, J.; Grzybowska, J.; Czerwiński, A.; Borowski, E., Quantitative structure-activity relationships in amphotericin B derivatives. *Biochemical Pharmacology* **1988**, *37* (5), 827-836.
69. Power, P.; Dunne, T.; Murphy, B.; Lochlainn, L. N.; Rai, D.; Borissow, C.; Rawlings, B.; Caffrey, P., Engineered synthesis of 7-oxo- and 15-deoxy-15-Oxo-Amphotericins: Insights into structure-activity relationships in polyene antibiotics. *Chem. Biol.* **2008**, *15* (1), 78-86.
70. Pawlak, J.; Sowinski, P.; Borowski, E.; Gariboldi, P., Stereostructure of perimycin A. *The Journal of antibiotics* **1995**, *48* (9), 1034-1038.
71. Zuckermann, R. N.; Kerr, J. M.; Kent, S. B.; Moos, W. H., Efficient method for the preparation of peptoids [oligo (N-substituted glycines)] by submonomer solid-phase synthesis. *J. Am. Chem. Soc.* **1992**, *114* (26), 10646-10647.
72. Kawabata, M.; Onda, M.; Mita, T., Effect of aggregation of amphotericin B on lysophosphatidylcholine micelles as related to its complex formation with cholesterol or ergosterol. *J. Biochem.* **2001**, *129* (5), 725-732.
73. Worthen, D. R.; Jay, M.; Bummer, P. M., Methods for the recovery and purification of polyene antifungals. *Drug Dev. Ind. Pharm.* **2001**, *27* (4), 277-286.
74. Palacios, D. S.; Anderson, T. M.; Burke, M. D., A Post-PKS oxidation of the amphotericin B skeleton predicted to be critical for channel formation is not required for potent antifungal activity. *J. Am. Chem. Soc.* **2007**, *129* (45), 13804-+.

75. NCCLS, Performance Standards for Antimicrobial Disk Susceptibility Tests, M2-A8, Approved standard 8th Edition. CLSI: 2003; Vol. 23, Number 1.
76. NCCLS, Reference Method for Broth Dilution Antifungal Susceptibility Testing of Yeasts; M27-A2 Approved Standard—Second Edition. 2002; Vol. 22, Number 15.
77. Perlman, D.; Semar, J. B., Preparation of amphotericin B-14C. *Biotechnology and Bioengineering* **1965**, 7 (1), 133-137.
78. Paquet, V.; Carreira, E. M., Significant improvement of antifungal activity of polyene macrolides by bisalkylation of the mycosamine. *Org. Lett.* **2006**, 8 (9), 1807-1809.
79. Mechlins.W; Schaffne.Cp; Ganis, P.; Avitabil.G, Structure and Absolute Configuration of Polyene Macrolide Antibiotic Amphotericin B. *Tetrahedron Lett.* **1970**, (44), 3873-&.
80. Ganis, P.; Avitabile, G.; Mechlinski, W.; Schaffner, C. P., Polyene Macrolide Antibiotic Amphotericin B - Crystal Structure of N-Iodoacetyl Derivative. *J. Am. Chem. Soc.* **1971**, 93 (18), 4560-+.
81. Smith, M. B., *Organic Chemistry - An Acid-Base Approach*. CRC Press: 2011.
82. Pérez, P.; Toro-Labbé, A., Characterization of Keto-Enol Tautomerism of Acetyl Derivatives from the Analysis of Energy, Chemical Potential, and Hardness. *The Journal of Physical Chemistry A* **2000**, 104 (7), 1557-1562.
83. Hart, H., Simple enols. *Chemical Reviews* **1979**, 79 (6), 515-528.
84. Lockwood, K. L., Solvent effect on the keto-enol equilibrium of acetoacetic ester. *Journal of Chemical Education* **1965**, 42 (9), 481.
85. Mountain, R. D., Microstructure and Hydrogen Bonding in Water-Acetonitrile Mixtures. *J. Phys. Chem. B* **2010**, 114 (49), 16460-16464.
86. Novak, P.; Skare, D.; Sekusak, S.; Vikić-Topić, D., Substituent, temperature and solvent effects on keto-enol equilibrium in symmetrical pentane-1,3,5-triones. Nuclear magnetic resonance and theoretical studies. *Croatica Chemica Acta* **2000**, 73 (4), 1153-1170.
87. Byrne, B.; Carmody, M.; Gibson, E.; Rawlings, B.; Caffrey, P., Biosynthesis of deoxyamphotericins and deoxyamphoteronolides by engineered strains of *Streptomyces nodosus*. *Chem. Biol.* **2003**, 10 (12), 1215-1224.

88. Ehrenfreund-Kleinman, T.; Azzam, T.; Falk, R.; Polacheck, I.; Golenser, J.; Domb, A. J., Synthesis and characterization of novel water soluble amphotericin B–arabinogalactan conjugates. *Biomaterials* **2002**, *23* (5), 1327-1335.
89. Lee, M.-J.; Kong, D.; Han, K.; Sherman, D. H.; Bai, L.; Deng, Z.; Lin, S.; Kim, E.-S., Structural analysis and biosynthetic engineering of a solubility-improved and less-hemolytic nystatin-like polyene in *Pseudonocardia autotrophica*. *Appl. Microbiol. Biotechnol.* **2012**, *95* (1), 157-168.
90. Currie, C. R.; Wong, B.; Stuart, A. E.; Schultz, T. R.; Rehner, S. A.; Mueller, U. G.; Sung, G.-H.; Spatafora, J. W.; Straus, N. A., Ancient Tripartite Coevolution in the Attine Ant-Microbe Symbiosis. *Science* **2003**, *299* (5605), 386.
91. Mueller, U. G.; Dash, D.; Rabeling, C.; Rodrigues, A., Coevolution between attine ants and actinomycete bacteria: a reevaluation. *Evolution* **2008**, *62* (11), 2894-2912.
92. Barke, J.; Seipke, R. F.; Grünschow, S.; Heavens, D.; Drou, N.; Bibb, M. J.; Goss, R. J.; Yu, D. W.; Hutchings, M. I., A mixed community of actinomycetes produce multiple antibiotics for the fungus farming ant *Acromyrmex octospinosus*. *BMC Biology* **2010**, *8* (1), 109.
93. Stephens, N.; Rawlings, B.; Caffrey, P., Versatility of Enzymes Catalyzing Late Steps in Polyene 67-121C Biosynthesis. *Biosci. Biotechnol. Biochem.* **2013**, *77* (4), 880-883.
94. De Poire, E.; Stephens, N.; Rawlings, B.; Caffrey, P., Engineered Biosynthesis of Disaccharide-Modified Polyene Macrolides. *Appl. Environ. Microbiol.* **2013**, *79* (19), 6156-6159.
95. Walmsley, S.; De Poire, E.; Rawlings, B.; Caffrey, P., Engineered biosynthesis and characterisation of disaccharide-modified 8-deoxyamphoteronolides. *Appl. Microbiol. Biotechnol.* **2017**, *101* (5), 1899-1905.
96. Jarzemska, K. N.; Kaminski, D.; Hoser, A. A.; Malinska, M.; Senczyna, B.; Wozniak, K.; Gagos, M., Controlled Crystallization, Structure, and Molecular Properties of Iodoacetylamphotericin B. *Cryst. Growth Des.* **2012**, *12* (5), 2336-2345.
97. Gagos, M.; Kaminski, D.; Arczewska, M.; Krajnik, B.; Mackowski, S., Spectroscopic Evidence for Self-Organization of N-Iodoacetylamphotericin B in Crystalline and Amorphous Phases. *J. Phys. Chem. B* **2012**, *116* (42), 12706-12713.